Metabolic engineering of *Streptomyces albus* for enhanced production of the reverse antibiotic nybomycin

Dissertation

zur Erlangung des Grades

des Doktors der Ingenieurwissenschaften

der Naturwissenschaftlich-Technischen Fakultät

der Universität des Saarlandes

von

Julian Stegmüller

Saarbrücken

2023

Tag des Kolloquiums:	4. April 2024
Prodekan:	Prof. Dr.-Ing. Michael Vielhaber
Berichterstatter:	Prof. Dr. Christoph Wittmann
	Prof. Dr. Andriy Luzhetskyy
Vorsitz:	Prof. Dr. Uli Kazmaier
Akad. Beisitzer:	Dr. Markus Neuber

Publications

Partial results of this work have been published in advance authorized by the Institute of Systems Biotechnology represented by Prof. Dr. Christoph Wittmann.

Peer-reviewed articles

Gläser, L., Kuhl, M., **Stegmüller, J**., Rückert, C., Myronovskyi, M., Kalinowksi, J., Luzhetskyy, A., Wittmann, C. (2021) Superior production of heavy pamamycin derivatives using a *bkdR* null mutant of *Streptomyces albus* J1074/R2*. Microb. Cell Fact*. 20, 111.

https://doi.org/10.1186/s12934-021-01602-6

Stegmüller, J., Rodríguez Estévez, M., Rückert, C., Shu, W., Gläser, L., Myronovskyi, M., Kalinowksi, J., Luzhetskyy, A., Wittmann, C. (2023) Systems metabolic engineering of the primary and secondary metabolism of *Streptomyces albidoflavus* enhances production of the reverse antibiotic nybomycin against multi-resistant *Staphylococcus aureus*. Metab. Eng. 81, 123-143.

https://doi.org/10.1016/j.ymben.2023.12.004

Conference contributions

Stegmüller, J., Kuhl, M., Gläser, L., Rebets, Y., Rückert, C., Kalinowksi, J., Luzhetskyy, A., Wittmann, C., „Heterologous production of the agrochemical pamamycin in metabolically engineered *Streptomyces albus* J1074/R2." GASB 4th conference, September 2 24 – 28, 2020, Virtual Conference

Danksagung

Besonders herzlich danke ich Prof. Dr. Christoph Wittmann, meinem Doktorvater, der nicht nur das Thema meiner Arbeit zur Verfügung stellte, sondern mich auch intensiv während des gesamten Forschungsprozesses betreute. Seine offene Tür, sein offenes Ohr und die zahlreichen wertvollen Lehren, die ich von ihm erhalten habe, sind für meine akademische Entwicklung von großem Wert. Prof. Dr. Wittmann vermittelte mir nicht nur fachliches Wissen, sondern ermutigte mich stets und gab mir den Glauben, die gesteckten Ziele zu erreichen. Diese außergewöhnliche und intensive Zeit hat nicht nur meine wissenschaftlichen Fähigkeiten, sondern auch meine persönliche Weiterentwicklung gefördert.

Ebenfalls möchte ich mich bei Prof. Dr. Andriy Luzhetskyy für die Koordination des BMBF geförderten Forschungsprojekts EXPLOMARE, die ausgezeichnete Zusammenarbeit in den vergangenen vier Jahren und für die sorgfältige Begutachtung meiner Arbeit bedanken.

Ein großes Dankeschön an Lars Gläser und Martin Kuhl für die ausführliche Einarbeitung in Sachen Kultivierung von *Streptomyces* und der dazugehörigen Analytik mittels LC/MS. Außerdem möchte ich mich bei Dr. Maksym Myronovskyi und Dr. Marta Rodríguez Estévez aus der Arbeitsgruppe Luzhetskyy für die Unterstützung bei gentechnischen Arbeiten mit *Streptomyces*, bedanken. Bei Dr. Christian Rückert möchte ich recht herzlich für die Durchführung und Auswertung der Transkriptomanalysen bedanken.

Ein besonderes Dankeschön gilt Michel Fritz, der mich unermüdlich im „Kampf“ mit eigensinnigen Analysegeräten wie Ionenchromatographie und LC/MS unterstütze.

Für die schönen Momente während und Abseits der Arbeit, möchte ich mich bei meinen Kollegen und Freunden Lars Gläser, Martin Kuhl, Demian Dietrich, Sarah Lisa Hoffmann, und Peng Cao bedanken. Ob Wakeboarding, Squash, Golfen, Laufen oder Badminton, es war immer ein super Ausgleich zum häufig stressigen Laboralltag.
Ein großer Dank gilt auch allen Kollegen, die mich während der Zeit am iSBio in vielerlei Hinsicht unterstützt und eine großartige Arbeitsatmosphäre geschaffen haben. Danke dir, Susanne Haßdenteufel für die abwechslungsreichen und humorvollen Gespräche über Gott und die Welt und deine Unterstützung in unzähligen anderen organisatorischen Angelegenheiten.

Ein großer Dank geht an meine Freundin Linda, die mich während der gesamten Zeit seelisch und moralisch unterstützt, und es auch in schwierigen Zeiten geschafft hat, mich aufzumuntern.

Zuletzt gilt mein Dank meiner Familie, die mir immer den notwendigen Rückhalt gegeben und mir die Zeit mit ihrer Unterstützung enorm erleichtert hat.

Table of contents

Summary

Streptomycetes, filamentous bacteria are well-known for their capability of producing bioactive secondary metabolites. With raised antimicrobial resistance of bacteria, these metabolites receive increased attention. Recently, the biosynthetic gene cluster of the reverse antibiotic nybomycin was found and its genes were firstly expressed heterologously in *S. albus*. The biosynthesis is complex since various building blocks are required. Nybomycin represents a promising antibiotic for the treatment of methicillin-resistant *Staphylococcus aureus* (MRSA). In this work, the aim was to improve the heterologous production in *S. albus*. In a minimal medium with mannitol as carbon source, 0.86 mg L^{-1} were produced in 275 h. Initial metabolic engineering attempts failed since the promoter P_{ermE*} was solely active during growth phase while main production occurred in stationary phase. Fluorescence-based promoter screening reveals the strong constitutive promoter P_{kasOP*} with superior activity in growth and production phase. Multiple rounds of engineering in the pentose phosphate pathway (PPP) and shikimic acid pathway (SAP), to improve the supply of nybomycin building blocks, doubled nybomycin production to 1.6 mg L^{-1}. Gene expression analysis, applying RNA-sequencing, revealed cluster-situated regulators *nybWXYZ*. Silencing the regulation by deletion of *nybWXYZ* yielded strain NYB-11, which produced 12 mg L^{-1} of nybomycin in a substrate optimized minimal medium containing 50 g L^{-1} mannitol.

Zusammenfassung

Streptomyceten, filamentöse Bakterien sind bekannt für ihre Fähigkeit bioaktive Sekundärmetabolite zu produzieren. Kürzlich wurden die Biosynthese Gene für das reverse Antibiotikum Nybomycin entdeckt und erstmals heterolog in *S. albus* exprimiert. Die Biosynthese ist komplex, da verschiedene Bausteine verwendet werden. Nybomycin stellt ein vielversprechendes Antibiotikum für die Behandlung von Methicillin-resistenten *Staphylococcus aureus* (MRSA) dar. Das Ziel dieser Arbeit war es, die heterologe Produktion in *S. albus* zu verbessern. In einem minimalen Wachstumsmedium auf Mannitol, wurden 0.86 mg L^{-1} in 275h produziert. Erste Versuche der Stammoptimierung scheiterten, da der verwendete Promoter P_{ermE*} lediglich in der Wachstumsphase aktiv war, während die Hauptproduktion in der stationären Phase ablief. Durch Fluoreszenz-basierte Promoter Studien, konnte der konstitutive Promoter P_{kasOP*} mit verbesserter Aktivität in Wachstums- und Produktionsphase gefunden werden. Mehrere Runden der Stammoptimierung im Pentose Phosphat Weg und im Shikimat Weg, um die Bereitstellung von Nybomycin Bausteinen zu verbessern, verdoppelten die Nybomycin Produktion auf 1.6 mg L^{-1}. Durch Gen Expressionsanalysen mittels RNA-Sequenzierung wurden die Cluster eigenen Regulatorgene *nybWXYZ* entdeckt. Das Unterdrücken der Regulation durch Deletion der Gene *nybWXYZ* in Stamm NYB-11, brachte eine Produktionssteigerung auf 12 mg L^{-1} Nybomycin in einem Substrat optimierten minimal medium mit 50 g L^{-1} Mannitol.

1 Introduction

1.1 General introduction

The genus *Streptomyces*, among the phylum *actinobacteria*, comprises Gram-positive filamentous bacteria from terrestrial and marine ecosystems (Macagnan et al., 2006). During their complex multi-staged life cycle, these cells propagate by vegetative mycelium formation, aerial hyphae production, and, finally, differentiation into new spores (Jones and Elliot, 2018; Kieser et al., 2000). The transition from vegetative to aerial growth is associated to a switch from primary to secondary metabolism, during which the most secondary metabolites are produced (Bibb, 2005; van Wezel and McDowall, 2011). This class of molecules is non-essential for growth (Demain and Fang, 2000), however, known to play a significant role in competing rivals (Chadwick and Whelan, 1992), and as effector of differentiation, e.g. pamamycin (Kuhl et al., 2020; McCann and Pogell, 1979), and germicidin (Petersen et al., 1993). Intriguingly, secondary metabolite-producing *Streptomyces* provide around two-thirds of all commercially available antibiotics (Barka et al., 2016; Kitani et al., 2011).

Excessive and incorrect use of antibiotics, however, is associated with emerging resistance. Methicillin-resistant *Staphylococcus aureus* (MRSA) a prominent hospital pathogen, causes thousands of deaths annually, while rapidly acquiring new resistances and thus hampering antibiotic treatment. Nybomycin, a pyridoquinolinedione-based metabolite, discovered in the 1950s, exhibits antibiotic activity against several pathogens including MRSA (Strelitz et al., 1955). Interestingly, inhibiting activity is, however, only observed against quinolone-resistant MRSA strains, subsequently sensitizing the strain to quinolone antibiotic again, by causing a backmutation in the affected gyrase A gene. Due to this special mode of action, nybomycin was termed `reverse` antibiotic, and regarded promising for potential future dual treatment using a combination of quinolone-antibiotics and nybomycin (Hiramatsu et al., 2012). The chemical synthesis of nybomycin is possible, however, laborious, time-consuming, and occurs at low yield (Forbis and Rinehart, 1971; Parkinson et al., 2015). The recent identification of the nybomycin biosynthetic gene cluster (BGC) in *Streptomyces albus* subsp. *chlorinus*, allowed the first generation of a heterologous nybomycin producer strain and provided a valuable proof

of principle (Rodriguez Estevez et al., 2018). Unfortunately, the production titer in the basic strain was low, limiting further exploration of the molecule.

1.2 Objectives

The aim of this work was to metabolically engineer a heterologous *Streptomyces* host to improve the production of nybomycin. Firstly, robust, and reliable methods for nybomycin extraction and analysis should be established. Next, the basic heterologous nybomycin producer *S. albus* 4N24 (Rodriguez Estevez et al., 2018) should be characterized for growth and nybomycin formation. Next, suitable promotors should be identified for tailored gene expression during the nybomycin production phase, using fluorescence-based gene expression screening. Subsequently, rational strain engineering of the carbon core metabolism, reactions for precursor supply, and the nybomycin biosynthetic pathway, should be conducted to improve product formation. The mutant strains should then be analyzed to combine promising gene targets, for the generation of even more efficient producers. Finally, RNA sequencing of selected strains should provide a systems view on gene expression of the nybomycin biosynthetic genes, as well as supporting and competing pathways.

2 Theoretical Background

2.1 The world of actinobacteria

Actinobacteria are Gram-positive filamentous bacteria with a high G+C content in their genome (Barka et al., 2016). They live in both terrestrial and marine ecosystems (Macagnan et al., 2006; Ribeiro da Cunha et al., 2019; Sarmiento-Vizcaino et al., 2018; Waksman et al., 2010). Since actinomycetes produce mycelium and propagate by sporulation like filamentous fungi, they are often considered as a translational form of fungi and bacteria. However, as all Gram-positive prokaryotes, actinomycetes are cellularly organized with a prokaryotic nucleoid and a peptidoglycan cell wall (Barka et al., 2016). *Actinobacteria* represent one of the largest taxonomic units among all 18 major lineages within the *Bacteria* domain (Ludwig et al., 2012; Ventura et al., 2007). Among the phylum *actinobacteria*, 15 genera are described, namely: *Tropheryma, Propionibacterium, Micromonospora, Salinispora, Mycobacterium, Nocardia, Corynebacterium, Gordonia, Rhodococcus, Leifsonia, Bifidobacterium, Gardnerella, Thermobifida, Frankia and Streptomyces* that are majorly distinguished by morphology (mycelial- and spore-chain morphology, spore chain length and melanin pigments) (Barka et al., 2016) and chemotaxonomy, including cell wall composition, whole-cell sugars, phospholipids, and menaquinones (Labeda, 1987). Meanwhile, sequencing technologies, allowing easy and cheap whole genome sequencing to conduct 16S rRNA and DNA-DNA hybridization analyses, also play an important role in the taxonomic classification of actinomycetes (Barka et al., 2016).

2.2 *Streptomyces*: cellular life cycle and natural product formation

Streptomyces represent the largest genus among *actinobacteria* (Lee et al., 2014). In soil samples, approximately 95% of the existing actinomycetes belong to the genus *Streptomyces* (Williams and Vickers, 1988). In this natural habitat they play a crucial role in recycling carbon from plant and fungi debris (Barka et al., 2016). Furthermore, *Streptomyces* possess large genomes organized in linear chromosomes, ranging in size from approximately 6-12 Mb (Harrison and Studholme, 2014). Their chromosomes are divided into the central ´core` region containing essential housekeeping genes (Hopwood, 2006) and two flanking ´arms`, containing non-essential genes, probably acquired by horizontal gene transfer to adapt to altered environmental conditions (Bentley et al., 2002; Hopwood, 2006)

Streptomyces contain large numbers (>20) of biosynthetic gene clusters (BGCs) encoding polyketide synthases (PKSs), non-ribosomal peptide synthetases (NRPSs) and other genes for the production of polyketides (Staunton and Weissman, 2001), peptides (Marahiel and Essen, 2009), bacteriocins (Moore, 2008), and other natural products (Nett et al., 2009). Approximately 75% of the commercially available antibiotics are derived from *Streptomyces* (Baltz, 2007; Berdy, 2005; Kinkel et al., 2014; Quinn et al., 2020), highlighting the importance of this genus with regard to development of new bioactive compounds particularly in the era of increasing antimicrobial resistance (AMR).

Streptomyces display a complex but well investigated life cycle that can be divided into three developmental forms, namely vegetative mycelium, aerial hyphae, and spores **(Figure 1)**. The common starting point of development is the germination of a free dormant spore. The following vegetative growth is characterized by linear tip extension and branching of the filaments at random intervals to build a dense network termed vegetative mycelium. Cell division during vegetative growth leads to cross-walls, separating hyphae into connected compartments (Wildermuth and Hopwood, 1970), containing multiple copies of the chromosome, giving *Streptomyces* the character of a multicellular bacterium (Claessen et al., 2014; Kois-Ostrowska et al., 2016).

Under unfavorable environmental conditions such as nutrient depletion, *Streptomyces* enter the second growth stage in which most antibiotics are produced (Bibb, 2005; van Wezel and

McDowall, 2011). Here, the vegetative mycelium is autolytically degraded by programmed cell death to supply nutrients for the formation of non-branching aerial hyphae (Méndez et al., 1985; Miguelez et al., 1999; Wildermuth, 1970). After the aerial hyphae growth has finished, the unbranched filaments start simultaneous septation to form chains of single genome pre-spores, that are further maturing to dormant spores (Jones and Elliot, 2018).

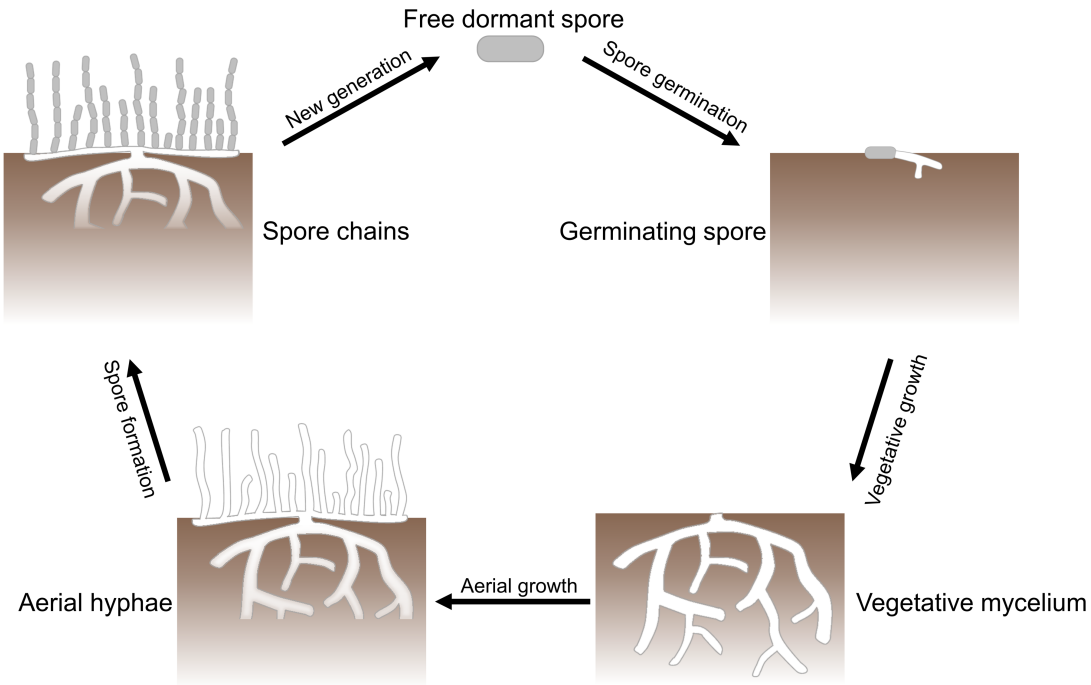

Figure 1: Developmental life cycle stages of *Streptomyces* species. In a nutrient-rich environment, free spores start germination, and subsequent formation of vegetative mycelium. Upon nutrient scarcity, the vegetative mycelium is autolytically degraded, serving as substrate for growth of the aerial hyphae. Afterwards, the unbranched hyphae start simultaneous septation to form a new generation of spores.

The development of *Streptomyces* and the production of secondary metabolites is highly connected (Barka et al., 2016; Kuhl et al., 2021). Obviously, regulatory genes involved in differentiation (such as *bld* and *whi*), also play a significant role in the regulation of secondary metabolite (antibiotic) formation (Elliot et al., 1998; Pope et al., 1996)

In the second phase (aerial hyphae formation phase, stationary phase), the cells shift to secondary metabolism, i.e., formation of secondary metabolites, often referred as natural product start (Puglisi, 2004; Stone and Williams, 1992). Apparently, secondary metabolite production and sporulation share some similarities (Bibb, 2005; van Wezel and McDowall, 2011). Estimations suggest that approximately 25 % of all known secondary metabolites –

more than one million – exploit biological activity such as antibiotic, antifungal, antiviral, immunosuppressive, antiparasitic, and anticancer (Demain, 2014), which may inhibit growth of competing microbes in the natural habitat (Hopwood, 1999). However, previous studies showed that secondary metabolites also play crucial roles in signaling, cell-cell communication (Davies, 2011; Willey and Gaskell, 2011), and differentiation (Kuhl et al., 2020; McCann and Pogell, 1979; Petersen et al., 1993).

Genes encoding secondary metabolites are usually organized in clusters that vary in size from several kilobases to more than 100 kilobases (Bentley et al., 2004; Bentley et al., 2002; Ikeda et al., 2003; Schwecke et al., 1995; Smanski et al., 2016). Emerging next generation sequencing technologies (Didelot et al., 2012), enabled inexpensive sequencing of several *Streptomyces* genomes. Driven by software tools to predict potential secondary metabolite gene clusters from genome sequences such as antiSMASH (Medema et al., 2011), the discovery and the development of new natural products evolved rapidly. However, BGCs often remain silent under conventional laboratory conditions (Liu et al., 2021b; Rodriguez Estevez et al., 2020). Several approaches to activate cryptic BGC have been described (Liu et al., 2021b). A common approach is the use of heterologous expression hosts or optimized chassis strains (Ahmed et al., 2020; Bu et al., 2019; Myronovskyi et al., 2018) for the expression of BGCs, obtained by either cloning (Hover et al., 2018; Rodriguez Estevez et al., 2018) or reconstruction (Ji et al., 2022; Ji et al., 2018) of the cluster genes. On the other hand, promoter engineering (Bai et al., 2015; Luo et al., 2015; Wang et al., 2019a), engineering of transcriptional regulation (Hackl and Bechthold, 2015; Liu et al., 2019; Zhu et al., 2017) or ribosome and RNA polymerase engineering (Li et al., 2019; Thong et al., 2018) in the native host is applied to activate silent BGCs. Another strategy is screening for antibiotic resistant mutants, that may alter the spectrum of produced secondary metabolites (Hosoya et al., 1998; Rodriguez Estevez et al., 2020; Shima et al., 1996).

Research on natural products started in the 1940s, since the first antibiotic penicillin was discovered in fungi (Fleming, 1929). Until the 1980s, the discovery reached a peak of 500 microbial bioactive compounds per year (Demain, 2014) including streptomycin and other aminoglycosides (Waksman and Schatz, 1945), cephalosporins (Bo, 2000) and tetracyclines

(Nelson and Levy, 2011). The discovery rate decreased dramatically in the 21st century for several reasons. Primarily, it was due to the loss of interest of pharmaceutical companies in developing these compounds due to low economic profit, resulting from the immense development costs caused by high screening efforts and long-term clinical trials (Livermore, 2011). Hence, natural products became unattractive, and pharmaceutical companies rather focused on high-throughput screening of synthetic compounds (Pereira and Williams, 2007). Certainly, the new high-throughput screening approach of synthetic compounds revealed a much lower hit rate compared to natural products (Weissman and Leadlay, 2005).

Starting with the discovery and the development of new natural products as antibiotics, antimicrobial resistance (AMR) emerged simultaneously (Fleming, 1929). Microbes, exposed to sub-lethal antibiotic concentrations, can establish resistance by acquiring spontaneous mutations (Kohanski et al., 2010; Salverda et al., 2017). Horizontal gene transfer, however, i.e., exchange of genetic material among bacteria including antibiotic resistance genes, enables easy and fast adaption to the sublethal environmental conditions (Roux and Blokesch, 2018). Common resistance mechanisms of bacteria rely on 1) drug inactivation by chemical modification of the molecule, 2) modification of drug binding sites to thwart interaction of the drug and its target, 3) insufficient intracellular drug accumulation by loss of porins or importers and efficient export of the molecule by efflux pumps, 4) formation of a biofilm, constituted of polymeric substances and other protecting molecules to build a mechanical and biochemical defense (Santajit and Indrawattana, 2016).

The development of multi drug resistant bacteria, particularly in clinical environments, is gaining more and more attention. The world health organization estimates the number of deaths caused by multi drug resistant bacteria by 2050 to around 10 million per year (Sun et al., 2019; WHO, 2014). Within the ESKAPE pathogens (*Enterococcus faecium, Staphylococcus aureus, Klebsiella pneumoniae, Acinetobacter baumannii, Pseudomonas aeruginosa* and *Enterobacter* species) (Santajit and Indrawattana, 2016), MRSA i.e. methicillin-resistant *Staphylococcus aureus* acquired multiple additional resistances to further antibiotics (Vestergaard et al., 2019), including other penicillins, cephalosporins, monobactams, carbapenems, cephems, and β-lactams and β-lactamase inhibitor

combinations (Dhungel et al., 2021) posing the threat of a devastating return to the pre-antibiotic era (Hassoun et al., 2017). Every year, MRSA infections cause more than 100,000 death cases with the highest burden in less developed regions e.g., lacking hygiene or a proper health care system. Extensive collaboration and appropriate policy decisions to brief about infection preventions, global access to essential antibiotic but also to support research and development for new antibiotics is required to tackle this problem (Murray et al., 2022).

Table 1: Clinically relevant compounds originating from *Streptomyces* species and their type

Compound	Type	species	Reference
Bialaphos	Herbicide	*S. hygrocopicus*	(Seto et al., 1983)
Bleomycin	Anticancer	*S. verticillus*	(Kong et al., 2018)
Chloramphenicol	Antibiotic	*S. venezuelae*	(Brock, 1961)
Cineromycin A + B	Antibiotic	*S. cinerochromogenes*	(Miyairi, 1966)
Clavulanic acid	Antibiotic	*S. clavuligerus*	(Higgens and Kastner, 1971)
Clindamycin	Antibiotic	*S. lincolnensis*	(Macleod et al., 1964)
Lincomycin	Antibiotic	*S. lincolnensis*	(Macleod et al., 1964)
Daptomycin	Antibiotic	*S. roseosporus*	(Eliopoulos et al., 1986)
Erythromycin	Antibiotic	*S. erythraeus*	(Washington and Wilson, 1985)
Fosfomycin	Antibiotic	*S. fradiae*	(Matthews et al., 2016)
Ivermectin	Antiparasitic	*S. avermitilis*	(Ottesen and Campbell, 1994)
Kanamycin	Antibiotic	*S. kanamyceticus*	(Umezawa, 1958)
Neomycin	Antibiotic	*S. fradiae* *S. albogriseus*	(Waksman and Lechevalier, 1949)
Nystatin	Antifungal	*S. noursei*	(Hazen and Brown, 1950)
Rapamycin	Antifungal, antitumor, immonusuppressive	*S. hygrocopicus*	(Sehgal, 2003)
Saframycins A-E	Anticancer	*S. lavendulae subsp. grasserius*	(Arai et al., 1980)
Streptomycin	Antibiotic	*S. griseus*	(Schatz et al., 2005)
Tetracycline	Antibiotic	*S. aureofaciens* *S. rimosus*	(Petkovic et al., 2006)
Vancomycin	Antibiotic	*Amycolatopsis orientalis*	(Geraci et al., 1956)

2.3 *Streptomyces albus* J1074 as heterologous expression workhorse

Streptomyces albus J1074, formerly known as *Streptomyces albus* G, was first mentioned almost 50 years ago, while describing its defective *Sal*I (*Sal*GI) restriction modification system (Chater and Wilde, 1976; Chater and Wilde, 1980; Rodicio and Chater, 1988). Notably, this feature allows easy and straightforward genetic manipulation which has greatly contributed to its development into an efficient expression host since then. *S. albus* J1074 possesses one of the smallest *Streptomyces* genomes known so far which comprises approximately 6.8 Mb and exhibits a high GC content of 73.3 % and encodes 5,832 predicted protein coding sequences. Interestingly, its two flanking chromosome `arms` are significantly smaller than those of *S. coelicolor* and other *Streptomycetes* (Zaburannyi et al., 2014). Furthermore, insertion elements within the genome are mainly located in the `core` region contrary to *S. coelicolor* where such transposases are found to be more concentrated in the `arms`. The small genome and its genetic organization enable fast growth and good genetic accessibility, making *S. albus* J1074 a widely used host for the heterologous expression of cryptic biosynthetic pathways and the production of secondary metabolites from diverse organisms (Baltz, 2010; Myronovskyi et al., 2014; Zaburannyi et al., 2014). This is underlined by various prominent examples, including the production of steffimycin (Gullon et al., 2006), fredericamycins (Wendt-Pienkowski et al., 2005), pamamycins (Rebets et al., 2015), iso-migrastatin (Feng et al., 2009), thiocoraline (Lombo et al., 2006), cyclooctatin (Kim et al., 2009), moenomycin (Makitrynskyy et al., 2010), and napyradiomycin (Winter et al., 2007), respectively. The *S. albus* J1074 expression platform was much improved by generating the cluster-free chassis *S. albus* Del14, upon the deletion of 15 native biosynthetic gene clusters encoding secondary metabolite biosynthetic pathways. The eliminiation of these undesired routes advanced production and allowed much more selective synthesis with reduced detection limits (Myronovskyi et al., 2018). The “clean” strain *S. albus* Del14 has also been validated as heterologous expression platform for fredericamycin C_2 (Rodriguez Estevez et al., 2020), benzanthric acid (Rodríguez Estévez et al., 2020), albucidin (Myronovskyi et al., 2020), dudomycins (Lasch et al., 2020), chelocardin (Lukezic et al., 2020), mansouramycin D (Shuai et al., 2022), huimycin (Shuai et al., 2020), bonsecamin

(Lasch et al., 2021), miramides (Paulus et al., 2022), and nybomycin (Rodriguez Estevez et al., 2018).

2.3.1 Systems metabolic engineering

Microbes offer genetic capabilities to produce a wide range of commercially relevant products, ranging from bulk chemicals including biofuels, solvents, organic acids, monomers, polymers, food supplements to high-value products such as pharmaceuticals, functional proteins or flavoring chemicals (Becker et al., 2018b; Becker and Wittmann, 2015). For competitive production, microbial cell factories need to enable attractive titer, yield and productivity (Lee and Kim, 2015). Classically, random mutagenesis and selection was used to obtain strains with improved performance. While this approach is still applied, however, the inherent accumulation of detrimental mutations during strain development poses a drawback on this strategy, (Lal et al., 1996; Parekh et al., 2000). Beneficially, the advent of genetic engineering technologies subsequently enabled a new way of designing and construction superior cell factories (Liu and Stephanopoulos, 2021; Yang et al., 2017) .

Nowadays, the generation of high performance cell factories is empowered by efficient systems metabolic engineering strategies that integrate systems biology, synthetic biology, and evolutionary engineering (Choi et al., 2016). On the experimental side, genomics, transcriptomics, proteomics, metabolomics and fluxomics, have provided a substantial knowledge gain for strain development (Becker and Wittmann, 2015; Lee and Kim, 2015). In addition, genome-based *in silico* metabolic modelling and simulation has greatly contributed to the prediction of strategies for subsequent pathway and protein engineering (Gustavsson and Lee, 2016). As example, genome-scale metabolic models (GSMM) have been constructed for several organisms, including *E. coli* (Edwards and Palsson, 2000; Reed et al., 2003), *B. subtilis* (Goelzer et al., 2008; Henry et al., 2009; Oh et al., 2007; Tanaka et al., 2012), *M. tuberculosis* (Beste et al., 2007; Kavvas et al., 2018), *C. glutamicum* (Becker et al., 2005; Becker et al., 2011; Feierabend et al., 2021; Wittmann and Heinzle, 2002), *S. cerevisiae* (Dobson et al., 2010; Forster et al., 2003) and *Streptomyces* sp. (Dang et al., 2017; Huang et al., 2011). Hereby, the integration of omics data sets into GSMM, provided a comprehensive

view on the cell metabolism (Kim et al., 2016; Monk et al., 2016). As example, GSMM guided the improvement of production of the antitumor drug FK506 in *Streptomyces tsukubaensis,* significantly (Huang et al., 2013a).

Transcriptomics is applied to determine dynamic gene expression differences between strains, culture conditions and growth phases, respectively, and offers a prominent tool to decipher global regulatory networks and identify potential targets for strain optimization (Becker and Wittmann, 2015). Whole-genome DNA microarrays and RNA sequencing technologies represent useful tools, with complementing advances in their field of application, respectively (Kogenaru et al., 2012). Whereas RNA sequencing offers more accurate quantitative measurement and the determination of absolute transcript abundance (Mantione et al., 2014), it is linked to substantially increased effort and costs. Microarray-based transcriptome analysis unveiled targets for strain improvement of recombinant proteins (Choi et al., 2003), amino acids such as L-glutamate (Stansen et al., 2005), L-lysine (Hayashi et al., 2006; Krömer et al., 2004) and related compounds such as diaminopentane (Kind et al., 2010b).

Since metabolic activities may not directly correlate with transcript levels, proteomics gained increased attention to enable a deeper understanding of cellular metabolism and cell physiology (Basan et al., 2015; Schmidt et al., 2016). Metabolomics, aiming at the quantification of (intracellular and extracellular) metabolites is more directly associated to the metabolic activities (Choi et al., 2019). Since intracellular metabolite levels, may change within short time, appropriate sampling protocols are crucial (Bolten et al., 2007; Pinu et al., 2019; Wittmann et al., 2004). To this end, different sampling approaches have been developed that allow, reliable intracellular metabolite quantification (Bolten et al., 2007; Gläser et al., 2020; Wittmann et al., 2004). Notably, metabolomics has proven valuable to drive strain engineering. As example, the production of 1-butanol in *E. coli*, could be efficiently improved after identifying a CoA imbalance using metabolomic profiling (Ohtake et al., 2017). Furthermore, the 1-butanol tolerance of *S. cerevisiae* was improved after revealing threonine, citric acid, trehalose, valine and pyroglutamic acid as tolerance promoting metabolites (Teoh et al., 2016; Teoh et al., 2015). Metabolome studies have, furthermore, been applied to guide the optimization of important commercial amino acids, including L-methionine (Krömer et al., 2005; Krömer et al.,

2006a; Krömer et al., 2006b), L-valine and L-leucine (Magnus et al., 2006), and L-lysine (Krömer et al., 2004). In the heterologous pamamycin producing strain *S. albus* J1074/R2 that uses CoA thioesters as starter and extender units, metabolite profiling and subsequent strain engineering optimized pamamycin production (Gummerlich et al., 2021).

Finally, fluxomics yields the deepest insights into the cellular metabolism. It determines the *in vivo* rates of metabolic reactions using tracer substrates that are labelled with ^{13}C and ^{15}N, then determine the resulting labelling patterns in metabolite formed during the tracer cultivations, using LC-MS (Schwechheimer et al., 2018a; van Winden et al., 2005), GC-MS (Wittmann, 2007), and NMR (Pickford, 2019; Schwechheimer et al., 2018b). The obtained labelling pattern is then used to calculate the flux distribution within the cell, providing most valuable insights for strain engineering (Wittmann, 2007). Various success stories have highlighted ^{13}C metabolic flux analysis as guiding tool for strain engineering and the overproduction of multiple compounds (Becker et al., 2009; Becker et al., 2005; Becker et al., 2011; Hoffmann et al., 2018; Lange et al., 2017; Schwechheimer et al., 2018a).

In addition, strong efforts have enabled the tailormade genomic engineering of microbes (d'Espaux et al., 2017; Pontrelli et al., 2018), whereby the genetic toolbox is constantly expanding and has been extended and applied, e.g. to *Chlostridium* sp. for acetone and butanol production (Kim et al., 2015; Qi et al., 2018), *Corynebacterium glutamicum* for amino acid production (Becker et al., 2007; Becker et al., 2011; Hoffmann et al., 2018; Park et al., 2014), *Yarrowia lipolytica* for lipid and fatty acid production (Qiao et al., 2017; Sagnak et al., 2018), and actinomycetes for the synthesis of natural products (Tong et al., 2015). Further advances in synthetic biology meanwhile allow the optimized reconstruction of existing pathways and the design of novel pathways (Paddon et al., 2013).

Likewise, systems metabolic engineering has been successfully applied to *Streptomyces* sp. for improved production of natural products. GSMM of diverse *Streptomyces* species have been constructed to identify and engineer potential target genes, resulting in improved strains for the production of pikromycin (Cho et al., 2022), rapamycin (Dang et al., 2017), FK506 (Huang et al., 2013a; Huang et al., 2013b), and ascomycin (Wang et al., 2017). Furthermore,

based on GSMM, an optimized feeding strategy for improved daptomycin production in *S. roseosporus* could be established (Huang et al., 2011). The refactoring of the large daptomycin BGC, based on transcription level analysis and expression balancing resulted in significant increased lipopeptide titers (Ji et al., 2022). Similarly, combinatorial metabolic engineering by the introduction of a refactored second copy of the pristinamycin BGC and the systematic manipulation of cluster-situated regulatory genes improved production (Li et al., 2015). Genomic comparison of a randomly mutagenized milbemycin producing strain and its corresponding non-producing wild type, revealed target genes from primary metabolism that influenced milbemycin production. The combinatorial engineering of these genes increased the product titer significantly (Liu et al., 2021a). Another promising strategy is a semi-rational approach by combining random mutagenesis with resistance marker reporter system to select for strains with high expression levels of the BGC genes. By applying this strategy, natamycin production in *S. gilvosporeus* was improved more than 3-fold (Wang et al., 2016). Moreover, the industrial salinomycin producer strain *S. albus* S12 was further improved, and subsequent comparative transcriptome analysis unveiled insights into relevant metabolic pathways (Zhang et al., 2019).

2.4 Nybomycins – promising reverse antibiotics

Nybomycins, pyridoquinolinedione-based metabolites, were discovered in 1955 (Strelitz et al., 1955). To date, various *Streptomyces* from terrestrial soil e.g. *Streptomyces* sp. AD-3-6 (Wang et al., 2019b) or *Streptomyces hyalinum* (Komaki et al., 2020), marine sediments e.g. *Streptomyces albus* subsp. *chlorinus* (Rodriguez Estevez et al., 2018), *Streptomyces* sp. MS44 (Arai et al., 2015) but also *Streptomyces* sp. Pe6 from the body of the carpenter ant *Camponotus vagus* (Zakalyukina et al., 2019) are known to produce nybomycins. Unfortunately, the natural isolates form only traces of the products and often exhibit poor genetic accessibility so that their use makes microbial nybomycin synthesis inefficient. Chemical synthesis of nybomycin, although successfully demonstrated, suffers from inefficiency as well, due to the need for ten synthetic steps with very low overall yield (Bardell-Cox et al., 2019; Forbis and Rinehart, 1970; Forbis and Rinehart, 1971; Forbis and Rinehart, 1973). Various nybomycin analogues or structurally related compounds such as deoxynybomycin, deoxynyboquinone or nybomycin B-D have been identified, recently **(Figure 2)** (Wang et al., 2019b).

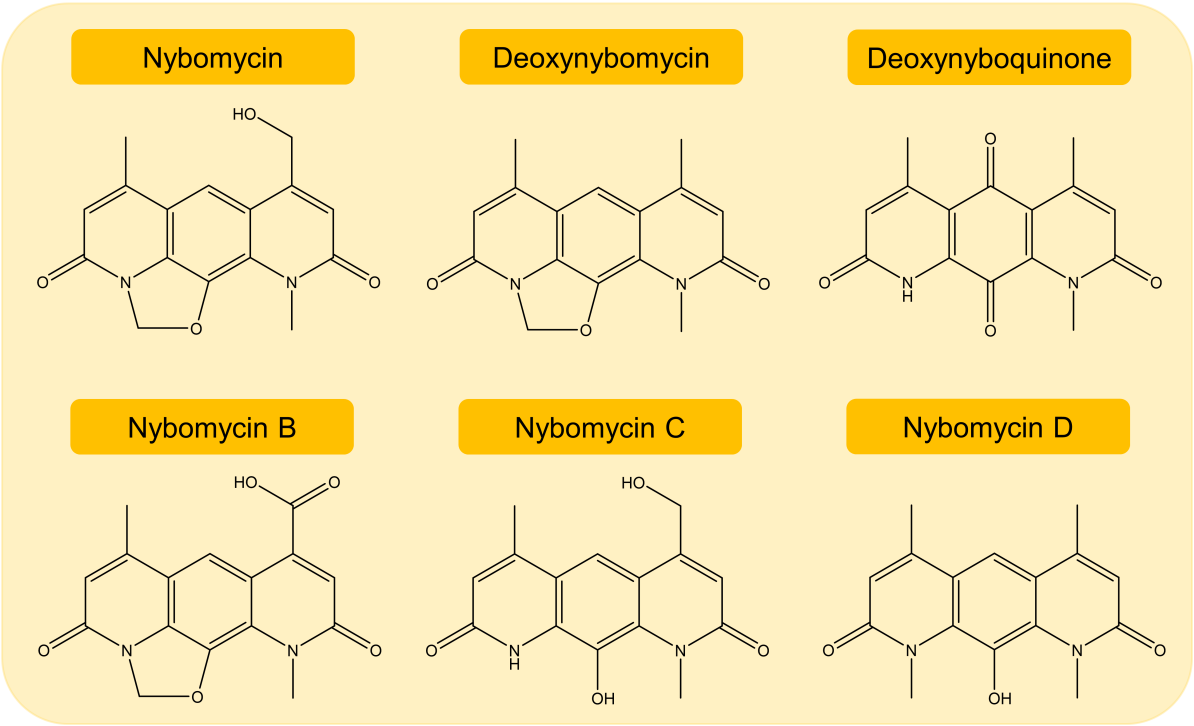

Figure 2: Nybomycin and its natural derivatives isolated from various *Streptomyces* species.

Initial investigations in 1955 with nybomycin revealed antiphage and antibacterial activity (Strelitz et al., 1955). Subsequent studies identified additional activity against Gram-positive *Mycobacterium smegmatis*, *Mycobacterium bovis* and *Mycobacterium tuberculosis* including clinically relevant strains under both aerobic and hypoxic conditions (Arai et al., 2015). Nybomycin treatment caused elongation of the cell bodies in *Mycobacterium sp*. that has been observed previously in mutants lacking genes involved in cell shape control and cell wall synthesis (Kang et al., 2005). Similarly, antibiotics acting on *E. coli* DNA replication and transcription such as nalidixic acid or ciprofloxacin also caused similar significant morphological changes (Nonejuie et al., 2013), allowing speculation that nybomycin might also target molecules involved in cell division or DNA replication and transcription. Further experiments confirmed this assumption by performing DNA binding assays, that revealed binding of nybomycin to plasmid DNA. These observations give evidence, that binding to genomic DNA of *Mycobacterium* sp. may be possible, causing inhibition of DNA replication and transcription, resulting in the described morphological changes and cell death (Arai et al., 2015). Altogether, nybomycin provides a new class of antibiotics for the potential treatment of Tuberculosis.

Furthermore, antibiotic activity was observed against Gram-positive clinically relevant quinolone-resistant *Staphylococcus aureus* (MRSA) strains possessing a S84L mutation in the *gyrA* gene, a type II topoisomerase that enables resistance to quinolone antibiotics, whereas strains with intact *gyrA* are not affected (Hiramatsu et al., 2012).

Topoisomerases represent a class of bacterial enzymes which are involved in genome maintenance and replication. They are classified as type I and type II topoisomerases, differing in the type of targeted DNA (single-strand DNA and double-strand DNA). DNA gyrase and topoisomerase IV, consisting of subunits $GyrA_2GyrB_2$ and $ParC_2ParE_2$ complexes, respectively, belong to the class type II topoisomerases, which are responsible for changes of the topological status of DNA during replication. Since DNA replication is an essential process in the cellular lifecycle, topoisomerases represent attractive targets for developing new antibiotics (Shiriaev et al., 2021). Quinolones represent a prominent class of antibiotics targeting bacterial topoisomerases (Chan et al., 2013). In general, quinolone antibiotics

capture bacterial DNA gyrase and topoisomerase IV by binding the enzyme-DNA complex, blocking subsequent ligation of the double strand break (Aldred et al., 2014; Drlica et al., 2009). The most common mechanism is binding of the quinolone to the serine residue of the *gyrA* subunit in the quinolone resistance-determining region via a hydrated magnesium ion bridge (Blower et al., 2016).

Quinolone-resistance is a frequent phenomenon that occurs when either one or both type II topoisomerase subunit genes (*parC* and *gyrA*) are mutated (Ferrero et al., 1994). However, Hiramatsu and co-workers found that nybomycin and deoxynybomycin only target mutated *gyrA* that comprised the substitution of serine by leucine at position 84 (Hiramatsu et al., 2012). Further investigations confirmed that the mutated ParC protein did not affect sensitivity to deoxynybomycin (Parkinson et al., 2015). Similarly, various microbes acquired quinolone-resistance by a mutated serine residue within the *gyrA* gene, as shown for *B. anthracis* (S85L) (Price et al., 2003), *E. coli* (S83L) (Vila et al., 1994), *A. baumannii* (S83L) (Vila et al., 1995), *Shigella sp*. (S83L) (Hirose et al., 2005; Mensa et al., 2008), vancomycin-resistant *Enterococcus* (S83I/R/Y) (Werner et al., 2010), *S. pneumoniae* (S81F/Y) (Bast et al., 2000), *K. pneumoniae* (S8F/Y) (Deguchi et al., 1997) and *N. gonorrhoeae* (S91F/Y) (Vernel-Pauillac et al., 2009).

Interestingly, the treatment of quinolone-resistant MRSA with nybomycin or deoxynybomycin results in very low numbers of survivors. Sequence analysis then revealed a backmutation in the *gyrA* gene, that made the mutants susceptible to quinolone antibiotics again. This feature of reversing resistance creates a new class of antibiotics termed `reverse antibiotics` **(Figure 3)** (Hiramatsu et al., 2012; Hiramatsu et al., 2015; Parkinson et al., 2015). Besides nybomycin, apigenin, a compound from the flavone class also exhibited reverse antibiotic activity against quinolone-resistant MRSA (Morimoto et al., 2015).

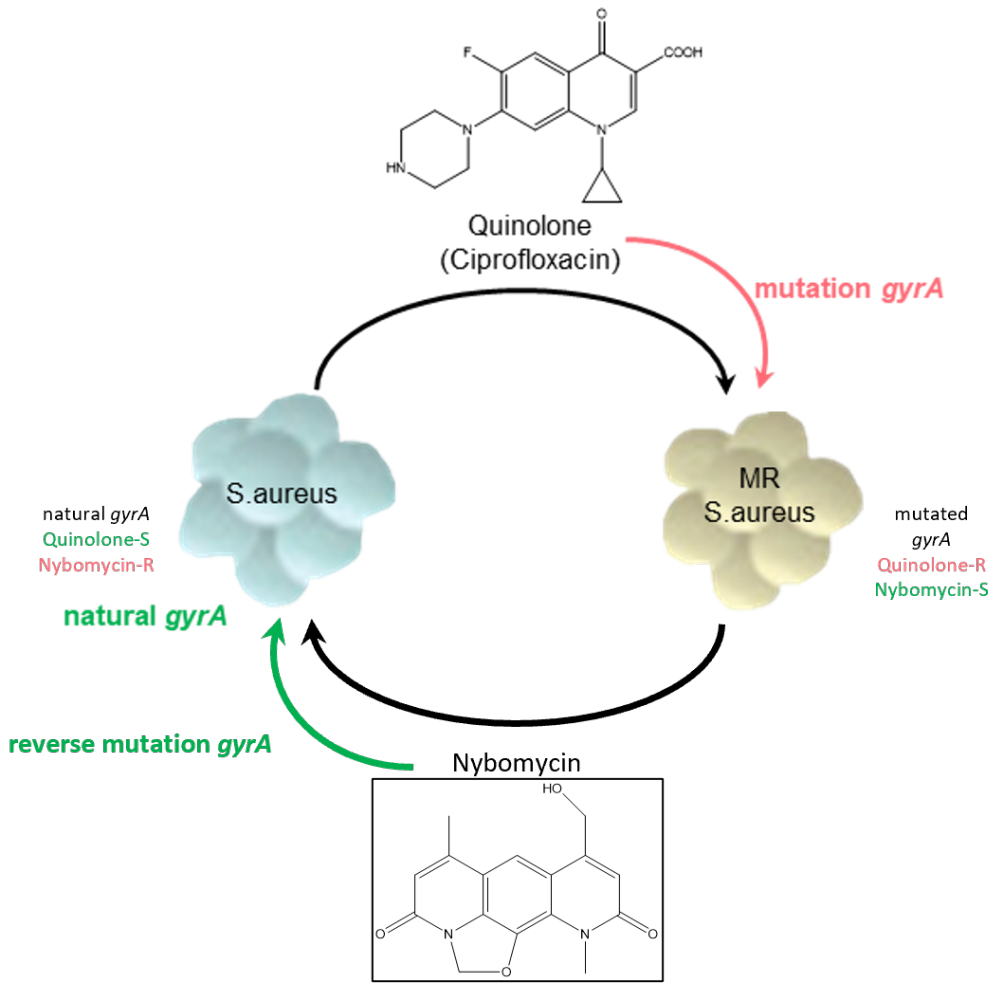

Figure 3: Nybomycin – the reverse antibiotic for quinolone resistance. Natural *S. aureus,* sensitive to quinolones and resistant to nybomycin, acquires a S84L mutation in gyrase A gene with high frequency (10^{-8}-10^{-9} (Parkinson et al., 2015)) upon quinolone treatment. Mutated *S. aureus* achieved quinolone resistance but becomes sensitive to nybomycin. Treatment with nybomycin reverses the mutation in *gyrA* with low frequency (10^{-10} (Parkinson et al., 2015)) making *S. aureus* susceptible to quinolone antibiotics again (Adapted from (Hiramatsu et al., 2015)

So far, little is known about the biological activity of nybomycin on Gram-negative microbes such as *E. coli*. The outer membrane of Gram-negative bacteria is difficult to be crossed by small molecules. Once entered through outer porins, small molecules are usually exported by efflux pumps (Richter et al., 2017). Initial results indicated activity of nybomycins against some of the tested *E. coli* strains (Strelitz et al., 1955). However, a later study did not observe activity of nybomycin on 14 tested *E. coli* isolates, likely due to an efflux pump that mediated resistance (Morimoto et al., 2013; Zakalyukina et al., 2019). This observation was confirmed by using a *E. coli* Δ*tolc* strain with increased permeability for antibiotics, that additionally acquired quinolone resistance by a mutation in *gyr*A (S83L or D87Y), by being sensitive to nybomycin

(Shiriaev et al., 2021). Interestingly, in contrast to *S. aureus*, the same *E. coli* strain with WT *gyrA*, was sensitive to nybomycin as observed for quinolone-resistance *E. coli*. The sensitivity of quinolone-sensitive and quinolone-resistant *E. coli* strains to nybomycin, might be due to preferential inhibition of topoisomerase IV rather than gyrase (Shiriaev et al., 2021). On the other hand, when testing the *E. coli* strain without increased permeability to antibiotics, deoxynybomycin poorly inhibited WT DNA gyrase *in vitro*, and in turn highly inhibited S83L mutated DNA gyrase, highlighting the importance of mutant DNA gyrase for sensitizing bacteria to deoxynybomycin (Parkinson et al., 2015).

Interestingly, the spheres of action of nybomycin and deoxynybomycin are not only limited to bacteria. Previous studies showed nybomycin toxicity against cancer cell lines A549 (human lung) and VA13 (lung fibroblast) (Zakalyukina et al., 2019). Furthermore, deoxynybomycin revealed selective growth inhibiting characteristics on cancer cell lines Saos-2 (human osteoblastic sarcoma), TMK-1 (gastric cancer) and THP-1 (monocytic leukemia), while survival of TIG-3 (normal human fibroblasts) was not affected (Egawa et al., 2000). Recent discovery of nybomycin analogues nybomycin D and deoxynyboquinone from *Streptomyces* sp. AD-3-6 reveal moderate and potent cytotoxicity against cancer cell lines A549 (human lung) and PC3 (human prostate), respectively (Wang et al., 2019b).

Deoxynybomycin selectively inhibits human topoisomerase I *in vitro,* whereas human topoisomerase II was not affected (Egawa et al., 2000). Moreover, human topoisomerase II was shown to be not significantly affected by a deoxynybomycin derivative *in vitro* (Hergenrother and Riley, 2022; Parkinson et al., 2015). In contrast, Shiriaev and colleagues propose the cytotoxic effect of nybomycin and derivatives caused by inhibition of human topoisomerase II, arguing with the protein sequence homology to bacterial GyrA at relevant positions (Shiriaev et al., 2021).

In preliminary toxicity tests, nybomycin was well tolerated by mice (Strelitz et al., 1955). Red blood cells did not show haemolysis, once treated with deoxynybomycin and derivatives (Parkinson et al., 2015) as observed for human fibroblasts (Egawa et al., 2000), suggesting that these compounds may be well-tolerated. Pharmakokinetic studies showed improved bioavailability of chemically modified deoxynybomycin derivatives whose 10-day oral

administration to mice revealed no serious symptoms. Furthermore, mice infected with quinolone resistant MRSA that were treated with the deoxynybomycin derivative, showed significantly increased survival rates (Parkinson et al., 2015).

2.4.1 Biosynthetic gene cluster and nybomycin biosynthesis

The nybomycin biosynthetic gene cluster was discovered in the marine strain *Streptomyces albus* subsp. *chlorinus* NRRL B-24108. A 36 kb DNA fragment containing the required set of genes for nybomycin biosynthesis represents 33 open reading frames **(Figure 6AB)** (Rodriguez Estevez et al., 2018). Structurally, the nybomycin core body shows similarity to streptonigrin, an antitumor antibiotic. Furthermore, nine open reading frames (*nybA* to *nybF* and *nybN* to *nybP*) reveal similarities on protein level.

In parallel to this work, the minimal nybomycin gene cluster required for full synthesis has been recently identified to include the reading frames *orf-02* to *nybT*. Interestingly, deletion of *orf-02*, possibly encoding a putative transposase and an endonuclease domain, abolished nybomycin production (personal communication, Marta Rodriguez Estevez, Andriy Luzhetskyy, Pharmaceutical Biotechnology, Saarland University). Further downstream, *nybT* turned out to be essential **(Figure 5A)**, resulting in a minimal set of genes required for nybomycin biosynthesis from *orf-02* to *nybT* **(Figure 5B)**.

A

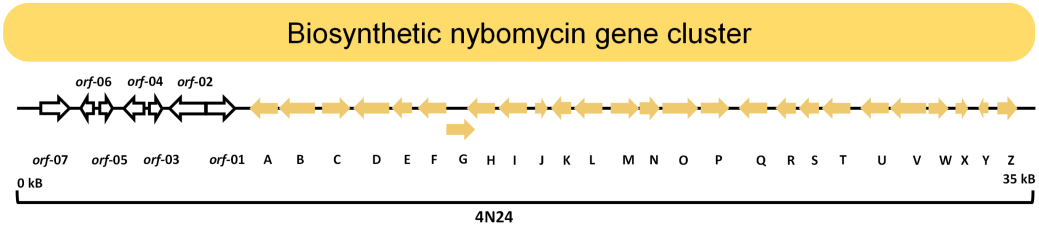

B

Gene	Proposed function
orf-07	Streptomycin 3”-adenyltransferase
orf-06	Hypothetical protein
orf-05	ATP-binding protein
orf-04	Hypothetical protein
orf-03	Hypothetical protein
orf-02	Hypothetical protein
orf-01	Hypothetical protein
nybA	3-carboxy-cis,cis-muconate cycloisomerase
nybB	FAD-binding protein
nybC	NADPH:quinone reductase
nybD	Anthranilate synthase
nybE	Isochorismatase
nybF	DAHP synthase
nybG	Hypothetical protein
nybH	Vicinal oxygen chelate protein
nybI	NAD(P)H:dehydrogenase
nybJ	Hypothetical protein
nybK	N-acetyltransferase
nybL	Aminohydrolase
nybM	Acetoacetyl-CoA synthetase
nybN	Aromatase/cyclase
nybO	Long-chain acyl-CoA synthetase
nybP	Salicylase hydroxylase
nybQ	Hypothetical protein
nybR	NAD-dependent epimerase
nybS	SAM-dependent methyltransferase
nybT	Isopenicilliin N synthase family oxygenase
nybU	Isopenicilliin N synthase family oxygenase
nybV	MFS transporter
nybW	Transcriptional regulator
nybX	Transcriptional regulator
nybY	Hypothetical protein
nybZ	Transcriptional regulator

Figure 4: Genetic organization of the nybomycin biosynthetic gene cluster in BAC 4N24. Genomic DNA fragment of *S. albus* subsp. *chlorinus* (A). Predicted genes and proposed function of the correlating gene products (B)

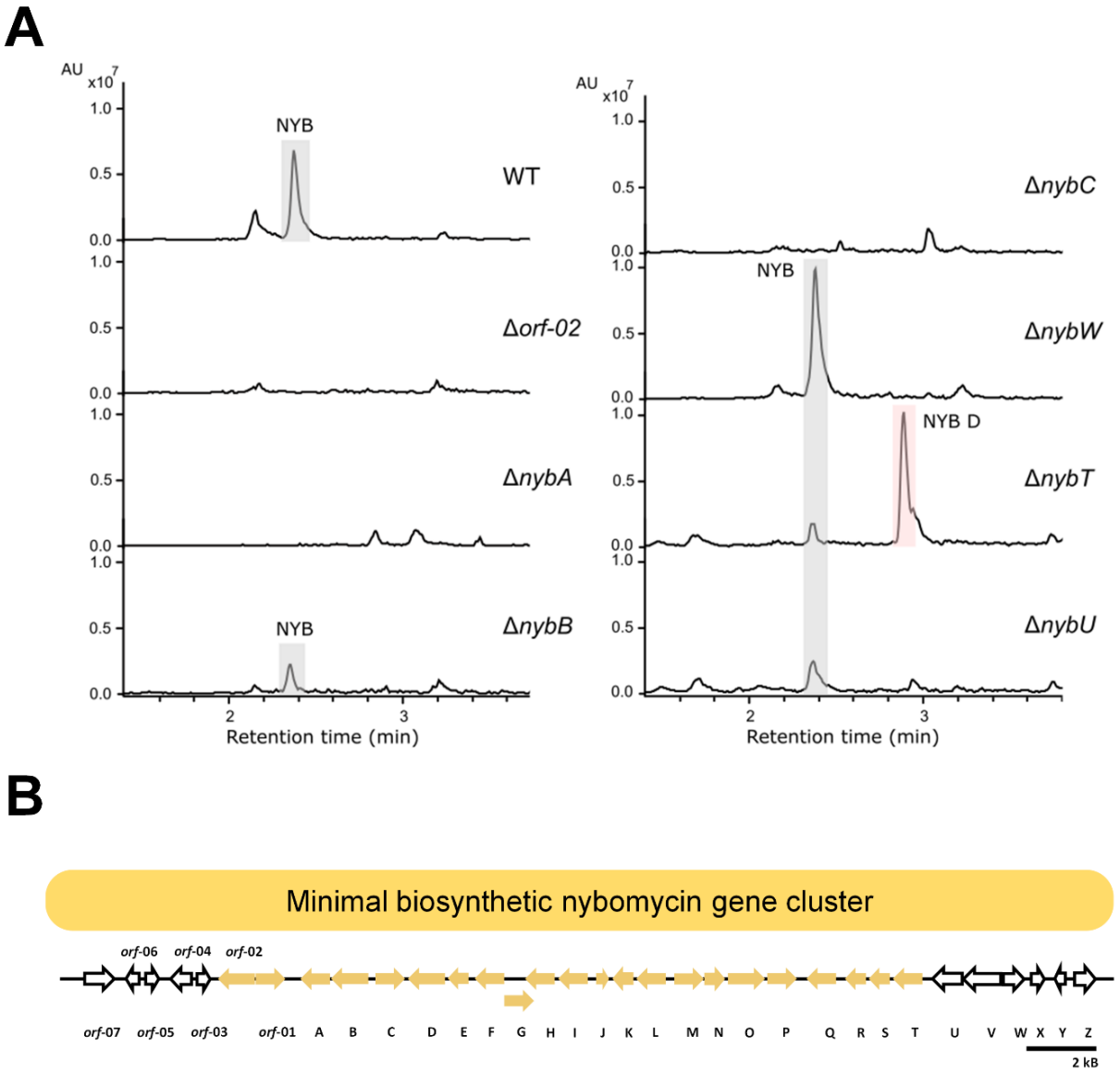

Figure 5: Characterization of the nybomycin BGC for identification of the minimal set of genes required. LC-MS analysis of cultivation extracts from *S. albus* 4N24 (WT) and the single gene deletion mutants *Δorf-02*, Δ*nybA*, Δ*nybB*, Δ*nybC*, Δ*nybW*, Δ*nybT*, and Δ*nybU.* Extracted chromatogram of *m/z* 299.10 ±0.1 Da (nybomycin) and m/z *285*.1 ±0.1 Da (intermediate)(A). Minimal nybomycin gene cluster. The genes from *orf-02* to *nybT* are essential for nybomycin biosynthesis, while the neighbored genes do not participate in the biosynthetic pathway (B).

Biochemically, erythrose 4-phosphate and phosphoenolpyruvate, supplied from the pentose phosphate (PP) and the Embden–Meyerhof–Parnas (EMP) pathways, respectively, are fused to 3-deoxy-D-arabino-hept-2-ulosonate 7-phosphate (DAHP). The reaction is catalyzed by 3-deoxy-D-arabinoheptulosonate 7-phosphate (DAHP) synthase encoded by *nybF*, XNR_0595, and XNR_4763. Subsequently, shikimic acid and chorismic acid are generated by mainly endogenous aromatic amino acid biosynthesis enzymes (AroABCEKQ) (Euverink, 1995; Parthasarathy et al., 2018). Similarly, chorismic acid serves as intermediate metabolite in biosynthesis of biologically active natural product, e.g. chloramphenicol (Vitayakritsirikul et al., 2016), anticapsin (Euverink, 1995), thermorubin (McCord et al., 2022), FK506 (Huang et al., 2013a), FK520 (Andexer et al., 2011), rapamycin (Andexer et al., 2011), unantimycins (Shen et al., 2020) and stravidins (Montaser and Kelleher, 2020). Further conversion of chorismic acid into the nybomycin core structure 4-aminoanthranilic acid (Gould and Erickson, 1988), is catalyzed by the gene products of *nybC*, *nybD*, *nybE, nybL* (Rodriguez Estevez et al., 2018). Hydroxylation, catalyzed by NybP and decarboxylation yields 2,6-diaminophenol. Catalyzed by the gene product of *nybK*, the aromatic ring is extended by the attachment of two acetoacetyl-CoA molecules to the amino groups, supplied by fusion of acetyl-CoA and malonyl-CoA catalyzed by NybM, from the ethylmalonyl-CoA pathway, following closure of the pyridine rings, yields intermediate 1, and methylation of the two nitrogen atoms, yielding intermediate 2, also known as Nybomycin D (Wang et al., 2019b). Subsequent formation of an oxazoline ring catalyzed by NybT or NybU provides deoxynybomycin following by final hydroxylation by NybB to yield nybomycin that is exported into the extracellular space by NybV (Rodriguez Estevez et al., 2018).

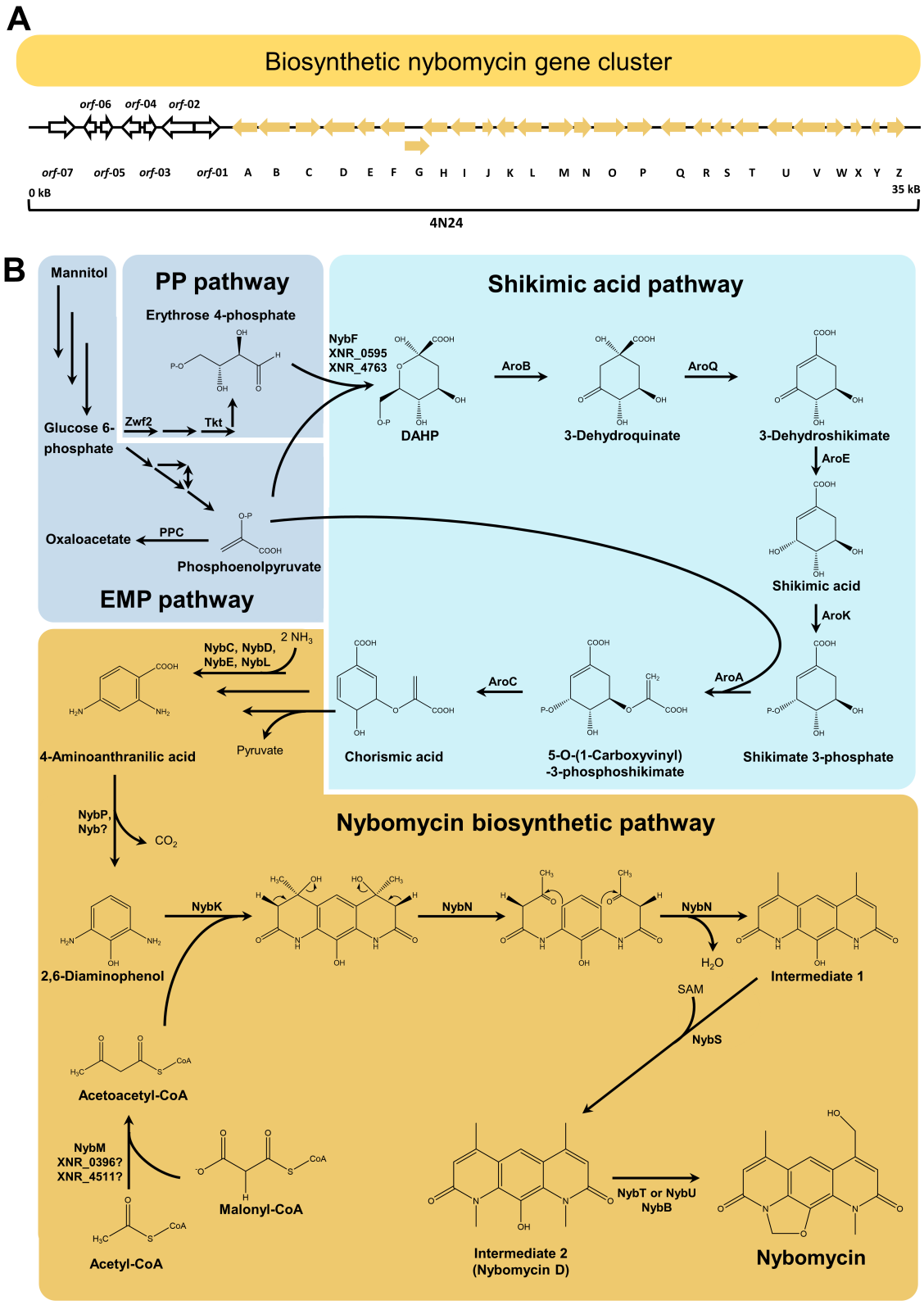

Figure 6: Pathway for biosynthesis of nybomycin in *S. albus* 4N24. Erythrose 4-phosphate and phosphoenolpyruvate are supplied from the PP and the EMP pathway to yield shikimic acid and chorismic acid, mainly via endogenous aromatic amino acid biosynthesis (AroABCEKQ) (Euverink, 1995; Parthasarathy et al., 2018). Further conversion into 4-aminoanthranilic acid is encoded by the genes *nybC, nybD, nybE*, and *nybL* following formation of 2,6-diaminophenol catalyzed by NybP. Next, the aromatic ring is extended by the attachment of two acetoacetyl-CoA molecules, supplied from the ethylmalonyl-CoA pathway, followed by closure of the pyridine rings, yielding intermediate 1, and methylation of the two nitrogen atoms, yielding intermediate 2. Subsequent formation of an oxazoline ring provides deoxynybomycin which is followed by final hydroxylation to yield nybomycin that is exported by NybV (Adapted from Rodriguez Estevez et al., 2018)

3 Materials and Methods

3.1 Bacterial strains and plasmids

S. albus Del14 and S. *albus* 4N24 were obtained from previous work (Rodriguez Estevez et al., 2018). *Streptomyces* sp. GBA 94-10 (Ian et al., 2014) and the heterologous nybomycin producers *Streptomyces* sp. GBA 94-10_4N24 and *Streptomyces* sp. Lv1-4_4N24 were kindly donated by Andriy Luzhetskyy (Pharmaceutical Biotechnology, Saarland University). *E. coli* DH10B was used for general cloning purposes (Thermo Fisher Scientific, Karlsruhe, Germany). *E. coli* ET12567/pUZ8002 served as donor for intergenic conjugation (Kieser et al., 2000). All strains and plasmids used in this study are listed in Table 2 and were kept as glycerol stocks at -80 °C.

Table 2: Bacterial strains and plasmids used in this work

Strains/Plasmids	Description	Reference
Strains		
E. coli		
DH10B	F– mcrA Δ(mrr-hsdRMS-mcrBC) φ80lacZΔM15 ΔlacX74 recA1 endA1 araD139 Δ (ara-leu)7697 galU galK λ– rpsL(StrR) nupG	Thermo Fisher Scientific
ET12567/pUZ8002	Non-methylating ET12567 containing non-transmissible RP4 derivative plasmid pUZ8002, Cm^R, Kan^R	(Kieser et al., 2000)
Streptomyces albus		
Del14 4N24	Del14 expressing BAC 4N24 for heterologous nybomycin production	(Rodriguez Estevez et al., 2018)
NYB-1A	Del14 4N24 expressing *tkt* (B591 RS24355) from *S. albus* sp. GBA 94-10 under control of P_{ermE*}	This work
NYB-1B	Del14 4N24 expressing *zwf2* (B591 RS24345) from *S. albus* sp. GBA 94-10 under control of P_{ermE*}	This work
NYB-1C	Del14 4N24 expressing *aro* I (NCgl0950) with the amino acid exchange S187C from *C. glutamicum* ATCC 13032 under control of P_{ermE*}	This work
NYB-2A	Del14 4N24 expressing *tkt* (B591_RS24355) from *S. albus* sp. GBA 94-10 under control of P_{kasOP*}	This work
NYB-2B	Del14 4N24 expressing *zwf2* (B591_RS24345) from *S. albus* sp. GBA 94-10 under control of P_{kasOP*}	This work

NYB-2C	Del14 4N24 with in-frame deletion of *ppc* (XNR 2069)	This work
NYB-2D	Del14 4N24 expressing *aroG* (P0AB91) with the amino acid exchange D146N from *E. coli* K12 under control of P_{kasOP*}	This work
NYB-2E	Del14 4N24 expressing *aro* I (NCgl0950) with the amino acid exchange S187C from *C. glutamicum* ATCC 13032 under control of P_{kasOP*}	This work
NYB-2F	Del14 4N24 expressing *nybF* (FM076 RS29120) from *S. albus* subsp. *chlorinus* NRRL B-24108 under control of P_{kasOP*}	This work
NYB-3A	Del14 4N24 expressing *nybM* (FM076 RS29150) from *S. albus* subsp. *chlorinus* NRRL B-24108 under control of P_{kasOP*}	This work
NYB-3B	Del14 4N24 expressing *nybV* (FM076 RS2919) from *S. albus* subsp. *chlorinus* NRRL B-24108 under control of P_{kasOP*}	This work
NYB-4A	Del14 4N24 expressing *tkt* (B591 RS24355) and *zwf2* (B591 RS24345) from *S. albus* sp. GBA 94-10 under control of P_{kasOP*}	This work
NYB-4B	Del14 4N24 expressing *nybF* (FM076 RS29120) from *S. albus* subsp. *chlorinus* NRRL B-24108 and *zwf2* (B591 RS24345) from *S. albus* sp. GBA 94-10) under control of P_{kasOP*}	This work
NYB-4C	Del14 4N24 expressing *nybF* (FM076 RS29120) from *S. albus* subsp. *chlorinus* NRRL B-24108 and *tkt* (B591 RS24355) from *S. albus* sp. GBA 94-10 under control of P_{kasOP*}	This work
NYB-4D	Del14 4N24 expressing *nybF* (FM076 RS29120) from *S. albus* subsp. *chlorinus* NRRL B-24108, *tkt* (B591 RS24355), and *zwf2* (B591 RS24345) from *S. albus* sp. GBA 94-10 under control of P_{kasOP*}	This work
NYB-5	Del14 4N24 with in-frame deletion of *nybW*	This work
NYB-6A	NYB-5 expressing *tkt* (B591 RS24355) and *zwf2* (B591 RS24345) from *S. albus* sp. GBA 94-10 under control of P_{kasOP*}	This work
NYB-6B	NYB-5 expressing *nybF* (FM076 RS29120) from *S. albus* subsp. *chlorinus* NRRL B-24108 and *zwf2* (B591 RS24345) from *S. albus* sp. GBA 94-10 under control of P_{kasOP*}	This work
NYB-6C	NYB-5 expressing *nybF* (FM076 RS29120) from *S. albus* subsp. *chlorinus* NRRL B-24108 and *tkt* (B591 RS24355) from *S. albus* sp. GBA 94-10 under control of P_{kasOP*}	This work
NYB-7	NYB-5 expressing *nybF* (FM076_RS29120) from *S. albus* subsp. *chlorinus* strain NRRL B-24108, and *tkt* (B591_RS24355) and *zwf2* (B591_RS24345) from *S. albus* sp. GBA 94-10 under control of P_{kasOP*}	This work

NYB-8	Del14 4N24 with in-frame deletion of *nybWX* replaced by kanamycin resistance gene	This work
NYB-9	Del14 4N24 with in-frame deletion of *nybWXYZ* replaced by kanamycin resistance gene	This work
NYB-10	NYB-8 expressing *nybF* (FM076 RS29120) from *S. albus* subsp. *chlorinus* NRRL B-24108 and *zwf2* (B591 RS24345) from *S. albus* sp. GBA 94-10 under control of P_{kasOP*}	This work
NYB-11	NYB-9 expressing *nybF* (FM076 RS29120) from *S. albus* subsp. *chlorinus* NRRL B-24108 and *zwf2* (B591 RS24345) from *S. albus* sp. GBA 94-10 under control of P_{kasOP*}	This work
Streptomyces sp. Lv1-4		
Lv1-4_4N24	Lv1-4 expressing BAC 4N24 for heterologous nybomycin production	Andriy Luzhetskyy, (Saarland University)
NYB-12A	Lv1-4_4N24 with in-frame deletion of *nybW*	This work
NYB-12B	NYB-12A expressing *nybF* (FM076 RS29120) from *S. albus* subsp. *chlorinus* NRRL B-24108 and *zwf2* (B591 RS24345) from *S. albus* sp. GBA 94-10 under control of P_{kasOP*}	This work
Streptomyces albus sp. GBA 94-10		
GBA 94-10		(Ian et al., 2014)
GBA 94-10_4N24	GBA 94-10 expressing BAC 4N24 for heterologous nybomycin production	Andriy Luzhetskyy, (Saarland University)
Streptomyces albus reporter strains		
RFP-1	Del14 4N24 expressing *mCherry* under control of P_{ermE*}	This work
RFP-2	Del14 4N24 expressing *mCherry* under control of P_{tipA}	This work
RFP-3	Del14 4N24 expressing *mCherry* under control of P_{SF14}	This work
RFP-4	Del14 4N24 expressing *mCherry* under control of P_{21}	This work
RFP-5	Del14 4N24 expressing *mCherry* under control of P_{SP43}	This work
RFP-6	Del14 4N24 expressing *mCherry* under control of P_{SP44}	This work
RFP-7	Del14 4N24 expressing *mCherry* under control of P_{kasOP*}	This work
RFP-8	Del14 4N24 expressing *mCherry* under control of P_{SP41}	This work

Plasmids/BACs		
4N24	BAC containing the full nybomycin biosynthetic gene cluster	(Rodriguez Estevez et al., 2018)
4N24 Δ*nybW*	4N24 with in-frame deletion of *nybW* (FM076 RS29200)	Andriy Luzhetskyy, (Saarland University)
4N24 Δ*nybWX_Kan*	4N24with in-frame deletion of *nybW* (FM076 RS29200), *nybX* (FM076_RS29205) replaced by kanamycin resistance gene	This work
4N24 Δ*nybWXYZ_Kan*	4N24with in-frame deletion of *nybW* (FM076 RS29200), *nybX* (FM076_RS29205), *nybY* (FM076_RS29210), *nybZ* (FM076_RS29215) replaced by kanamycin resistance gene	This work
pRT801	Integrative plasmid containing *oriT*, *attP*, *int* phiBT1, and *aac3(IV)* gene	This work
pKG1132	Suicide vector for genome-based modification of *actinobacteria*, comprising *ori* for *E. coli*, and Am^R and *gusA* gene as selection marker	(Barton et al., 2018)
pKG1132hyg	Suicide vector for genome-based modification of *actinobacteria*, comprising *ori* for *E. coli*, and Am^R and *gusA* gene as selection marker	(Gläser et al., 2021)
pDppc4	Suicide vector derivative of pKG1132hyg for in-frame deletion of gene XNR 2069 in 4N24	This work
pBT1H	Integrative plasmid containing *oriT*, *attP*, *int* phiBT1, *hph*,	This work
pBT1HP	Integrative plasmid containing *oriT*, *attP*, *int* phiBT1, *hph*, P_{ermE*}, *tfd*	This work
pBT1H-*tkt*1	integrative plasmid containing P_{ermE*}, *tkt*, HygR	This work
pBT1H-*zwf*2	integrative plasmid containing P_{ermE*}, *zwf2*, HygR	This work
pBT1HP-*aro*lfbr	integrative plasmid containing P_{ermE*}, *aro*lfbr, HygR	This work
pBT1HP-er*mCherry*	integrative plasmid containing P_{ermE*}, *mCherry*, Hyg^R	This work
pBT1H-kasOP*-mCherry	integrative plasmid containing P_{kasOP*}, *mCherry*, Hyg^R	This work
pBT1H-P21-mCherry	integrative plasmid containing P_{21}, *mCherry*, Hyg^R	This work
pBT1H-PtipA-mCherry	integrative plasmid containing P_{tipA}, *mCherry*, Hyg^R	This work
pBT1H-SF14P-mCherry	integrative plasmid containing P_{SF14}, *mCherry*, Hyg^R	This work
pBT1H-SP41-mCherry	integrative plasmid containing P_{SP41}, *mCherry*, Hyg^R	This work

pBT1H-SP43-mCherry	integrative plasmid containing P_{SP43}, *mCherry*, Hyg^R	This work
pBT1H-SP44-mCherry	integrative plasmid containing P_{SP44}, *mCherry*, Hyg^R	This work
pBT1H-kasOP*-tkt	integrative plasmid containing P_{kasOP*}, *tkt*, Hyg^R	This work
pBT1H-kasOP*-zwf2	integrative plasmid containing P_{kasOP*}, *zwf*2, Hyg^R	This work
pBT1H-kasOP*-nybV	integrative plasmid containing P_{kasOP*}, *nybV*, Hyg^R	This work
pBT1H-kasOP*-nybM	integrative plasmid containing P_{kasOP*}, *nybM*, Hyg^R	This work
pBT1H-pkasOP*-nybF	integrative plasmid containing P_{kasOP*}, *nybF*, Hyg^R	This work
pBT1H-*kasOP**-*aroG*fbr	integrative plasmid containing P_{kasOP*}, *aroG*fbr, Hyg^R	This work
pBT1H-*kasOP**-*aroI*fbr	integrative plasmid containing P_{kasOP*}, *aroI*fbr, Hyg^R	This work
pBT1H-kasOP*-nybF-zwf2	integrative plasmid containing P_{kasOP*}, *nybF*, *zwf*2, Hyg^R	This work
pBT1H-kasOP*-nybF-tkt	integrative plasmid containing P_{kasOP*}, *nybF*, *tkt*, Hyg^R	This work
pBT1H-kasOP*-tkt-zwf2	integrative plasmid containing P_{kasOP*}, *tkt*, *zwf*, Hyg^R	This work
pBT1H-kasOP*-nybF-tkt-zwf2	integrative plasmid containing P_{kasOP*}, *nybF*, *tkt*, *zwf2*, Hyg^R	This work

3.2 Molecular biology and genetic engineering

The software SnapGene (GSL Biotech LLC, San Diego, USA) was used for strain, plasmid, and primer design, respectively. DNA fragments of interest were amplified by PCR (2× Phusion High-Fidelity PCR Master Mix with GC Buffer, Thermo Scientific, Waltham, MA, USA) using sequence specific primers **(Appendix, Table 7).** Prior to assembly, the amplified fragments were extended with 20bp overhangs at their 5´-end. Afterwards, they were purified (Wizard SV Gel, PCR Clean-Up System, Promega, Mannheim, Germany) following *in vitro* assembly with the linearized vector, obtained by treatment with endonucleases leaving blunt ends (*Eco*RV, *Sna*BI, *Pvu*II) and alkaline phosphatase. The Gibson assembly reaction mix contained 157.5 mM Tris·HCl (pH 7.5), 15.75 mM of $MgCl_2$, 15.75 mM of DTT, 42 mg μL^{-1} of PEG-800, 0.6 mg μL^{-1} of NAD, 25 mU μL^{-1} of Phusion High-Fidelity DNA Polymerase (Thermo Fisher Scientific), 7.5 mU μL^{-1} T5 exonuclease (Epicentre, Madison, USA), 4 U μL^{-1} Taq Ligase (Thermo Fisher Scientific), and 0.3 mM dNTPs. The assembled plasmids were transferred into *E. coli* DH10B cells by heat shock (Sambrook and Russell, 2001), followed by selection. Subsequently, the plasmids were multiplied in the cloning host, isolated (QIAprep Spin MiniPrep Kit, Qiagen, Hilden, Germany), and verified for correctness by PCR, restriction digestion, and sequencing (Genewiz Germany GmbH, Leipzig, Germany). Afterwards, they were transferred into the methylation-deficient donor *E. coli* ET12567/pUZ8002 and subsequently transferred into *Streptomyces* by intergenic conjugation (Kieser et al., 2000). In short, *Streptomyces* spores, obtained from four-day old mannitol soy (MS) agar plates, were washed off using sterile water, mixed with *E. coli* ET12567/pUZ8002 (containing the recombinant plasmid of interest) and plated on fresh MS agar. After incubation for 16h at 30°C, the plates were overlayed with phosphomycin (200 µg mL^{-1}) and hygromycin (50 µg mL^{-1}). Exconjugants were passaged to fresh MS plates, again containing phosphomycin and hygromycin. The desired genomic integration of the DNA was verified by PCR and sequencing. Integrase-mediated site-specific recombination using *phiBT1* integrase and its associated *attP* attachment site was used to integrate the expression plasmids into gene XNR_3921 (integral membrane protein) within the genome of *S. albus (Gregory et al., 2003)*. When using suicide plasmids for in-frame gene deletion, 3 µL X-Gluc (100 mg mL^{-1}) was sprinkled onto spores, followed incubation for 20-30

min at 30°C, to evaluate for blue coloration. Blue-stained exconjugants, that had undergone a single crossover were passaged on MS agar without selection pressure, washed off, diluted serially, and plated on MS agar supplemented with X-Gluc (40 µg mL^{-1}) to screen for white colonies that had undergone the second crossover. White colonies were analyzed by PCR to differentiate between the desired mutant and the reverted wild type. For gene deletions within the nybomycin cluster, the gene of interest was individually substituted via Red/ET recombineering for a resistance marker which was later removed, and the resulting knock-out BAC variants were introduced in *S. albus* Del14 via conjugation (Myronovskyi et al., 2018).

3.3 Growth media

E. coli strains were cultured in liquid LB medium. Solid LB medium was obtained by adding 20 g L^{-1} of agar (Becton Dickinson, Heidelberg, Germany). For sporulation, *Streptomyces* strains were grown on MS agar, containing per liter: 20 g of D-mannitol (Sigma Aldrich, Taufkirchen, Germany), 20 g of soy flour (Schoenenberger Hensel, Magstadt, Germany), and 20 g of agar (Becton Dickinson). Where required, kanamycin (50 µg mL^{-1}), hygromycin B (50 µg mL^{-1} for *Streptomyces*, 100 µg mL^{-1} for *E. coli*), and apramycin (50 µg mL^{-1}) were supplemented for selection. When using suicide vectors for gene deletions, 5-bromo-4-chloro-1H-indol-3-yl β-D-glucopyranosiduronic acid (X-Gluc, 40 µg mL^{-1}) was added to the LB plate medium for blue-white screening.

For nybomycin production, strains were pre-cultured in liquid ISP medium (pH 7.2) containing per liter: 3 g of yeast extract (Beckton Dickinson) and 5 g of tryptone (Beckton Dickinson). For secondary metabolite expression and *nyb* cluster characterization, *Streptomyces* strains were grown in liquid DNPM medium (40 g L^{-1} dextrin, 7.5 g L^{-1} soytone, 5 g L^{-1} baking yeast, and 21 g L^{-1} MOPS, pH 6.8). Main cultures to overproduce nybomycin were grown in chemically defined minimal medium (MMM) containing per liter: 10 g of D-mannitol, 15 g of $(NH_4)_2SO_4$, 20.9 g of MOPS, 0.5 g of K_2HPO_4, 1 g of NaCl, 0.55 g of $CaCl_2$, 0.2 g of $MgSO_4 \cdot 7H_2O$, 0.02 g of $FeSO_4 \cdot 7H_2O$, 2 mg of $FeCl_3 \cdot 6H_2O$, 2 mg of MnSO4·H_2O, 0.5 mg of ZnSO4·H_2O, 0.5 mg of $CuCl_2 \cdot 2H_2O$, 0.2 mg of $Na_2B_4O_7 \cdot 10H_2O$, 0.1 mg of $(NH_4)6Mo_7O_{24} \cdot 4H_2O$, 1 mg of nicotinamide, 1 mg of riboflavin, 0.5 mg of thiamine hydrochloride, 0.5 mg of pyridoxine hydrochloride, 0.2 mg of biotin and 0.1 mg of p-aminobenzoic acid. An adapted defined minimal medium (MM#2) was used for nybomycin production in strain Lv1-4 background containing per liter: 10 g of D-mannitol, 7 g of $(NH_4)_2SO_4$, 20.9 g of MOPS, 0.5 g of K_2HPO_4, 1 g of NaCl, 0.55 g of $CaCl_2$, 0.2 g of $MgSO_4 \cdot 7H_2O$, 4 mg of thiamine hydrochloride, 4 mg of pyridoxine hydrochloride, 10 mg of biotin, 40 mg of Inositol and 8 mg of pantothenic acid. Additionally, for nybomycin production, DNPM with 40g L^{-1} and DNPM with 75 g L^{-1} Dextrin was used, respectively.

3.4 Cultivation

3.4.1 Nybomycin production in shake flasks

Liquid cultures were incubated in 500 mL baffled shake flasks (10% filing volume) on an orbital shaker at 230 rpm, 75% relative humidity, and 28 °C (5 cm shaking diameter, Multitron, Infors AG, Bottmingen, Switzerland). The medium was supplemented with 30 g glass beads (soda-lime glass, 5 mm, Sigma-Aldrich). Spores from a single colony grown for 3-5 days on MS agar plates were harvested and inoculated to the first pre-culture on ISP medium which was incubated overnight. Then, cells were collected (5,000 x *g*, 25 °C, 6 min) and resuspended in minimal or complex medium for the second pre-culture, following again incubation overnight. Again, cells were collected (5,000 x *g*, 25 °C, 6 min) and used to inoculate the main culture, again in minimal or complex medium, as described below. All growth and production experiments were conducted as biological triplicate.

3.4.2 Strain screening at miniaturized scale

For screening experiments, the first and the second pre-culture were conducted in shake flasks, as described in chapter 3.4.1. For the screening, a microplate-based microbioreactor was used (Biolector I, Beckman Coulter GmbH, Baesweiler, Germany). The main cultivation was conducted in 48-well flower plates with photometric on-line monitoring of the cell concentration (OD_{620}) (1,300 rpm, 28°C, 80% relative humidity). Each well was filled with 1 mL minimal mannitol medium. All experiments were conducted as triplicate.

3.5 Analytical methods

3.5.1 Quantification of cell concentration

Measuring optical density (OD) at a certain wavelength is a quick and commonly used method to follow growth during cultivation. However, OD measurements show some drawbacks such as morphological changes of the cells, saturation at high cell concentrations or the influence by ambient light (Boss et al., 2018). Additionally, many analyses are normalized to cell dry weight (CDW). Indeed, it is possible to measure CDW whenever required during a culture process. However, it is much easier to determine a correlation factor between OD_{600} and CDW once, to apply it in future cases. It is noteworthy, that such correlation factors only apply for the used optical device, organism and medium. The correlation factor in minimal medium using mannitol as carbon source is shown in **Table 3** and **Figure 7**.

In this regard, cells were collected from broth by centrifugation (5,000 x *g*, 4 °C, 6 min) and washed twice with 0.9% NaCl. Subsequently, the pellets were freeze-dried, and the cell dry weight (CDW) was gravimetrically measured (HB43-S, Mettler-Toledo, Columbus, OH, USA) (Kuhl et al., 2020). In addition, the cell concentration was analysed as optical density (OD_{600}) at a wavelength of 600 nm. Systematic analysis of strains *S. albus* 4N24, Lv1-4_4N24 and GBA 94-10_4N24 cultures yielded linear correlations between CDW and OD_{600} (Kuhl et al., 2020). Measurements were conducted in triplicate.

Table 3: OD – CDW correlation factors for heterologous nybomycin producer strains and applicability

Strain	OD – CDW correlation factor	Applicability
S. albus 4N24	CDW [g L^{-1}] = 0.438 × OD_{600}	growth and stationary phase
Lv1-4_4N24	CDW [g L^{-1}] = 0.658 × OD_{600}	growth phase
94-10_4N24	CDW [g L^{-1}] = 0.453 × OD_{600}	growth and stationary phase

Interestingly, this factor is applicable for growth and stationary phase for strains *S. albus* 4N24 and 94-10_4N24, even though the culture and cells apparently change their viscosity, density, and morphology. Hence, these correlations are usually applicable in growth phase only (Gläser et al., 2021; Kuhl et al., 2020), as it was observed for strain Lv1-4_4N24.

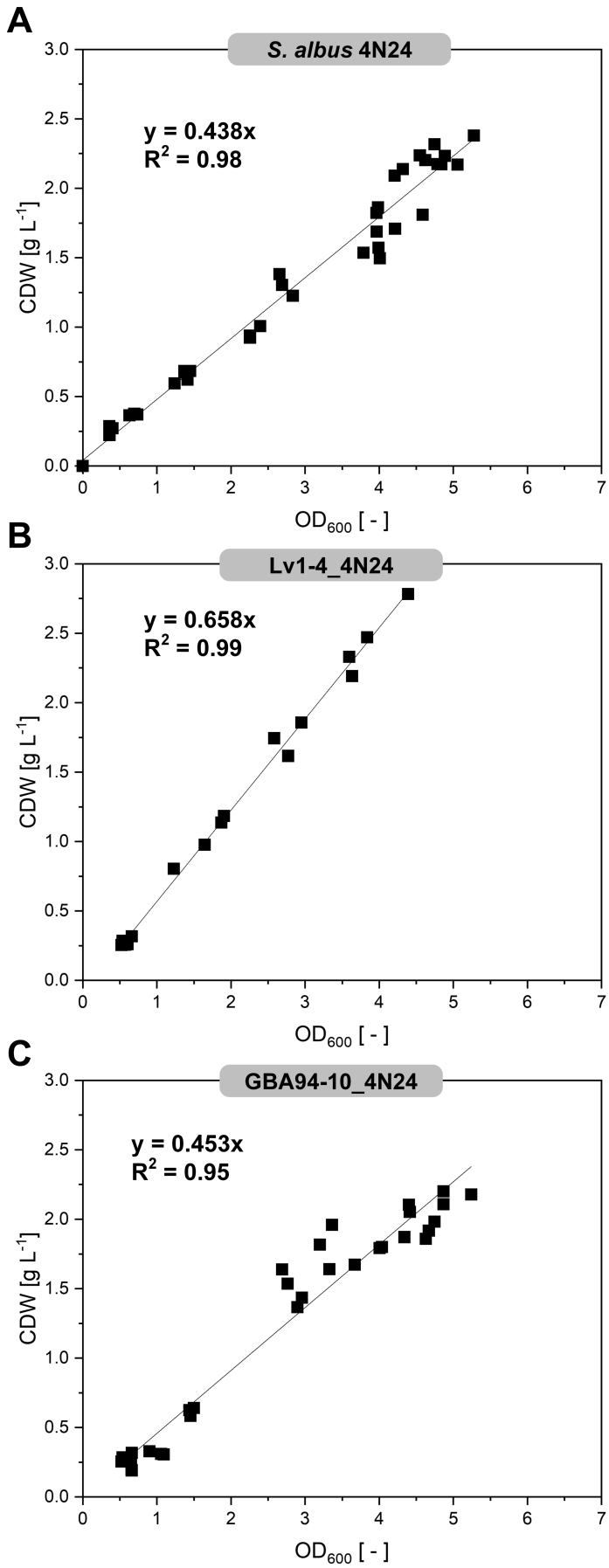

Figure 7: OD – CDW correlations of heterologous nybomycin producer strains in minimal mannitol medium. (A) *S. albus* 4N24 growth and stationary phase, (B) Lv1-4_4N24 growth phase only, (C) GBA94-10_4N24 growth and stationary phase.

3.5.2 Quantification of sugars

Quantification of mannitol was conducted by isocratic HPLC (Agilent Series 1260 Infinity, Agilent), using an Aminex HPX-87H column (300x7.8 mm 9 µm, Bio-Rad, Hercules, CA, USA) at 65 °C as stationary phase and 3 mM H_2SO_4 as mobile phase at a flow rate of 0.5 mL min^{-1}. Detection and quantification of the separated analytes was accomplished by refractive index measurement, using external standards. External standards were used for quantification.

3.5.3 Quantification of inorganic ions

Phosphate was quantified by HPIC (Dionex Integrion; Thermo Fisher Scientific) as previously described (Kuhl et al., 2020). Ammonium was analysed by HPIC (Dionex Integrion; Thermo Fisher Scientific) using a Dionex IonPac CS16-4µm (2 x 250 mm, Thermo Fisher Scientific) and 30 mM methanesulfonic acid as mobile phase (40°C, 0.16 ml min^{-1}). For detection, conductivity measurement was applied. External standards were used for quantification.

3.5.4 Quantification of nybomycin

Nybomycin was extracted from the culture broth using n-butanol. In short, 200 µL broth was mixed with 600 µL butanol and incubated for 15 min (1,400 rpm, 23°C, Thermomixer F1.5 Eppendorf, Wesseling, Germany). The organic phase was collected (20,000 x *g*, 5 min, 4°C). Subsequently, 400 µL butanol was mixed with the aqueous phase for a second extraction step. Afterwards, the two organic fractions were collected, and the solvent was removed by freeze drying. The obtained solid was dissolved in a mixture of methanol and DMSO (1:1) and clarified from debris (20,000 x *g*, 10 min, 4°C). Quantification of nybomycin was conducted using LC-ESI-MS/MS comprising a HPLC system (Agilent Infinity, 1290 System, Santa Clara, CA, USA), coupled to a triple quadrupole mass spectrometer (QTRAP 6500+, AB Sciex, Darmstadt, Germany). Separation was conducted on a C18 column (Vision HT C18 HighLoad, 100 mm × 2 mm, 1.5 µm, Dr. Maisch, Ammerbuch-Entringen, Germany) at 45 °C, applying a linear gradient (0-7 min, 10% B to 90% B) of eluent B (0.1% formic acid in acetonitrile) against eluent A (0.1 % formic acid in water) at a flow rate of 500 µL min^{-1}. Nybomycin was detected in the positive mode using selected ion monitoring of the $[M + H]^+$ adduct (*m/z* 299.1) (Rodriguez

Estevez et al., 2018). Quantification was based on external standards (Cayman Chemical, Ann Arbor, USA).

3.6 Transcriptomics

Sample preparation and RNA sequencing was done as biological triplicate as previously described (Gläser et al., 2021; Kuhl et al., 2020; Kuhl et al., 2021). In short, cells (1 mL broth) were collected by centrifugation (20,000 x g, 4 °C, 1 min) and immediately frozen in liquid nitrogen. RNA was extracted with the Qiagen RNA Mini kit (Qiagen, Hilden, Germany) according to the manufacturer's instructions. Residual DNA was removed by digestion with 10 U RNase-free DNase I (Thermo Scientific) for 1 h in the presence of RiboLock RNase inhibitor (Thermo Scientific). After DNA digestion, the RNA was again purified with the same kit. RNA quality was checked by Trinean Xpose (Gentbrugge, Belgium) and the Agilent RNA 6000 Nano Kit on an Agilent 2100 Bioanalyzer (Agilent Technologies, Böblingen, Germany). Ribosomal RNA (rRNA) molecules were removed from the total RNA with the Ribo-Zero rRNA Removal Kit (Illumina, San Diego, USA). The removal of rRNA was checked with the Agilent RNA 6000 Pico Kit on an Agilent 2100 Bioanalyzer (Agilent Technologies). Libraries of cDNA were prepared with the TruSeq Stranded mRNA Library Prep Kit (Illumina, San Diego, USA), and the resulting cDNA was sequenced paired end on an Illumina HiSeq 1500 system using 2x 75 bp read length. Reads were mapped to the *S. albus* J1074/R2 genome sequence (CP059254.1) with Bowtie2 using standard settings (Langmead and Salzberg, 2012) except for increasing the maximal allowed distance for paired reads to 600 bases. For visualization of read alignments and raw read count calculation, ReadXplorer 2.2.3 was used (Hilker et al., 2014). Using the resulting data, DESeq2 (Love et al., 2014) was used to QC the data sets via, among others, calculation of the sample to sample distances **(Figure 62)** and PCA **(Figure 63)**. In addition, DESeq2 was used to calculate DGE data sets. Raw data sets (sequenced reads) as well as processed data sets (input matrix & normalized read counts from DESeq2) are available from GEO (GSE240471). For statistical analysis, a student's t-test was carried out and the data were filtered for genes with a log2-fold change $\geq$ 1 (p-value $\leq$ 0.05). Hierarchical clustering was conducted, using the software package gplots (R core team 2014; Warnes et al., 2016). RNA extraction, sequencing, and data processing was conducted by Christian Rückert (Cebitec Bielefeld).

4 Results and Discussion

4.1 Streamlining of workflows for genomic modification of *Streptomyces* strains

Towards the desired nybomycin producing cell factories as central goal of this work, efficient and precise workflows for genetic engineering of the microbes of interest appeared crucial. Admittedly, *Streptomyces* are far more difficult to manipulate than most other industrial microbes. Therefore, the initial steps of the work focused on the adaptation and optimization of genetic engineering workflows.

4.1.1 Adaption of replication-deficient suicide vectors for homologous recombination

Suicide vectors, replicative in *E. coli* but replication-deficient in *Streptomyces*, respectively, are commonly used for genomic modification of *Streptomyces*, including in-frame deletions, insertions, and replacements. Hereby, antibiotic selection forces the integration of the vector during a first homologous recombination event. Subsequently, the vector backbone is excised by a second homologous recombination event upon omitting the selection pressure. For the planned work, the recently generated suicide vector pKG1132, containing the *gus*A gene for blue-white screening in *actinobacteria* and the apramycin resistance gene, respectively, was available (Barton et al., 2018). The basic heterologous nybomycin producer *S. albus 4N24* to be used, however, was resistant to apramycin upon insertion of the BAC 4N24 (Rodriguez Estevez et al., 2018), making pKG1132 inapplicable. Therefore, the apramycin resistance gene *aac(3)-IV* was replaced by the hygromycin resistance gene *hph* to enable the use of the vector for genetic engineering purposes in this work.

In short, the vector backbone pKG1132, lacking the apramycin resistance gene, was amplified by PCR and assembled with the PCR amplified hygromycin resistance gene by Gibson assembly which yielded the new plasmid pKG1132hyg **(Figure 8)**. Subsequently, restriction digestion using restriction enzymes (*Mlu*I / *EcoR*I) and Sanger sequencing verified the correctness of the vector.

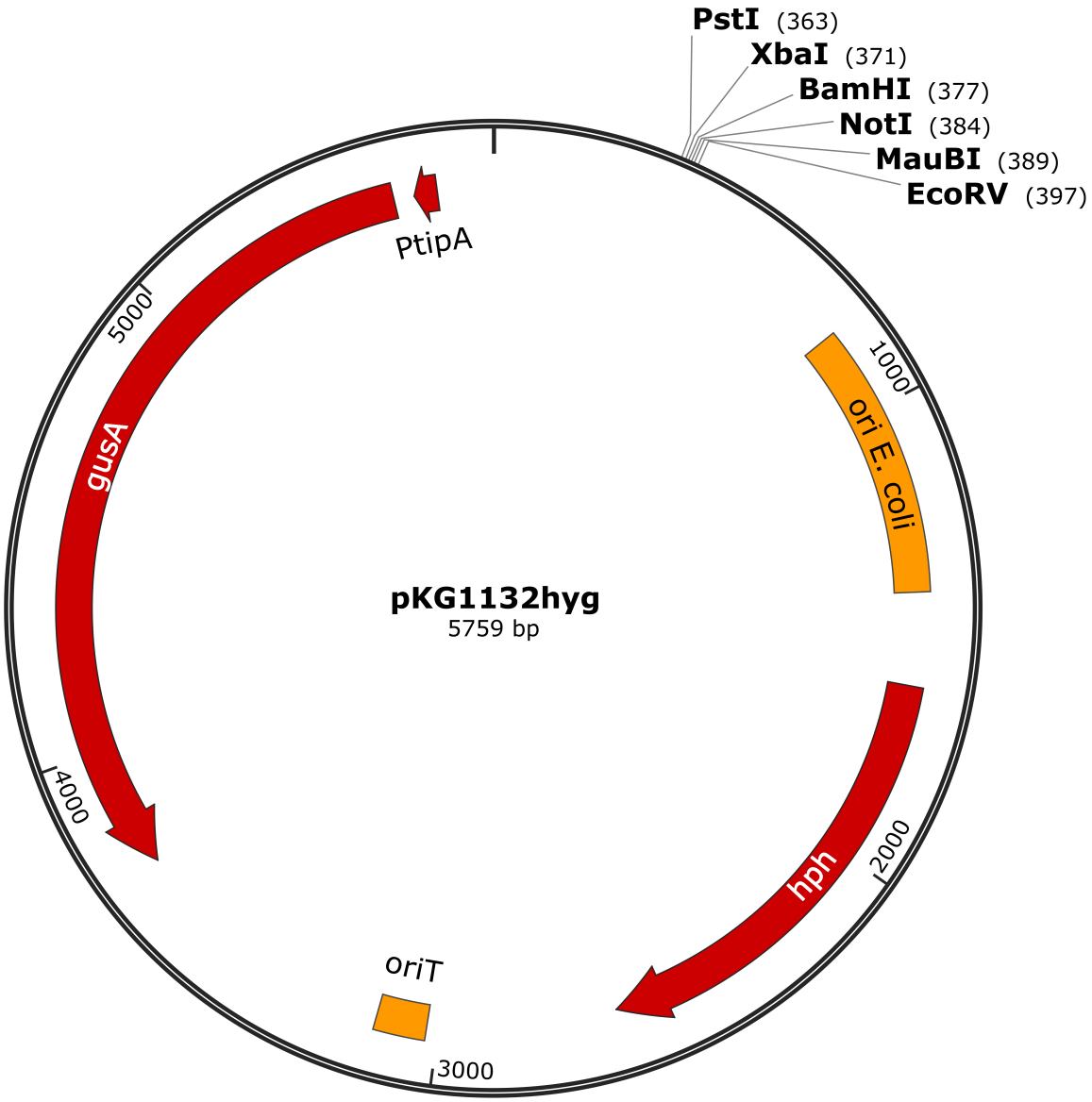

Figure 8: Plasmid map of the constructed suicide vector pKG1132hyg. The gene *hph* (hygromycin B phosphotransferase) enabled hygromycin resistance. The ori *E. coli* mediated plasmid replication in *E. coli*. The gene *gusA* (β-glucuronidase) enabled blue-white screening and the locus oriT (origin of transfer) enabled conjugative DNA transfer from *E. coli* into *Streptomyces*.

4.1.2 Refactoring of plasmids for integrase-coupled cloning purposes

In *Streptomyces*, site-specific recombinases are commonly used for the integration of plasmids and the excision of selection markers (Myronovskyi and Luzhetskyy, 2013). They display an easy, fast, and efficient tool for the genetic engineering of *Streptomyces* (Baltz, 2012; Bierman et al., 1992). Recombinases, such as Int-phiC31, Int-phiBT1, Int-VWB, Int-pSAM2, Cre, Dre, and Flp, recognise specific attachment sites in the genome to promote recombination of two specific DNA sequences called *attP* and *attB* (Myronovskyi and Luzhetskyy, 2013). The BAC

4N24, comprising the nybomycin BGC, had been previously integrated into the host using Int-phiC31 (Rodriguez Estevez et al., 2018). Due to this change, the genomic *attB* attachment site was already used up. Hence, another recombinase system was required which tackled an alternative attachment site. In addition, a switch to the hygromycin resistance gene (*hph*) was needed (see 4.1.1). Here, the integrative vectors pRT801 (Gregory et al., 2003) and pTOS (Herrmann et al., 2012) were selected. They express recombinases Int-phiBT1 and Int-VWB, respectively.

For the desired re-construction, the vector backbones pRT801 and pTOS were linearized by PCR amplification lacking the apramycin resistance gene (*aac(3)-IV)* and assembled with the hygromycin resistance gene (*hph*), yielding pBT1H **(Figure 12)** and pTOShyg **(Figure 10)**, respectively. Colony PCR, using sequence specific primers which bound in the vector backbone and in the inserted *hph* gene, were used to check the assembled vectors. Further verification by restriction digestion using the restriction enzymes i) *Sal*I / *EcoR*I (2646, 983, 802, 648, 557bp) **(Figure 9)**, ii) *Hinc*II (3294, 817, 802, 557, 166bp) for pTOShyg, and iii) *Sal*I (2226, 1546, 802, 557, 257bp) for pBT1H **(Figure 11)** and Sanger sequencing, respectively, further confirmed the correctness of the vector sequences.

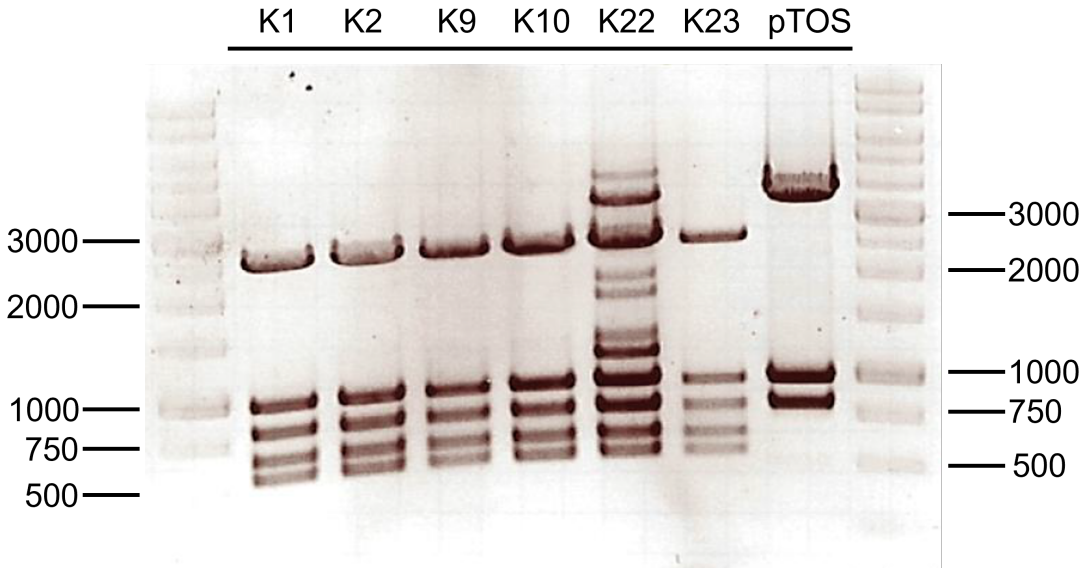

Figure 9: 1% Agarose gel electrophoresis of the vector pTOShyg digested with *Sal*I / *EcoR*I

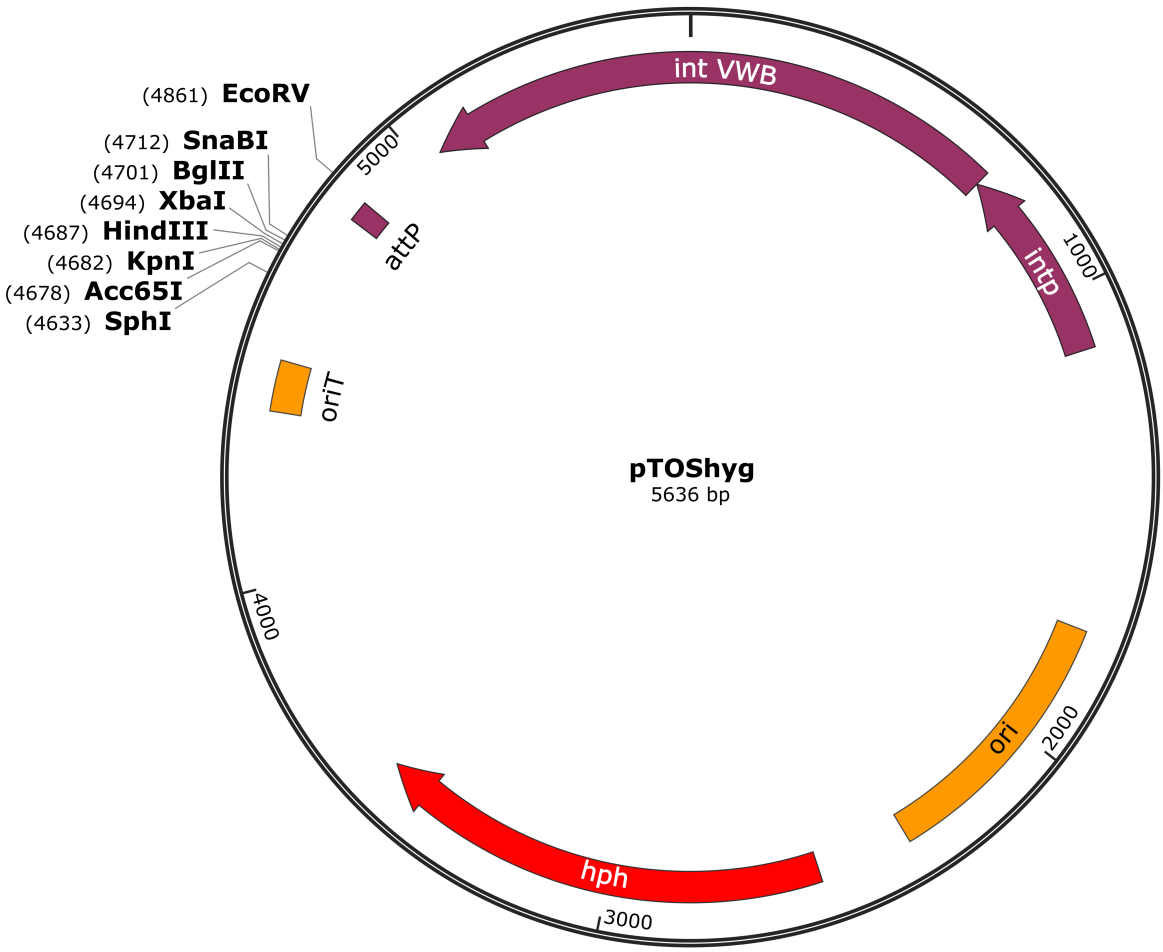

Figure 10: Plasmid map of the constructed integrative vector pTOShyg. The Gene *hph* (hygromycin B phosphotransferase) enabled hygromycin resistance. The ori mediated plasmid replication in *E. coli*. The gene intVWB (recombinase) enabled integration into *attP* site (attachment site for recombinase) and the locus oriT (origin of transfer) enabled conjugative DNA transfer *E. coli* into *Streptomyces*.

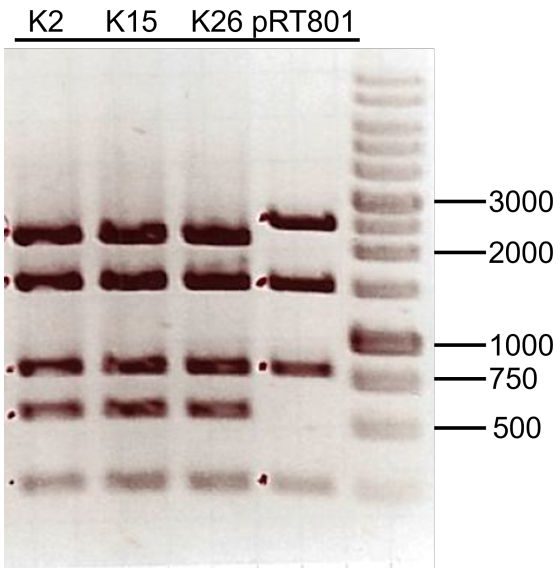

Figure 11: 1% Agarose gel electrophoresis of the vector pBT1H digested with *Sal*I

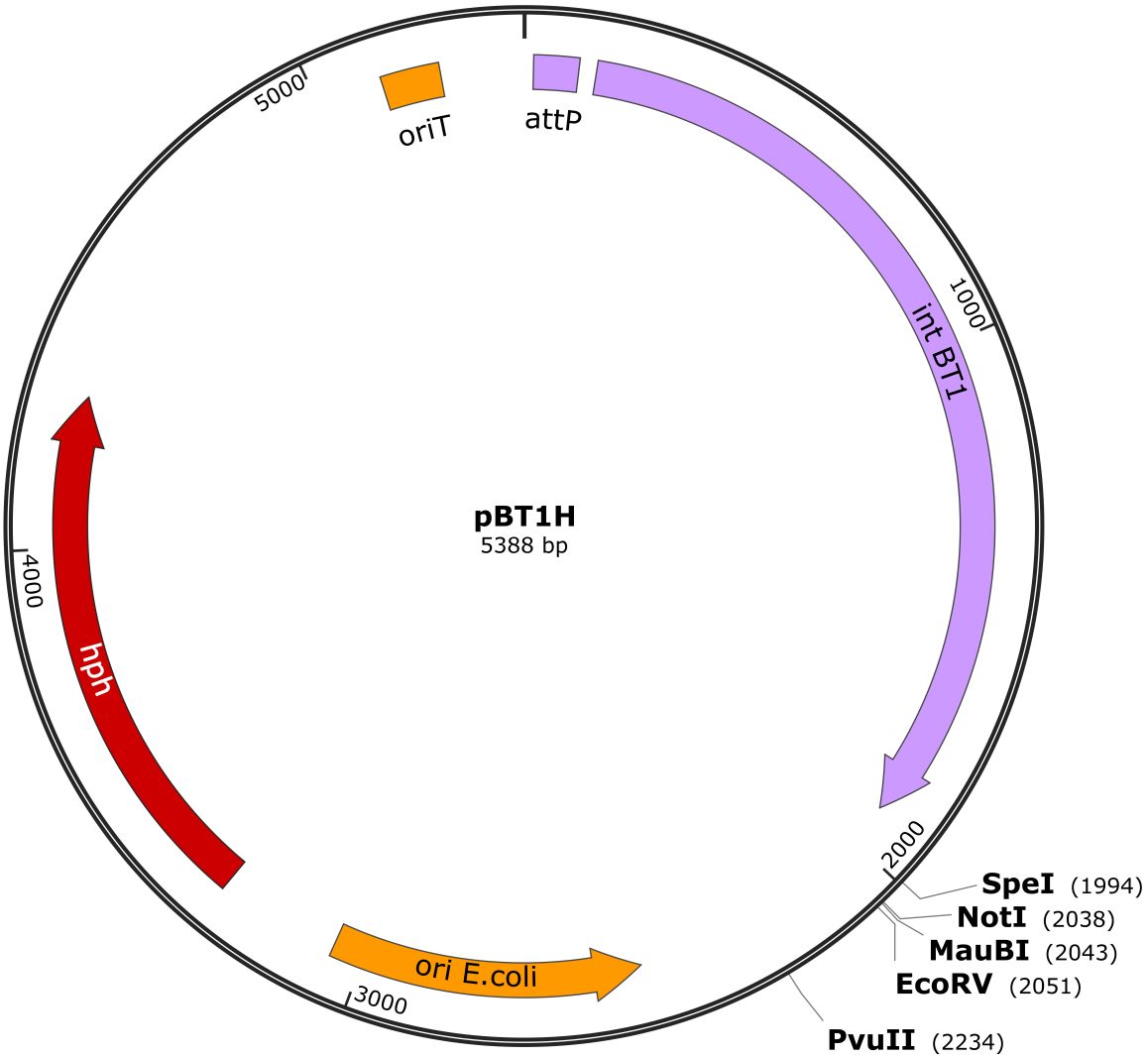

Figure 12: Plasmid map of the constructed integrative vector pBT1H. The Gene *hph* (hygromycin B phosphotransferase) enabled hygromycin resistance. The ori *E. coli* mediated plasmid replication in *E. coli*. The gene intBT1 (recombinase) enabled integration into *attP* site (attachment site for recombinase) and the locus oriT (origin of transfer) enabled conjugative DNA transfer *E. coli* into *Streptomyces*.

To simplify cloning efforts when using pBT1H, a refined version of the expression vector was created. For later expression of genes of interest, the constitutive promoter P_{ermE*} (Myronovskyi and Luzhetskyy, 2016), a ribosome binding site (RBS, underlined) AATGAACCGTTGGAGGCAAACACAT (Horbal et al., 2018), the blunt-end *Sna*BI restriction site (TAC*GTA) and the fd terminator (Wu et al., 2018) were selected.

The different elements (P_{ermE*} with RBS, *Sna*BI and 20bp overhangs as well as the fd terminator sequence with overhangs) were amplified by PCR and assembled with *Pvu*II linearized pBT1H to obtain pBT1HP **(Figure 13)**. Colony PCR, restriction digestion using the

restriction enzymes i) *Hincl*I and ii) *Sac*I / *EcoR*I and Sanger sequencing verified the correctness of the vector sequence.

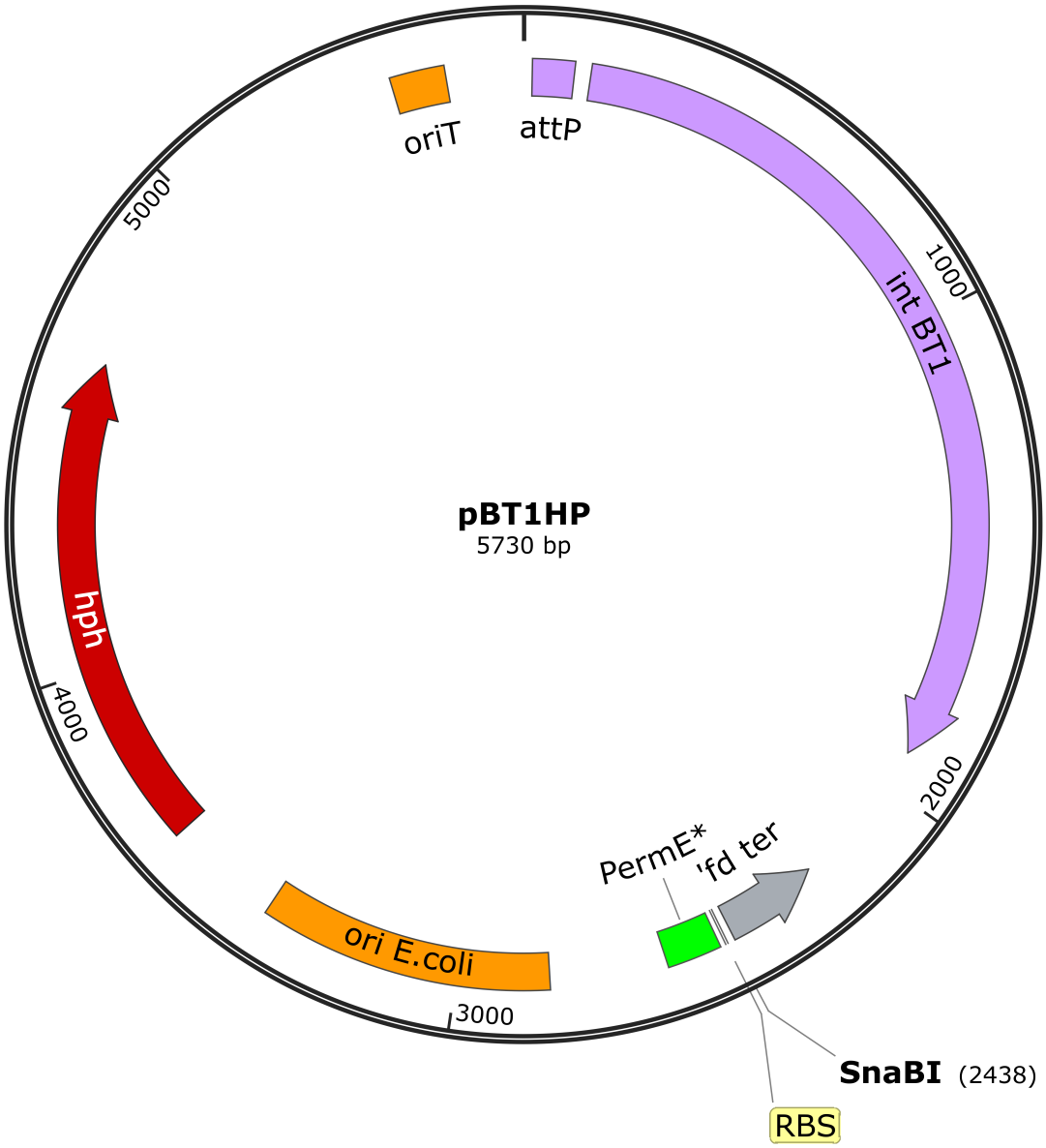

Figure 13: Plasmid map of the constructed integrative vector pBT1HP. The Gene *hph* (hygromycin B phosphotransferase) enabled hygromycin resistance. The ori *E. coli* mediated plasmid replication in *E. coli*. The gene intBT1 (recombinase) enabled integration into *attP* site (attachment site for recombinase) and the locus oriT (origin of transfer) enabled conjugative DNA transfer *E. coli* into *Streptomyces*. The restriction site *SnaB*I (blunt-end) enabled linearization for Gibson assembly allowing gene expression under control of the constitutive promoter *ermE** (P_{ermE*}). The terminator sequence 'fd ter enables transcription termination.

4.1.3 Improved cell lysis for colony PCR

Colony PCR, using viable cells containing genomic or plasmid DNA of interest as template for PCR screening, is a commonly applied method for fast and reliable screening of Gram-

negative and Gram-positive microbes, including *E. coli* (Pereira et al., 2023) and *C. glutamicum* (Becker et al., 2018a; Liu et al., 2017). Thereby, cells are lysed at 98 °C during the initial denaturation step of the PCR, causing the release of DNA and other cell components. However, the cell wall structure and thus, the thermal stability of microbial cells differs between genera, making this technique not applicable in *Streptomyces*. The extraction of gDNA and plasmid DNA, required as PCR template, is commonly conducted using expensive extraction kits applying binding matrices or time-consuming performing cell lysis and ethanol precipitation of the DNA (Gupta, 2019).

Hence, a quick and scalable method to extract DNA from *Streptomyces* aerial hyphae or spores as template for PCR screenings was established, based on literature (Sun et al., 2014). In general, three solutions were required to run the protocol. The resuspension solution (1) (10 mM TRIS, 1 mM EDTA, pH 7.6), was used to resuspend the cells. Next, an alkaline lysis solution (2) (0.4 M KOH, 10 mM EDTA) was added, and the mixture was incubated for 5 minutes at 70°C, followed by neutralization solution (3) (0.4M TRIS-HCl, pH 4.0) (Table 4).

Table 4: Titration experiment to achieve proper cell lysis applicable as template in PCR

Solution	Volume [mL]	pH	Function
(1)	27	7.6	Resuspension
(2)	3	12.2	Lysis
(3)	3	8.8	Neutralization
(3)	2	8.2	

Finally, protocol was transferred to small scale for colony PCR, using only 27 µL of solution (1), 3 µL of solution (2) and 5 µL of solution (3). Afterwards, 1 µL of the lysis mixture was used in a 20 µL PCR reaction. As example, the use of this protocol yielded clear bands for all tested clones **(Figure 14)**. This procedure was applied throughout this work.

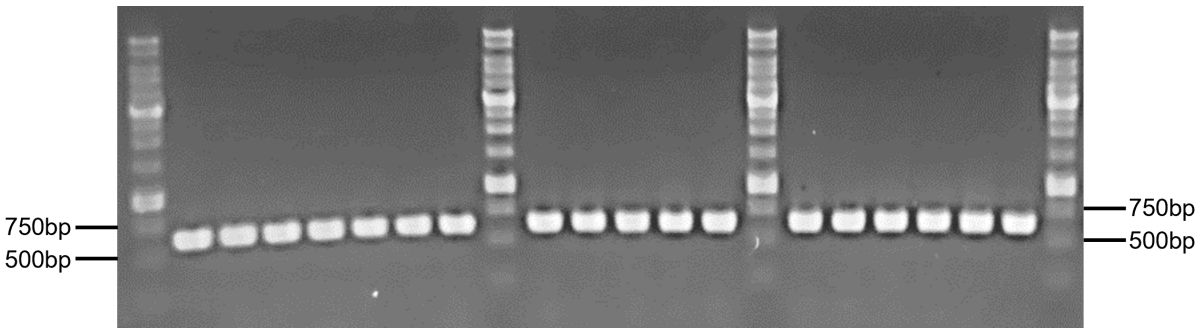

Figure 14: Colony PCR. Spores were treated as described and used as PCR template. The expected fragment size was 625bp. It was amplified from gDNA of *S. albus* after the integration of plasmid pBT1H using the primers IntBT1_Lv1-4_ch2_F and IntBT1_Salb_ch2_R.

4.2 Nybomycin extraction and quantification

For reproducible and reliable nybomycin analysis, the extraction, and the subsequent quantification of the nybomycin displayed crucial steps. The extraction of natural products from culture broth, supernatant, and biomass is commonly conducted by extraction, using organic solvents (Rodriguez Estevez et al., 2018). Different to previous work, ethyl acetate was replaced by n-butanol as the solvent because of higher efficiency (personal communication Marta Rodriguez-Estevez, Andriy Luzhetskyy, Pharmaceutical Biotechnology, Saarland University). Additionally, the volumetric ratio of n-butanol to culture broth was increased from 1:1 to 3:1. First efforts yielded, however, unreproducible results with deviations between technical replicates. To overcome this problem, multiple extraction steps (up to three) were conducted and separately evaluated. In the first extraction step, the culture broth was mixed with n-butanol. After incubation and centrifugation, the organic phase was collected. In the second extraction step, n-butanol was mixed with the remaining aqueous phase, following collection of the organic phase. This was repeated in the third extraction step. Subsequent measurement revealed that 82 % of the nybomycin was extracted during the first extraction step. In the second and third extraction step, 15 % and 3% of nybomycin were found, respectively **(Figure 15)**. Obviously, single extraction resulted in incomplete recovery of the product, making a second extraction inevitable. However, the cost-benefit relation for a third extraction seemed not reasonable. Finally, the use of n-butanol, the increases of volumetric ratio of n-butanol to broth to 3:1, and two extraction steps were found useful and reliable and used further on.

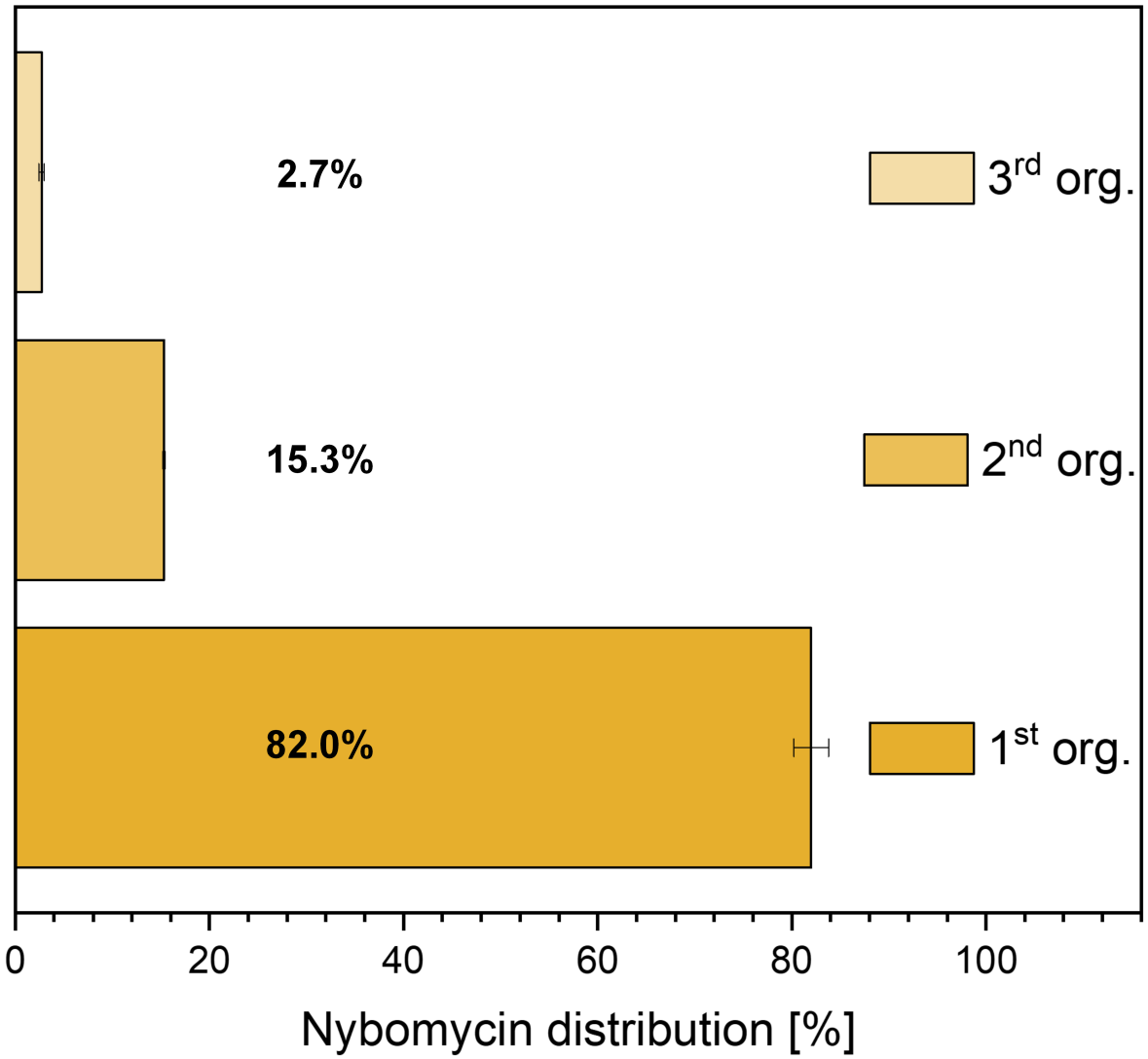

Figure 15: Nybomycin distribution among multistep solvent extraction process. The data represent mean values and corresponding standard deviations from three biological replicates.

For nybomycin quantification, liquid chromatography coupled to mass spectrometry (LC-MS) was used, including an 18-minute-long chromatographic separation (Rodriguez Estevez et al., 2018). As described in the previous protocol, the injection volume (1 µL) and the eluents (A, 0.1 % formic acid in MQ water; B, 0.1 % formic acid in acetonitrile) were maintained but small changes in the flow rate, gradient and runtime were introduced to optimize the analysis. The flow rate was reduced from 0.6 mL min^{-1} to 0.5 mL min^{-1} to reduce the column pressure to maximal 620 bar and thus, the danger to exceed the pressure limit of the column (1000 bar). The process time was reduced to 7 minutes by concurrent adaptation of the gradient **(Figure 16)**. Starting with 10% organic eluent B allowed almost complete binding of the analytes for 0.5 minutes. An increase of eluent B to 50% within 2.5 minutes, during which nybomycin was

eluted after around 2.2 minutes, allowed appropriate separation of the product from other extracted compounds, followed by an equilibration step (gradient to 90% eluent B) for 1 minute, and a subsequent gradient to 10% eluent B within 1 minute and 2 minutes of equilibration. Pure nybomycin (Cayman Chemical) was used to for method establishment **(Figure 17A)**. Extracts, obtained from culture broth of *S. albus* 4N24 were used for validation of the method **(Figure 17B)**.

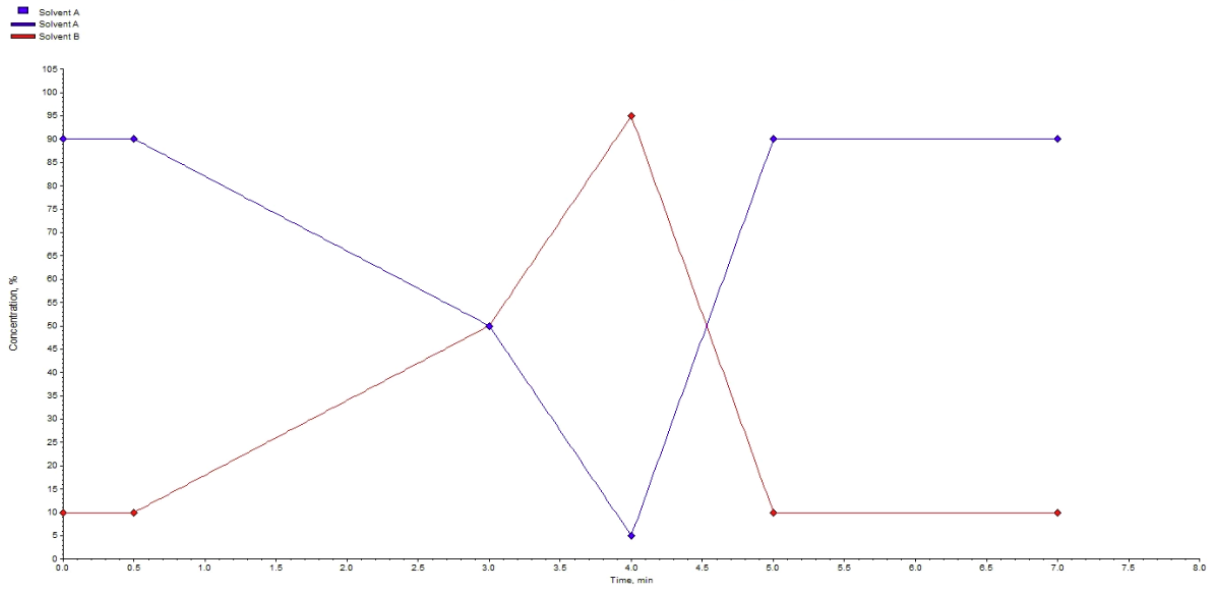

Figure 16: Gradient profile of eluent A and eluent B for nybomycin analysis using LC-MS.

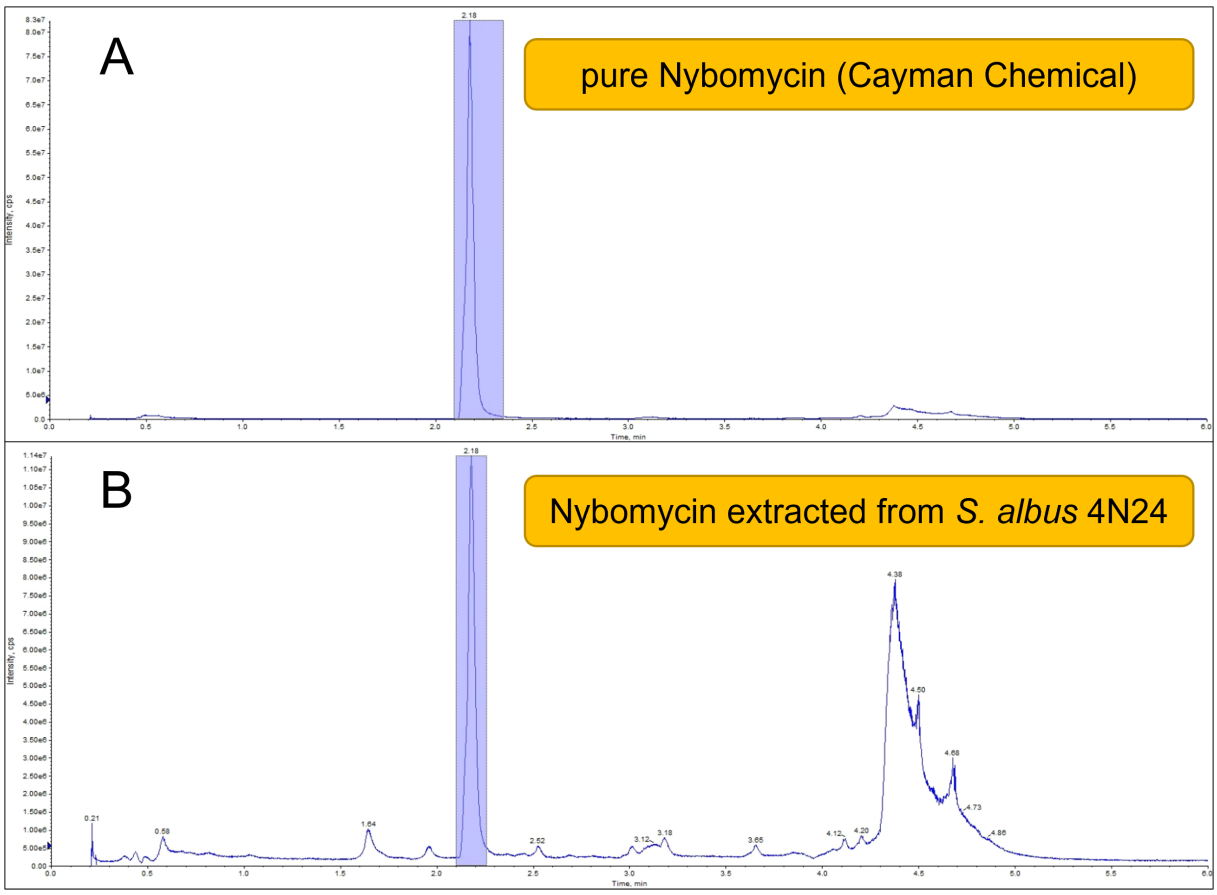

Figure 17: LC-MS chromatogram of the optimized nybomycin analysis procedure. Extracted chromatograms of *m/z* 299.10 Da (nybomycin) for the pure substance supplied from Cayman chemical (A) and n-butanol extracted sample from strain *S. albus* 4N24 grown in minimal mannitol medium (B).

4.3 Nybomycin production in the basic producer *S. albus 4N24*

The heterologous production of nybomycin in *S. albus* 4N24, grown in complex medium was described recently (Rodriguez Estevez et al., 2018). In our study, a defined medium using mannitol as sole carbon source was chosen, which promised to avoid unresolvable cellular responses that would have likely resulted from undefined complex medium ingredients (Schwechheimer et al., 2018a; Schwechheimer et al., 2018b) and facilitate the elucidation of the planned metabolic engineering efforts (Gläser et al., 2021).

S. albus 4N24 was grown in shake flasks. Over 275 h, *S. albus* 4N24 formed 860 µg L^{-1} of nybomycin when grown in minimal medium **(Figure 18)**. Once inoculated, the cells started to grow exponentially with a specific growth rate µ of 0.1 h^{-1}, while co-consuming mannitol, ammonium, and phosphate. Within 24 h, the supplemented phosphate was depleted. The incipient phosphate limitation caused an immediate slowdown of growth. The cell concentration increased further until mannitol was exhausted after 32 h which caused a growth stop. Interestingly, nybomycin was detectable already during the growth phase, different to most secondary metabolites being exclusively producing in the stationary phase (Kuhl et al., 2020; Ruiz et al., 2010; Seyedsayamdost, 2019). The production start was likely triggered by the simultaneously occurring phosphate limitation (Gläser et al., 2021). Taken together, 20% of nybomycin was formed during the growth phase. The stationary phase turned out to be the major phase of production (80%) **(Figure 18)**. During growth, the pH dropped to around 6, which is easily tolerable for the cells, however, stabilized around pH 7 in the stationary phase.

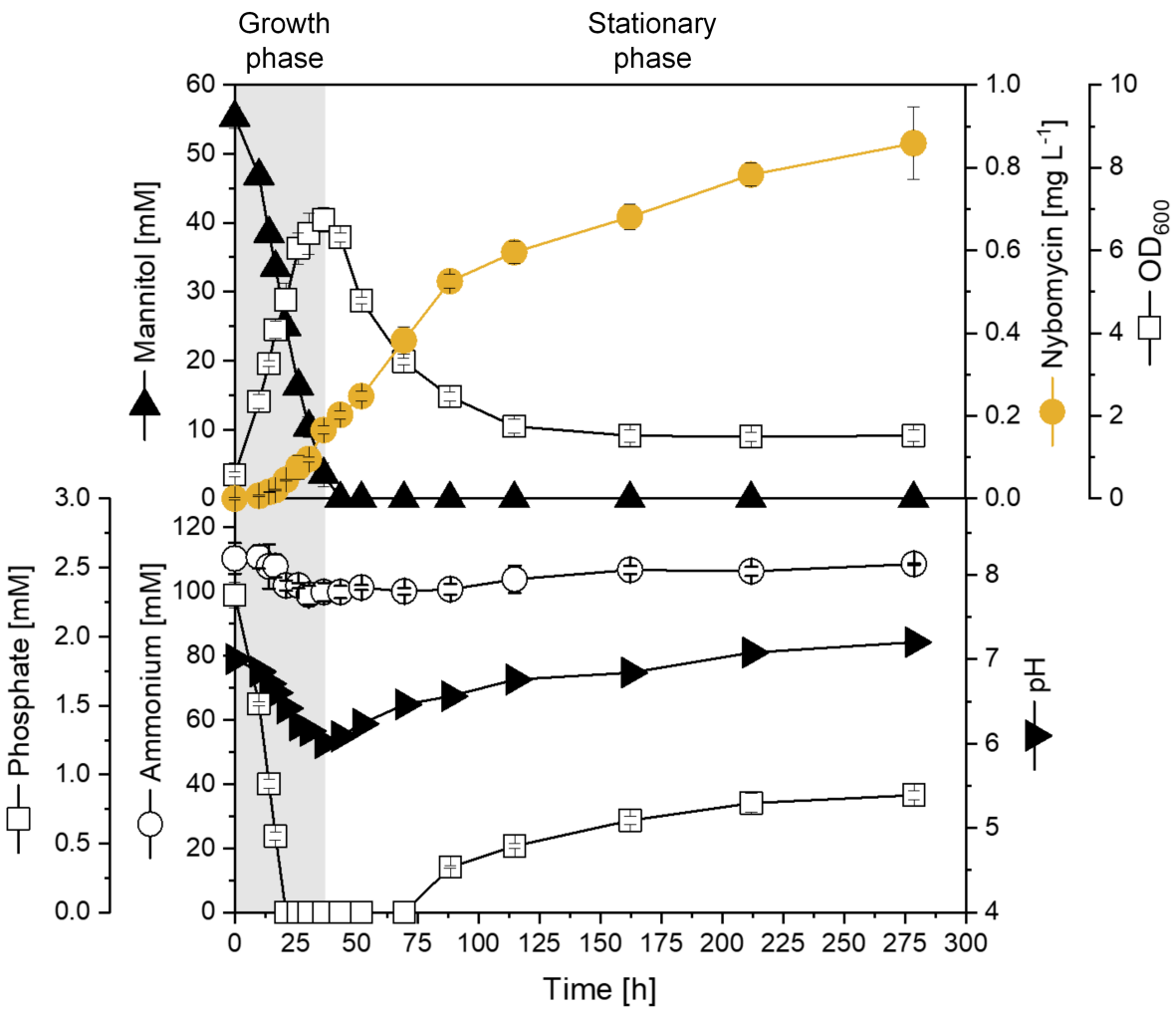

Figure 18: Cultivation time profile of the basic producer strain *S. albus* 4N24. The data comprise the cultivation profile of strain *S. albus* 4N24 grown in minimal mannitol medium including analysis of OD_{600} (open squares, upper panel), nybomycin (yellow circles, upper panel), mannitol (solid triangles, upper panel), phosphate (open squares, lower panel), ammonium (open circles, lower panel) and pH (solid squares, lower panel). The data represent mean values and corresponding standard deviations from three biological replicates.

To localize the product during the cultivation, biomass and supernatant were analyzed separately. Prior to extraction, the cell pellet was resuspended in 1x PBS to mimic identical starting conditions. During extraction, both phases, organic and aqueous, were measured individually. Nybomycin was found in the supernatant with 68.6 %, while 9.2 % were found in the aqueous phase **(Figure 19)**. In total 31.4 % were found in the biomass, split into 24.4 % and 7.0 % in organic and aqueous phase, respectively. The export mechanism is not fully described yet, however, a cluster-situated exporter, encoded by *nybV*, might play a crucial role in export. Nevertheless, cell lysis during growth, causing an unintended release of nybomycin into culture broth, may also contribute. Transporter proteins for certain secondary metabolites,

however, are often located within their corresponding BGCs such as for pamamycin (Rebets et al., 2015), moenomycin (Ostash et al., 2012) and balhimycin (Menges et al., 2007). Naturally, passive diffusion across the cell wall of small molecules is possible, however, has not been described for nybomycin, so far. It remains unclear, why, despite the existence of a nybomycin exporter, around 30 % of nybomycin are not found in the biomass. One possible explanation is an insufficient export capacity. However, titers are still in mg L^{-1} scale, making this assumption questionable. On the other hand, it is possible, that the product is indeed exported, but will stick to the cell wall rather than dissolving in the aqueous supernatant. Nonetheless, it is worth trying to improve nybomycin export by overexpression of the known transporter *nybV*.

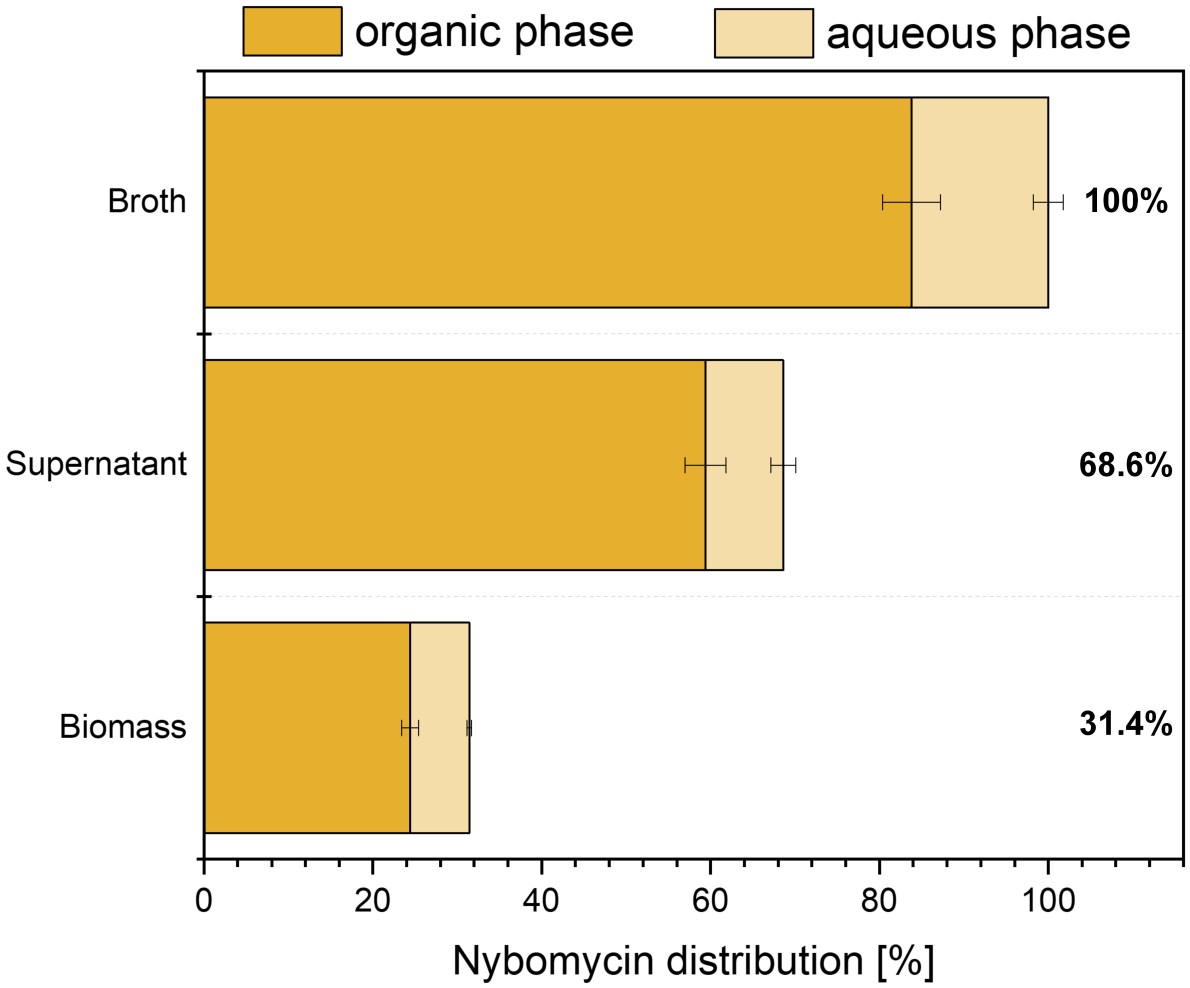

Figure 19: Localization of nybomycin in *S. albus* 4N24 during batch cultivation. The data represent the separate inspection of supernatant and biomass regarding to nybomycin analysis as well as nybomycin distribution among organic and aqueous phase during solvent extraction process. The data represent mean values and corresponding standard deviations from three biological replicates.

4.4 Systems metabolic engineering of *S. albus* 4N24: Precursor supply, flux channeling and deregulation

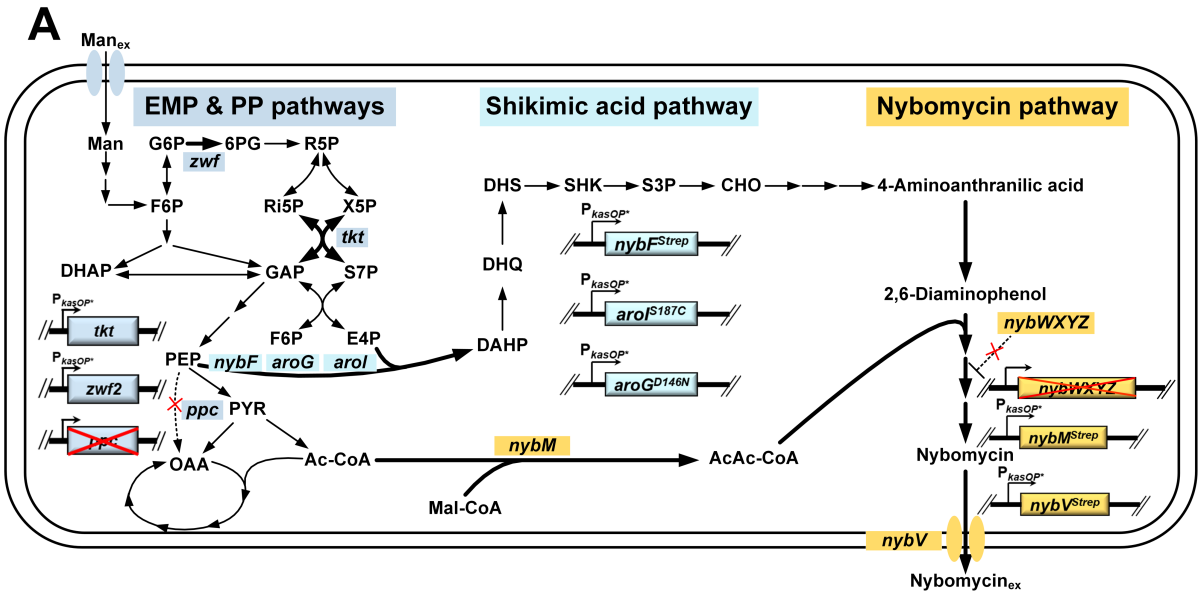

Figure 20: Metabolic pathway design to produce nybomycin in *Streptomyces albus* Del14. The overview illustrates the targets of the stepwise metabolic engineering in the primary metabolism including EMP and PP pathways (blue), shikimic acid pathway (light blue), supplying precursors for biosynthesis of the secondary metabolite nybomycin (yellow).

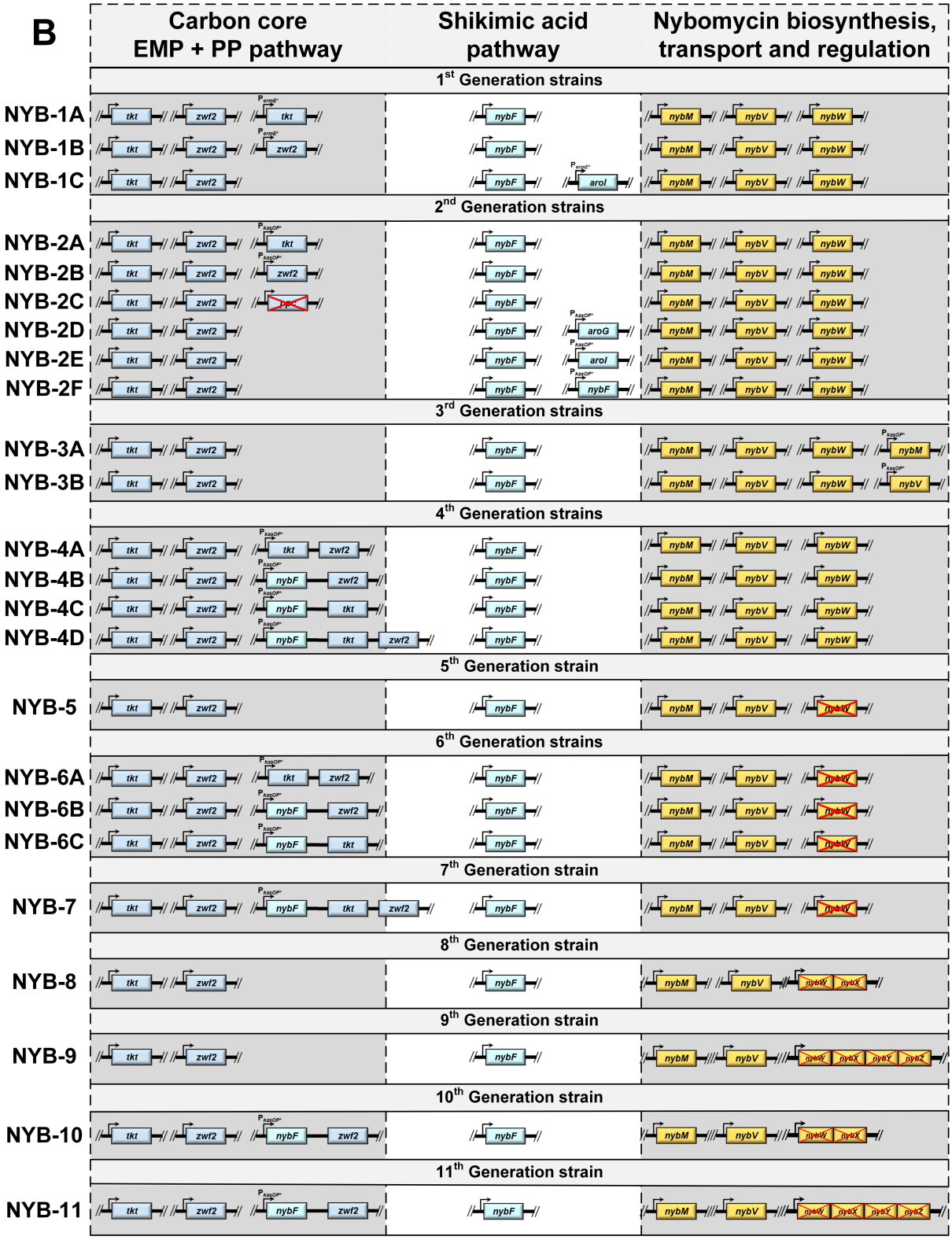

Figure 21: Overview of engineered 1st, 2nd, 3rd, 4th, 5th, 6th, 7th, 8th, 9th, 10th and 11th generation *S. albus* 4N24 strains by its genetic characteristics. Genetic changes for each producer implanted into the primary metabolism (carbon core metabolism, synthesis of the precursor shikimic acid, supply of CoA thioester precursors) and the secondary metabolism (nybomycin biosynthesis, regulation, and export), respectively. All changes were implemented stepwise into the chromosome of the basic nybomycin producer *S. albus* 4N24 that had been previously derived upon heterologous expression of the nybomycin gene cluster from *S. albus subsp. chlorinus* (Rodriguez Estevez et al., 2018). Further details on the created strains can be found in chapters 4.4.1 - 4.6.3.

4.4.1 Targeted expression of PP and SA pathway genes

Nybomycin biosynthesis starts from E4P and PEP while the PP pathway and, further downstream, the SA pathway, supplied all carbon to form 2,6-diaminophenol, the centrepiece of nybomycin **(Figure 6)**. In a first metabolic engineering step, two native PP pathway genes were selected for overexpression to explore the potential of an enhanced precursor supply: *tkt* (encoding transketolase A in the reversible branch) and *zwf2* (encoding glucose 6-phosphate dehydrogenase in the oxidative branch) **(Figure 20)**. The overexpression of each gene had previously proven efficient to (i) increase the PP pathway flux in the actinobacterium *C. glutamicum* (Becker et al., 2007; Becker et al., 2011) and (ii) the formation of PP pathway-based natural products, including violacein and deoxyviolacein in *E. coli* (Rodrigues et al., 2013) and FK506 in *S. tsukubaensis* (Huang et al., 2013a). The genes were separately integrated each under control of the strong constitutive promotor P_{ermE*} (Garcia-Gutierrez et al., 2020) into the chromosome of *S. albus* 4N24, leading to strains NYB-1A (4N24 P_{ermE*} *tkt*) and NYB-1B (4N24 P_{ermE*} *zwf2*) **(Figure 21)**.

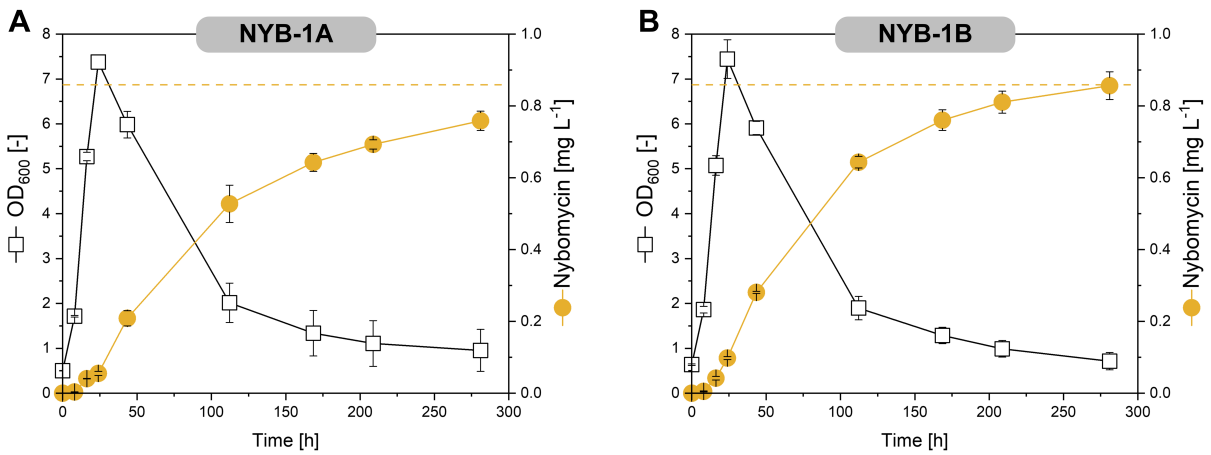

Figure 22: Time profiles for growth and nybomycin production of engineered 1st generation strains. The data represent OD_{600} (open squares) and nybomycin titer (yellow circles) of *tkt* (NYB-1A) and *zwf2* (NYB-1B) expressing strains driven by P_{ermE*} grown in minimal mannitol medium. The dashed yellow lines indicate the nybomycin titer of the basic producer *S. albus* 4N24. The data shows mean values and corresponding standard deviations from three biological replicates.

Both mutant strains exhibited similar growth compared to the reference strain in minimal medium containing mannitol as carbon source, but none was found improved in nybomycin production. NYB-1A reached a nybomycin titer 760 µg L^{-1} **(Figure 22A)**, whereas NYB-1B produced 860 µg L^{-1} **(Figure 22B)**.

Next, flux through the shikimic acid pathway was targeted for improvement. To this end, the *aro* I^{S187C} gene from *C. glutamicum* was selected for heterologous expression in *S. albus* 4N24. The gene encoded a feedback-resistant DAHP synthase (*aro* type-I DS) from the SA pathway, which had been successfully used to increase aromatic amino acid biosynthesis (Liao et al., 2001). **(Figure 20, Figure 21)**. The constructed strain NYB-1C (4N24 P_{ermE*} *aro* I^{S187C}), however, did not differ in nybomycin production too (data not shown).

Two possibilities arose to explain the somewhat surprising lack of improvement in the three strains NYB-1A, NYB-1B, and NYB-1C: (i) insufficient expression of the target genes and/or (ii) independence of nybomycin formation from precursor supply. Regarding the first, P_{ermE*} represented a well-known promotor which had been successfully used many times to drive gene expression in *Streptomyces* (Chen et al., 2012; Huo et al., 2012; Kallifidas et al., 2018; Lu et al., 2016; Ma et al., 2020; Mo et al., 2019; van Wezel et al., 2000). However, as promoters can vary in their strength depending on the conditions and appropriate promoter functionality was crucial for successful strain engineering, experimental benchmarking of P_{ermE*} was necessary.

4.4.2 Evaluation of expression dynamics of P_{ermE*}

For this purpose, the reporter strain *S. albus* RFP-1 (4N24 P_{ermE*} *mCherry*) was constructed. The construct was integrated into the chromosome using the phiBT1 integration site, resulting in the expression of mCherry under control of P_{ermE*}. **(Figure 24A)**. Most previous studies on promotor strength in *Streptomyces* relied on end-point measurement of expression (Bibb et al., 1994; Seghezzi et al., 2011; Siegl et al., 2013). However, *S. albus* exhibited distinct dynamics in nybomycin production **(Figure 18)** so that it appeared important to measure gene expression dynamically as well. The obtained reporter strain was therefore analysed on-line for growth and fluorescence (Kohlstedt et al., 2018). Interestingly, mCherry was found to be

exclusively expressed during the first 40 h of cultivation, i. e. during the phase of cell growth **(Figure 23)**. The fluorescence remained unchanged during the entire stationary phase, revealing a previously overlooked dependence of P_{ermE*} activity on the growth status of *S. albus* (Myronovskyi and Luzhetskyy, 2016). In terms of nybomycin production, which in *S. albus* predominantly occurred in stationary phase, the dynamic expression pattern of P_{ermE*} appeared unfavorable, as it resulted in a temporal mismatch of the expression of target genes with the major phase of production, in which the precursors would have been needed.

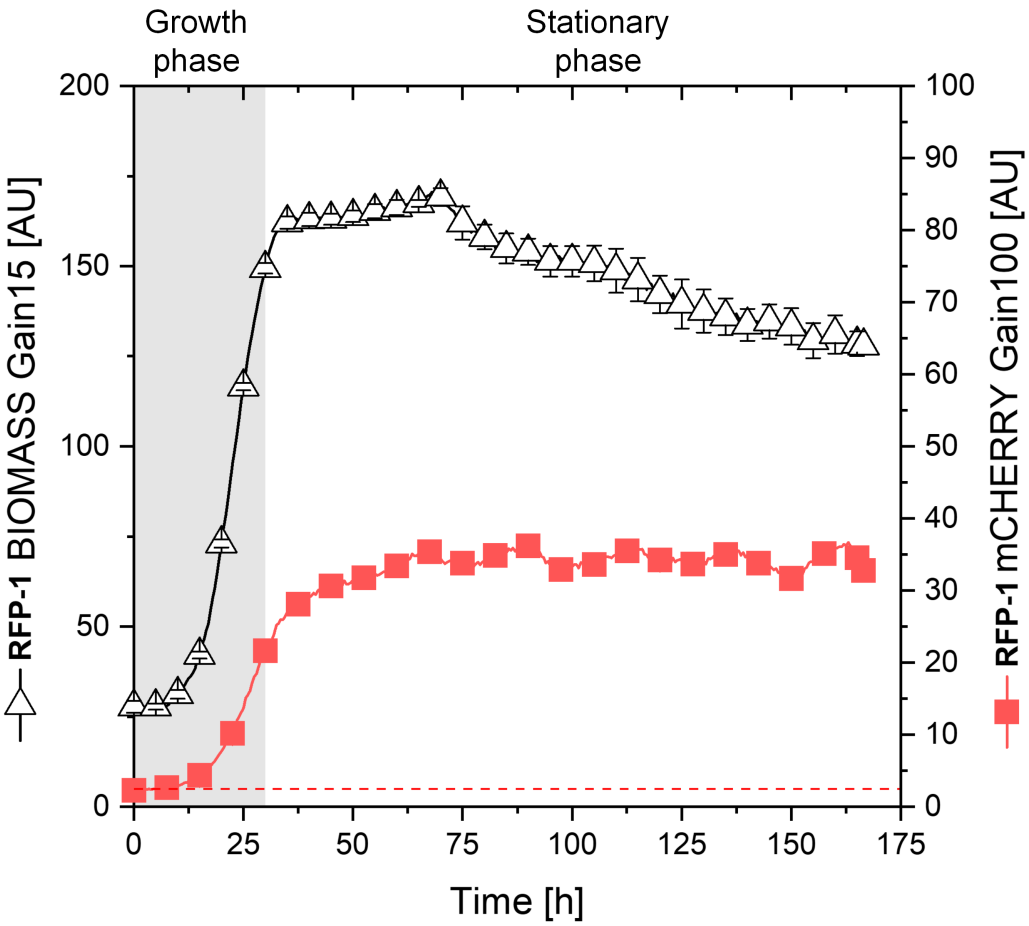

Figure 23: Benchmarking P_{ermE*} by online monitoring of fluorescence signal. The data show time profiles for biomass (open triangles) and fluorescence signal (red squares) of strain *S. albus* RFP-1 grown in minimal mannitol medium using microplate-based microbioreactor. The dashed red line illustrates the background signal of the reference strain *S. albus* 4N24. The data represent mean values and corresponding standard deviations from three biological replicates.

4.5 Identification of a suitable promoter systems

4.5.1 Promoter screening for production-associated gene expression

In a next step, superior promotors to drive production-associated gene expression were searched. Seven alternative promotors were selected: the thiostrepton-inducible promotor P_{tipA} conferring substantial uninduced activity (Myronovskyi and Luzhetskyy, 2016), the synthetic promoter P_{21} (Siegl et al., 2013), the constitutive phage-derived promotor P_{SF14} (Labes et al., 1997) as well as the deregulated promotor variant P_{kasOP*} and its synthetic derivatives P_{SP41}, P_{SP43}, and P_{SP44} (Bai et al., 2015) **(Figure 24A)**. Each promotor was cloned in front of mCherry, and the respective plasmids were integrated into the chromosome of *S. albus*, yielding the reporter strains RFP-2 to RFP-8 (**Figure 24A, Table 2**). They were all characterized for dynamic expression strength. The promotors differed strongly in their dynamic expression pattern **(Figure 24B)**. P_{tipA} appeared inactive throughout the entire culture, indicating that uninduced activity was insignificant, different from previous observations (Myronovskyi and Luzhetskyy, 2016). P_{SF14} was found weaker than P_{ermE*}, the opposite of what had been observed in *S. lividans* (Labes et al., 1997) underlining the importance of case specific evaluation. P_{21} was similarly strong as P_{ermE*}. The activity of P_{21} and P_{SF14} was almost entirely restricted to the growth phase **(Figure 24C)**. None of these alternative promotors appeared useful to drive precursor supply for nybomycin production.

This picture completely changed, when analysing the P_{kasOP*} -based promotors. The two variants P_{SP43} and P_{SP44} were found three-fold more active than P_{ermE*} based on final fluorescence **(Figure 24B)**. P_{kasOP*} and its synthetic derivative P_{SP41} were the two best promotors, exhibiting the highest overall activity (seven-fold higher than P_{ermE*}) and, importantly, a constantly high expression throughout the whole culture process, including the stationary phase, in which most of the nybomycin was made **(Figure 24C)**.

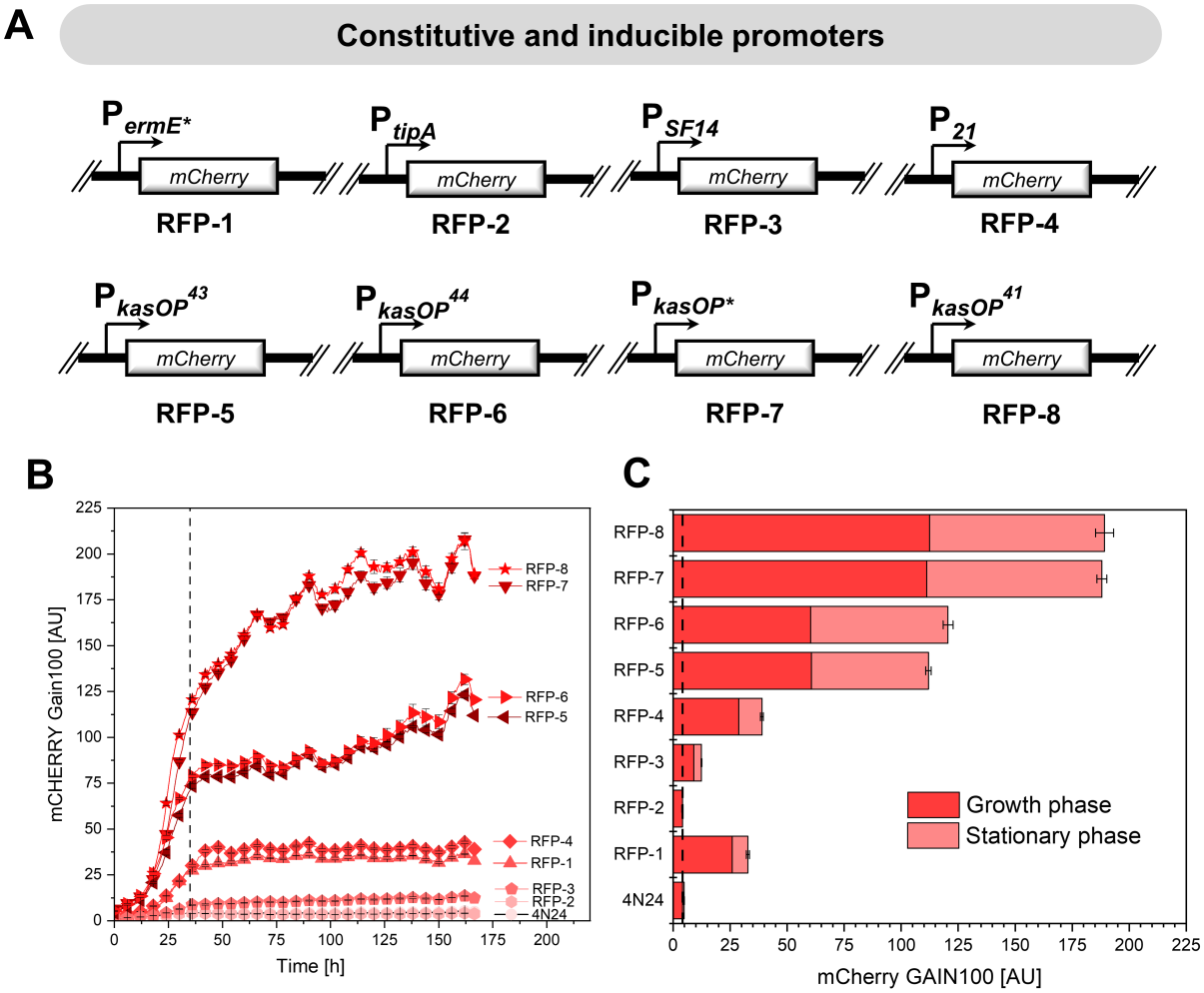

Figure 24: Evaluation of heterologous promotors for expression efficiency in *S. albus* 4N24 during the nybomycin production process. Features of the tested promoters and genetic design of mCherry-based fluorescent reporter constructs (A). The data represent dynamics of mCherry expression of reporter strains RFP-1 to RPF-8 in minimal mannitol medium using microplate-based microbioreactor. The vertical dashed line represents the transition from growth to stationary phase (B). Time-resolved expression strength during the growth and the stationary phase. The vertical dashed line represents the background fluorescence signal of the reference strain *S. albus* 4N24 (C). The data represent mean values and corresponding standard deviations from three biological replicates.

4.5.2 Tailor-made gene overexpression by the synthetic P_{kasOP*}

The best promotor P_{kasOP*} was used to overexpress *tkt* and *zwf*2 for enhanced supply of the PP pathway intermediate E4P, again through implementation both genes individually **(Figure 21)**. Favorably, the two mutants NYB-2A (4N24 P_{kasOP*} *tkt*) and NYB-2B (4N24 P_{kasOP*} *zwf2*) accumulated 29% and 31% more nybomycin, i. e. 1,071 and 1,093 µg L^{-1}, respectively **(Figure 25AB, Figure 33A)**. At the same time, the maximum specific nybomycin production rate was increased up to 50% **(Figure 33B)**. The significant improvement was important in two aspects.

It revealed that the synthesis of nybomycin was limited by the supply of its central carbon moiety and, moreover, proved the high value of P_{kasOP*} for tailor-made gene expression of production-supporting genes.

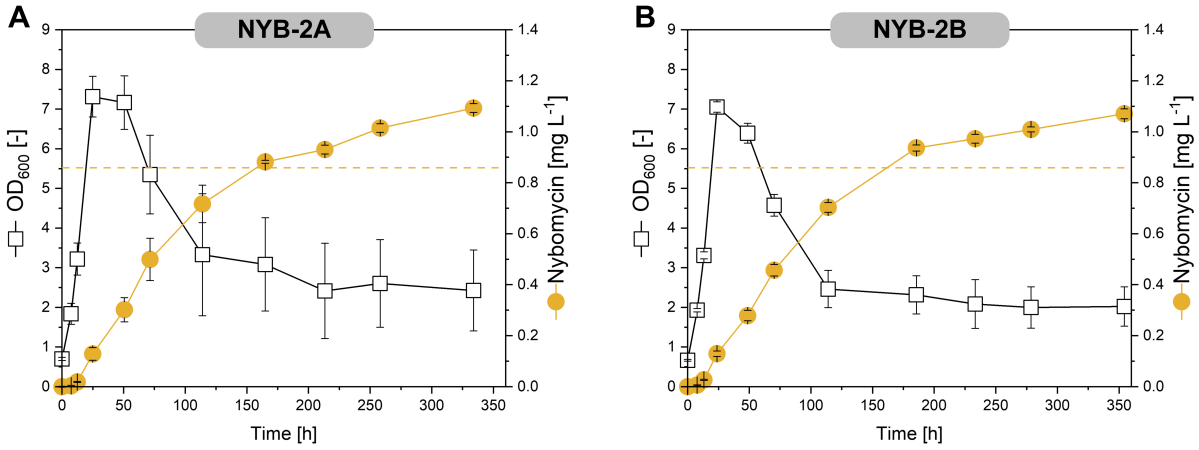

Figure 25: Time profiles for growth and nybomycin production of engineered 2nd generation strains. The data represent OD_{600} (open squares) and nybomycin titer (yellow circles) of *tkt* (NYB-2A) (A) and *zwf2* (NYB-2B) (B) expressing strains driven by P_{kasOP*} grown in minimal mannitol medium. The dashed yellow lines indicate the nybomycin titer of the basic producer *S. albus* 4N24. The data represent mean values and corresponding standard deviations from three biological replicates.

Next, DAHP synthase (DS) emerged as relevant point of control **(Figure 20)** (Sander et al., 2019), given its impact on the formation of SA pathway-based products, such as salvianic acid (Yao et al., 2013), violacein (Rodrigues et al., 2013), caffeic acid (Zhang and Stephanopoulos, 2013), and avenanthramides (Eudes et al., 2013). To overcome a potential limitation at this step, P_{kasOP*} was used to heterologously express genes from two different donors that encoded feedback-resistant variants of the enzyme: *aroG*^{D146N} (NYB-2D) from *E. coli* (Kikuchi et al., 1997) and *aro I*^{S187C} (NCgl0950, NYB-2E) from *C. glutamicum* (Liao et al., 2001) **(Figure 21)**. Beneficially, the mutants achieved a 20% higher nybomycin titer and a 15% increased productivity **(Figure 26AB, Figure 33)**. Interestingly, the *nyb* cluster itself also comprised a DS-encoding gene, namely *nybF*. Overexpressing this gene resulted in a further increased titer (1,160 µg L^{-1}) in the new strain NYB-2F **(Figure 26C)**. The volumetric productivity was increased even by 40% **(Figure 33)**.

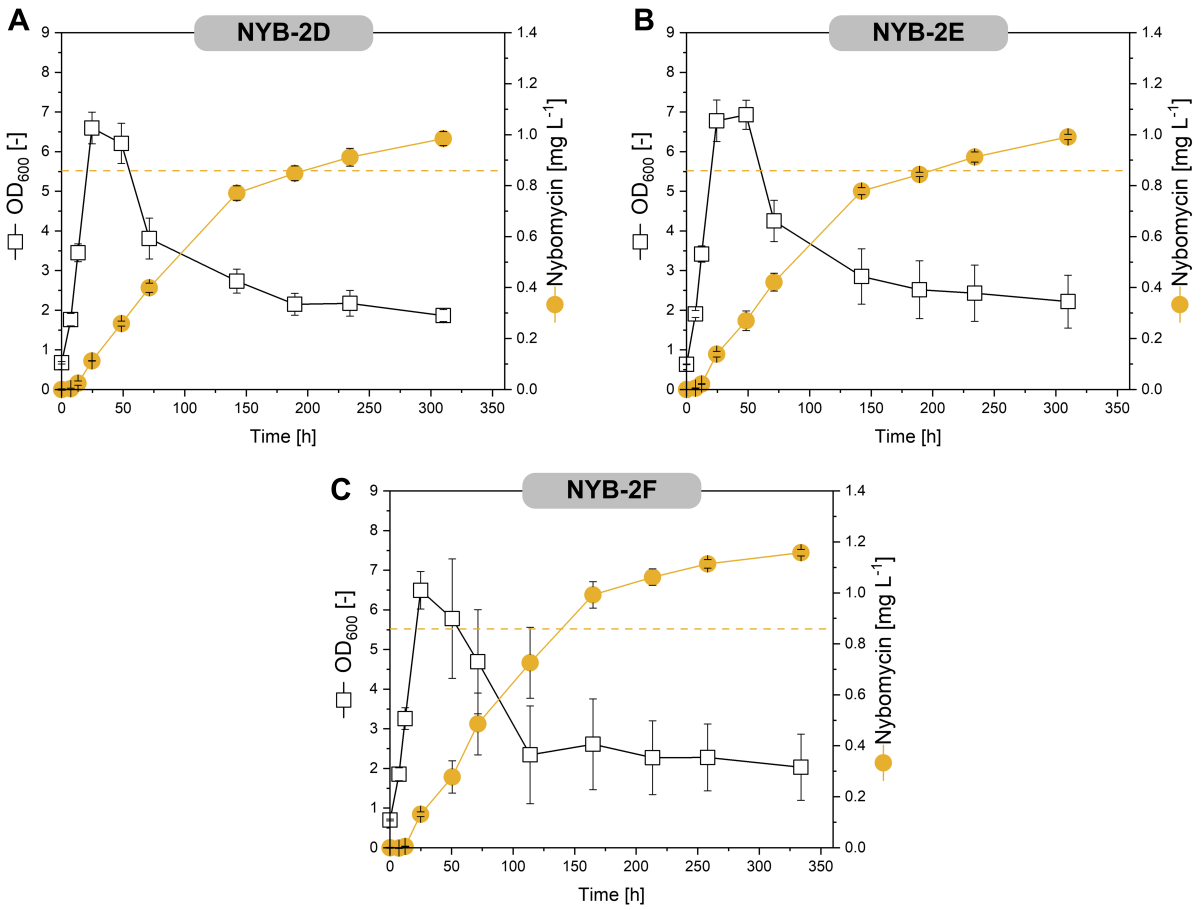

Figure 26: Time profiles for growth and nybomycin production of engineered 2nd generation strains. The data shows OD_{600} (open squares) and nybomycin titer (yellow circles) of *aroG*^{D146N} from *E. coli* (NYB-2D) (A), *aro I*^{S187C} from *C. glutamicum* (NYB-2E) (B) and *nybF* (NYB-2F) (C) expressing strains driven by P_{kasOP*} grown in minimal mannitol medium. The dashed yellow lines indicate the nybomycin titer of the basic producer *S. albus* 4N24. The data represent mean values and corresponding standard deviations from three biological replicates.

This extra improvement was eventually caused by better expression of the GC-rich *nybF* gene (75%), probably due to its more suited codon usage (Rohles et al., 2022; Weiland et al., 2023) or by superior kinetics of the NybF protein. The aligned amino acid sequences revealed 52 % identity between AroG and Aro I (95% coverage), while almost no conserved regions of AroG and Aro I were detected with NybF **(Figure 27A)**. Obviously, NybF differed substantially from the other enzymes. However, *C. glutamicum* possesses another DAHP synthase, denoted Aro II (NCgl2098) (Ikeda, 2006), a plant-like type II DAHP synthase (Walker et al., 1996). Interestingly, NybF revealed 37% similarity to Aro II (91% coverage) **(Figure 27A)**. So far, metabolic engineering for the production of aromatic amino acids and related derivatives, commonly recruited type I feedback-resistant enzyme variants from *E. coli* (AroG, AroF, AroH) or *C. glutamicum* (Aro I) (Rodriguez et al., 2014), where it seems that type II enzymes were

largely neglected. Based on our findings, however, type II DAHP synthases seem to deserve a closer look for future metabolic and enzyme engineering to overproduce aromatic amino acids and related derivatives.

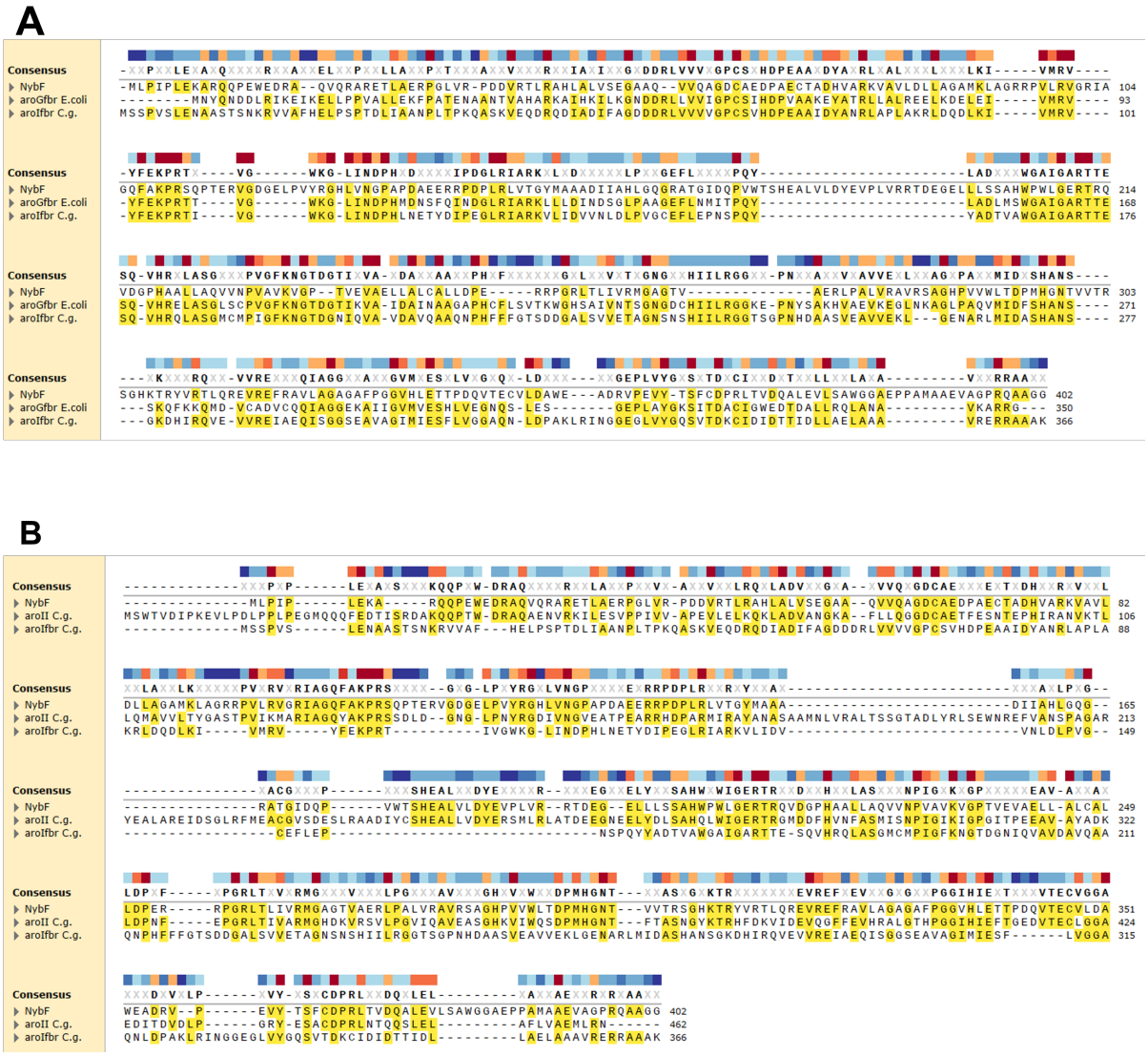

Figure 27: Protein sequence alignments of DAHP synthases from *Streptomyces*, *C. glutamicum* and *E. coli*. Alignment of NybF (*S. albus* subsp. *Chlorinus*), AroG^{D146N} (*E. coli*) and Aro I^{S187C} (*C. glutamicum*) (A). Alignment of NybF (*S. albus* subsp. *Chlorinus*), Aro I^{S187C} (*C. glutamicum*) and Aro II (*C. glutamicum*) (B).

Next, re-direction of PEP from the EMP pathway towards nybomycin production was aimed **(Figure 6, Figure 20)**. To this end, the gene *ppc*, coding for PEP-consuming phosphoenolpyruvate carboxylase was deleted in-frame in the genome of *S. albus*, resulting in strain NYB-2C (4N24 *Δppc*). The deletion strain, however, needed almost 100 h to reach the maximum cell concentration **(Figure 28A)**, while producing almost two-fold less nybomycin

(470 µg L^{-1}) **(Figure 28A, Figure 33A)**. When growing NYB-2C in a complex DNPM medium, the growth retardation could be partially recovered but nybomycin production remained far below that of the parent strain **(Figure 28B)**. Previously, a *Δppc* mutant of *Corynebacterium glutamicum* was not affected in growth on minimal media (Peters-Wendisch et al., 1993). In addition, the deletion of *ppc* in *S. tsukubaensis* affected growth on complex medium only slightly (Huang et al., 2013a). Genetically, the three strains comprised the same set of enzymes around the pyruvate node, namely pyruvate carboxylase, phosphoenolpyruvate carboxylase, pyruvate kinase, phosphoenolpyruvate carboxykinase, and malic enzyme, offering the same options to redirect fluxes upon genetic perturbation (Becker et al., 2008; Huang et al., 2013a; Meza et al., 2012). A possible explanation for the different behaviour could be the used carbon sources, *i. e.* mannitol on one hand (this work) and, on the other hand, glucose (Peters-Wendisch et al., 1993). Mannitol-grown *actinobacteria* exhibit a highly different intracellular flux distribution as compared to glucose (Hoffmann et al., 2018; Hoffmann et al., 2021), and, therefore, might respond differently to the absence of *ppc*. What remained unclear, however, was the reason for the negative effect of the *ppc* deletion on nybomycin production. Previously, increased production of FK506 (built from chorismic acid as precursor) was observed in a *ppc* deletion mutant of *S. tsukubaensis* (Huang et al., 2013a). More work would be needed to understand the underlying effects better.

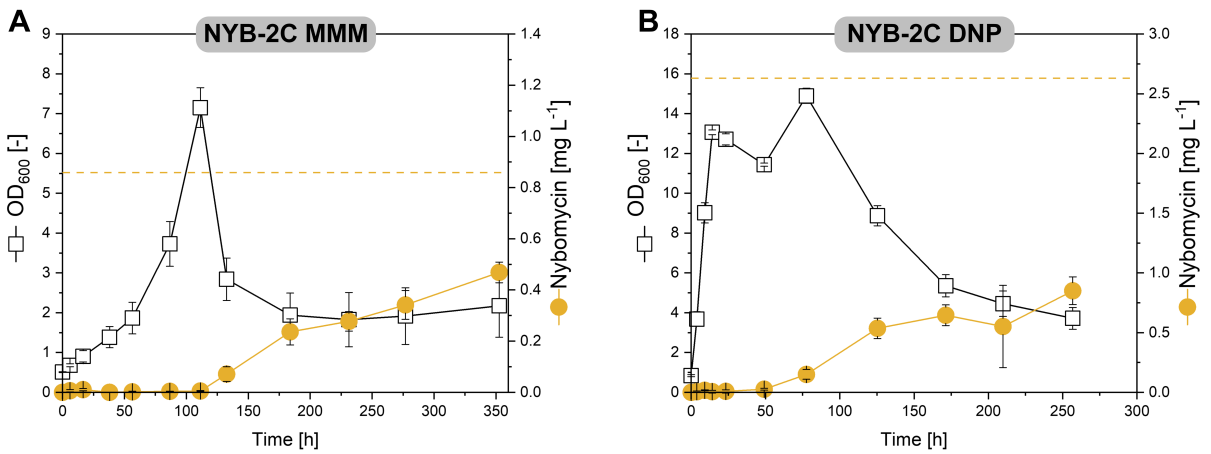

Figure 28: Time profiles for growth and nybomycin production of engineered NYB-2C strain. The data represent OD_{600} (open squares) and nybomycin titer (yellow circles) of *Δppc* (NYB-2C) deletion strain grown in minimal mannitol medium (A) and complex DNP medium (B). The dashed yellow lines indicate the nybomycin titer of the basic producer *S. albus* 4N24. The data represent mean values and corresponding standard deviations from three biological replicates.

Next, focus was on the nybomycin biosynthetic pathway. Spurred by the fact that nybomycin production could be driven by enhanced precursor supply **(Figure 25, Figure 26)**, overexpression of *nybM*, encoding acetoacetyl-CoA synthase which supplied two acetoacetyl-CoA residues to assemble the nybomycin core **(Figure 6, Figure 20, Figure 21),** was targeted. The created strain NYB-3A (4N24 P_{kasOP*} *nybM*), however, formed only 300 µg L^{-1} of the antibiotic, almost three-fold less than the basic producer **(Figure 29A, Figure 33)**. Furthermore, the mutant was heavily impaired in vitality, growing much slower, compared to the basic strain **(Figure 29A)**. Previously, the overexpression of acetoacetyl-CoA synthase in *S. cerevisiae* resulted in a similar phenotype in the way that it did not increase (acetoacetyl-CoA-based) sesquiterpene production, and it was concluded that the advanced supply of acetoacetyl-CoA could potentially stimulate its thiolysis and result in a futile cycle (Tippmann et al., 2017). In this regard, acetoacetyl-CoA synthase overexpression in NYB-3A might have affected the availability of malonyl-CoA, a key precursor of native fatty acid biosynthesis that requires fine-tuned balancing to avoid limiting and even toxic effects (Pizer et al., 2000).

Furthermore, the nybomycin cluster contained *nybV*, encoding for a putative transporter. As shown in parallel studies, the deletion of this gene reduced nybomycin formation in *S. albus* 4N24 (personal communication Marta Rodriguez-Estevez, Andriy Luzhetskyy, Pharmaceutical Biotechnology, Saarland University). Therefore, enhanced product export was aimed for. To this end, the *nybV* overexpressing strain NYB-3B was generated (4N24 P_{kasOP*} *nybV*). However, the transporter mutant showed weak growth and low nybomycin production **(Figure 29B, Figure 33A)**. This finding differed from previous examples that reported increased production of tetracycline (Yin et al., 2017), pristinamycin (Jin et al., 2010), and avermectin (Qiu et al., 2011) in strains with increased export capacity. On the other hand, increased abundance of native and heterologous transporters has been shown to potentially reduce the integrity of the cell membrane and thus cell viability (Wagner et al., 2007), particularly when the protein of interest was overexpressed at high level (Kind et al., 2011; Rohles et al., 2022). Taken together, none of the two targets appeared useful for further engineering of *S. albus*.

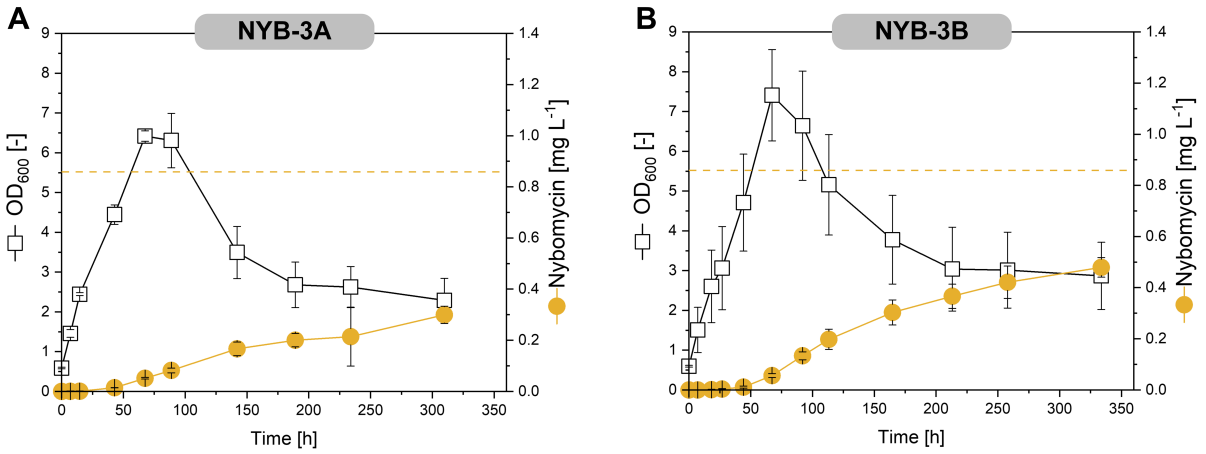

Figure 29: Time profiles for growth and nybomycin production of engineered 3rd generation strains. The data represents OD_{600} (open squares) and nybomycin titer (yellow circles) of *nybM* (NYB-3A) (A) and *nybV* (NYB-3B) (B) expressing strains driven by P_{kasOP*} grown in minimal mannitol medium. The dashed yellow lines indicate the nybomycin titer of the basic producer *S. albus* 4N24. The data represent mean values and corresponding standard deviations from three biological replicates.

4.6 Combinatorial effects of genes promoting nybomycin production

4.6.1 Synergistic impact of *tkt*, *zwf* and *nybF* expression

As shown, individual overexpression of the native genes *tkt*, and *zwf2*, and the heterologous genes *aroG*^{D146N} (*E. coli*), *aro I*^{S187C} (*C. glutamicum*), and *nybF* (*S. albus*, subsp. *chlorinus*), allowed to enhance nybomycin production, while other targets failed. Based on these findings, a combination of beneficial targets could enable further improvement. Hereby, focus was placed on complementary combinations of *tkt*, *zwf2*, and *nybF*, and double combinations and the triple combination were created, yielding strains NYB-4A (P_{kasOP*} *tkt zwf2*), NYB-4B (P_{kasOP*} *nybF zwf2*), NYB-4C (P_{kasOP*} *nybF tkt*), and NYB-4D (P_{kasOP*} *nybF tkt zwf2*) **(Figure 21)**. The double combination mutants enabled substantial improvement in terms of titer and productivity. The co-expression of *nybF* with a PP pathway gene was most successful. It resulted in almost two-fold more nybomycin in strains NYB-4B (1,644 µg L^{-1}) and NYB-4C (1,638 µg L^{-1}) as compared to the basic producer **(Figure 30BC, Figure 33A)**. The corresponding increase in maximum productivity was even three-fold (NYB-4B) and four-fold (NYB-4C) **(Figure 33B)**. Notably, the combinatorial effects for the two strains were more than additive. As example, the titer increase for the NYB-4B strain was more than 50% higher (+779 µg L^{-1}) than the sum of the increase observed for the single overexpression strains (+511 µg L^{-1}). The co-expression of two PP pathway genes *tkt* and *zwf2* in strain NYB-4A, yielded 1,3347 µg L^{-1} **(Figure 30A)**. Surprisingly, the triple mutant (NYB-4D) that overexpressed *nybF*, *tkt* and *zwf2,* revealed weak performance **(Figure 30D)**, and was even less efficient than the basic producer, although its growth was unchanged. Eventually, the combined effects were too strong and caused an imbalance in metabolism, as observed before. Similarly, previous metabolic engineering efforts caused unforeseen effects on antibiotic formation and sporulation in *S. lividans* due to high intracellular NADPH levels (Jin et al., 2017).

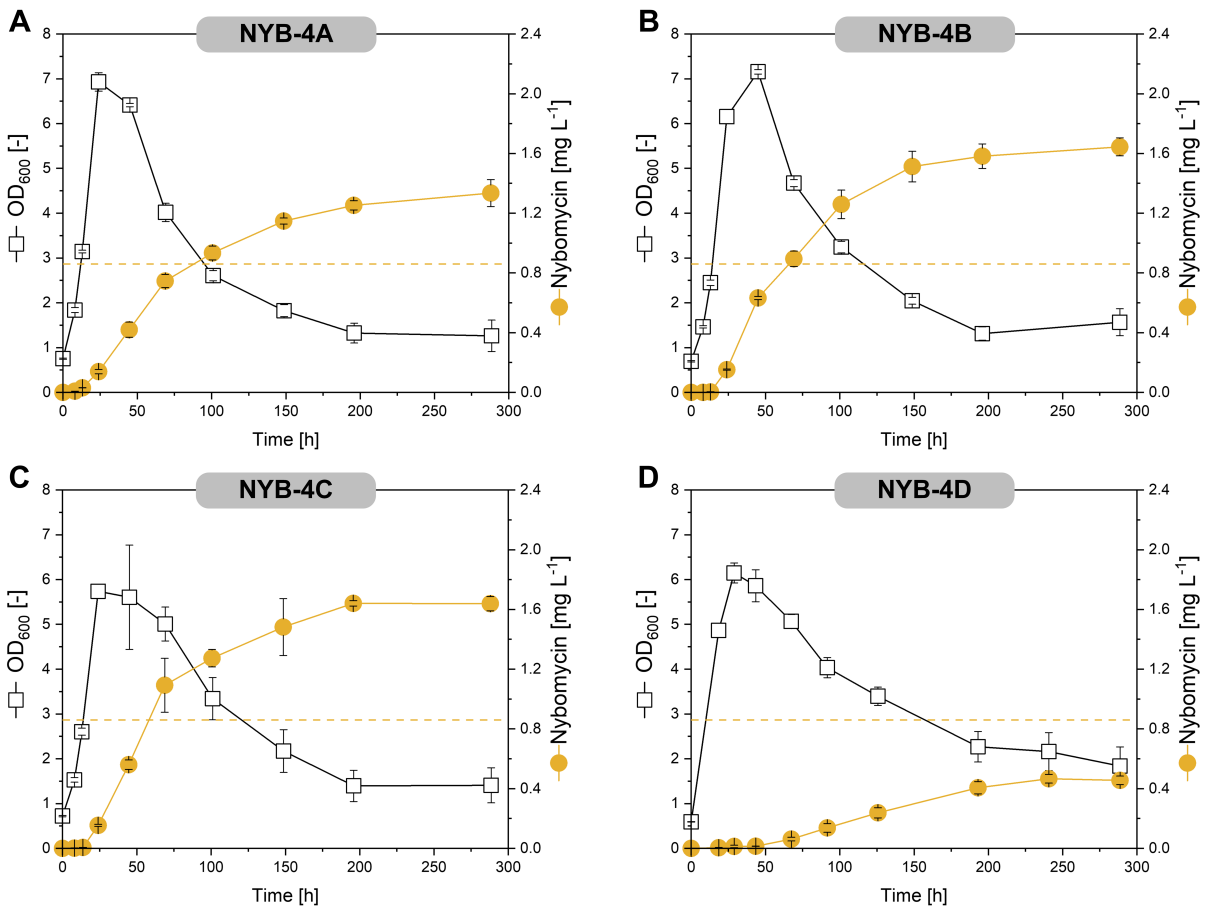

Figure 30: Time profiles for growth and nybomycin production of engineered combinatorial 4th generation strains. The data show OD_{600} (open squares) and nybomycin titer (yellow circles) of *tkt zwf2* (NYB-4A) (A), *nybF zwf* (NYB-4B) (B), *nybF tkt* (NYB-4C) (C) and *nybF tkt zwf2* (NYB-4D) (D) expressing strains driven by P_{kasOP*} grown in minimal mannitol medium. The dashed yellow lines indicate the nybomycin titer of the basic producer *S. albus* 4N24. The data represent mean values and corresponding standard deviations from three biological replicates.

4.6.2 Influence of regulator *nybW* on nybomycin titer and productivity

As shown, metabolic engineering efforts that were directed to individual steps of the terminal assembly of nybomycin, failed to provide the product at higher level **(Figure 20, Figure 33)**. It was hypothesized that the nybomycin pathway might require a balanced expression of its different genes to achieve increased flux, as previously observed during metabolic engineering of other microbial biosynthetic routes (Giesselmann et al., 2019; Jones et al., 2015). For coordinated activation, biosynthetic gene clusters for natural products typically contain specific regulator genes (Bednarz et al., 2019; Liu et al., 2013; Schwentner et al., 2019) and the removal of such regulatory elements had been found helpful to overproduce the antibiotics daptomycin (Mao et al., 2017) and chromomycin (Sun et al., 2018), respectively.

Previously, *nybW* had been suggested as a potential regulatory element of the nybomycin pathway, based on sequence homology (Rodriguez Estevez et al., 2018). Interestingly, the deletion of *nybW* had enabled slightly improved nybomycin production during qualitative inspection for functional characterization of the cluster **(Figure 5A**). Therefore, the regulator deficient mutant *S. albus* NYB-5 (4N24 Δ*nybW*) was constructed **(Figure 21)**. When grown on the minimal mannitol medium, strain NYB-5 achieved a nybomycin titer of 1,418 µg L^{-1}, 70% more than the basic strain **(Figure 31)**. Hereby, the strain grew well, indicating that the genetic modification did not interfere with vitality. The biggest change in the mutant, however, was a drastically accelerated production. Nybomycin formation started much earlier, while cells were still growing, resulting in a production rate that was higher than that of all other strains **(Figure 31, Figure 33)**. While the basic strain produced nybomycin mainly in the stationary phase, the regulatory mutant accumulated the product in both phases, regardless of the growth state. The maximum titer could therefore be reached already after 125 h, offering to strongly shorten the overall process. This acceleration appeared useful, as secondary metabolites are produced mainly in the late growth or stationary phase (Ferraiuolo et al., 2021) so that the industrial processes using *Streptomyces* are usually very long and result in low productivities (Pereira et al., 2008).

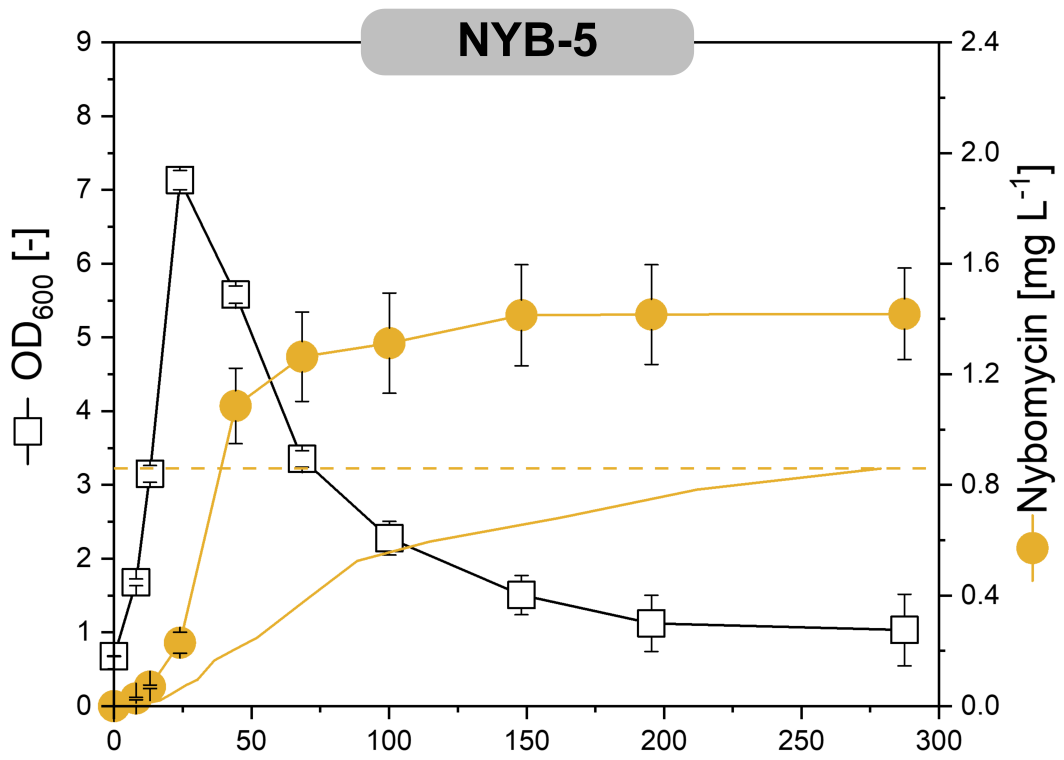

Figure 31: Time profile for growth and nybomycin production of engineered 5th generation strain NYB-5. The data represent OD_{600} (open squares) and nybomycin titer (yellow circles) of 4N24 *ΔnybW* (NYB-5) grown in minimal mannitol medium. The solid and dashed yellow lines indicate the nybomycin production profile and the final nybomycin titer of the basic producer *S. albus* 4N24, respectively. The data represent mean values and corresponding standard deviations from three biological replicates.

4.6.3 Benefits of combining primary metabolism engineering and cluster deregulation

Subsequently, the Δ*nybW* mutation was combined with all other high-performance targets. A set of sixth generation producers was constructed, comprising three-target combinations, i. e. NYB-6A (4N24 Δ*nybW* P_{kasOP*} *tkt zwf2),* NYB-6B (4N24 Δ*nybW* P_{kasOP*} *nybF zwf2)*, and NYB-6C (Δ*nybW* P_{kasOP*} *nybF tkt*). The Δ*nybW* modification massively increased the productivity in all strains, revealing beneficial synergetic effects of the targets **(Figure 33B)**. Hereby, strains NYB-6B and NYB-6C achieved the highest titer **(Figure 32BC, Figure 33A**). All three mutants showed the favourable growth state-decoupled production phenotype. A quadruple mutant, namely NYB-7 (4N24 Δ*nybW* P_{kasOP*} *nybF tkt zwf2*) was constructed as well. Nybomycin production in this strain, however, was almost abandoned (70 µg L^{-1}) **(Figure 32D, Figure 33A)**. Obviously, the growth-deficiency of the parent strain NYB-4D could not be rescued by deletion of the regulator. In comparison to the basic strain, the two best producers NYB-6B

and NYB-6C formed the reverse antibiotic at almost two-fold higher titer and up to seven-fold higher productivity. Taken together, systems metabolic engineering of *S. albus* 4N24 through several cycles of optimization, substantially upgraded nybomycin production.

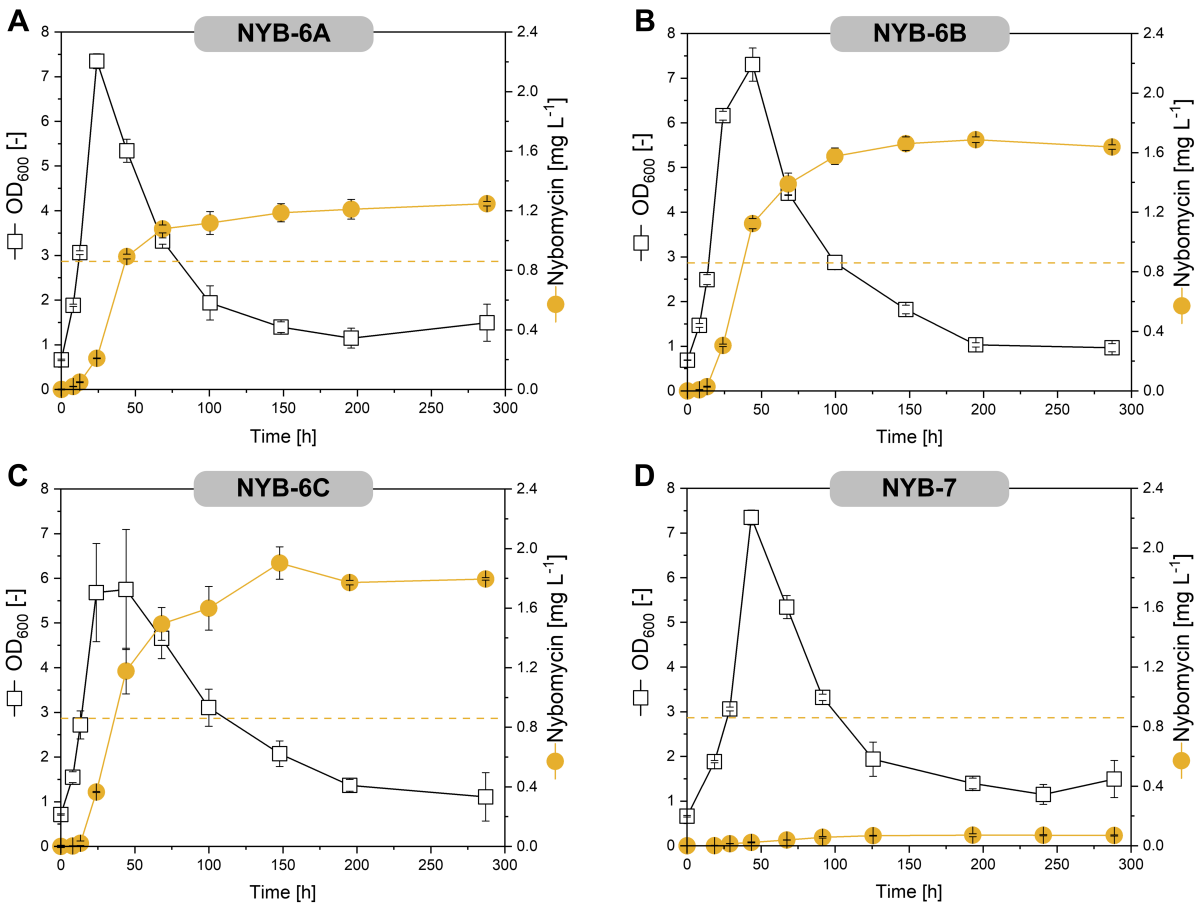

Figure 32: Time profiles for growth and nybomycin production of engineered 6th and 7th generation strains. The data represent OD_{600} (open squares) and nybomycin titer (yellow circles) of *tkt zwf2* (NYB-6A) (A), *nybF zwf* (NYB-6B) (B), *nybF tkt* (NYB-6C) (C) and *nybF tkt zwf2* (NYB-7) (D) expressing *ΔnybW* strains driven by P_{kasOP*} grown in minimal mannitol medium. The dashed yellow lines indicate the nybomycin titer of the basic producer *S. albus* 4N24. The data represent mean values and corresponding standard deviations from three biological replicates.

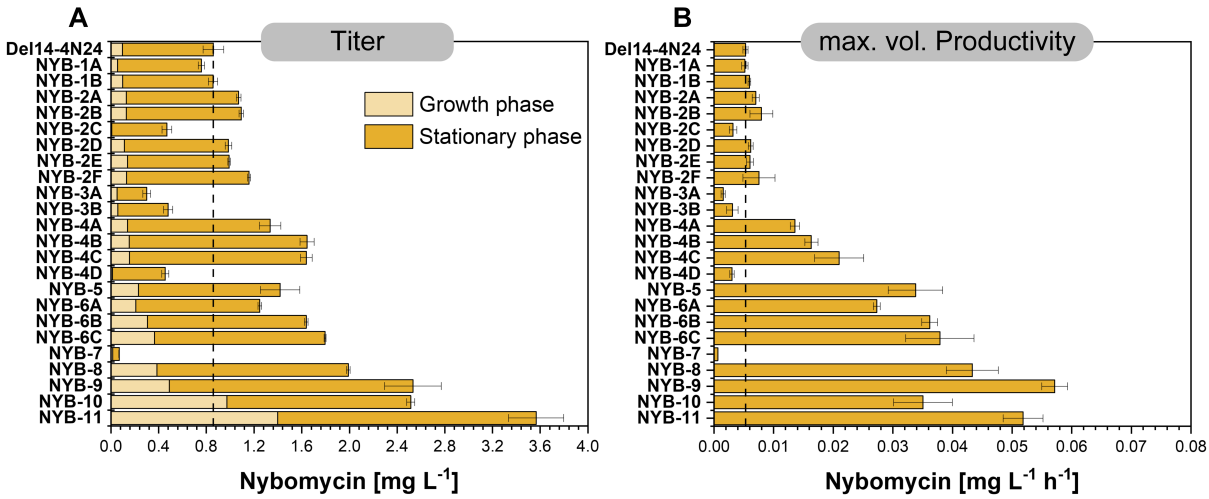

Figure 33: Overview of nybomycin titer and maximal volumetric productivity of generated strains. The data display nybomycin titer split in production during growth (light yellow) and stationary phase (yellow) (A) and maximal volumetric productivity (B) of all engineered *S. albus* strains grown in minimal mannitol medium with 10 g L^{-1} mannitol. Black dashed line indicates the respective reference values for the basic producer strain *S. albus* 4N24 in the same culture conditions. The data represent mean values and corresponding standard deviations from three biological replicates.

4.7 Optimization of the production process

S. albus NYB-6B was chosen to benchmark the achieved performance. First, a dextrin-based DNP medium, a complex mixture that is commonly chosen for natural product formation in *Streptomyces* (Ahmed et al., 2020; Paulus et al., 2022; Rodríguez Estévez et al., 2020), including the previous production of nybomycin in *S. albus* 4N24 (Rodriguez Estevez et al., 2018) was used. When grown on a formulation with 40 g L^{-1} of dextrin (DNP40), the NYB-6B overproducer formed 4.1 mg L^{-1} of nybomycin, almost 60% more than the basic strain **(Figure 34B)**. Interestingly, the production mainly occurred during the initial growth phase. The use of an increased dextrin level (75 g L^{-1}, DNP75) resulted in a prolongation of production and a final nybomycin titer of 5.5 mg L^{-1} **(Figure 34C)**.

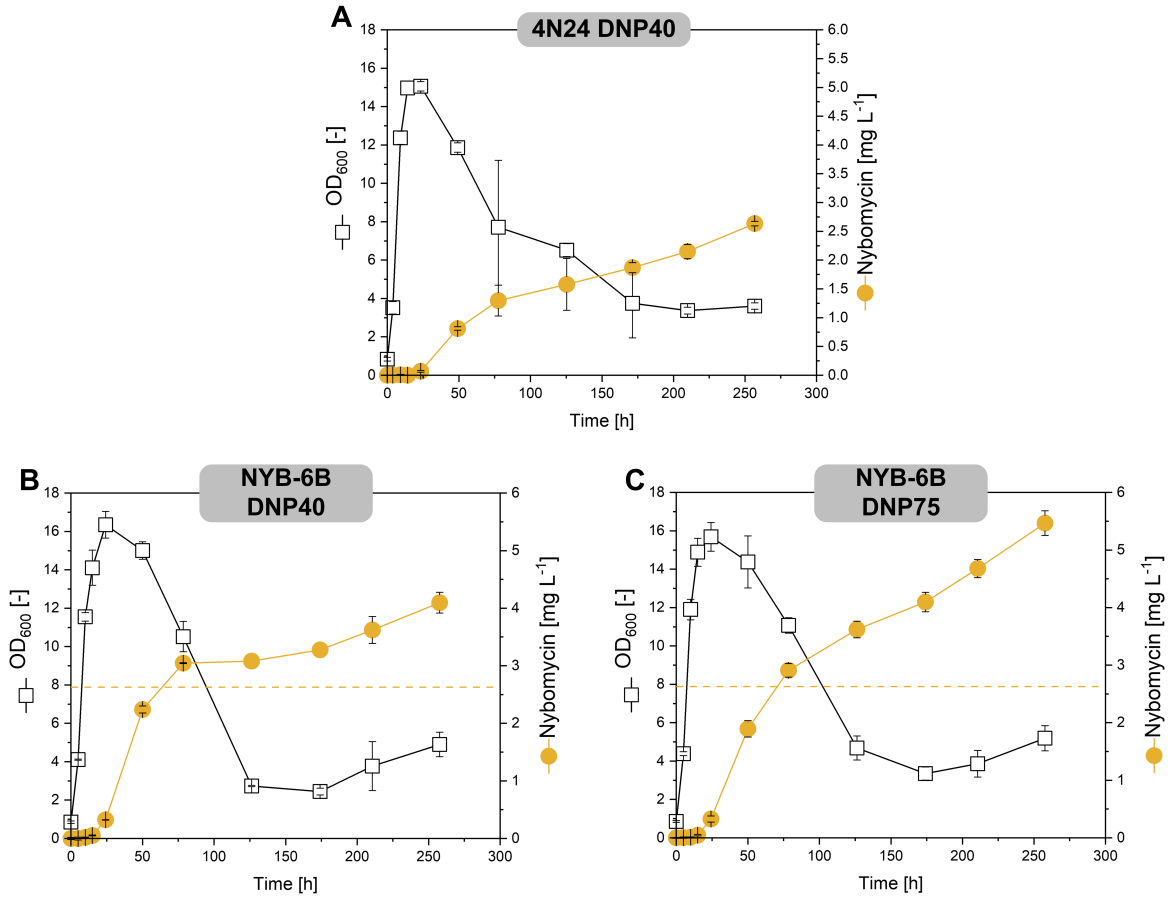

Figure 34: Time profiles for growth and nybomycin production of *S. albus* 4N24 and engineered NYB-6B strains in complex medium. The data outline OD_{600} (open squares) and nybomycin titer (yellow circles) of the basic producer strain (*S. albus* 4N24, DNP40) (A) and the *nybF zwf* (NYB-6B) expressing strain with deletion of *nybW* in DNP40 (B) and DNP75 (C) medium, respectively. The dashed yellow lines indicate the nybomycin titer of the basic producer *S. albus* 4N24. The data represent mean values and corresponding standard deviations from three biological replicates.

Next, the strain was studied on the minimal medium formulation at increased initial mannitol (25 g L^{-1}, 50 g L^{-1}, 75 g L^{-1}) and phosphate levels (1.0 g L^{-1}, 2.0 g L^{-1}, 3.0 g L^{-1}) **(Figure 35)**. The recombinant strain performed well in all set-ups and reached a final nybomycin titer of 7.2 mg L^{-1} (7,185 µg L^{-1}) for the highest substrate level tested, reflecting an overall 8.3-fold improvement of production. The higher the initial concentration of mannitol, the longer the nybomycin production was sustained and the higher was the final titer. Admittedly, growth of the cells was slightly delayed when using 75 g L^{-1} mannitol, so that the production required about 200 h. At 25 and 50 g L^{-1} mannitol, growth was not affected, and biomass was built up quickly, until mannitol was completely consumed. Accordingly, the maximum titer was reached earlier, resulting in a substantially higher maximum productivity **(Figure 33)**. Notably in all cases, the product was already formed in the presence of phosphate; the deregulated cluster expression enabled this superior production phenotype.

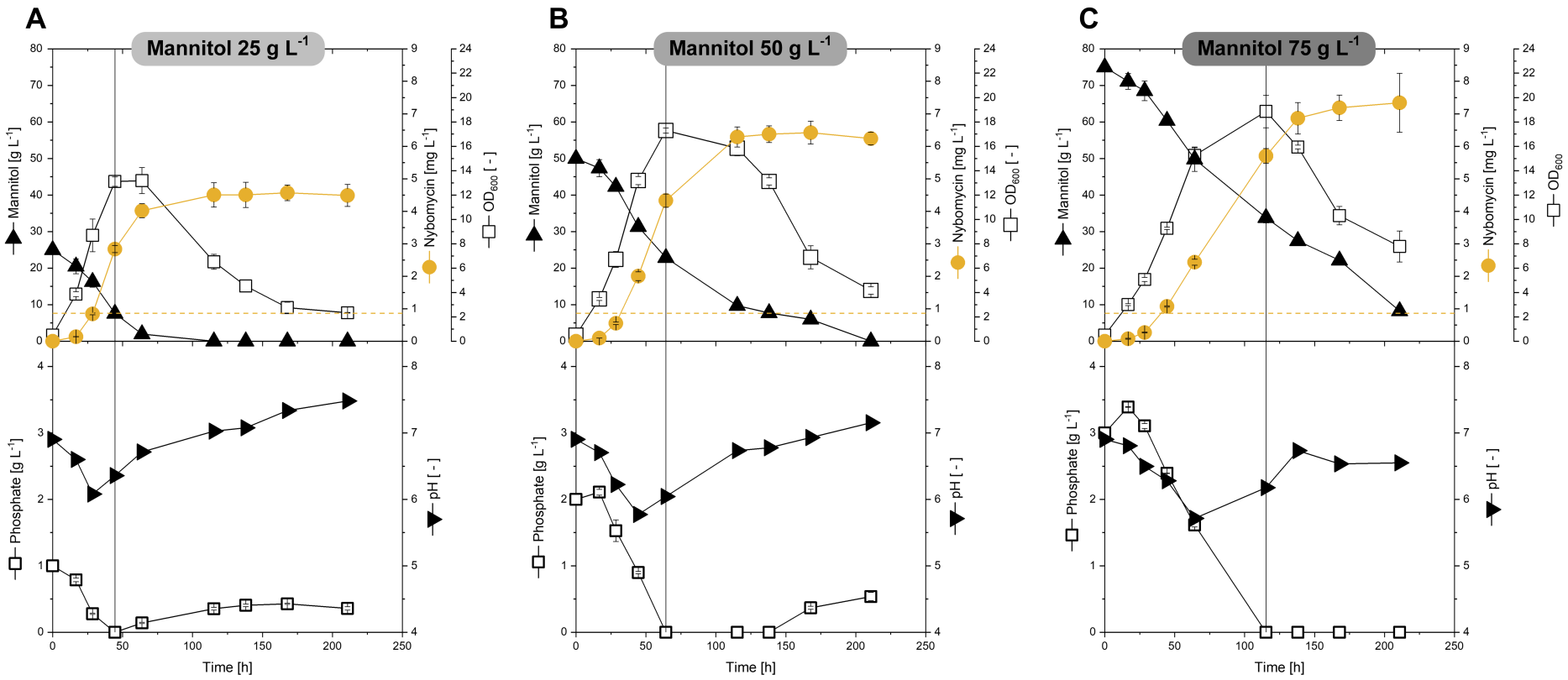

Figure 35: Cultivation time profiles of the engineered top producer strain NYB-6B in optimized minimal mannitol medium. The data represent strain NYB-6B grown in minimal mannitol medium with adapted mannitol (25 g L^{-1}, 50 g L^{-1} and 75 g L^{-1}) and phosphate (1 g L^{-1}, 2 g L^{-1} and 3 g L^{-1}) concentrations including analysis of OD_{600} (open squares, upper panel), nybomycin (yellow circles, upper panel), mannitol (solid triangles, upper panel), phosphate (open squares, lower panel) and pH (solid squares, lower panel). The dashed yellow lines indicate the nybomycin titer of the basic producer *S. albus* 4N24 grown in minimal mannitol medium with common mannitol (10 g L^{-1}) and phosphate (0.5 g L^{-1}) concentrations. The data represent mean values and corresponding standard deviations from three biological replicates.

4.8 Transcriptomic insights

4.8.1 Gene expression of *S. albus* 4N24 in the growth and the stationary phase

Next, RNA sequencing of *S. albus* Del14 4N24 was conducted to shed light on the changes related to the shift from growth (13 h) to nybomycin production (70 h) **(Figure 18)**, given the highly informative value of transcriptomic data to evaluate metabolically engineered strains (Kohlstedt et al., 2014; Kohlstedt et al., 2022; Schilling et al., 2007). The expression of 2044 out of totally 5790 encoded genes (35.3 %) significantly differed between the growth and the production phase (log2-fold change $\geq$ 1, p $\leq$ 0.05), whereby 868 genes were found downregulated, and 1176 genes were found upregulated.

Regarding the high-flux pathways of carbon core metabolism, precursor supply, and nybomycin biosynthesis, the analysis provided important insights **(Figure 36)**. Expectable from the depletion of mannitol and the stop of growth, the cells downregulated genes encoding mannitol import and metabolization (up to log2-fold 5.7), the EMP pathway, and most TCA cycle enzymes during the stationary phase. This picture matched with related strains (Hwang et al., 2019; Lee et al., 2022). An interesting exception was the upregulation of genes encoding the succinate dehydrogenase complex II (5662, 5663, and 5664) and the upstream conversion of L-glutamate to succinate. The succinate dehydrogenase complex has a unique dual function, in that it converts succinate to fumarate in the TCA cycle and channels electrons to the respiratory chain (Huang and Millar, 2013; Park et al., 1995) thereby preventing the production of superoxide anion ($O2^-$), an oxygen reactive species (Dalla Pozza et al., 2020; Hwang et al., 2014). Eventually, its upregulation was linked to protection. Furthermore, the cells activated catabolic routes for the degradation of branched-chain amino acids (L-valine, L-leucine, L-isoleucine) and lipids, respectively (log2-fold up to 5.7), eventually to mobilize internal carbon (Gläser et al., 2021) **(Figure 36)**. Notably, these pathways yielded acetyl-CoA as central intermediate (Fujita et al., 2007; Kaiser and Heinrichs, 2018; Massey et al., 1976; Pavoncello et al., 2022). In addition, the cells upregulated routes to synthetize acetoacetyl-CoA from acetyl-CoA. Nybomycin biosynthesis required CoA-based carbon so that, overall, the activated acetyl-CoA supply appeared favorable. Eventually, it was even sufficient. This

would at least explain the fact, that the overexpression of *nybM* did not provide any improvement in production. In terms of precursor supply, however, genes encoding enzymes of the PP pathway and the shikimate and chorismate routes were found reduced in expression during the production phase **(Figure 36)**, presumably limiting the supply of 4-aminoanthranilate for nybomycin biosynthesis **(Figure 6)**. In this regard, the overexpression of *zwf* and *tkt*, as well as the DAHP-encoding variants $aroG^{D146N}$, $aro\ I^{S187C}$, and *nybF*, respectively, appeared as good choice to overcome the naturally occurring downregulation.

The expression pattern of the nybomycin cluster, inspected next, was very surprising. The cluster was highly expressed during the non-producing growth phase and largely downregulated during the major nybomycin production phase. During the major production phase, almost all cluster genes were reduced in expression (log2-fold changes up to -3.4). except for *nybV*, encoding the nybomycin exporter, and the presumable regulators *nybX, nybZ*, and *nybY*. This diametral behavior appeared extremely unfavorable in terms of production performance. Typically, BGCs are activated when cells enter the stationary phase and start forming natural products, and this is regarded a major feature for high-level production (Bobek et al., 2021; Gramajo et al., 1993; Holt et al., 1992; Kormanec et al., 2014; Novakova et al., 2022; Zhu et al., 2022). Regarding global regulation, genes encoding sigma factors and presumed regulators revealed complex changes over time, which mirrored the picture, observed for other *S. albus* Del14 derivatives (Gläser et al., 2021), when shifting from growth to the stationary phase **(Table 8).**

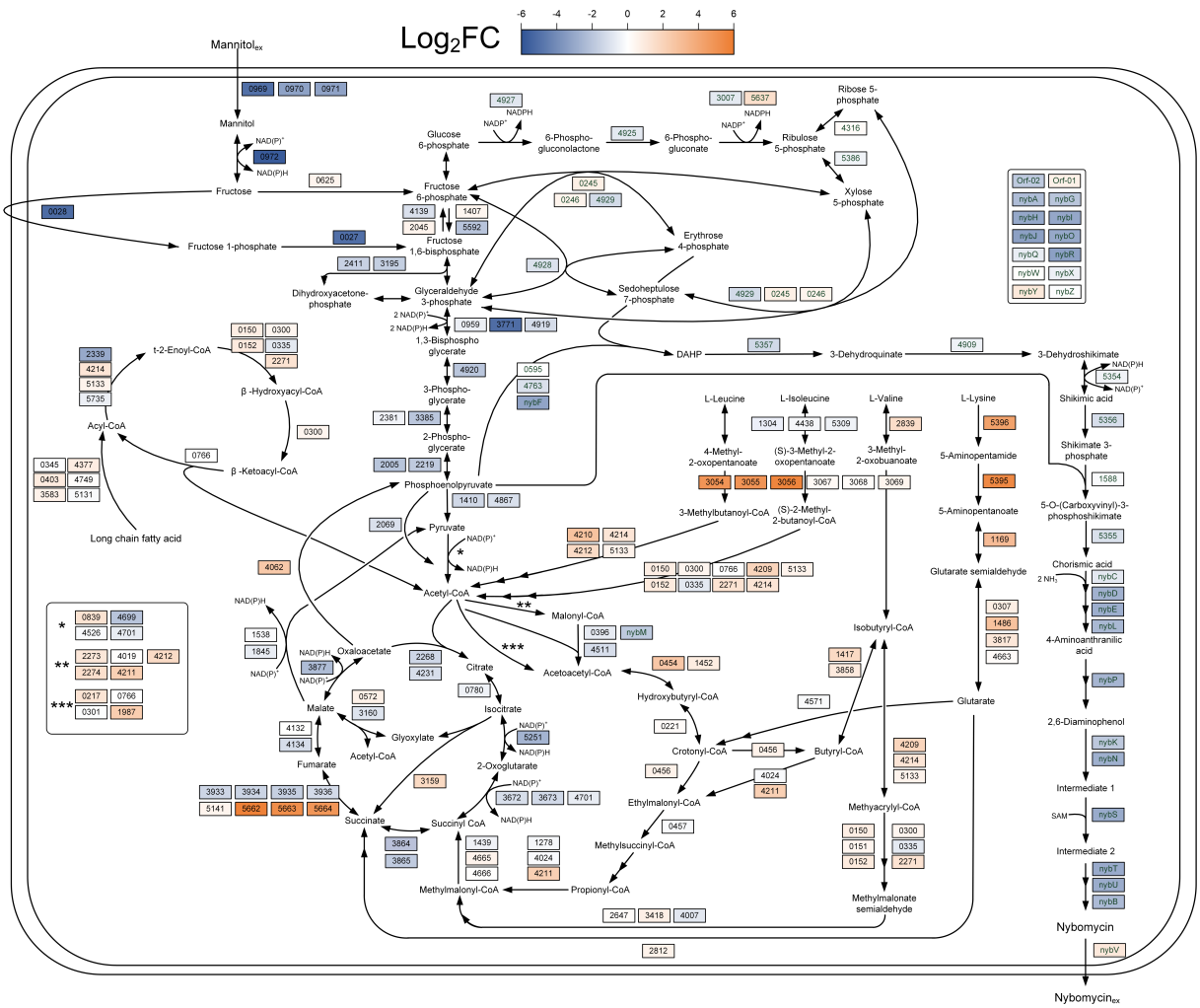

Figure 36: Dynamic gene expression changes of the basic nybomycin producer *S. albus* 4N24. The data reflect expression differences between the growth phase (13 h, used as reference) and the major nybomycin production phase (70 h) and include genes encoding enzymes of major catabolic and anabolic pathways, nybomycin biosynthesis, and precursor supply. Enzymes were assigned to certain reactions based on KEGG pathway maps and gene annotations, obtained during RNA sequencing. For all samples, the biological replicates clustered closely indicating an excellent data quality (**Figure 62**, **Figure 63**). The data represent mean values and corresponding standard deviations from three biological replicates.

4.8.2 Transcriptomic changes of advanced nybomycin producers

Next, the transcriptome in different producers was compared to trace effects that resulted from the successive rounds of strain engineering (**Figure 37)**. To this end, a genealogy of three differently performing *zwf*-based mutants was performed: NYB-2B (*zwf*), NYB-4B (*nybF zwf*), and NYB-6B (*ΔnybW nybF zwf*). In addition, the *tkt*-based derivative NYB-6C (*ΔnybW nybF tkt*) was included, but to cut a long story short, it was almost identical to NYB-6B, except for the two differently engineered genes. Generally, targeted genes (*nybF, zwf* and *tkt*) were found

strongly overexpressed during the growth as well the production phase, unravelling that (i) the P_{kasOP*} promotor reliably enabled increased expression and (ii) the genetic modifications indeed boosted increase nybomycin production. Based on these findings, its recommended to use the synthetic P_{kasOP*} promotor and its derivatives **(Figure 24)** for metabolic engineering efforts in *S. albus* and related strains (Ahmed et al., 2020), which require growth-independent constitutive overexpression of target genes.

Notably, the deletion of *nybW* increased the expression of several upstream cluster genes, namely *nybQRSTUV*, whereby the increase for *nybUV* was much higher than that of the other genes **(Figure 37B)**. Within the cluster, the genes *nybQRSTUV* were transcribed in the same direction **(Figure 4A)**, allowing the conclusion that their expression was under control of the NybW repressor.

The expression data of the other 18 cluster genes during the major production phase were, however, surprising. Compared to the basic producer, the strains NYB-4B, NYB-6B, and NYB-6C exhibited a strong down-regulation of these genes. This change indicated a serious bottleneck, limiting production. All advanced strains, for unknown reason, exhibited a slightly elevated expression of *nybXYZ*, encoding for two regulators (*nybX, nybZ*) and a small protein (87 AA) of unknown function **(Figure 4A)**. Considering that the regulators were presumably repressors, their upregulation could have indeed caused the observed downregulation of most of the cluster genes, i. e. all genes that were not controlled by n*ybW*. Interestingly, the single gene deletion strains *nybX*, *nybY*, and *nybZ* exhibited massively reduced nybomycin titers which, at first glance, seemed to rule out the elimination of the regulatory genes as a target for optimization (personal communication, Marta Rodriguez Estevez, Andriy Luzhetskyy, Pharmaceutical Biotechnology, Saarland University). The unraveled expression dynamics, however, indicated that the regulators acted together or depended on each other, so that the remaining repressor genes in single gene deletion mutants could have been still able to repress the cluster.

On the other hand, the genetic modifications of the primary metabolism affected the expression of the correspondingly chosen target gene rather locally but did not cause broader effects, e. g. within the EMP and PP pathways, the TCA cycle, and related routes **(Figure 37CDEF)**. This

observation implied that genes encoding enzymes, upstream or downstream of the modified step in the corresponding pathway, were sufficiently expressed to enable increased flux but still display promising targets for additional enhancement in the future (Becker et al., 2005; Buschke et al., 2013; Kind et al., 2010a; Rohles et al., 2016).

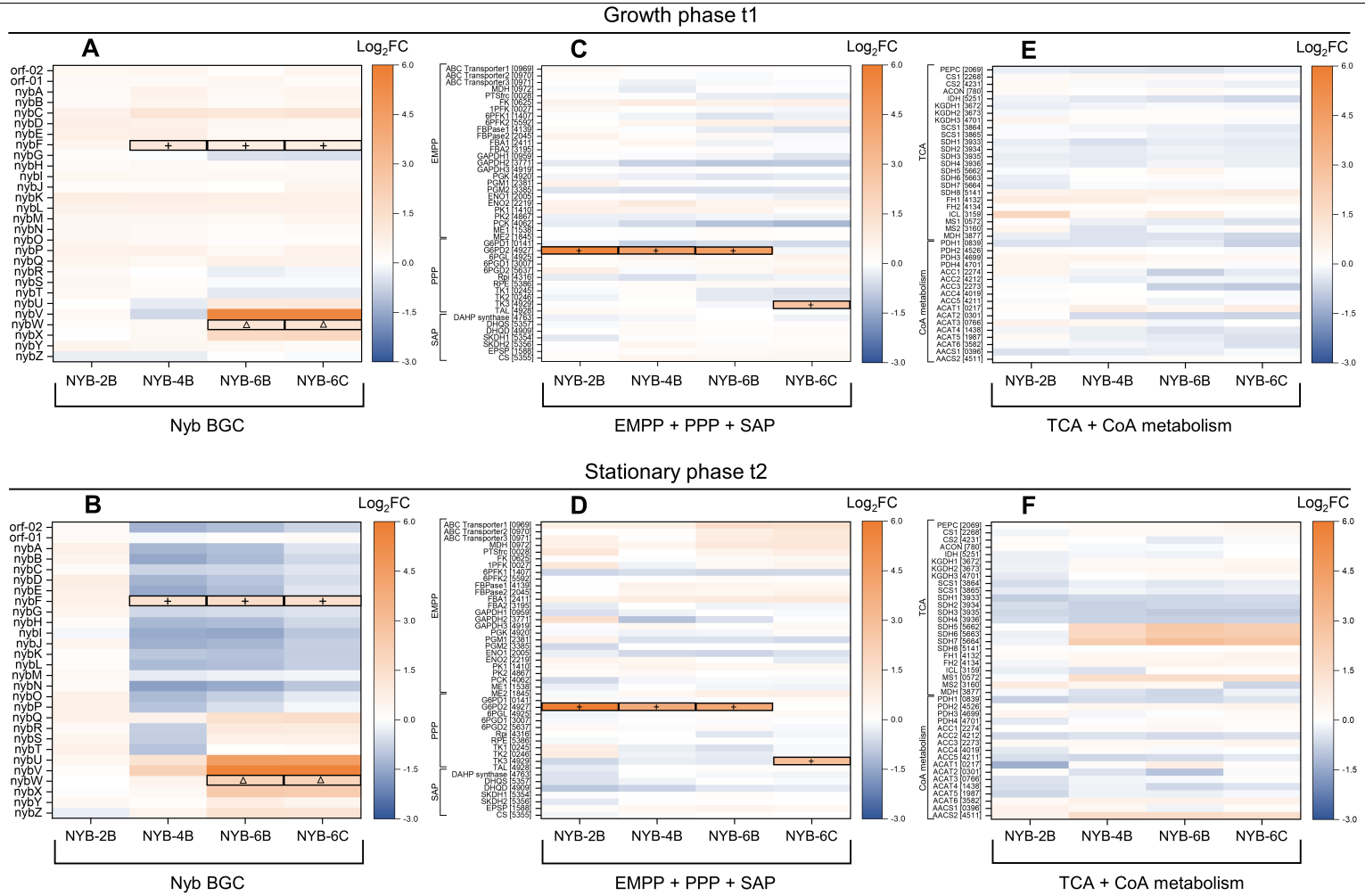

Figure 37: Global gene expression in different mutants of *S. albus* 4N24, metabolically engineered for nybomycin overproduction. The data reflect differences between the strains 4N24, NYB-2B, NYB-4B, NYM-6B, and NYB-6C during the growth phase (13 h) and the major nybomycin production phase (70 h). The data for the basic producer 4N24, analyzed after 13 h, are used as reference. The displayed genes include nybomycin biosynthesis (A, B), the Emden-Meyerhof-Parnas (EMP), the pentose phosphate (PP), and the shikimic acid (SA) pathways (C, D), as well as the TCA cycle and the reactions linked to the metabolism of CoA thioesters (E, F). Enzymes were assigned to certain reactions based on KEGG pathway maps and gene annotations, obtained during RNA sequencing. One should notice that (in the corresponding strains NYB-6B and NYB-6C) *nybW* was only partially deleted without affecting its promotor region to exclude neighboring effects. The detected *nybW* expression in NYB-6B and NYB-6C therefore proved the sustained activity of the promotor but did not reflect the expression of a functional NybW protein. The data represent mean values and corresponding standard deviations from three biological replicates.

4.9 Combinatorial engineering of primary and secondary metabolism

To elucidate the control of the cluster, engineering its regulatory part in strain 4N24 was targeted. Therefore, the genes *nybWX* and *nybWXYZ*, respectively, were replaced by a kanamycin resistance gene. The new strains NYB-8 (4N24 Δ*nybWX*) and NYB-9 (4N24 Δ*nybWXYZ*) were grown in mannitol minimal medium, after verifying the correctness of the introduced mutations by PCR and sequencing. NYB-8 accumulated 1,990 µg L^{-1} of nybomycin, while NYB-9 formed even 2,533 µg L^{-1}, up to three-fold more than the basic strain 4N24 **(Figure 38EF)**. Importantly, the data revealed that several regulators synergistically cooperated to control the expression of the cluster. The regulator NybW controlled the expression of *nybQRSTUV,* while the regulators encoded *nybXYZ* modulated the transcription of cluster genes further upstream. Therefore, the combined elimination of *nybW* plus *nybX* or *nybW* plus *nybXYZ*, respectively, was required to override the natural control and release the cluster from repression, whereas the single deletion of either *nybW, nybX, nybY*, or *nybZ* was not sufficient. Often, bacterial gene clusters contain several cluster-situated regulatory elements (Novakova et al., 2022; Sun et al., 2018; Zhu et al., 2017). The encoded multifunctional regulators can form a complex intricate regulatory network (Tsypik et al., 2021), as also observed here.

Merging all the obtained knowledge, final combinations applying the optimized primary metabolic pathway layout with the optimized layout of the nybomycin biosynthetic pathway were created. To this end, the de-regulated cluster mutants NYB-8 and NYB-9 were equipped with the best targets from the primary metabolism. Transformation of NYB-8 and NYB-9 with the integrative plasmid pBT1H-kasOP*-nybF-zwf2 resulted in the new strains NYB-10 (4N24 Δ*nybWX* P_{kasOP*} *nybF zwf2*) and NYB-11 (4N24 Δ*nybWXYZ* P_{kasOP*} *nybF zwf2*), respectively. Favourably, both cell factories produced more nybomycin than any other strain created before **(Figure 38GH)**. When tested in batch cultures, NYB-10 accumulated 2,557 µg L^{-1} of nybomycin, while NYB-11 even formed 3,567 µg L^{-1}, more than four-fold more than 4N24 **(Figure 33A)**. It was interesting to note that the major improvement in production occurred during the later culture stage, well matching with the newly in-built de-repression of the nybomycin cluster.

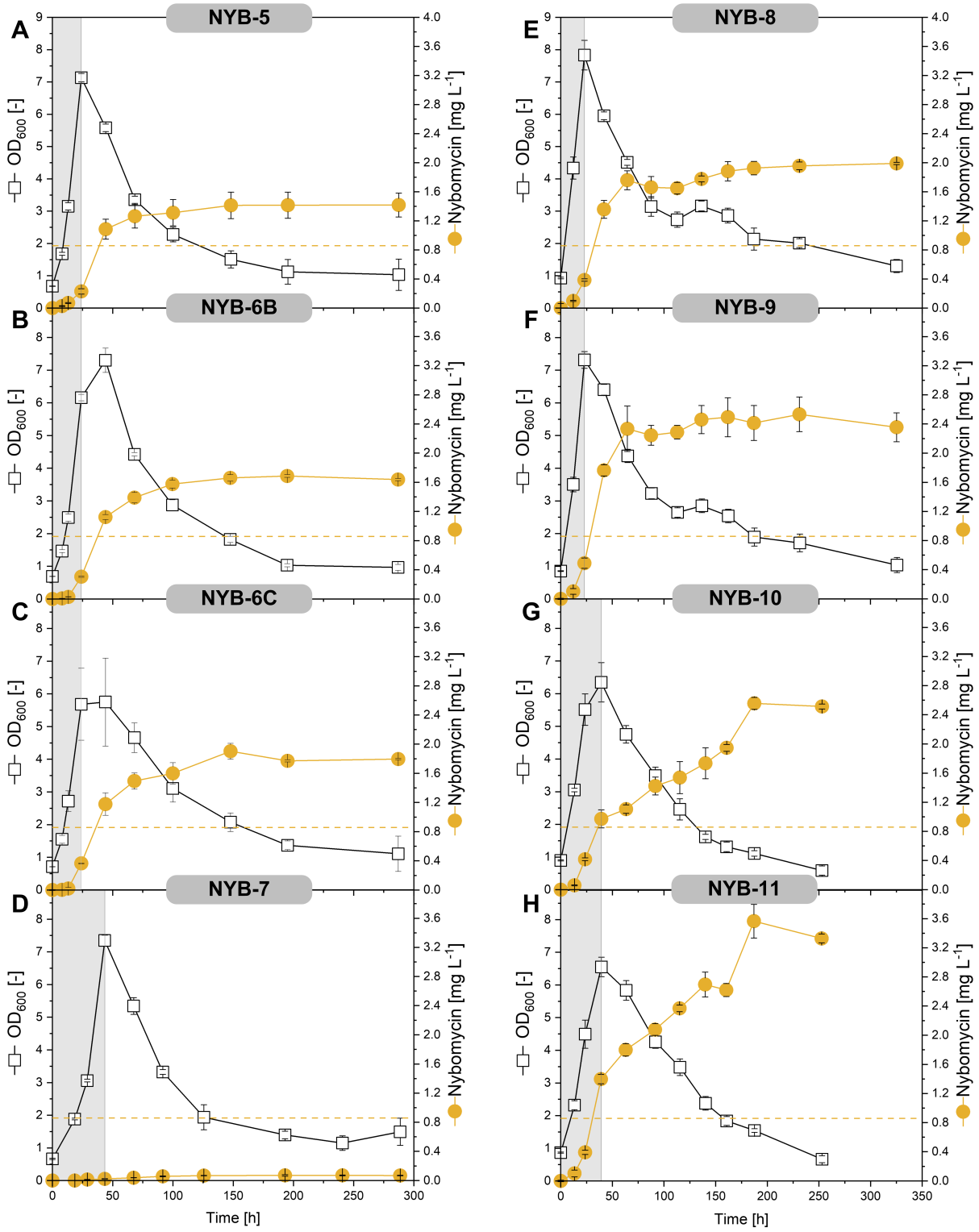

Figure 38: Time profiles for growth and nybomycin production in the advanced nybomycin cell factories *Streptomyces albus* NYB-5 (A), NYB-6B (B), NYB-6C (C), NYB-7 (D), NYB-8 (E), NYB-9 (F), NYB-10 (G), and NYB-11 (H). All strains were grown in shake flasks on minimal mannitol medium with 10 g L^{-1} mannitol. The corresponding genetic layouts are given in **Figure 21** and **Table 2**, respectively. The data outline OD_{600} (open squares) and nybomycin titer (yellow circles). Yellow dashed lines indicate the titer of the basic producer *S. albus* 4N24. The data represent mean values and corresponding standard deviations from three biological replicates.

Finally, the strains NYB-8, NYB-9, NYB-10, and NYB-11 were benchmarked on 50 g L^{-1} mannitol medium **(Figure 39, Figure 40)**. All mutants exhibited excellent production performance, whereby strain NYB-11 performed best during both culture phases and achieved the highest final nybomycin titer of 12 mg L^{-1}. Overall, systems metabolic engineering and a superior bioprocess at high initial substrate levels enabled an almost fifteen-fold increase in production of nybomycin from previous developments.

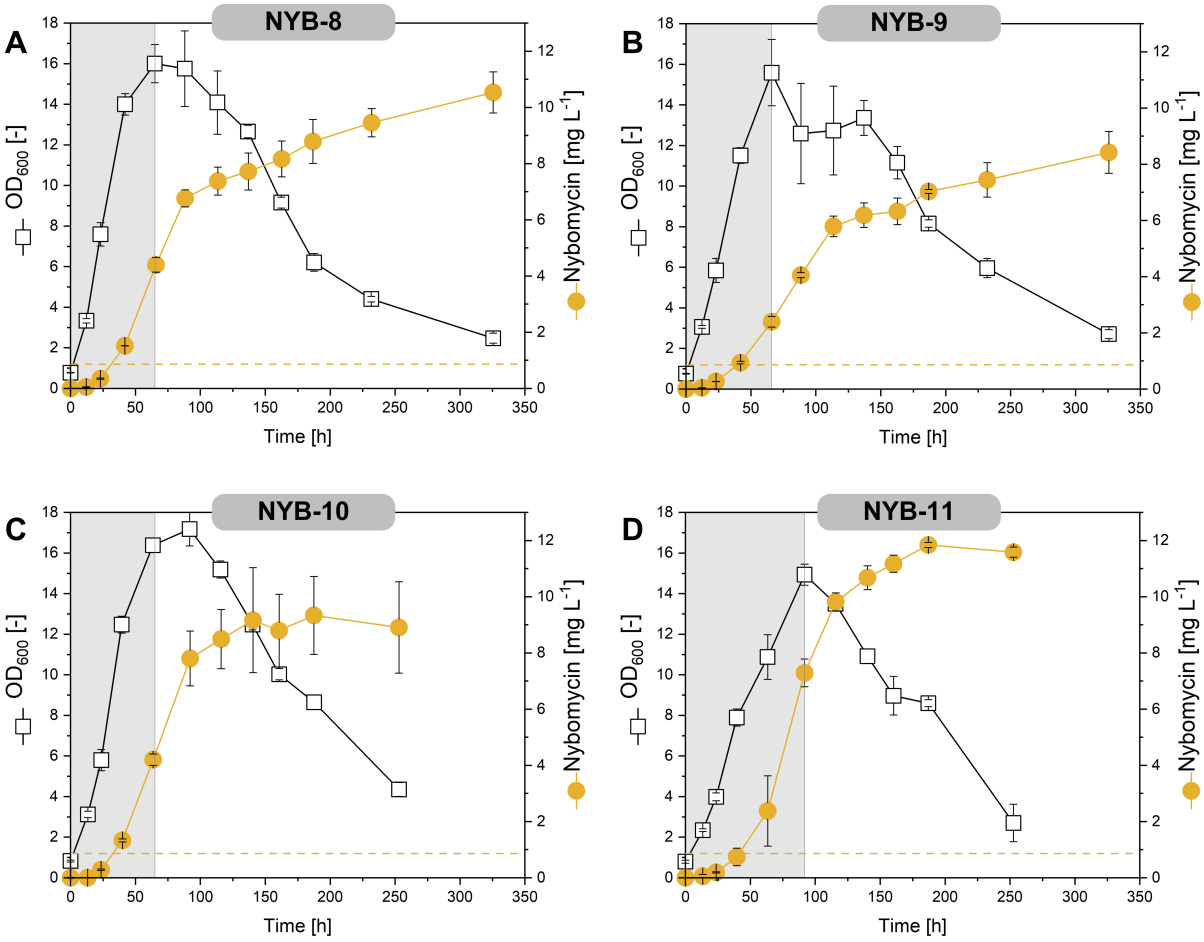

Figure 39: Benchmarking the created *Streptomyces albus* nybomycin producers in batch processes. The data show the growth and production profiles of strains NYB-8 (A), NYB-9 (B), NYB-10 (C), and NYB-11 (D) including OD_{600} (open squares) and nybomycin titer (yellow circles) on minimal medium with 50 g L^{-1} mannitol. Yellow dashed lines indicate the titer of the basic producer *S. albus* 4N24. The data represent mean values and corresponding standard deviations from three biological replicates.

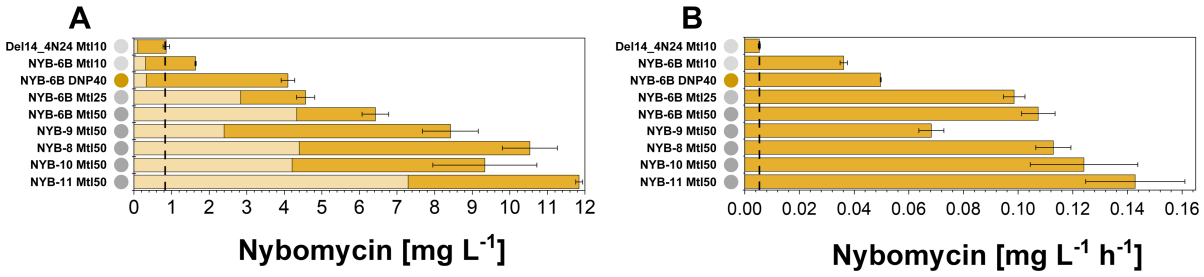

Figure 40: Overview of strains in optimized medium. The data represent the final titer (A) and the maximum volumetric productivity (B) for different mutants (4N24, NYB-6B, Nyb-8, NYB-9, NYB-10, NYB-11). The strains were grown on different media, including DNP40 with 40 g L^{-1} of dextrin and minimal mannitol medium with 10 (Mtl10), 25 (Mtl25), and 50 g L^{-1} (Mtl50) of mannitol, respectively. Black dashed lines indicate the values of the basic producer *S. albus* 4N24. The data represent mean values and corresponding standard deviations from three biological replicates.

4.10 Towards other heterologous nybomycin producers

4.10.1 Evaluating other heterologous hosts for nybomycin production

Beyond *S. albus* 4N24, other heterologous hosts were finally evaluated for their nybomycin production performance. For these studies, the previously used defined mannitol-based minimal medium was used.

Streptomyces sp. Lv1-4_4N24 formed 2,320 µg L^{-1} of nybomycin over 250 h of growth **(Figure 41B)**. The supplemented phosphate 0.5 g L^{-1} was depleted after around 56 h, initiating the transition to the stationary phase until mannitol was consumed after around 75 h. Again, nybomycin was produced during the exponential growth phase. Interestingly, more than half (55%) of the total nybomycin was produced during this phase, while only 45% of nybomycin was produced during the stationary phase **(Figure 41B, Table 5)**.

Strain 94-10_4N24 produced 123 µg L^{-1} of nybomycin within 225 h of cultivation. It exhibited the poorest production performance among the three strains. Phosphate was not depleted at all, and remained at a very low level after 75 h **(Figure 41C, Table 5)**. However, mannitol was consumed after 67 h, resulting in transient fructose accumulation (data not shown). Cells stopped growing once the available sugar was depleted. Furthermore, nybomycin was detectable after 70h. Production mainly occurred during the stationary phase (90%).

Among the three producers, huge differences in growth, production and genetic accessibility were observed. *S. albus* 4N24 exhibited the fastest growth with a decent nybomycin production. Furthermore, this strain offered an easy handling and exhibited only weak pellet formation, simplifying cultivation and product extraction. The parent strain, *S. albus* Del14 (derived from J1074) is a well-known heterologous host, and prominent for being easily modifiable (Myronovskyi and Luzhetskyy, 2013; Zaburannyi et al., 2014).

Lv1-4_4N24 exhibited slow growth but the highest product titer. Nevertheless, the strain turned out difficult in handling. Integration by recombinase-based system was found generally possible. However, different tests revealed a much lower transformation efficiency as compared to *S. albus*, and modification by homologous recombination using the pKG1132hyg suicide vector turned out not successful (data not shown).

94-10_4N24 exhibited slow growth and a low product titer. Genetic engineering was found challenging but possible (data not shown).

Table 5: Comparison of growth and production characteristics of three heterologous nybomycin producer strains

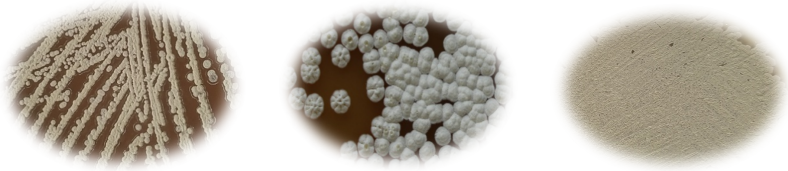

	***S. albus* 4N24**	**Lv1-4_4N24** marine, Ukrainian coast	**94-10_4N24** marine sponge, Trondheim fjord
Nybomycin [µg L^{-1}]	**859**	**2,322**	**123**
Cultivation time [h]	250	250	225
Production in % growth ph.	20	55	10
Production in % stationary ph.	80	45	90
spec. growth rate µ	0.10	0.04	0.03
Generation time [h]	6.7	15.6	20.1

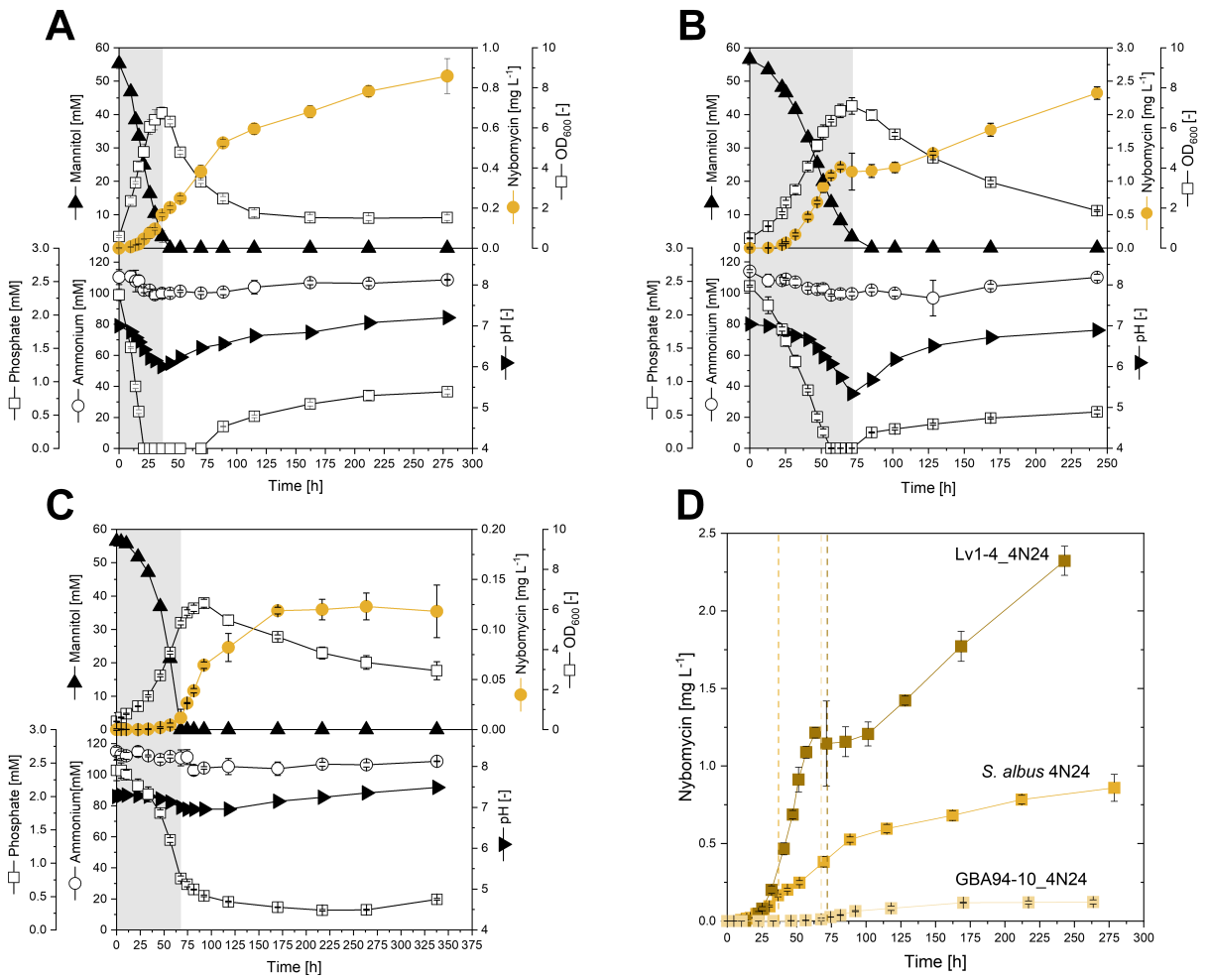

Figure 41: Cultivation time profiles of three heterologous nybomycin producer strains. The data represent strains *S. albus* 4N24 (A), Lv1-4_4N24 (B) and GBA94-10_4N24 (C) grown in minimal mannitol medium including analysis of OD_{600} (open squares, upper panel), nybomycin (yellow circles, upper panel), mannitol (solid triangles, upper panel), phosphate (open squares, lower panel), ammonium (open circles, lower panel) and pH (solid squares, lower panel). Comparison of nybomycin production of all heterologous producer strains (D). Dashed lines indicate the transition from growth to stationary phase for the corresponding strains. The data represent mean values and corresponding standard deviations from three biological replicates.

4.10.2 Transfer of the metabolic engineering strategy to strain *Streptomyces* Lv1-4

Since Lv1-4_4N24 was an efficient nybomycin producer, the metabolic engineering strategy, successfully applied to *S. albus* 4N24, was now tested for strain Lv1-4. For this purpose, BAC 4N24 Δ*nybW* was integrated into strain Lv1-4, yielding NYB-12A. Next, both Lv1-4-based strains were grown in a modified minimal medium (MM#2) with 10 g L^{-1} mannitol but some minor changes, since this medium offered slightly better growth for strain Lv1-4 (personal communication Wei Shu, Systems Biotechnology, Saarland University).

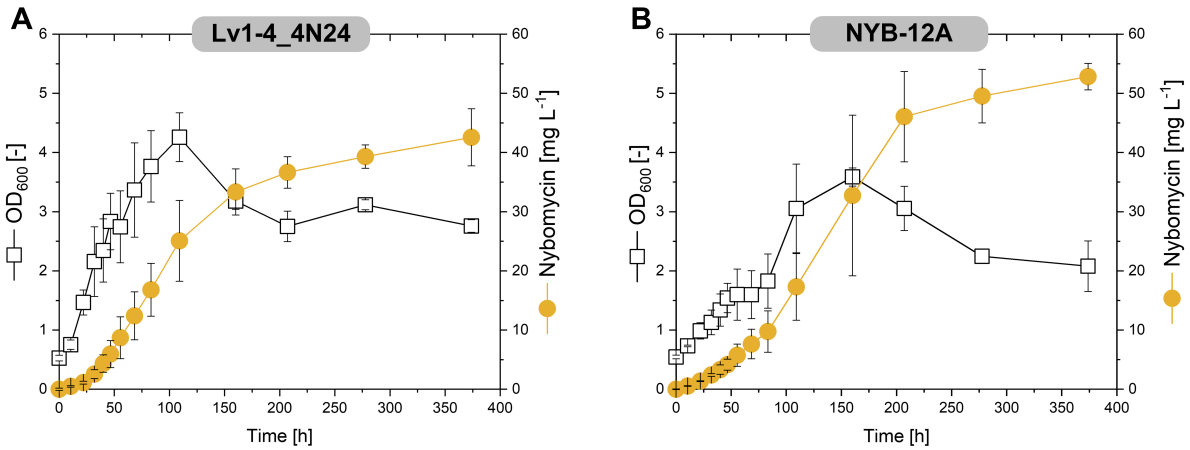

Figure 42: Time profiles for growth and nybomycin production of Lv1-4_4N24 basic producer and engineered NYB-12A. The data show OD_{600} (open squares) and nybomycin titer (yellow circles) of strains Lv1-4_4N24 (A) and Lv1-4_4N24_ΔnybW (NYB-12A) (B) grown in minimal mannitol medium. The data represent mean values and corresponding standard deviations from three biological replicates.

Unexpectedly, Lv1-4_4N24 and NYB-12A exhibited massively improved nybomycin production in the adapted minimal medium grown for almost 400 h, with titers of 43 mg L^{-1} and 53 mg L^{-1}, respectively. As observed for *S. albus,* possessing similar BAC modification, the deletion of *nybW* increased the final nybomycin titer.

To further improve the nybomycin titer, the previously best expression plasmid pBT1H-kasOP*-nybF-zwf2 with target genes *nybF* and *zwf* under control of the very strong constitutive promoter P_{kasOP*}, was integrated into NYB-12A to yield NYB-12B. Grown for 400 h, strain NYB-12B, expressing two additional genes, namely *nybF* and *zwf,* no difference in the strain's fitness was observed. However, the nybomycin titer in the novel strain reached only 15 mg L^{-1}. Taking a deeper look into the strain backgrounds of *S. albus* and Lv1-4 reveals that in *S. albus* 15 native BGC had been deleted to obtain a clean strain (Myronovskyi et al., 2018). In contrast, Lv1-4 represented a rather new species with so far unknown native BGCs. In the *S. albus* Del14 clean strain, a positive effect may be observed since no or less secondary metabolites biosynthesis routes that may benefit from the shifted flux, are available. In the native Lv1-4 background, possessing 28 BGCs (**Table 6A)** (Blin et al., 2023) for the formation of secondary metabolites, compared to remaining predicted 11 BGCs in *S. albus* Del14 (**Table 6B)** (Blin et al., 2023), many different other products may also profit and thus decrease the

overall nybomycin production. For example: lydicamycins, polyketides and nonribosomal peptides, constituted of eleven malonyl-CoA and six methylmalonyl-CoA molecules derived by type I PKS pathway, additionally containing a tetramic acid moiety coupled to the polyketide chain (Komaki et al., 2015). Caniferolides, 36-membered polyol macrolides, incorporating methylmalonyl-CoA as starter units (Pérez-Victoria et al., 2019). Altogether, in strain Lv1-4 more competing biosynthesis pathways to nybomycin formation exist, highlighting the benefit of a clean strain.

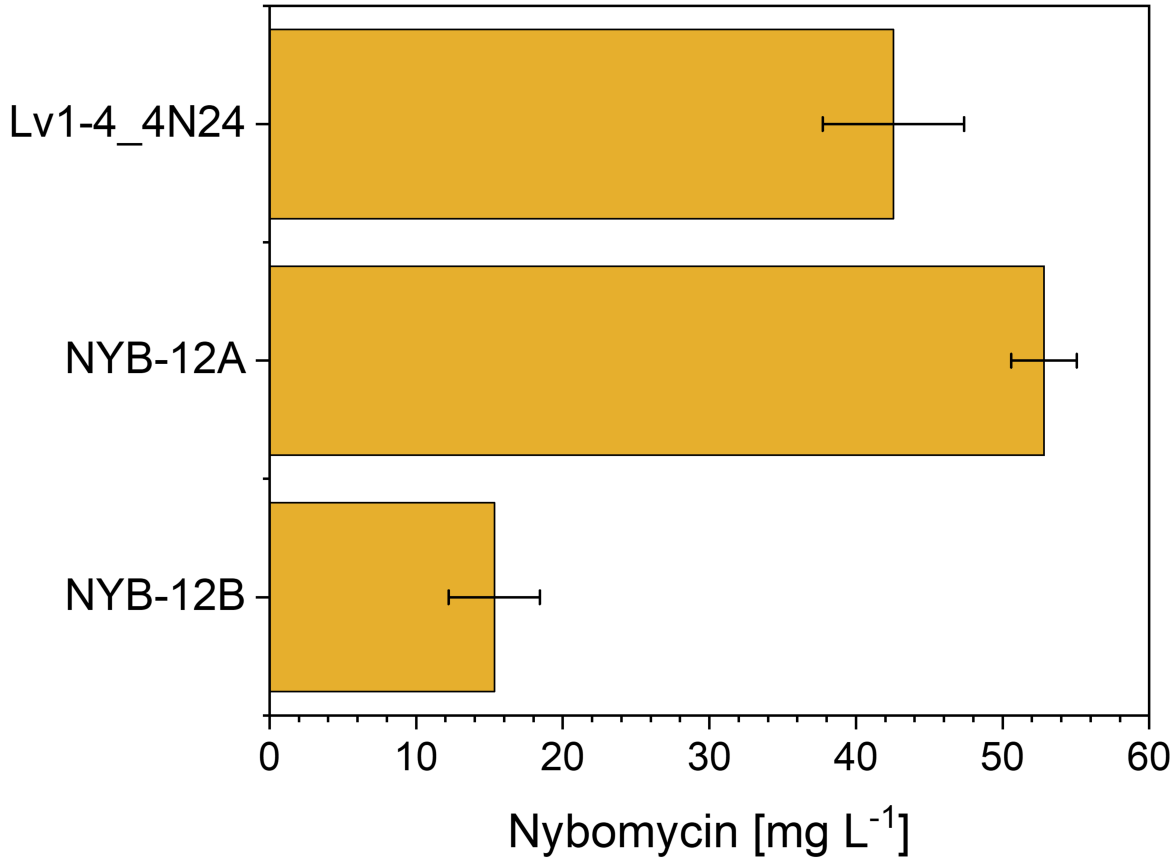

Figure 43: Strain comparison of Lv1-4_4N24 and its derivatives NYB-12A and NYB-12B. The data show the final nybomycin titer in MM#2 medium with 10 g L^{-1} mannitol after growth for 400h. The data represent mean values and corresponding standard deviations from three biological replicates.

Table 6: antiSMASH analysis for secondary metabolite BGCs in *Streptomyces sp.* Lv1-4 (A) and *Streptomyces albus* Del14 (B). antiSMASH version 7.0.0 (Blin et al., 2023).

A

Streptomyces sp. Lv1-4

Region	Type	From	To	Most similar known cluster		Similarity
Region 1	butyrolactone	65,112	74,061			
Region 2	terpene, T1PKS, NRPS-like, PKS-like, oligosaccharide	465,200	655,675	caniferolide A/caniferolide B/caniferolide C/caniferolide D	Polyketide:Modular type I polyketide	61%
Region 3	other, NRPS, NRPS-like	701,208	757,694	antipain	NRP	100%
Region 4	butyrolactone	822,306	833,036	hygrocin A/hygrocin B	Polyketide	6%
Region 5	RiPP-like	1,041,387	1,052,487			
Region 6	lanthipeptide-class-i	1,118,928	1,141,870	sceliphrolactam	Polyketide	8%
Region 7	other, nucleoside	1,152,263	1,193,519	pseudouridimycin	Other:Nucleoside	100%
Region 8	T1PKS, hglE-KS	1,277,527	1,328,052	hexacosalactone A	Other	6%
Region 9	terpene	1,467,962	1,493,492	hopene	Terpene	69%
Region 10	lanthipeptide-class-i	2,028,763	2,055,238			
Region 11	butyrolactone	2,262,874	2,273,851			
Region 12	NI-siderophore	2,447,331	2,460,472	synechobactin C9/synechobactin C11/synechobactin 13/synechobactin 14/synechobactin 16/synechobactin A/synechobactin B/synechobactin C	Other	9%
Region 13	NRPS-like, NRPS, lassopeptide	4,031,666	4,106,908	ulleungdin	RiPP:Lassopeptide	100%
Region 14	LAP	4,284,309	4,306,577			
Region 15	terpene	4,356,047	4,376,805	salinomycin	Polyketide:Modular type I polyketide	6%
Region 16	terpene	4,860,169	4,878,635	clipibycyclene	Alkaloid	6%
Region 17	terpene	5,908,267	5,929,328	ebelactone	Polyketide	5%
Region 18	T1PKS	5,996,238	6,040,905	melanin	Other	40%
Region 19	ectoine	6,957,181	6,967,597	ectoine	Other:Ectoine	100%
Region 20	NI-siderophore	7,050,718	7,059,417	desferrioxamine E	Other	100%
Region 21	NI-siderophore	7,761,952	7,776,809	peucechelin	NRP	25%
Region 22	T1PKS, NRPS, NRP-metallophore, melanin, aminopolycarboxylic-acid, hglE-KS, NRPS-like	7,914,438	8,145,641	lydicamycin	NRP+Polyketide:Modular type I polyketide	96%
Region 23	T2PKS	8,170,924	8,243,439	spore pigment	Polyketide	83%
Region 24	RiPP-like	8,271,447	8,278,850	hexacosalactone A	Other	4%
Region 25	NAPAA	8,317,128	8,353,799	stenothricin	NRP:Cyclic depsipeptide	13%
Region 26	lanthipeptide-class-iii, T3PKS	8,444,239	8,494,296	SapB	RiPP:Lanthipeptide	100%
Region 27	RiPP-like	8,575,877	8,587,049			
Region 28	NRPS	8,642,046	8,693,367	bonnevillamide D/bonnevillamide E	NRP	6%

B

***Streptomyces albus* Del14**

Region	Type	From	To	Most similar known cluster		Similarity
Region 1	terpene	271,049	296,211	hopene	Terpene	76%
Region 2	RiPP-like	377,482	385,318	hexacosalactone A	Other	4%
Region 3	NI-siderophore	1,153,252	1,166,646	synechobactin C9/synechobactin C11/synechobactin 13/synechobactin 14/synechobactin 16/synechobactin A/synechobactin B/synechobactin C	Other	9%
Region 4	terpene	1,747,160	1,768,212	julichrome Q3-3/julichrome Q3-5	Polyketide	25%
Region 5	RiPP-like	2,423,718	2,433,101	goadsporin	RiPP:LAP	12%
Region 6	lanthipeptide-class-iii	2,575,711	2,598,290	AmfS	RiPP:Lanthipeptide	80%
Region 7	LAP	3,724,962	3,747,253	surugamide A/surugamide D	NRP	38%
Region 8	NI-siderophore	4,492,588	4,504,408	desferrioxamin B	Other	100%
Region 9	ectoine	5,387,484	5,397,882	ectoine	Other	100%
Region 10	RiPP-like	6,145,776	6,155,383			
Region 11	RiPP-like	6,235,571	6,246,938	streptamidine	RiPP:Other	75%

Since strain NYB-12A exhibited the highest nybomycin titer in MM#2, the mannitol and phosphate concentrations were adapted as for *S. albus*, to further improve the bioprocess. Therefore, the best conditions, obtained from the *S. albus* process were chosen: Mannitol 50 g L^{-1}, K_2HPO_4 2 g L^{-1} and Mannitol 75 g L^{-1}, K_2HPO_4 3 g L^{-1}. In 400 h of growth, strain NYB-12A reached a final titer of around 70 mg L^{-1} for both conditions, 50 g L^{-1} and 75 g L^{-1} mannitol, respectively. However, the high initial concentrations of mannitol reduced the growth rate, and no complete depletion of mannitol was reached when using 75 g L^{-1}. Nevertheless, an increase in nybomycin titer from 53 mg L^{-1} to around 70 mg L^{-1} for higher mannitol concentrations were reached in strain NYB-12A, representing the highest nybomycin titer ever, so far **(Figure 44)**. Due to incomplete usage of mannitol, even higher titers may be possible with elongated cultivation time, since previous Lv1-4- production studies revealed that a significant amount of nybomycin (45%, **Table 5**) is produced after mannitol depletion **(Figure 41B)**.

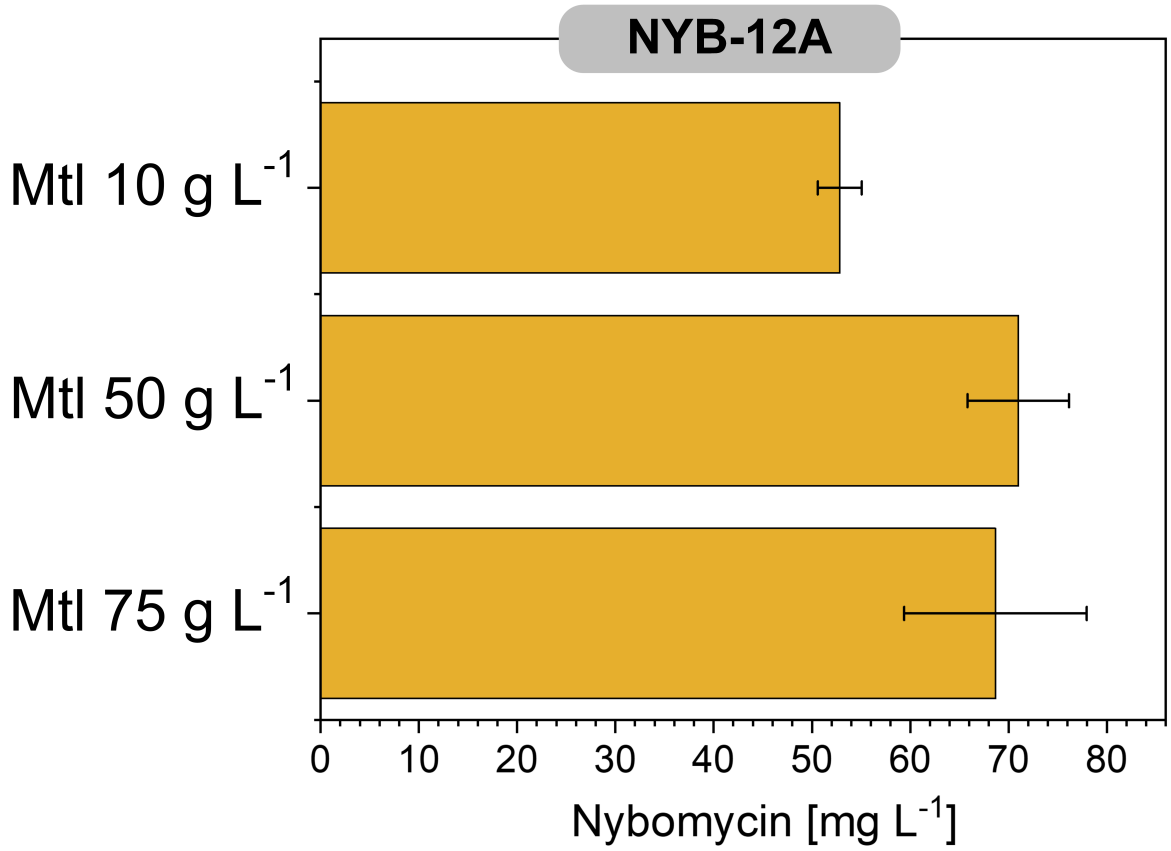

Figure 44: Nybomycin production of strain NYB-12A in MM#2 medium with optimized substrate concentrations. The data shows the final nybomycin titer after growth for 400h. The data represent mean values and corresponding standard deviations from three biological replicates.

5 Conclusions

As shown, metabolically engineered *S. albus* 4N24 (Rodriguez Estevez et al., 2018) was rebuilt into a powerful cell factory to overproduce nybomycin, a reverse antibiotic of substantial interest. Several rounds of metabolic engineering provided strains with successively improved nybomycin titer, an important step to explore the interesting molecule further which requires elevated amounts for e. g. activity and stability testing, toxicity screening, and mode-of-action studies. Notably, the de-regulation of the expression of the *nyb* cluster through the elimination of the regulator gene *nybW* enabled efficient production during the growth phase as well as the stationary phase, which allowed to substantially shorten the production process. The acceleration appeared useful, as secondary metabolites are produced mainly in the late growth or stationary phase (Ferraiuolo et al., 2021) so that industrial processes using *Streptomyces* are usually very long and suffer from low productivities (Pereira et al., 2008). The chosen host and the established process both supported the selective production of nybomycin, promising a facilitated purification in the future. On one hand, all *Streptomyces albus* producers of the NYB family created in this work, were based on the pre-engineered cluster-free chassis *S. albus* Del14, eliminating any potential interference from native natural products of the host (Myronovskyi et al., 2018). In addition, the use of a lean, minimal medium, as shown here, allowed to avoid the typical impurities that result from the use of complex ingredients.

Conceptually, a systems-wide strain engineering strategy was aimed for, because this approach had proven most successful to overproduce e. g. amino acids and organic acids, typically demanding for a set of different cellular precursors, at very high titers and yields (Becker et al., 2011; Kind et al., 2013; Kind et al., 2014; Rohles et al., 2016). Likewise, the synthesis of the nybomycin molecule required precursors from various routes **(Figure 6).** The best strain NYB-11 produced 12 mg L^{-1} of nybomycin, fifteen-fold more than the basic producer, used as starting point. Hereby, the improvement was enabled by the combination of targets from primary and secondary metabolism which synergistically contributed to the enhanced production. It appears straightforward to apply similar approaches to other *S. albus* based producers which have been created by heterologous cluster expression without further

optimization (Estevez et al., 2020; Myronovskyi et al., 2018). A key step to success in this work was the identification and implementation of appropriate promoters to drive gene expression. Based on our findings, the synthetic promoter derivatives can be recommended for broader use, given their constitutive nature. However, other genetic backgrounds or production media might change this picture, suggesting additional case-specific tests with on-line recording of promoter dynamics, as done here. Finally, beneficial findings from *S. albus* strain engineering were transferred to the superior nybomycin production host Lv1-4. Combined with the adapted medium composition a final nybomycin titer of 70 mg L^{-1} was achieved.

6 Outlook

Starting from the basic heterologous nybomycin producer strain *S. albus* 4N24, metabolic engineering was applied and enabled and a 4.5-fold improved titer. Additionally promising genes, not tested so far in this work, namely *aroB* and *aroK* encoding enzymes of the shikimic acid pathway **(Figure 6)** are known as bottlenecks in aromatic amino acid production in other microbes (Dell and Frost, 1993). Previously, these genes were overexpressed in chloramphenicol-producing *S. venezuelae* which doubled the titer (Vitayakritsirikul et al., 2016). The expression data from *S. albus* 4N24 of this work revealed a downregulation of several SA pathway genes during the main production (stationary) phase **(Figure 36, Figure 37)**, rendering *aroB* and *aroK* as promising targets for further strain engineering.

Furthermore, several nybomycin derivatives **(Figure 2)** with distinct biological activity and solubilities exist in nature (Wang et al., 2019b). The improved nybomycin producer NYB-11 could serve as starting point for the generation of a nybomycin D or deoxynyboquinone by deleting of inserting the required genes.

Among the species *Streptomyces*, huge differences in heterologous nybomycin formation were observed. The host strain Lv1-4_4N24 exhibited the best production performance **(Figure 41)**. Given the findings here, a fully deregulated producer with the deletion of *nybWXYZ*, as done for *S. albus*, appears promising to create.

Since *Streptomyces* are capable of consuming different types of sugars combined with tolerance to harsh environmental conditions (Sivalingam et al., 2019), the use of sustainable seaweed extracts as substrate is obvious. Especially brown algae including *Himanthalia elongata*, *Sargassum muticum*, *Saccharina latissima* and *Undaria pinnatifida* contain a huge fraction of mannitol (Poblete-Castro et al., 2020). Several basic chemicals such as L-lysine, lactate, ethanol or butanol has been produced by using seaweed hydrolysates (Hoffmann et al., 2021; Poblete-Castro et al., 2020). A sustainable production of complex chemicals from sustainable resources would make biotechnological production even more interesting.

7 Appendix

7.1 Primers

Table 7: Primers used in this study

Primer name	Sequence 5`-->3`
PR_{pBT1H}_1	ACACCGCCCCCGGCGCCTGAGCTCATGAGCGGAGAACGAG
PR_{pBT1H}_2	AGCAGGGATTCTTGTGTCATGACATTGCACTCCACCGCTG
PR_{pBT1H}_3	CAGCGGTGGAGTGCAATGTCATGACACAAGAATCCCTGCTCC
PR_{pBT1H}_4	CTCGTTCTCCGCTCATGAGCTCAGGCGCCGGGGGCGGTGTC
PR_{pDppc4}_1	GATCCGCGGCCGCGCGCGATTCCGAGTTCGGCAAGGGTGC
PR_{pDppc4}_2	TGCAAGGAGCCGCACCTGTGTGACGGCGGGACGTACCACG
PR_{pDppc4}_3	CGTGGTACGTCCCGCCGTCACACAGGTGCGGCTCCTTGCAG
PR_{pDppc4}_4	GACATGATTACGAATTCGATGGCGGAGGCGTGAGCGGG
PR_{pBT1HP}_1	GAAACTGTTGAAAGTACGTAATGTGTTTGCCTCCAACGG
PR_{pBT1HP}_2	TGGCCGATTCATTAATGCAGTCGATCTTGACGGCTGGCG
PR_{pBT1HP}_3	CGGGAAACCTGTCGTGCCAGCGATGGTTGTTGTCATTGTC
PR_{pBT1HP}_4	ACCGTTGGAGGCAAACACATTACGTACTTTCAACAGTTTCAGCGG
PR_{ermE*}_1	GGATCCGCGGCCGCGCGCGATTCGATCTTGACGGCTGGCG
PR_{ermE*}_2	GTGGTCGGCTTGGTGCTCACATGTGTTTGCCTCCAACGG
PR_{ermE*}_3	AGCGGGTTCGCTCCGTGCAGATGTGTTTGCCTCCAACGG
PR_{tkt}_1	ACCGTTGGAGGCAAACACATGTGAGCACCAAGCCGACCAC
PR_{tkt}_2	TCCGCTGAAACTGTTGAAAGTCCTACAGCTACAGAGTGG
PR_{zwf}_1	ACCGTTGGAGGCAAACACATCTGCACGGAGCGAACCCGC
PR_{zwf}_2	TCCGCTGAAACTGTTGAAAGGCTGGAGGTGGTGTCCGTC
PR_{tfd}_1	ACCACTCTGTAGCTGTAGGACTTTCAACAGTTTCAGCGG
PR_{tfd}_2	TGACGGACACCACCTCCAGCCTTTCAACAGTTTCAGCGG
PR_{tfd}_3	GACATGATTACGAATTCGATCGATGGTTGTTGTCATTGTC
$PR_{permCherry}$_1	GTTGGAGGCAAACACATTACATGGTGAGCAAGGGCGAGG
$PR_{permCherry}$_2	GCTGAAACTGTTGAAAGTACTTACTTGTACAGCTCGTCCATG
PR_{kasOP*}	TGGCCGATTCATTAATGCAGTGTTCACATTCGAACGGTCTCTGCTTTGA CAACATGCTGTGCGGTGTTGTAAAGTCGTGGCCAATGAACCGTTGGAG GCAAAC
PR_{P21}	TGGCCGATTCATTAATGCAGTGTGCGGGCTCTAACACGTCCTAGTATG GTAGGATGAGCAAAATGAACCGTTGGAGGCAAAC
PR_{pTipA}	TGGCCGATTCATTAATGCAGGAACGTCCGGGCTTGCACCTCACGTCAC GTGAGGAGGCAGCGTGGACGGCGAATGAACCGTTGGAGGCAAAC
PR_{SP41}	TGGCCGATTCATTAATGCAGTGTTCACATTCGAACCGTCTCTGCTTTGA CAACATGCTGTGCGGTGTTGTAAAGTCCAGCTGAATGAACCGTTGGAG GCAAAC
PR_{SP43}	TGGCCGATTCATTAATGCAGTGTTCACATTCGAACCGTCTCTGCTTTGA CACGGACAAGCGCTATGGTGTAAAGTCGTGGCCAATGAACCGTTGGAG GCAAAC
PR_{SP44}	TGGCCGATTCATTAATGCAGTGTTCACATTCGAACCGTCTCTGCTTTGA CAACATGCTGTGCGGTGTTGTAAAGTCTGGTGTAATGAACCGTTGGAG GCAAAC
PR_{SF14P}	TTGGCCGATTCATTAATGCAGCCTATCCAGGAGATATTATGAGTTACGT AGACCTACGCCTTGACCTTGATGAGGCGGCGTGAGCTACAATCAATAC TCGATTAATGAACCGTTGGAGGC
$PR_{kasOP*-nybF-zwf}$_1	AGCGGGTTCGCTCCGTGCAGATGTGTTTGCCTCCAACGGTTCATTTCA GCCCCCCGCCGCCTGCC

$PR_{kasOP^*\text{-}nybF\text{-}zwf}$_2	GGCAGGCGGCGGGGGGCTGAAATGAACCGTTGGAGGCAAACACATCTGCACGGAGCGAACCCGC
$PR_{kasOP^*\text{-}nybF\text{-}tkt}$_1	GTGGTCGGCTTGGTGCTCACATGTGTTTGCCTCCAACGGTTCATTTCAGCCCCCCGCCGCCTGCC
$PR_{kasOP^*\text{-}nybF\text{-}tkt}$_2	GGCAGGCGGCGGGGGGCTGAAATGAACCGTTGGAGGCAAACACATGTGAGCACCAAGCCGACCAC
$PR_{kasOP^*\text{-}tkt\text{-}zwf}$_1	AGCGGGTTCGCTCCGTGCAGATGTGTTTGCCTCCAACGGTTCATTTCAGCGCTGAGCGGCGGCGA
$PR_{kasOP^*\text{-}tkt\text{-}zwf}$_2	TCGCCGCCGCTCAGCGCTGAAATGAACCGTTGGAGGCAAACACATCTGCACGGAGCGAACCCGC
DnybWXYZ_Kan_F	ATTTCGGAGGTGAACGTCATCGCAGACAAAGAGCGCACGAAGAGCCGTTTGCTAAAGGAAGCGGAACACG
DnybWX_Kan_R	GTCCGCTCGGCGCAGTCCCGCGATGAGGAGAGCGACCAGCCGGCGGGCGTCGCCTGATGCGGTATTTTC
DnybWXYZ_Kan_F	ATTTCGGAGGTGAACGTCATCGCAGACAAAGAGCGCACGAAGAGCCGTTTGCTAAAGGAAGCGGAACACG
DnybWXYZ_Kan_R	GTCTCCCCCGGGCGCGGTGTGCCGCAGCAGAGGGCCGGTGTGGCGCTGGAGGGCGCCTGATGCGGTATTTTC

7.2 Vector maps

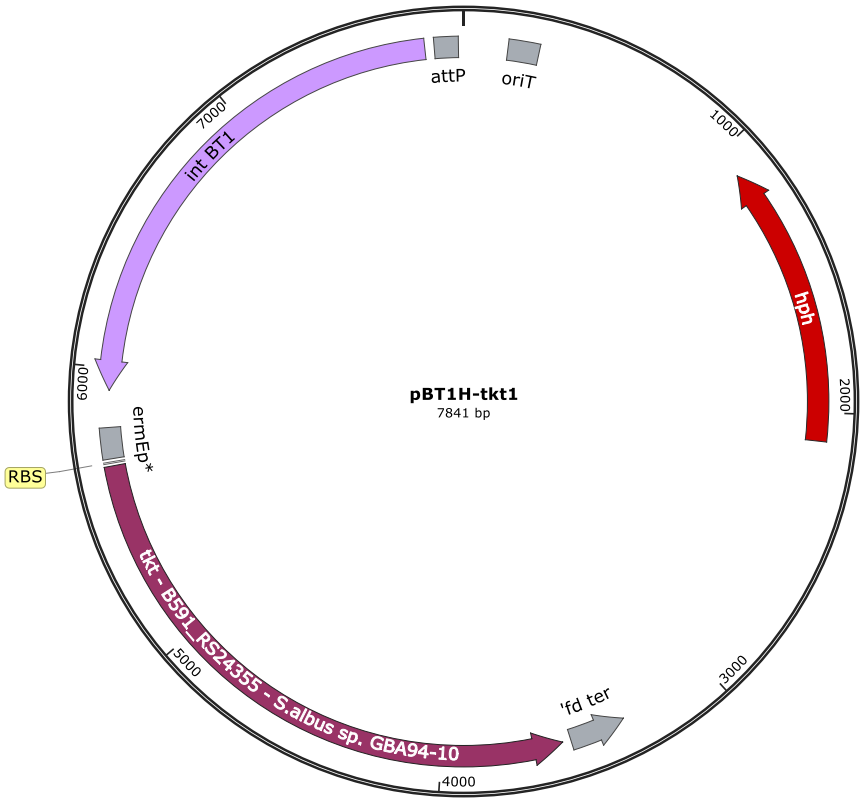

Figure 45: Vector map expression plasmid pBT1H-tkt1

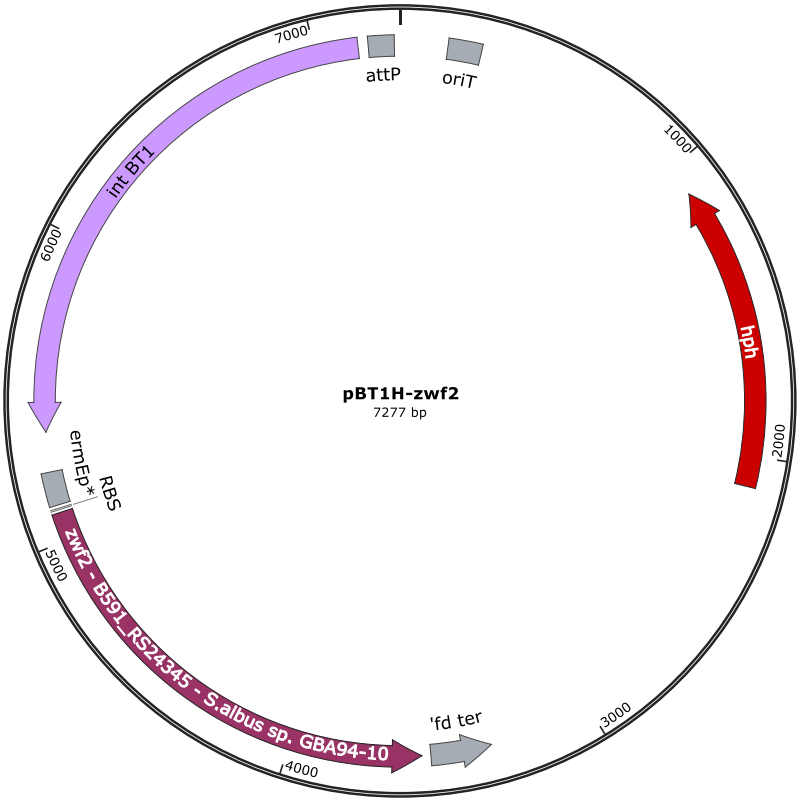

Figure 46: Vector map expression plasmid pBT1H-zwf2

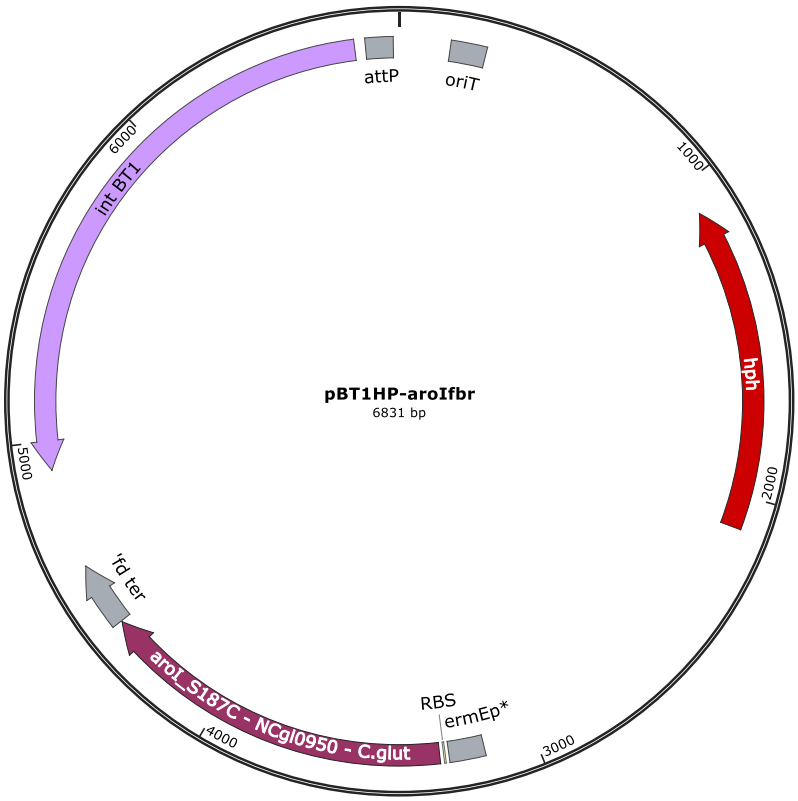

Figure 47: Vector map expression plasmid pBT1HP-aroIfbr

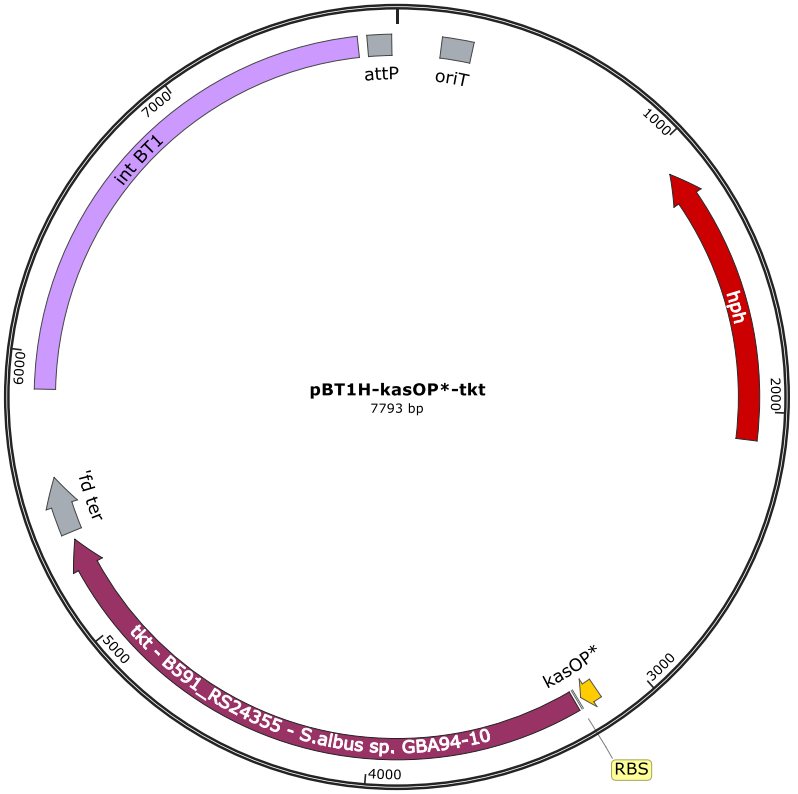

Figure 48: Vector map expression plasmid pBT1H-kasOP*-tkt

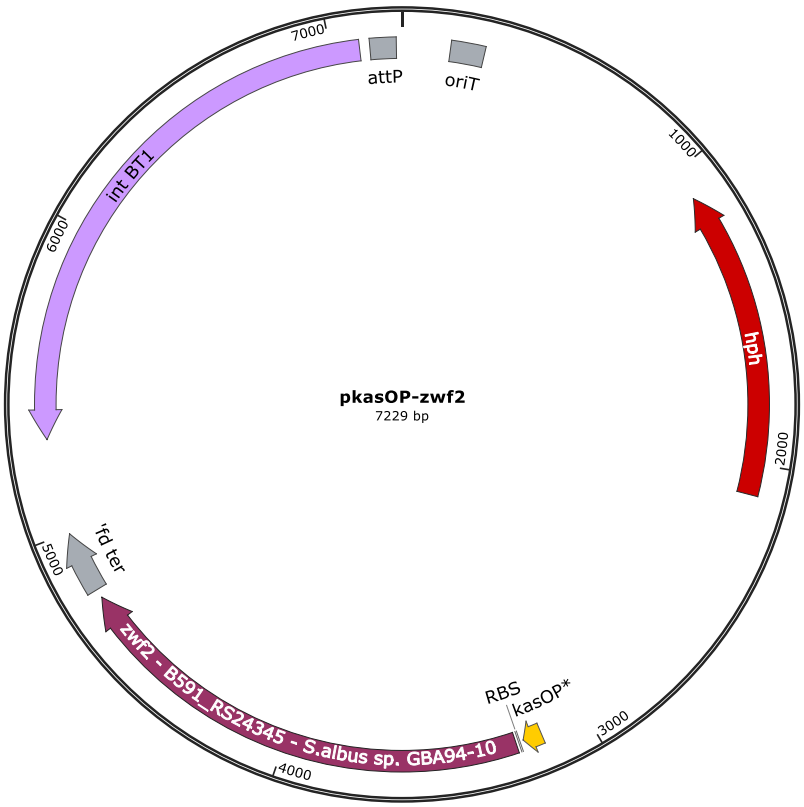

Figure 49: Vector map expression plasmid pBT1H-kasOP*-zwf2

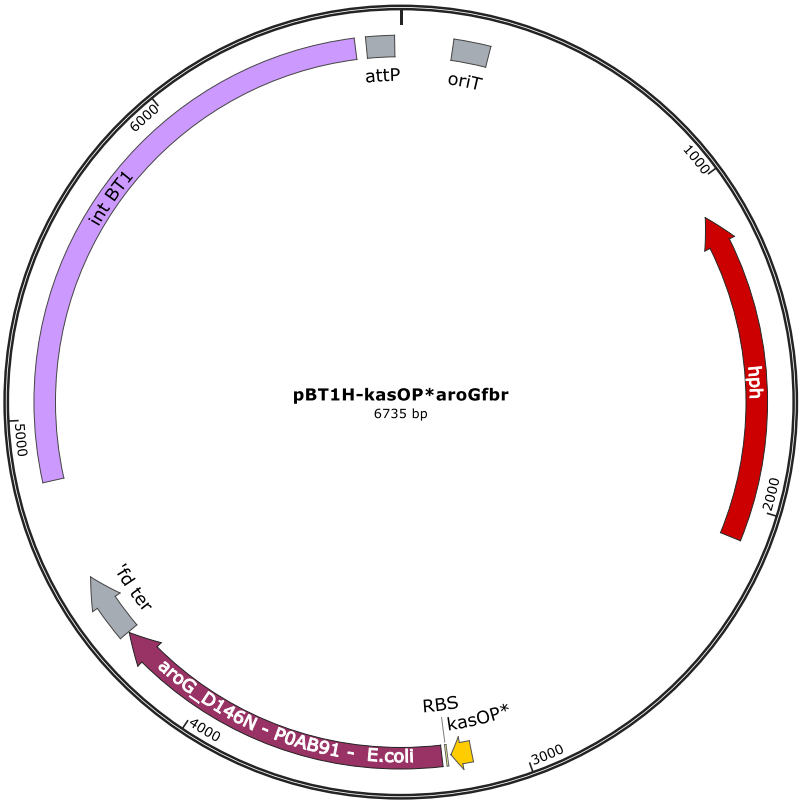

Figure 50: Vector map expression plasmid pBT1H-kasOP*-aroGfbr

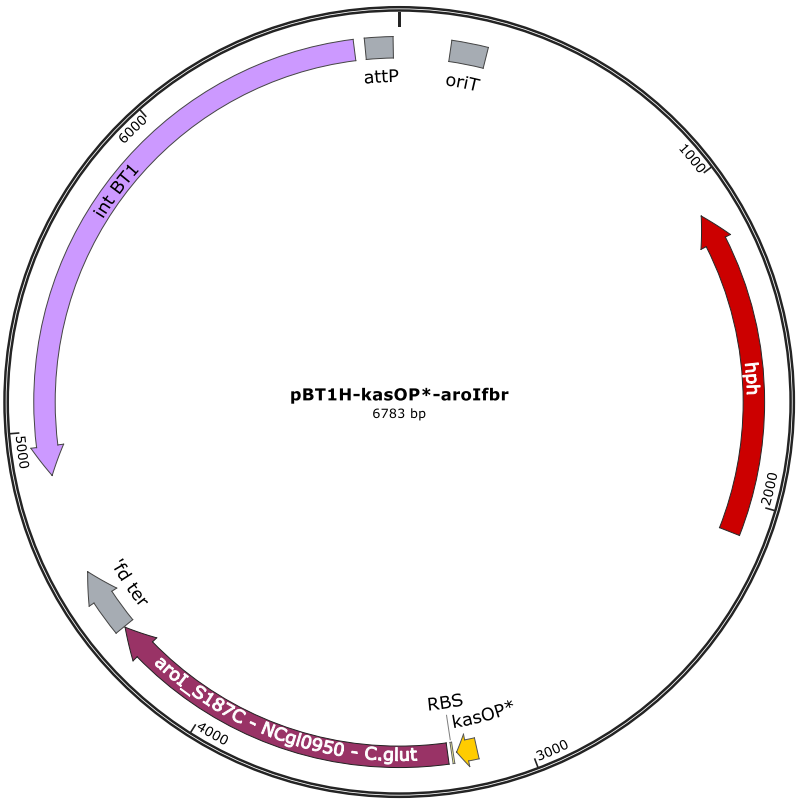

Figure 51: Vector map expression plasmid pBT1H-kasOP*-aroIfbr

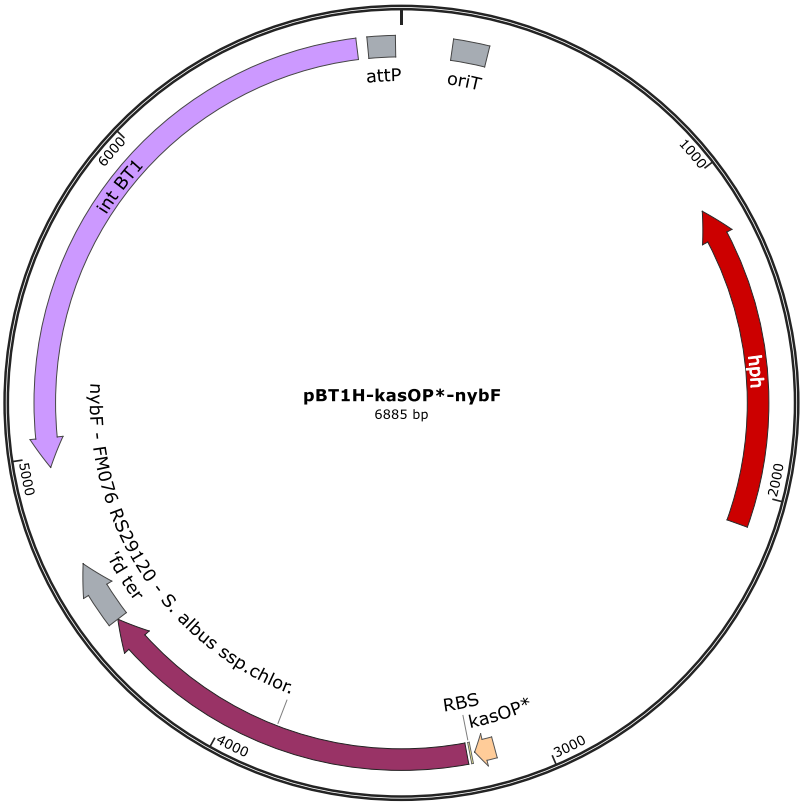

Figure 52: Vector map expression plasmid pBT1H-kasOP*-nybF

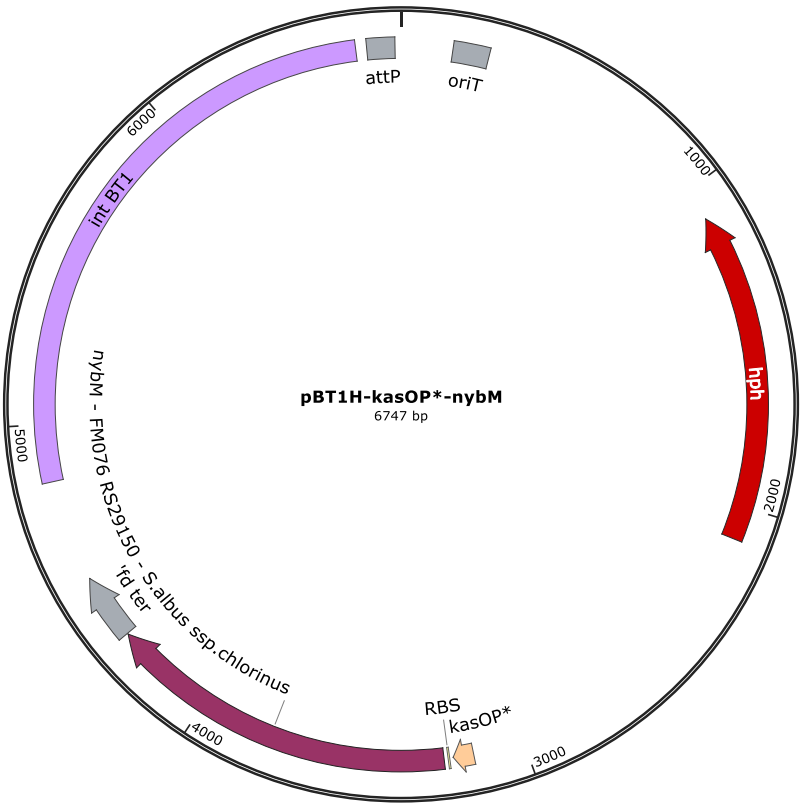

Figure 53: Vector map expression plasmid pBT1H-kasOP*-nybM

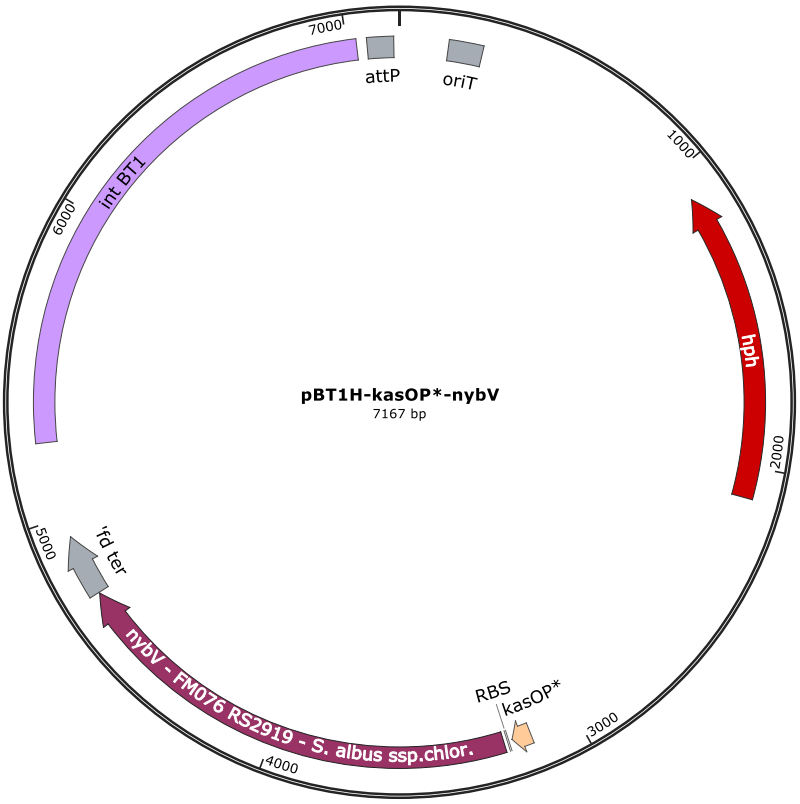

Figure 54: Vector map expression plasmid pBT1H-kasOP*-nybV

7.3 DNA sequences of expressed genes

```
GTGAGCACCAAGCCGACCACCACAGACTTCGAGTGGACCACAGAGGACCA    50
GCGGGCCGTCGACACCGTCCGCGTCCTGGCCGCAGACGCCGTACAGAAGG   100
TCGGCAACGGCCATCCCGGTACGGCGATGAGCCTCGCGCCGGCCGCGTAC   150
ACCCTCTTCCAGAAGGTGATGCGGCACGACCCGGCGGACGCCGACTGGAC   200
GGGGCGCGACCGCTTCGTCCTCTCCGTGGGCCACTCGTCCCTGACCCTCT   250
ACATCCAGCTCTACCTGGCCGGCTTCGGCCTGGAGCTGGACGACCTGAAG   300
GCCTTCCGCAGCTGGGGTTCGAAGACCCCCGGGCACCCGGAGTACGGCCA   350
CACCACCGGCGTGGAGACCACCACCGGCCCGCTCGGGCAGGGTGTGGCCA   400
ACGCGGTGGGCATGGCCATGGCCGCGCGGTACGAGCGCGGGCTGTTCGAC   450
CCGGAGGCGGCCGAGGGCACCTCCCCGTTCGACCACCACATCTACTGCAT   500
CGCCGGTGACGGCTGCCTCCAGGAGGGCATCTCCGCCGAGGCCTCCTCCA   550
CCGCCGGGCACCAGAAGCTCGGCAACCTGATCATGCTGTGGGACGACAAC   600
CACATCTCGATCGAGGGCGACACCGAGACGGCCGTCTCCGAGGACACCCT   650
CAAGCGGTACGAGGCGTACGGCTGGCACGTGCAGCGGGTGGCGCCCAAGG   700
AGAACGGCGACCTGGACCCGGCCGCCCTGTACGAGGCGATCGAGGCGGCG   750
AAGGCGGAGACCGGGCGTCCCTCCTTCATCGCGATGCGCTCGATCATCGC   800
GTGGCCGGCCCCGAACGCGCAGAACACCGAGGCCGCACACGGCTCGGCGC   850
TCGGCGAGGACGAGGTCGCCGCCACCAAGCGCGTCCTCGGCTTCGACCCG   900
GAGAAGAGCTTCGAGGTCTCCGACGAGGTCCTGGCGTACACCCGTGGCGC   950
GCTGGACCGCGGCCGCGAGCTGCGCGCCGAGTGGGAGAAGGGGTACGCCG  1000
CCTGGCGCACCGCCAACCCGGAGCACGCCGCGCTCTTCGACCGCGTCGCC  1050
GCCGGCGAGCTGCCCGAGGGCTGGGAGGACGCGCTGCCGGTCTTCGAGAC  1100
CGGCAAGGCCGTCGCCACCCGTGCCGCCTCCGGCAAGATCCTCCAGGCAC  1150
TCGGTGCGGTCGTGCCCGAGCTGTGGGGCGGCTCCGCCGACCTGGCCGGC  1200
TCGAACAACACGACGATCGACAAGACCTCGTCGTTCCTGCCCGCCGGCAA  1250
CCCGCTGCCGGAGGCCGACCCGTACGGCCGAACCATCCACTTCGGCATCC  1300
GTGAGCACGCGATGGCCGCCGAGATGAACGGCATCCAGCTCCACGGCAAC  1350
ACCCGCATCTACGGCGGCACGTTCCTGGTCTTCTCCGACTACATGCGCAA  1400
CGCGGTGCGCCTCTCCGCGCTGATGCACCTGCCGGTGACCTACGTGTGGA  1450
CGCACGACTCGATCGGCCTCGGCGAGGACGGCCCGACCCACCAGCCGGTG  1500
GAGCACCTGGCCGCGCTGCGCGCCATCCCGGGTCTCAACCTGGTCCGCCC  1550
GGCCGACGCCAACGAGACGGTCGTCGCCTGGCGCGAGATCATGCGCCGGT  1600
GGACCAAGGTGTACGGCAAGGGCGCCCCGCACGGTCTGGCGCTGACCCGC  1650
CAGGGCGTACCGACCTACGAACTGAACGAGAACGCGGCCCGTGGCGGTTA  1700
CGTCCTCGCGGAGGCCGAGGGCGGCGAGCCGCAGGTCATCCTGATCGGCA  1750
CCGGCTCCGAGGTGCAGCTGGCCGTCGAGGCCCGCGAGCAGCTCCAGGCG  1800
GCCGGCGTGCCCACCCGGGTGGTCTCCGTGCCGTGTGTCGAGTGGTTCGA  1850
GGAGCAGGACGAGGCGTACCGCGAGTCGGTGCTGCCGCGTGCCGTGCGCG  1900
CGCGGGTGGCGGTCGAGGCCGGCATCGGCCTGACCTGGCACCGCTTCGTG  1950
GGCGACGCCGGCCGGATCGTCTCGCTGGAGCACTTCGGTGCCTCGGCGGA  2000
CGCGAAGGTGCTGTTCCGCGAGTTCGGCTTCACCGCGGACGCGGTCGCCG  2050
AGGCCGCCCGGGAATCCCTCGCCGCCGCTCAGCGCTGA              2088
```

Figure 55: DNA sequence gene *tkt* - B591_RS24355 - *Streptomyces albus* sp. GBA 94-10

```
CTGCACGGAGCGAACCCGCTTCGTGACGCCGCGGACCGACGGCTCCCGCG    50
TATCGCGGGGCCGTCGGGCCTGGTCATCTTCGGCGTCACCGGCGACCTGT   100
CCCGCAAGAAGCTGATGCCCGCCGTCTACGACCTGGCCAACCGCGGCCTC   150
CTGCCCCCGGGCTTCTCCCTGATCGGGTTCGCCCGGCGCGAGTGGCAGGA   200
CCAGGACTTCGCCGAGGTCGTCCACGACGCCGTCAAGGAGTACGCCCGCA   250
CGCCCTTCCGCGAGGAGGTCTGGCAGCAGCTGGCCCAGGGCATGCGGTTC   300
GTCCAGGGCACCTTCGACGACGACGCGTCGTTCGAGACCCTCAAGGCGAC   350
CATGGAGGAGCTGGACAAGGAGCAGGGCACGGGCGGCAACTTCGCCTTCT   400
ACCTCTCCGTCCCGCCGAAGTTCTTCCCCAAGGTCGTCCAGCAGCTCAAG   450
AAGCACGGCCTGGCCGACGCCCCCGAGGGCTCCTGGCGCCGCGCCGTCAT   500
CGAGAAGCCGTTCGGCCACGACCTGGCCTCGGCCCGCGAGCTCAACGAGA   550
TCGTGCACGAGGTGTTCGCCCCGGACCAGGTGTTCCGGATCGACCACTAC   600
CTCGGCAAGGAGACCGTCCAGAACATCCTGGCGCTCCGCTTCGCCAACAC   650
CATGTTCGAGCCGCTGTGGAACCGGTCGTACGTCGACCACGTGCAGATCA   700
CCATGGCGGAGGACATCGGCATCGGAGGCCGGGCCGGTTACTACGACGGC   750
ATCGGCGCCGCCCGCGACGTCATCCAGAACCACCTGCTCCAGCTGATGGC   800
GCTGACCGCCATGGAGGAGCCCGCCTCCTTCGAGGCCAACGCGCTGGTGG   850
CGGAGAAGGCCAAGGTCCTCGGCGCCGTCCGGCTCCCCGAGGACCTGGGC   900
AAGGACACGGTCCGCGCGCAGTACTCGGCGGGCTGGCAGGGCGGCGAGAA   950
GGCCGTCGGCTACCTGGAGGAGGAGGGGATCAACCCCCGCTCCAAGACCG  1000
ACACCTACGCCGCCGTGAAGCTGGAGGTCGACAACCGCCGCTGGGCGGGC  1050
GTCCCCTTCTACCTGCGGACCGGCAAGCGGCTGGGCCGCCGGGTCACCGA  1100
GATCGCGGTGGTCTTCCAGCGCGCCCCGCACTCCCCGTTCGACACCACGA  1150
CCACGGAGGAGCTGGGCCACAACGCCCTGGTCATCCGGGTCCAGCCGGAC  1200
GAGGGCGTGACCGTGCGGTTCGGCTCGAAGGTGCCCGGCACCTCGATGGA  1250
GGTCCGGGACGTGTCGATGGACTTCGCCTACGGCGAGTCCTTCACCGAGT  1300
CCAGCCCCGAGGCGTACGAGCGGCTCATCCTCGACGTGCTGCTCGGCGAC  1350
GCCAACCTCTTCCCGCGCACCGAGGAGGTCGAGCTGTCCTGGCGCATCCT  1400
CGACCCGATCGAGGAGTACTGGGACACCCACCGCAAGCCGGCGCAGTACC  1450
CGGCCGGCAGCTGGGGGCCCAAGGAGGCGGACGAGATGCTCGCACGAGAC  1500
GGACGGAGCTGGCGCCGGCCATGA                            1524
```

Figure 56: DNA sequence gene *zwf*2 - B591_RS24345 - *Streptomyces albus* sp. GBA 94-10

```
ATGAATTATCAGAACGACGATTTACGCATCAAAGAAATCAAAGAGTTACT    50
TCCTCCTGTCGCATTGCTGGAAAAATTCCCCGCTACTGAAAATGCCGCGA   100
ATACGGTTGCCCATGCCCGAAAAGCGATCCATAAGATCCTGAAAGGTAAT   150
GATGATCGCCTGTTGGTTGTGATTGGCCCATGCTCAATTCATGATCCTGT   200
CGCGGCAAAAGAGTATGCCACTCGCTTGCTGGCGCTGCGTGAAGAGCTGA   250
AAGATGAGCTGGAAATCGTAATGCGCGTCTATTTTGAAAAGCCGCGTACC   300
ACGGTGGGCTGGAAAGGGCTGATTAACGATCCGCATATGGATAATAGCTT   350
CCAGATCAACGACGGTCTGCGTATAGCCCGTAAATTGCTGCTTGATATTA   400
ACGACAGCGGTCTGCCAGCGGCAGGTGAGTTTCTCAATATGATCACCCCA   450
CAATATCTCGCTGACCTGATGAGCTGGGGCGCAATTGGCGCACGTACCAC   500
CGAATCGCAGGTGCACCGCGAACTGGCATCAGGGCTTTCTTGTCCGGTCG   550
GCTTCAAAAATGGCACCGACGGTACGATTAAAGTGGCTATCGATGCCATT   600
AATGCCGCCGGTGCGCCGCACTGCTTCCTGTCCGTAACGAAATGGGGGCA   650
TTCGGCGATTGTGAATACCAGCGGTAACGGCGATTGCCATATCATTCTGC   700
GCGGCGGTAAAGAGCCTAACTACAGCGCGAAGCACGTTGCTGAAGTGAAA   750
GAAGGGCTGAACAAAGCAGGCCTGCCAGCACAGGTGATGATCGATTTCAG   800
CCATGCTAACTCGTCCAAACAATTCAAAAAGCAGATGGATGTTTGTGCTG   850
ACGTTTGCCAGCAGATTGCCGGTGGCGAAAAGGCCATTATTGGCGTGATG   900
GTGGAAAGCCATCTGGTGGAAGGCAATCAGAGCCTCGAGAGCGGGGAGCC   950
GCTGGCCTACGGTAAGAGCATCACCGATGCCTGCATCGGCTGGGAAGATA  1000
CCGATGCTCTGTTACGTCAACTGGCGAATGCAGTAAAAGCGCGTCGCGGG  1050
TAA                                                 1053
```

Figure 57: DNA sequence gene *aroG*_D146N - P0AB91 - *E. coli*

```
ATGAGTTCTCCAGTCTCACTCGAAAACGCGGCGTCAACCAGCAACAAGCG    50
CGTCGTGGCTTTCCACGAGCTGCCTAGCCCTACAGATCTCATCGCCGCAA   100
ACCCACTGACACCAAAGCAGGCTTCCAAGGTGGAGCAGGATCGCCAGGAC   150
ATCGCTGATATCTTCGCTGGCGACGATGACCGCCTCGTTGTCGTTGTGGG   200
ACCTTGCTCAGTTCACGATCCTGAAGCAGCCATCGATTACGCAAACCGCC   250
TGGCTCCGCTGGCAAAGCGCCTTGATCAGGACCTCAAGATTGTCATGCGC   300
GTGTACTTCGAGAAGCCTCGCACCATCGTCGGATGGAAGGGATTGATCAA   350
TGATCCTCACCTCAACGAAACCTACGACATCCCAGAGGGCTTGCGCATTG   400
CGCGCAAAGTGCTTATCGACGTTGTGAACCTTGATCTCCCAGTCGGCTGC   450
GAATTCCTCGAACCAAACAGCCCTCAGTACTACGCCGACACTGTCGCATG   500
GGGAGCAATCGGCGCTCGTACCACCGAATCTCAGGTGCACCGCCAGCTGG   550
CTTCTGGGATGTGTATGCCAATTGGTTTCAAGAACGGAACTGACGGAAAC   600
ATCCAGGTTGCAGTCGACGCGGTACAGGCTGCCCAGAACCCACACTTCTT   650
CTTCGGAACCTCCGACGACGGCGCGCTGAGCGTCGTGGAGACCGCAGGCA   700
ACAGCAACTCCCACATCATTTTGCGCGGCGGTACCTCCGGCCCGAATCAT   750
GATGCAGCTTCGGTGGAGGCCGTCGTCGAGAAGCTTGGTGAAAACGCTCG   800
TCTCATGATCGATGCTTCCCATGCTAACTCCGGCAAGGATCATATCCGAC   850
AGGTTGAGGTTGTTCGTGAAATCGCAGAGCAGATTTCTGGCGGTTCTGAA   900
GCTGTGGCTGGAATCATGATTGAGTCCTTCCTCGTTGGTGGCGCACAGAA   950
CCTTGATCCTGCGAAATTGCGCATCAATGGCGGTGAAGGCCTGGTGTACG  1000
GACAGTCTGTGACCGATAAGTGCATCGATATTGACACCACCATCGATTTG  1050
CTCGCTGAGCTGGCCGCAGCAGTAAGGGAACGCCGAGCAGCAGCCAAGTA  1100
A                                                   1101
```

Figure 58: DNA sequence gene *aroI*_S187C - NCgl0950 - *C. glutamicum* ATCC13032

```
atgctccccattcccttggaaaaggcgcggcaacagccggaatgggagga     50
ccgggcgcaggtgcagcgcgcgcgggagaccctggccgagcgccccggac    100
tcgtccggccggacgacgtgcggacgctgcgtgcccatctggccctcgtc    150
agcgagggcgcggcccaggtcgtgcaggccggtgactgcgcggaggaccc    200
ggccgagtgcacggcggaccacgtcgcgcgcaaggtggccgtgctcgacc    250
tgctcgccggtgcgatgaagctggccgggcggcgtccggtgctgcgggtg    300
ggccggatcgcgggacagttcgccaagccgcggtcgcagccgaccgagcg    350
tgtcggggacggcgaactccccgtctaccggggccacctggtcaacggac    400
cggcgccggacgcggaggagaggcgccccgacccgctgcgtctggtcacc    450
gggtacatggccgccgccgacatcatcgcccacctcggacagggccgtgc    500
caccggcatcgaccagccggtgtggaccagccacgaggcgctggtcctcg    550
actacgaggtccccctggtgcgccggaccgacgagggggagctgctgctc    600
tcctcggcccactggccctggctcggggagcgcacccgccaggtggacgg    650
gccgcacgcggcgctgctcgcccaggtggtcaaccctgtcgccgtcaagg    700
tggggcccacggtggaggtggccgagctgctggcgctgtgcgccctgctg    750
gacccggagcggcgcccgggccggctgacgctgatcgtgcggatgggcgc    800
cgggacggtggccgagcggctgcccgcgctggtccgcgcggtgcggtcgg    850
ccgggcatccggtggtgtggctgaccgatccgatgcacggcaacacggtg    900
gtcacccgcagcggccacaagacgcggtacgtccgcacgttgcagcgcga    950
ggtccgcgagttccgcgccgtgctggccggggccggtgcgttccccggcg   1000
gtgtgcacctggagacgacgcccgaccaggtcaccgagtgcgtgctcgac   1050
gcctgggaggccgaccgggtcccggaggtctacacgagcttctgcgaccc   1100
gcggctcaccgtcgaccaggcgctcgaggtcctgagcgcctggggcgggg   1150
ccgaaccgccggcgatggcggccgaggtggccgggccgcggcaggcggcg   1200
gggggctga                                            1209
```

Figure 59: DNA sequence gene *nybF* - FM076 RS29120 - *Streptomyces albus* subsp. *chlorinus* NRRL B-24108

```
ATGGCCCCTGGAGCAGCACCGGTCCATGACGCCGAAGCGATCGGAATTCT    50
CGGCACCGGTTCCTGTCTTCCCGGAAAGGTCGTCACCAACGACGAGGTCG   100
GCGCACCGGCCGGCGTGACGGACGAGTGGATCACCCGGAAGACCGCCATC   150
CGCGAACGCCGCTGGGCGAAGGCGGACGAGGCCACCTCCGACCTGGCGGC   200
GATGGCCGCGCGCGCCGCGCTCGACGACGCGGGGGTCTGCCCGGCGGACA   250
TCTCCCTCGTCGTGGTGGCGACCTCCACACCCGACGCGCCCCAGCCGCCC   300
ACCGCCACCGCGGTCGCCGCCGAACTCGGCGTCCCGGCCGGCACCCCGGC   350
GTTCGACATCAACGCGGTGTGCAGCGGCTTCGTCTTCGCGCTGACCGCGG   400
CGGAGCGCATGATCCGCGGCACGGGCGGCCACGCCGTCGTCATCGGCGCC   450
GACATCTACTCGCGCACTCTCGACCCCACCGACCGCAGGACCGTCGTGCT   500
CTTCGGCGACGGCGCCGGAGCCGTGGTGCTGGGGCCCACCGCGACCGGAG   550
GTGTCCTCGCCACCGAGCTGGCCACCTTCCCGCAGGAACGGGACCTGATC   600
CGGGTCCCCGCGGGCGGCTCCCGGATACCCGCGTCCCGGGCCTCGGTCGA   650
GGAGGGCCTCCACTACTTCGCCATGGACGGCCCGGCGGTCCGCCACTTCG   700
TGGAGAACCGGGTCGGGCCGCTGATCCGCTCCTTCCTCGACCGCCATCTG   750
GCGGACCGCGCCCGGCGCGCGCACTTCGTCCCCCACCAGGCCAACGGGCG   800
GATGATCGCCGCGCTCGCCGACAGCCTCGGCTTTTTGCCGGAGCACACGC   850
ATACGACGGTGCGGTTCCTCGGCAACACCGGTGCCGCGTCGGTGCCGGTC   900
ACCCTCGACCGGGCCGCCGACCGGCTCGTGCCCGGCGACCTGGTGGTGCT   950
CGCCGGGTTCGGCGGCGGCATGGCCGCGGGCCTGGCCCTGGTCGAATGGC  1000
GGACGACGCGGGCCGGCGGGCGCGGCGGAAAGAGCCGTGCCGCCCTCGCG  1050
GCCGACGGGACCTGA                                     1065
```

Figure 60: DNA sequence gene *nybM* - FM076 RS29150 - *Streptomyces albus* subsp. *chlorinus* NRRL B-24108

```
GTGACAGACATCAAGCAAGAAGCCCCGGCTCCCCCCGCTCAGTCCCCGAA    50
ACGCTGGTGGGCCCTCCCCGTCGTGAGCCTGGCCCAGCTGATGGTCGTGC   100
TGGACGCGACCATCGTGAACATCGCCCTTCCCTCGGCCCAGCAGGACCTG   150
GGAATGTCGGACGCCGACCGGCACTGGGTCATCACCGCCTACGCCCTCGC   200
CTTCGGCGGGCTGCTGCTCGTGGGCGGCCGGGTGTGCGGCGCCCTCGGCC   250
ACCGCCGCTCCTTCACCCTCAGCCTGATCGGCTTCGCCGTGACCTCCGCG   300
CTCGGCGGAGCCGCGAACTCCGCGGGCATGCTGTTCGCCGCCCGCGCGGG   350
CCAGGGAGTCTTCGCCGCCCTCCTGGCGCCGGCCGCGCTGTCCCTGCTGA   400
TCCTGACGTTCACCGACGGGCGCGAACGGGGGAAGGCCTTCGGTGTGTTC   450
GCCGGGGTCGGCGCCGGCGGCGCGGCCCTGGGCGTGGTGGCCGGCGGTCT   500
GCTCACCGAGTACACCGACTGGCGCTGGTGCCTCTACATCAACGTCCCGA   550
TGGCCGCCCTCGCCCTGCTGGGCGTGCCGTTCATCATCCGGGACCGCCCC   600
AGCGGCACCCTGCGCCACCTGGACCTTCCCGGGGTGCTGCTCAGCGTCGC   650
CGGCCTCGTCTGCCTGGTCTACGGCTTCACCCAGGCCGAACCGCACGGCT   700
GGGGCGACCCGAAGGTGCTCTCCCTGCTGATCGGCGGCATCGTGCTGCTG   750
GGGCTGTTCGTCCTGGTCGAGGCCCGGACGGGGCACCCGCTGCTGCCGCT   800
GCGCATCCTCGCCCACCGCACACGGGGCGTCGCCTTCGTCTCCGTGTGCG   850
TGATGTTCATCGCGATGTTCGGCTTCTACCTGTTCGTCAGCTACTACACG   900
CAGACGATCCTCGGCTACTCACCCGTCAAGGCGGGCATGACGCTGCTGGT   950
GAACGCCGTGTGCACCACCATCGGCGCGATGCTGATCGCCGGAAAGCTGA  1000
CCGGCCGCGTCCCGGCGAACGTGCTGATCGCGGGCAGCCTGCTCTCCTCC  1050
GCCCTCGGCATGCTGATCCTCACCCAGCTGGAAGTGGACAGCTCCAACGT  1100
CTTCCTCGTCTATCTGACCCCCGCGATGATCCTGACGGGGCTCGGACTCG  1150
GCTGCCTGCTGGCGGCGGCGACCAACATGGCGACGGTGGAACTGGGCCAC  1200
GCCGAGGCGGGTGTCGCCTCAGCCGCGTACAACACGGTGCAGCAGGTGGG  1250
CGCCGCGTTCGGTACCGCTCTGCTCAACTCGATCGCTACCAGCGTCACCG  1300
GTGACTACCTCAAGGAGCACGGGGCCGGCCCGGAATCCGTCAACGCCGGG  1350
ACCGTGCACGGATACACGGTGGCGCTGTGGGTCGCCTTCGGCATCCTCCT  1400
CGCCGGTGCGGTGGCCGTCGCCCTCTTCTCCCGGCGCCGGGACAGCGAGG  1450
GCCGGCCGGAGGCCGTCCTCGAGTCCACGCACTGA                 1485
```

Figure 61: DNA sequence gene *nybV* - FM076 RS2919 - *Streptomyces albus* subsp. *chlorinus* NRRL B-24108

Table 8: Dynamic gene expression changes of the basic nybomycin producer *S. albus* 4N24. The data reflect log2-fold expression differences between the growth phase (13 h, set as reference) and the major nybomycin production phase (70 h) and include genes encoding sigma factors and potential regulators (Gläser et al., 2021). n=3

Gene	Annotation	Log2-fold change
SAD14N_0615	RNA polymerase sigma factor ECF subfamily	0.9
SAD14N_0683	RNA polymerase sigma factor ECF subfamily	-1.2
SAD14N_0749	RNA polymerase sigma factor ECF subfamily	0.0
SAD14N_0776	ROK-family transcriptional regulator	-0.3
SAD14N_1043	RNA polymerase, sigma 70 subunit, RpoD	0.4
SAD14N_1044	Sporulation transcription factor	2.4
SAD14N_1071	PpGpp synthetase/hydrolase	0.4
SAD14N_1132	BldB protein	0.5
SAD14N_1222	[Protein-PII] uridylyltransferase	-0.3
SAD14N_1223	Nitrogen regulatory protein P-II	-0.6
SAD14N_1224	Ammonium transporter	-0.1
SAD14N_1225	NsdA	2.9
SAD14N_1256	Transcriptional regulator, IclR family	-1.7
SAD14N_1391	Neutral zinc metalloprotease	-0.8
SAD14N_1515	RNA polymerase ECF-subfamily sigma factor	0.2
SAD14N_1539	arginine/ornithine binding protein	-0.7
SAD14N_1554	Nucleotide-binding protein	1.3
SAD14N_1574	HTH-type transcriptional repressor dasR	1.3
SAD14N_1584	RNA polymerase sigma factor RpoE, ECF subfamily	-0.2
SAD14N_1656	RNA polymerase sigma factor SigE, ECF subfamily	0.5
SAD14N_1798	sporulation and cell division protein SsgA	1.3
SAD14N_1962	Two-component system histidine kinase	-0.7
SAD14N_1963	Two-component system response regulator	-0.1
SAD14N_2142	RNA polymerase principal sigma factor hrdD	0.7
SAD14N_2151	Small membrane protein	1.9
SAD14N_2166	RdlB protein	2.1
SAD14N_2167	RdlA protein	2.5
SAD14N_2231	Transcriptional regulator AfsR	0.5
SAD14N_2232	AfsS	-2.2
SAD14N_2250	RNA polymerase ECF-subfamily sigma factor	1.6
SAD14N_2306	Factor C protein	0.0
SAD14N_2570	Phosphate regulon transcriptional regulatory protein PhoB (SphR)	1.5
SAD14N_2571	Phosphate regulon sensor protein PhoR (SphS)	1.7
SAD14N_2597	Universal stress protein UspA	-0.2
SAD14N_2728	Transcriptional regulator, Crp/Fnr family	-0.9
SAD14N_2735	WblA	1.5
SAD14N_2757	RNA polymerase ECF-subfamily sigma factor	-0.6
SAD14N_2760	Hypothetical protein	-0.3
SAD14N_2769	serine/threonine protein kinase	0.2
SAD14N_2903	sulfate transporter	1.2
SAD14N_2943	Two-component system sensor histidine kinase/response regulator	2.8

SAD14N_2992	NUDIX family hydrolase	0.5
SAD14N_3046	50S ribosomal protein L34	-0.1
SAD14N_3174	aromatase/cyclase	0.2
SAD14N_3275	Spermidine synthase	0.2
SAD14N_3298	Arsenic-transport integral membrane protein arsC	0.5
SAD14N_3323	TetR-family transcriptional regulator	-1.0
SAD14N_3489	Hypothetical protein	-0.4
SAD14N_3527	3-dehydroquinate dehydratase	1.7
SAD14N_3720	NADH-ubiquinone oxidoreductase chain G	-1.0
SAD14N_3805	30S ribosomal protein S7	0.8
SAD14N_3945	ATPase	0.1
SAD14N_3984	D-aminopeptidase	-0.4
SAD14N_3996	Integral membrane protein	-0.6
SAD14N_3997	Hypothetical protein	0.1
SAD14N_3998	CsbD family protein	0.3
SAD14N_4039	6-phosphogluconate dehydrogenase NAD-binding protein	1.0
SAD14N_4181	Secretory protein	-1.4
SAD14N_4476	1-aminocyclopropane-1-carboxylate deaminase	1.4
SAD14N_4658	Two-component system response regulator	-2.4
SAD14N_4681	Hypothetical protein	1.2
SAD14N_5022	Iron-regulated ABC-type transporter	2.6
SAD14N_5117	Sporulation-control protein	1.5
SAD14N_5152	glycosyltransferase	2.1
SAD14N_5153	Hypothetical protein	1.9
SAD14N_5208	Hypothetical protein	-2.1
SAD14N_5283	RarA	0.6
SAD14N_5315	50S ribosomal protein L20	1.4
SAD14N_5340	Acetyltransferase	0.4
SAD14N_5362	Secreted protein	-0.1
SAD14N_5529	ATP/GTP-binding protein	2.5
SAD14N_5625	ACT domain-containing protein	2.0
SAD14N_5652	DUF397 domain containing protein	0.8

7.4 Quality control of RNA sequencing data

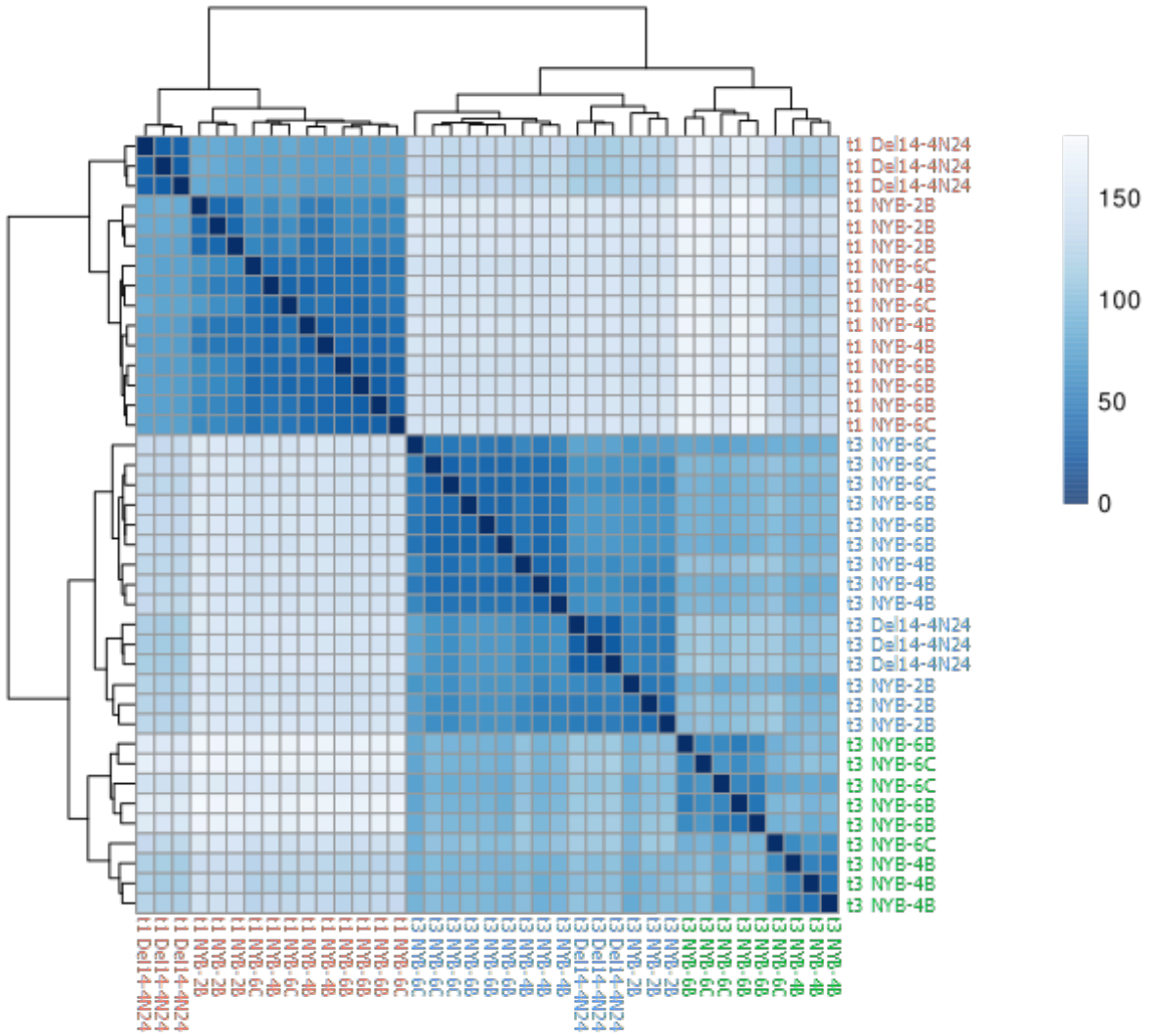

Figure 62: Statistical evaluation of gene expression profiles of *Streptomyces albus* 4N24 and different derivatives using sample to sample distances. For calculation of normalized read counts, the raw read count data were processed by DESeq2.

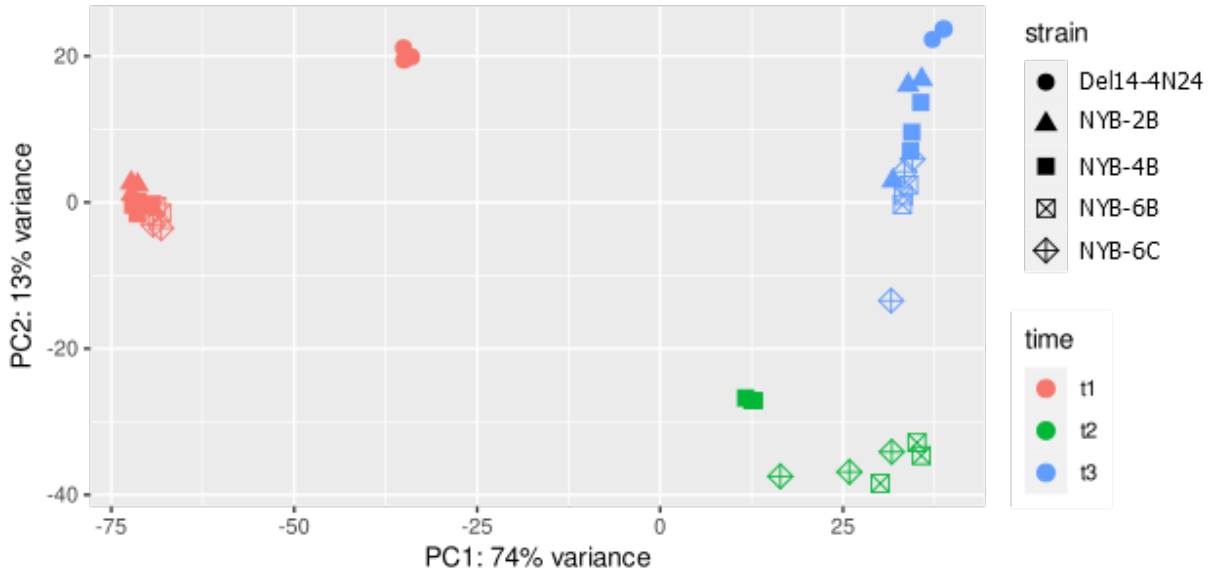

Figure 63: Statistical evaluation of gene expression profiles of *Streptomyces albus* 4N24 and different derivatives using PCA. Global transcription profiling of the cultures was conducted using RNA sequencing during the production process growth after 13 h (t1), 48 h (t2), and 70 h (t3). For calculation of normalized read counts, the raw read count data were processed by DESeq2 (Love et al., 2014), including regularized log transformation (with blind dispersion estimation enabled). Subsequently, PCA was performed and visualized using ggplot2 (Wickham et al., 2016). n=3.

8 References

Ahmed, Y., Rebets, Y., Estévez, M. R., Zapp, J., Myronovskyi, M., Luzhetskyy, A., 2020. Engineering of *Streptomyces lividans* for heterologous expression of secondary metabolite gene clusters. Microb Cell Fact. 19**,** 020-1277.

Aldred, K. J., Kerns, R. J., Osheroff, N., 2014. Mechanism of quinolone action and resistance. Biochemistry. 53**,** 1565-74.

Andexer, J. N., Kendrew, S. G., Nur-e-Alam, M., Lazos, O., Foster, T. A., Zimmermann, A.-S., Warneck, T. D., Suthar, D., Coates, N. J., Koehn, F. E., et al., 2011. Biosynthesis of the immunosuppressants FK506, FK520, and rapamycin involves a previously undescribed family of enzymes acting on chorismate. Proceedings of the National Academy of Sciences. 108**,** 4776-4781.

Arai, M., Kamiya, K., Pruksakorn, P., Sumii, Y., Kotoku, N., Joubert, J. P., Moodley, P., Han, C., Shin, D., Kobayashi, M., 2015. Anti-dormant mycobacterial activity and target analysis of nybomycin produced by a marine-derived *Streptomyces* sp. Bioorg Med Chem. 23**,** 3534-41.

Arai, T., Takahashi, K., Ishiguro, K., Mikami, Y., 1980. Some chemotherapeutic properties of two new antitumor antibiotics, saframycins A and C. Gan. 71**,** 790-6.

Bai, C., Zhang, Y., Zhao, X., Hu, Y., Xiang, S., Miao, J., Lou, C., Zhang, L., 2015. Exploiting a precise design of universal synthetic modular regulatory elements to unlock the microbial natural products in *Streptomyces*. Proc Natl Acad Sci U S A. 112**,** 12181-6.

Baltz, R. H., Antimicrobials from Actinomycetes : Back to the Future Actinomycetes are the source of most clinically relevant antibiotics in use today and may continue to. 2007.

Baltz, R. H., 2010. *Streptomyces* and *Saccharopolyspora* hosts for heterologous expression of secondary metabolite gene clusters. J Ind Microbiol Biotechnol. 37**,** 759-72.

Baltz, R. H., 2012. *Streptomyces* temperate bacteriophage integration systems for stable genetic engineering of actinomycetes (and other organisms). Journal of Industrial Microbiology and Biotechnology. 39**,** 661-672.

Bardell-Cox, O. A., White, A. J. P., Aragon, L., Fuchter, M. J., 2019. Synthetic studies on the reverse antibiotic natural products, the nybomycins. Medchemcomm. 10, 1438-1444.

Barka, E. A., Vatsa, P., Sanchez, L., Gaveau-Vaillant, N., Jacquard, C., Meier-Kolthoff, J. P., Klenk, H. P., Clement, C., Ouhdouch, Y., van Wezel, G. P., 2016. Taxonomy, Physiology, and Natural Products of *Actinobacteria*. Microbiol Mol Biol Rev. 80, 1-43.

Barton, N., Horbal, L., Starck, S., Kohlstedt, M., Luzhetskyy, A., Wittmann, C., 2018. Enabling the valorization of guaiacol-based lignin: Integrated chemical and biochemical production of cis,cis-muconic acid using metabolically engineered *Amycolatopsis* sp ATCC 39116. Metab Eng. 45, 200-210.

Basan, M., Hui, S., Okano, H., Zhang, Z., Shen, Y., Williamson, J. R., Hwa, T., 2015. Overflow metabolism in *Escherichia coli* results from efficient proteome allocation. Nature. 528, 99-104.

Bast, D. J., Low, D. E., Duncan, C. L., Kilburn, L., Mandell, L. A., Davidson, R. J., de Azavedo, J. C., 2000. Fluoroquinolone resistance in clinical isolates of *Streptococcus pneumoniae*: contributions of type II topoisomerase mutations and efflux to levels of resistance. Antimicrob Agents Chemother. 44, 3049-54.

Becker, J., Klopprogge, C., Herold, A., Zelder, O., Bolten, C. J., Wittmann, C., 2007. Metabolic flux engineering of L-lysine production in *Corynebacterium glutamicum* -over expression and modification of G6P dehydrogenase. J Biotechnol. 132, 99-109.

Becker, J., Klopprogge, C., Schröder, H., Wittmann, C., 2009. Metabolic engineering of the tricarboxylic acid cycle for improved lysine production by *Corynebacterium glutamicum*. Appl Environ Microbiol. 75, 7866-9.

Becker, J., Klopprogge, C., Wittmann, C., 2008. Metabolic responses to pyruvate kinase deletion in lysine producing *Corynebacterium glutamicum*. Microb Cell Fact. 7, 8.

Becker, J., Klopprogge, C., Zelder, O., Heinzle, E., Wittmann, C., 2005. Amplified expression of fructose 1,6-bisphosphatase in *Corynebacterium glutamicum* increases in vivo flux through the pentose phosphate pathway and lysine production on different carbon sources. Appl Environ Microbiol. 71, 8587-96.

Becker, J., Kuhl, M., Kohlstedt, M., Starck, S., Wittmann, C., 2018a. Metabolic engineering of *Corynebacterium glutamicum* for the production of cis, cis-muconic acid from lignin. Microb Cell Fact. 17**,** 115.

Becker, J., Rohles, C. M., Wittmann, C., 2018b. Metabolically engineered *Corynebacterium glutamicum* for bio-based production of chemicals, fuels, materials, and healthcare products. Metab Eng. 50**,** 122-141.

Becker, J., Wittmann, C., 2015. Advanced Biotechnology: Metabolically Engineered Cells for the Bio-Based Production of Chemicals and Fuels, Materials, and Health-Care Products. Angewandte Chemie International Edition. 54**,** 3328-3350.

Becker, J., Zelder, O., Hafner, S., Schroder, H., Wittmann, C., 2011. From zero to hero--design-based systems metabolic engineering of *Corynebacterium glutamicum* for L-lysine production. Metab Eng. 13**,** 159-68.

Bednarz, B., Kotowska, M., Pawlik, K. J., 2019. Multi-level regulation of coelimycin synthesis in *Streptomyces coelicolor* A3(2). Appl Microbiol Biotechnol. 103**,** 6423-6434.

Bentley, S. D., Brown, S., Murphy, L. D., Harris, D. E., Quail, M. A., Parkhill, J., Barrell, B. G., McCormick, J. R., Santamaria, R. I., Losick, R., et al., 2004. SCP1, a 356,023 bp linear plasmid adapted to the ecology and developmental biology of its host, *Streptomyces coelicolor* A3(2). Mol Microbiol. 51**,** 1615-28.

Bentley, S. D., Chater, K. F., Cerdeno-Tarraga, A. M., Challis, G. L., Thomson, N. R., James, K. D., Harris, D. E., Quail, M. A., Kieser, H., Harper, D., et al., 2002. Complete genome sequence of the model actinomycete *Streptomyces coelicolor* A3(2). Nature. 417**,** 141-7.

Berdy, J., 2005. Bioactive microbial metabolites. J Antibiot (Tokyo). 58**,** 1-26.

Beste, D. J. V., Hooper, T., Stewart, G., Bonde, B., Avignone-Rossa, C., Bushell, M. E., Wheeler, P., Klamt, S., Kierzek, A. M., McFadden, J., 2007. GSMN-TB: a web-based genome-scale network model of *Mycobacterium tuberculosis* metabolism. Genome Biology. 8**,** R89.

Bibb, M. J., 2005. Regulation of secondary metabolism in *streptomycetes*. Curr Opin Microbiol. 8**,** 208-215.

Bibb, M. J., White, J., Ward, J. M., Janssen, G. R., 1994. The mRNA for the 23S rRNA methylase encoded by the ermE gene of *Saccharopolyspora erythraea* is

translated in the absence of a conventional ribosome-binding site. Mol Microbiol. 14, 533-45.

Bierman, M., Logan, R., O'Brien, K., Seno, E. T., Rao, R. N., Schoner, B. E., 1992. Plasmid cloning vectors for the conjugal transfer of DNA from *Escherichia coli* to *Streptomyces* spp. Gene. 116, 43-9.

Blin, K., Shaw, S., Augustijn, H. E., Reitz, Z. L., Biermann, F., Alanjary, M., Fetter, A., Terlouw, B. R., Metcalf, W. W., Helfrich, E. J. N., et al., 2023. antiSMASH 7.0: new and improved predictions for detection, regulation, chemical structures and visualisation. Nucleic Acids Res.

Blower, T. R., Williamson, B. H., Kerns, R. J., Berger, J. M., 2016. Crystal structure and stability of gyrase–fluoroquinolone cleaved complexes from *Mycobacterium tuberculosis*. Proceedings of the National Academy of Sciences. 113, 1706-1713.

Bo, G., 2000. Giuseppe Brotzu and the discovery of cephalosporins. Clinical Microbiology and Infection. 6, 6-8.

Bobek, J., Mikulová, A., Šetinová, D., Elliot, M., Čihák, M., 2021. 6S-Like scr3559 RNA Affects Development and Antibiotic Production in *Streptomyces coelicolor*. Microorganisms. 9.

Bolten, C. J., Kiefer, P., Letisse, F., Portais, J. C., Wittmann, C., 2007. Sampling for metabolome analysis of microorganisms. Anal Chem. 79, 3843-9.

Boss, E., Sherwood, C. R., Hill, P., Milligan, T., 2018. Advantages and Limitations to the Use of Optical Measurements to Study Sediment Properties. Applied Sciences. 8, 2692.

Brock, T. D., 1961. Chloramphenicol. Bacteriol Rev. 25, 32-48.

Bu, Q.-T., Yu, P., Wang, J., Li, Z.-Y., Chen, X.-A., Mao, X.-M., Li, Y.-Q., 2019. Rational construction of genome-reduced and high-efficient industrial *Streptomyces* chassis based on multiple comparative genomic approaches. Microb Cell Fact. 18, 16.

Buschke, N., Becker, J., Schäfer, R., Kiefer, P., Biedendieck, R., Wittmann, C., 2013. Systems metabolic engineering of xylose-utilizing *Corynebacterium glutamicum* for production of 1,5-diaminopentane. Biotechnol J. 8, 557-70.

Chadwick, D. J., Whelan, J., Secondary metabolites: their function and evolution. 1992.

Chan, P. F., Huang, J., Bax, B. D., Gwynn, M. N., 2013. Recent Developments in Inhibitors of Bacterial Type IIA Topoisomerases. Antibiotics (Basel). pp. 263-297.

Chater, K. F., Wilde, L. C., 1976. Restriction of a bacteriophage of *Streptomyces albus* G involving endonuclease SalI. J Bacteriol. 128**,** 644-50.

Chater, K. F., Wilde, L. C., 1980. *Streptomyces albus* G mutants defective in the *Sal*GI restriction-modification system. J Gen Microbiol. 116**,** 323-34.

Chen, D., Zhang, Q., Cen, P., Xu, Z., Liu, W., 2012. Improvement of FK506 production in *Streptomyces tsukubaensis* by genetic enhancement of the supply of unusual polyketide extender units via utilization of two distinct site-specific recombination systems. Appl Environ Microbiol. 78**,** 5093-103.

Cho, M. K., Lee, B. T., Kim, H. U., Oh, M. K., 2022. Systems metabolic engineering of *Streptomyces venezuelae* for the enhanced production of pikromycin. Biotechnol Bioeng. 119**,** 2250-2260.

Choi, J. H., Lee, S. J., Lee, S. J., Lee, S. Y., 2003. Enhanced production of insulin-like growth factor I fusion protein in *Escherichia coli* by coexpression of the down-regulated genes identified by transcriptome profiling. Appl Environ Microbiol. 69**,** 4737-42.

Choi, K. R., Jang, W. D., Yang, D., Cho, J. S., Park, D., Lee, S. Y., 2019. Systems Metabolic Engineering Strategies: Integrating Systems and Synthetic Biology with Metabolic Engineering. Trends Biotechnol. 37**,** 817-837.

Choi, K. R., Shin, J. H., Cho, J. S., Yang, D., Lee, S. Y., 2016. Systems Metabolic Engineering of *Escherichia coli*. EcoSal Plus. 7.

Claessen, D., Rozen, D. E., Kuipers, O. P., Sogaard-Andersen, L., van Wezel, G. P., 2014. Bacterial solutions to multicellularity: a tale of biofilms, filaments and fruiting bodies. Nat Rev Microbiol. 12**,** 115-24.

d'Espaux, L., Ghosh, A., Runguphan, W., Wehrs, M., Xu, F., Konzock, O., Dev, I., Nhan, M., Gin, J., Reider Apel, A., et al., 2017. Engineering high-level production of fatty alcohols by *Saccharomyces cerevisiae* from lignocellulosic feedstocks. Metab Eng. 42**,** 115-125.

Dalla Pozza, E., Dando, I., Pacchiana, R., Liboi, E., Scupoli, M. T., Donadelli, M., Palmieri, M., 2020. Regulation of succinate dehydrogenase and role of succinate in cancer. Seminars in Cell & Developmental Biology. 98**,** 4-14.

Dang, L., Liu, J., Wang, C., Liu, H., Wen, J., 2017. Enhancement of rapamycin production by metabolic engineering in *Streptomyces hygroscopicus* based on genome-scale metabolic model. J Ind Microbiol Biotechnol. 44, 259-270.

Davies, J., 2011. How to discover new antibiotics: harvesting the parvome. Curr Opin Chem Biol. 15, 5-10.

Deguchi, T., Fukuoka, A., Yasuda, M., Nakano, M., Ozeki, S., Kanematsu, E., Nishino, Y., Ishihara, S., Ban, Y., Kawada, Y., 1997. Alterations in the GyrA subunit of DNA gyrase and the ParC subunit of topoisomerase IV in quinolone-resistant clinical isolates of *Klebsiella pneumoniae*. Antimicrob Agents Chemother. 41, 699-701.

Dell, K. A., Frost, J. W., 1993. Identification and removal of impediments to biocatalytic synthesis of aromatics from D-glucose: rate-limiting enzymes in the common pathway of aromatic amino acid biosynthesis. J Am Chem Soc. 115, 11581-11589.

Demain, A. L., 2014. Importance of microbial natural products and the need to revitalize their discovery. J Ind Microbiol Biotechnol. 41, 185-201.

Demain, A. L., Fang, A., 2000. The natural functions of secondary metabolites. Adv Biochem Eng Biotechnol. 69, 1-39.

Dhungel, S., Rijal, K. R., Yadav, B., Dhungel, B., Adhikari, N., Shrestha, U. T., Adhikari, B., Banjara, M. R., Ghimire, P., 2021. Methicillin-Resistant Staphylococcus aureus (MRSA): Prevalence, Antimicrobial Susceptibility Pattern, and Detection of mecA Gene among Cardiac Patients from a Tertiary Care Heart Center in Kathmandu, Nepal. Infect Dis (Auckl). 14, 11786337211037355.

Didelot, X., Bowden, R., Wilson, D. J., Peto, T. E. A., Crook, D. W., 2012. Transforming clinical microbiology with bacterial genome sequencing. Nature Reviews Genetics. 13, 601-612.

Dobson, P. D., Smallbone, K., Jameson, D., Simeonidis, E., Lanthaler, K., Pir, P., Lu, C., Swainston, N., Dunn, W. B., Fisher, P., et al., 2010. Further developments towards a genome-scale metabolic model of yeast. BMC Systems Biology. 4, 145.

Drlica, K., Hiasa, H., Kerns, R., Malik, M., Mustaev, A., Zhao, X., 2009. Quinolones: action and resistance updated. Curr Top Med Chem. 9, 981-98.

Edwards, J. S., Palsson, B. O., 2000. The *Escherichia coli* MG1655 *in silico* metabolic genotype: Its definition, characteristics, and capabilities. Proceedings of the National Academy of Sciences. 97**,** 5528-5533.

Egawa, K., Yamori, T., Nosaka, C., Kunimoto, S., Takeuchi, T., Nos, K., 2000. Deoxynybomycin is a selective anti-tumor agent inducing apoptosis and inhibiting topoisomerase I. Biol Pharm Bull. 23**,** 1036-40.

Eliopoulos, G. M., Willey, S., Reiszner, E., Spitzer, P. G., Caputo, G., Moellering, R. C., Jr., 1986. In vitro and in vivo activity of LY 146032, a new cyclic lipopeptide antibiotic. Antimicrob Agents Chemother. 30**,** 532-5.

Elliot, M., Damji, F., Passantino, R., Chater, K., Leskiw, B., 1998. The *bld*D gene of *Streptomyces coelicolor* A3(2): a regulatory gene involved in morphogenesis and antibiotic production. J Bacteriol. 180**,** 1549-55.

Eudes, A., Juminaga, D., Baidoo, E. E., Collins, F. W., Keasling, J. D., Loque, D., 2013. Production of hydroxycinnamoyl anthranilates from glucose in *Escherichia coli*. Microb Cell Fact. 12**,** 62.

Euverink, G.-J., 1995. Aromatic amino acid biosynthesis in actinomycetes.

Feierabend, M., Renz, A., Zelle, E., Noh, K., Wiechert, W., Drager, A., 2021. High-Quality Genome-Scale Reconstruction of *Corynebacterium glutamicum* ATCC 13032. Front Microbiol. 12**,** 750206.

Feng, Z., Wang, L., Rajski, S. R., Xu, Z., Coeffet-LeGal, M. F., Shen, B., 2009. Engineered production of iso-migrastatin in heterologous *Streptomyces* hosts. Bioorg Med Chem. 17**,** 2147-53.

Ferraiuolo, S. B., Cammarota, M., Schiraldi, C., Restaino, O. F., 2021. Streptomycetes as platform for biotechnological production processes of drugs. Appl Microbiol Biotechnol. 105**,** 551-568.

Ferrero, L., Cameron, B., Manse, B., Lagneaux, D., Crouzet, J., Famechon, A., Blanche, F., 1994. Cloning and primary structure of Staphylococcus aureus DNA topoisomerase IV: a primary target of fluoroquinolones. Mol Microbiol. 13**,** 641-53.

Fleming, A., 1929. On the Antibacterial Action of Cultures of a Penicillium, with Special Reference to their Use in the Isolation of *B. influenzæ*. Br J Exp Pathol. 1929 Jun;10(3):226-36.

Forbis, R. M., Rinehart, K. L., Jr., 1970. Nybomycin. IV. Total synthesis of deoxynybomycin. J Am Chem Soc. 92**,** 6995-6.

Forbis, R. M., Rinehart, K. L., Jr., 1971. Nybomycin. V. Total synthesis of nybomycin. J Antibiot (Tokyo). 24, 326-7.

Forbis, R. M., Rinehart, K. L., Jr., 1973. Nybomycin. VII. Preparative routes to nybomycin and deoxynybomycin. J Am Chem Soc. 95, 5003-13.

Forster, J., Famili, I., Fu, P., Palsson, B. O., Nielsen, J., 2003. Genome-scale reconstruction of the *Saccharomyces cerevisiae* metabolic network. Genome Res. 13, 244-53.

Fujita, Y., Matsuoka, H., Hirooka, K., 2007. Regulation of fatty acid metabolism in bacteria. Mol Microbiol. 66, 829-39.

Garcia-Gutierrez, C., Aparicio, T., Torres-Sanchez, L., Martinez-Garcia, E., de Lorenzo, V., Villar, C. J., Lombo, F., 2020. Multifunctional SEVA shuttle vectors for actinomycetes and Gram-negative bacteria. Microbiologyopen. 9, 1135-1149.

Geraci, J. E., Heilman, F. R., Nichols, D. R., Wellman, E. W., Ross, G. T., 1956. Some laboratory and clinical experiences with a new antibiotic, vancomycin. Antibiot Annu. 90-106.

Giesselmann, G., Dietrich, D., Jungmann, L., Kohlstedt, M., Jeon, E. J., Yim, S. S., Sommer, F., Zimmer, D., Muhlhaus, T., Schroda, M., et al., 2019. Metabolic engineering of *Corynebacterium glutamicum* for high-level ectoine production: Design, combinatorial assembly, and implementation of a transcriptionally balanced heterologous ectoine pathway. Biotechnol J. 14, e1800417.

Gläser, L., Kuhl, M., Jovanovic, S., Fritz, M., Vögeli, B., Erb, T. J., Becker, J., Wittmann, C., 2020. A common approach for absolute quantification of short chain CoA thioesters in prokaryotic and eukaryotic microbes. Microb Cell Fact. 19, 160.

Gläser, L., Kuhl, M., Stegmüller, J., Rückert, C., Myronovskyi, M., Kalinowski, J., Luzhetskyy, A., Wittmann, C., 2021. Superior production of heavy pamamycin derivatives using a *bkdR* deletion mutant of *Streptomyces albus* J1074/R2. Microb Cell Fact. 20, 111.

Goelzer, A., Bekkal Brikci, F., Martin-Verstraete, I., Noirot, P., Bessières, P., Aymerich, S., Fromion, V., 2008. Reconstruction and analysis of the genetic and metabolic regulatory networks of the central metabolism of *Bacillus subtilis*. BMC Systems Biology. 2, 20.

Gould, S. J., Erickson, W. R., 1988. Isolation of 4-aminoanthranilic acid: a new shikimate pathway product from *Streptomyces flocculus*. J Antibiot (Tokyo). 41, 688-9.

Gramajo, H. C., Takano, E., Bibb, M. J., 1993. Stationary-phase production of the antibiotic actinorhodin in *Streptomyces coelicolor* A3(2) is transcriptionally regulated. Mol Microbiol. 7, 837-45.

Gregory, M. A., Till, R., Smith, M. C., 2003. Integration site for *Streptomyces* phage phiBT1 and development of site-specific integrating vectors. J Bacteriol. 185, 5320-3.

Gullon, S., Olano, C., Abdelfattah, M. S., Brana, A. F., Rohr, J., Mendez, C., Salas, J. A., 2006. Isolation, characterization, and heterologous expression of the biosynthesis gene cluster for the antitumor anthracycline steffimycin. Appl Environ Microbiol. 72, 4172-83.

Gummerlich, N., Manderscheid, N., Rebets, Y., Myronovskyi, M., Gläser, L., Kuhl, M., Wittmann, C., Luzhetskyy, A., 2021. Engineering the precursor pool to modulate the production of pamamycins in the heterologous host *S. albus* J1074. Metab Eng. 67, 11-18.

Gupta, N., 2019. DNA Extraction and Polymerase Chain Reaction. J Cytol. 36, 116-117.

Gustavsson, M., Lee, S. Y., 2016. Prospects of microbial cell factories developed through systems metabolic engineering. Microb Biotechnol. 9, 610-617.

Hackl, S., Bechthold, A., 2015. The Gene *bldA*, a regulator of morphological differentiation and antibiotic production in *streptomyces*. Arch Pharm. 348, 455-62.

Harrison, J., Studholme, D. J., 2014. Recently published *Streptomyces* genome sequences. Microb Biotechnol. 7, 373-80.

Hassoun, A., Linden, P. K., Friedman, B., 2017. Incidence, prevalence, and management of MRSA bacteremia across patient populations-a review of recent developments in MRSA management and treatment. Crit Care. 21, 211.

Hayashi, M., Ohnishi, J., Mitsuhashi, S., Yonetani, Y., Hashimoto, S., Ikeda, M., 2006. Transcriptome analysis reveals global expression changes in an industrial L-lysine producer of *Corynebacterium glutamicum*. Biosci Biotechnol Biochem. 70, 546-50.

Hazen, E. L., Brown, R., 1950. Two antifungal agents produced by a soil actinomycete. Science (New York, N.Y.). 112, 423.

Henry, C. S., Zinner, J. F., Cohoon, M. P., Stevens, R. L., 2009. iBsu1103: a new genome-scale metabolic model of *Bacillus subtilis* based on SEED annotations. Genome Biology. 10, R69.

Hergenrother, P. J., Riley, A. P., Topoisomerase inhibitors with antibacterial and anticancer activity. U.S. Patent No. 11274106, 2022.

Herrmann, S., Siegl, T., Luzhetska, M., Petzke, L., Jilg, C., Welle, E., Erb, A., Leadlay, P. F., Bechthold, A., Luzhetskyy, A., 2012. Site-specific recombination strategies for engineering actinomycete genomes. Appl Environ Microbiol. 78, 1804-12.

Higgens, C. E., Kastner, R. E., 1971. *Streptomyces clavuligerus* sp. nov., a β-Lactam Antibiotic Producer. Int J Syst Evol Microbiol. 21, 326-331.

Hiramatsu, K., Igarashi, M., Morimoto, Y., Baba, T., Umekita, M., Akamatsu, Y., 2012. Curing bacteria of antibiotic resistance: reverse antibiotics, a novel class of antibiotics in nature. Int J Antimicrob Agents. 39, 478-85.

Hiramatsu, K., Sasaki, T., Morimoto, Y., 2015. Future Chemotherapy Preventing Emergence of Multi-Antibiotic Resistance. Juntendo Medical Journal. 61, 249-256.

Hirose, K., Terajima, J., Izumiya, H., Tamura, K., Arakawa, E., Takai, N., Watanabe, H., 2005. Antimicrobial susceptibility of *Shigella sonnei* isolates in Japan and molecular analysis of *S. sonnei* isolates with reduced susceptibility to fluoroquinolones. Antimicrob Agents Chemother. 49, 1203-5.

Hoffmann, S. L., Jungmann, L., Schiefelbein, S., Peyriga, L., Cahoreau, E., Portais, J. C., Becker, J., Wittmann, C., 2018. Lysine production from the sugar alcohol mannitol: Design of the cell factory *Corynebacterium glutamicum* SEA-3 through integrated analysis and engineering of metabolic pathway fluxes. Metab Eng. 47, 475-487.

Hoffmann, S. L., Kohlstedt, M., Jungmann, L., Hutter, M., Poblete-Castro, I., Becker, J., Wittmann, C., 2021. Cascaded valorization of brown seaweed to produce l-lysine and value-added products using *Corynebacterium glutamicum* streamlined by systems metabolic engineering. Metab Eng. 67, 293-307.

Holt, T. G., Chang, C., Laurent-Winter, C., Murakami, T., Garrels, J. I., Davies, J. E., Thompson, C. J., 1992. Global changes in gene expression related to antibiotic synthesis in *Streptomyces hygroscopicus*. Mol Microbiol. 6, 969-80.

Hopwood, D. A., 1999. Forty years of genetics with *Streptomyces*: from in vivo through *in vitro* to *in silico*. Microbiology. 145, 2183-2202.

Hopwood, D. A., 2006. Soil to genomics: the *Streptomyces* chromosome. Annu Rev Genet. 40, 1-23.

Horbal, L., Siegl, T., Luzhetskyy, A., 2018. A set of synthetic versatile genetic control elements for the efficient expression of genes in *Actinobacteria*. Sci Rep. 8, 491.

Hosoya, Y., Okamoto, S., Muramatsu, H., Ochi, K., 1998. Acquisition of certain streptomycin-resistant (str) mutations enhances antibiotic production in bacteria. Antimicrob Agents Chemother. 42, 2041-7.

Hover, B. M., Kim, S.-H., Katz, M., Charlop-Powers, Z., Owen, J. G., Ternei, M. A., Maniko, J., Estrela, A. B., Molina, H., Park, S., et al., 2018. Culture-independent discovery of the malacidins as calcium-dependent antibiotics with activity against multidrug-resistant Gram-positive pathogens. Nature Microbiology. 3, 415-422.

Huang, D., Jia, X., Wen, J., Wang, G., Yu, G., Caiyin, Q., Chen, Y., 2011. Metabolic flux analysis and principal nodes identification for daptomycin production improvement by *Streptomyces roseosporus*. Appl Biochem Biotechnol. 165, 1725-39.

Huang, D., Li, S., Xia, M., Wen, J., Jia, X., 2013a. Genome-scale metabolic network guided engineering of *Streptomyces tsukubaensis* for FK506 production improvement. Microb Cell Fact. 12, 52.

Huang, D., Xia, M., Li, S., Wen, J., Jia, X., 2013b. Enhancement of FK506 production by engineering secondary pathways of *Streptomyces tsukubaensis* and exogenous feeding strategies. J Ind Microbiol Biotechnol. 40, 1023-37.

Huang, S., Millar, A. H., 2013. Succinate dehydrogenase: the complex roles of a simple enzyme. Current Opinion in Plant Biology. 16, 344-349.

Huo, L., Rachid, S., Stadler, M., Wenzel, S. C., Muller, R., 2012. Synthetic biotechnology to study and engineer ribosomal bottromycin biosynthesis. Chem Biol. 19, 1278-87.

Hwang, M.-S., Rohlena, J., Dong, L.-F., Neuzil, J., Grimm, S., 2014. Powerhouse down: Complex II dissociation in the respiratory chain. Mitochondrion. 19, 20-28.

Hwang, S., Lee, N., Jeong, Y., Lee, Y., Kim, W., Cho, S., Palsson, B. O., Cho, B. K., 2019. Primary transcriptome and translatome analysis determines transcriptional and translational regulatory elements encoded in the *Streptomyces clavuligerus* genome. Nucleic Acids Res. 47, 6114-6129.

Ian, E., Malko, D. B., Sekurova, O. N., Bredholt, H., Rückert, C., Borisova, M. E., Albersmeier, A., Kalinowski, J., Gelfand, M. S., Zotchev, S. B., 2014. Genomics of sponge-associated *Streptomyces* spp. closely related to *Streptomyces albus* J1074: insights into marine adaptation and secondary metabolite biosynthesis potential. PLoS One. 9, e96719.

Ikeda, H., Ishikawa, J., Hanamoto, A., Shinose, M., Kikuchi, H., Shiba, T., Sakaki, Y., Hattori, M., Omura, S., 2003. Complete genome sequence and comparative analysis of the industrial microorganism *Streptomyces avermitilis*. Nat Biotechnol. 21, 526-31.

Ikeda, M., 2006. Towards bacterial strains overproducing L-tryptophan and other aromatics by metabolic engineering. Appl Microbiol Biotechnol. 69, 615-26.

Ji, C. H., Kim, H., Je, H. W., Kwon, H., Lee, D., Kang, H. S., 2022. Top-down synthetic biology approach for titer improvement of clinically important antibiotic daptomycin in *Streptomyces roseosporus*. Metab Eng. 69, 40-49.

Ji, C. H., Kim, J. P., Kang, H. S., 2018. Library of Synthetic *Streptomyces* Regulatory Sequences for Use in Promoter Engineering of Natural Product Biosynthetic Gene Clusters. ACS Synth Biol. 7, 1946-1955.

Jin, X. M., Chang, Y. K., Lee, J. H., Hong, S. K., 2017. Effects of Increased NADPH Concentration by Metabolic Engineering of the Pentose Phosphate Pathway on Antibiotic Production and Sporulation in *Streptomyces lividans* TK24. J Microbiol Biotechnol. 27, 1867-1876.

Jin, Z., Jin, X., Jin, Q., 2010. Conjugal transferring of resistance gene ptr for improvement of pristinamycin-producing *Streptomyces pristinaespiralis*. Appl Biochem Biotechnol. 160, 1853-64.

Jones, J. A., Vernacchio, V. R., Lachance, D. M., Lebovich, M., Fu, L., Shirke, A. N., Schultz, V. L., Cress, B., Linhardt, R. J., Koffas, M. A., 2015. ePathOptimize: A

Combinatorial Approach for Transcriptional Balancing of Metabolic Pathways. Sci Rep. 5, 11301.

Jones, S. E., Elliot, M. A., 2018. 'Exploring' the regulation of *Streptomyces* growth and development. Curr Opin Microbiol. 42, 25-30.

Kaiser, J. C., Heinrichs, D. E., 2018. Branching Out: Alterations in Bacterial Physiology and Virulence Due to Branched-Chain Amino Acid Deprivation. mBio. 9.

Kallifidas, D., Jiang, G., Ding, Y., Luesch, H., 2018. Rational engineering of *Streptomyces albus* J1074 for the overexpression of secondary metabolite gene clusters. Microb Cell Fact. 17, 25.

Kang, C. M., Abbott, D. W., Park, S. T., Dascher, C. C., Cantley, L. C., Husson, R. N., 2005. The *Mycobacterium tuberculosis* serine/threonine kinases PknA and PknB: substrate identification and regulation of cell shape. Genes Dev. 19, 1692-704.

Kavvas, E. S., Seif, Y., Yurkovich, J. T., Norsigian, C., Poudel, S., Greenwald, W. W., Ghatak, S., Palsson, B. O., Monk, J. M., 2018. Updated and standardized genome-scale reconstruction of *Mycobacterium tuberculosis* H37Rv, iEK1011, simulates flux states indicative of physiological conditions. BMC Systems Biology. 12, 25.

Kieser, T., Bibb, M. J., Buttner, M. J., Chater, K. F., Hopwood, D. A., 2000. Practical *Streptomyces* Genetics. The John Innes Foundation, Norwich, UK.

Kikuchi, Y., Tsujimoto, K., Kurahashi, O., 1997. Mutational analysis of the feedback sites of phenylalanine-sensitive 3-deoxy-D-arabino-heptulosonate-7-phosphate synthase of *Escherichia coli*. Appl Environ Microbiol. 63, 761-2.

Kim, M., Rai, N., Zorraquino, V., Tagkopoulos, I., 2016. Multi-omics integration accurately predicts cellular state in unexplored conditions for *Escherichia coli*. Nat Commun. 7, 13090.

Kim, S., Jang, Y. S., Ha, S. C., Ahn, J. W., Kim, E. J., Lim, J. H., Cho, C., Ryu, Y. S., Lee, S. K., Lee, S. Y., et al., 2015. Redox-switch regulatory mechanism of thiolase from *Clostridium acetobutylicum*. Nat Commun. 6, 8410.

Kim, S. Y., Zhao, P., Igarashi, M., Sawa, R., Tomita, T., Nishiyama, M., Kuzuyama, T., 2009. Cloning and heterologous expression of the cyclooctatin biosynthetic gene cluster afford a diterpene cyclase and two p450 hydroxylases. Chem Biol. 16, 736-43.

Kind, S., Jeong, W. K., Schröder, H., Wittmann, C., 2010a. Systems-wide metabolic pathway engineering in *Corynebacterium glutamicum* for bio-based production of diaminopentane. Metab Eng. 12**,** 341-51.

Kind, S., Jeong, W. K., Schröder, H., Zelder, O., Wittmann, C., 2010b. Identification and elimination of the competing N-acetyldiaminopentane pathway for improved production of diaminopentane by *Corynebacterium glutamicum*. Appl Environ Microbiol. 76**,** 5175-80.

Kind, S., Kreye, S., Wittmann, C., 2011. Metabolic engineering of cellular transport for overproduction of the platform chemical 1,5-diaminopentane in *Corynebacterium glutamicum*. Metab Eng. 13**,** 617-627.

Kinkel, L. L., Schlatter, D. C., Xiao, K., Baines, A. D., 2014. Sympatric inhibition and niche differentiation suggest alternative coevolutionary trajectories among Streptomycetes. The ISME Journal. 8**,** 249-256.

Kitani, S., Miyamoto, K. T., Takamatsu, S., Herawati, E., Iguchi, H., Nishitomi, K., Uchida, M., Nagamitsu, T., Omura, S., Ikeda, H., et al., 2011. Avenolide, a *Streptomyces hormone* controlling antibiotic production in *Streptomyces avermitilis*. Proc Natl Acad Sci U S A. 108**,** 16410-5.

Kogenaru, S., Yan, Q., Guo, Y., Wang, N., 2012. RNA-seq and microarray complement each other in transcriptome profiling. BMC Genomics. 13**,** 629.

Kohanski, M. A., DePristo, M. A., Collins, J. J., 2010. Sublethal antibiotic treatment leads to multidrug resistance via radical-induced mutagenesis. Mol Cell. 37**,** 311-20.

Kohlstedt, M., Sappa, P. K., Meyer, H., Maass, S., Zaprasis, A., Hoffmann, T., Becker, J., Steil, L., Hecker, M., van Dijl, J. M., et al., 2014. Adaptation of *Bacillus subtilis* carbon core metabolism to simultaneous nutrient limitation and osmotic challenge: a multi-omics perspective. Environ Microbiol. 16**,** 1898-1917.

Kohlstedt, M., Starck, S., Barton, N., Stolzenberger, J., Selzer, M., Mehlmann, K., Schneider, R., Pleissner, D., Rinkel, J., Dickschat, J. S., et al., 2018. From lignin to nylon: Cascaded chemical and biochemical conversion using metabolically engineered *Pseudomonas putida*. Metab Eng. 47**,** 279-293.

Kohlstedt, M., Weimer, A., Weiland, F., Stolzenberger, J., Selzer, M., Sanz, M., Kramps, L., Wittmann, C., 2022. Biobased PET from lignin using an engineered cis, cis-muconate-producing *Pseudomonas putida* strain with superior robustness, energy and redox properties. Metab Eng. 72**,** 337-352.

Kois-Ostrowska, A., Strzałka, A., Lipietta, N., Tilley, E., Zakrzewska-Czerwińska, J., Herron, P., Jakimowicz, D., 2016. Unique Function of the Bacterial Chromosome Segregation Machinery in Apically Growing *Streptomyces* - Targeting the Chromosome to New Hyphal Tubes and its Anchorage at the Tips. PLOS Genetics. 12, e1006488.

Komaki, H., Hosoyama, A., Kimura, A., Ichikawa, N., Igarashi, Y., Tamura, T., 2020. Classification of '*Streptomyces hyalinum*' Hamada and Yokoyama as *Embleya hyalina* sp. nov., the second species in the genus *Embleya*, and emendation of the genus *Embleya*. Int J Syst Evol Microbiol. 70, 1591-1595.

Komaki, H., Ichikawa, N., Hosoyama, A., Fujita, N., Igarashi, Y., 2015. Draft genome sequence of marine-derived *Streptomyces sp*. TP-A0598, a producer of anti-MRSA antibiotic lydicamycins. Standards in genomic sciences. 10, 58.

Kong, J., Yi, L., Xiong, Y., Huang, Y., Yang, D., Yan, X., Shen, B., Duan, Y., Zhu, X., 2018. The discovery and development of microbial bleomycin analogues. Appl Microbiol Biotechnol. 102, 6791-6798.

Kormanec, J., Novakova, R., Mingyar, E., Feckova, L., 2014. Intriguing properties of the angucycline antibiotic auricin and complex regulation of its biosynthesis. Appl Microbiol Biotechnol. 98, 45-60.

Krömer, J. O., Fritz, M., Heinzle, E., Wittmann, C., 2005. In vivo quantification of intracellular amino acids and intermediates of the methionine pathway in *Corynebacterium glutamicum*. Anal Biochem. 340, 171-3.

Krömer, J. O., Heinzle, E., Schroder, H., Wittmann, C., 2006a. Accumulation of homolanthionine and activation of a novel pathway for isoleucine biosynthesis in *Corynebacterium glutamicum* McbR deletion strains. J Bacteriol. 188, 609-18.

Krömer, J. O., Heinzle, E., Wittmann, C., 2006b. Quantification of S-adenosyl methionine in microbial cell extracts. Biotechnol Lett. 28, 69-71.

Krömer, J. O., Sorgenfrei, O., Klopprogge, K., Heinzle, E., Wittmann, C., 2004. In-depth profiling of lysine-producing *Corynebacterium glutamicum* by combined analysis of the transcriptome, metabolome, and fluxome. J Bacteriol. 186, 1769-84.

Kuhl, M., Gläser, L., Rebets, Y., Rückert, C., Sarkar, N., Hartsch, T., Kalinowski, J., Luzhetskyy, A., Wittmann, C., 2020. Microparticles globally reprogram *Streptomyces albus* toward accelerated morphogenesis, streamlined carbon

core metabolism, and enhanced production of the antituberculosis polyketide pamamycin. Biotechnol Bioeng. 117, 3858-3875.

Kuhl, M., Rückert, C., Gläser, L., Beganovic, S., Luzhetskyy, A., Kalinowski, J., Wittmann, C., 2021. Microparticles enhance the formation of seven major classes of natural products in native and metabolically engineered *actinobacteria* through accelerated morphological development. Biotechnol Bioeng. 118, 3076-3093.

Labeda, D. P., Actinomycete taxonomy: generic characterization. 1987.

Labes, G., Bibb, M., Wohlleben, W., 1997. Isolation and characterization of a strong promoter element from the *Streptomyces ghanaensis* phage I19 using the gentamicin resistance gene (aacC1) of Tn 1696 as reporter. Microbiology. 143 (Pt 5), 1503-1512.

Lal, R., Khanna, R., Kaur, H., Khanna, M., Dhingra, N., Lal, S., Gartemann, K.-H., Eichenlaub, R., Ghosh, P. K., 1996. Engineering Antibiotic Producers to Overcome the Limitations of Classical Strain Improvement Programs. Crit Rev Microbiol. 22, 201-255.

Lange, A., Becker, J., Schulze, D., Cahoreau, E., Portais, J.-C., Haefner, S., Schröder, H., Krawczyk, J., Zelder, O., Wittmann, C., 2017. Bio-based succinate from sucrose: High-resolution ^{13}C metabolic flux analysis and metabolic engineering of the rumen bacterium *Basfia succiniciproducens*. Metab Eng. 44, 198-212.

Lasch, C., Stierhof, M., Estevez, M. R., Myronovskyi, M., Zapp, J., Luzhetskyy, A., 2020. Dudomycins: New Secondary Metabolites Produced After Heterologous Expression of an Nrps Cluster from *Streptomyces albus* ssp. *Chlorinus* Nrrl B-24108. Microorganisms. 8.

Lasch, C., Stierhof, M., Estevez, M. R., Myronovskyi, M., Zapp, J., Luzhetskyy, A., 2021. Bonsecamin: A New Cyclic Pentapeptide Discovered through Heterologous Expression of a Cryptic Gene Cluster. Microorganisms. 9.

Lee, L. H., Zainal, N., Azman, A. S., Eng, S. K., Goh, B. H., Yin, W. F., Ab Mutalib, N. S., Chan, K. G., 2014. Diversity and antimicrobial activities of *actinobacteria* isolated from tropical mangrove sediments in Malaysia. ScientificWorldJournal. 2014, 698178.

Lee, S. Y., Kim, H. U., 2015. Systems strategies for developing industrial microbial strains. Nat Biotechnol. 33, 1061-72.

Lee, Y., Lee, N., Hwang, S., Kim, W., Cho, S., Palsson, B. O., Cho, B. K., 2022. Genome-scale analysis of genetic regulatory elements in *Streptomyces avermitilis* MA-4680 using transcript boundary information. BMC Genomics. 23**,** 68.

Li, L., Zhao, Y., Ruan, L., Yang, S., Ge, M., Jiang, W., Lu, Y., 2015. A stepwise increase in pristinamycin II biosynthesis by *Streptomyces pristinaespiralis* through combinatorial metabolic engineering. Metab Eng. 29**,** 12-25.

Li, Z.-y., Bu, Q.-t., Wang, J., Liu, Y., Chen, X.-a., Mao, X.-m., Li, Y.-Q., 2019. Activation of anthrachamycin biosynthesis in *Streptomyces chattanoogensis* L10 by site-directed mutagenesis of *rpoB*. Journal of Zhejiang University-SCIENCE B. 20**,** 983-994.

Liao, H. F., Lin, L. L., Chien, H. R., Hsu, W. H., 2001. Serine 187 is a crucial residue for allosteric regulation of *Corynebacterium glutamicum* 3-deoxy-D-arabino-heptulosonate-7-phosphate synthase. FEMS Microbiol Lett. 194**,** 59-64.

Liu, G., Chater, K. F., Chandra, G., Niu, G., Tan, H., 2013. Molecular regulation of antibiotic biosynthesis in *streptomyces*. Microbiol Mol Biol Rev. 77**,** 112-43.

Liu, J., Wang, Y., Lu, Y., Zheng, P., Sun, J., Ma, Y., 2017. Development of a CRISPR/Cas9 genome editing toolbox for *Corynebacterium glutamicum*. Microb Cell Fact. 16**,** 205.

Liu, L., Cheng, Y., Lyu, M., Zhao, X., Wen, Y., Li, J., Chen, Z., 2019. AveI, an AtrA homolog of *Streptomyces avermitilis*, controls avermectin and oligomycin production, melanogenesis, and morphological differentiation. Appl Microbiol Biotechnol. 103**,** 8459-8472.

Liu, N., Stephanopoulos, G., 2021. Metabolic Engineering Perspectives. Metab Eng. pp. 1-21.

Liu, Y., Wang, H., Li, S., Zhang, Y., Cheng, X., Xiang, W., Wang, X., 2021a. Engineering of primary metabolic pathways for titer improvement of milbemycins in *Streptomyces bingchenggensis*. Appl Microbiol Biotechnol. 105**,** 1875-1887.

Liu, Z., Zhao, Y., Huang, C., Luo, Y., 2021b. Recent Advances in Silent Gene Cluster Activation in *Streptomyces*. Front Bioeng Biotechnol. 9.

Livermore, D. M., 2011. Discovery research: the scientific challenge of finding new antibiotics. J Antimicrob Chemother. 66**,** 1941-4.

Lombo, F., Velasco, A., Castro, A., de la Calle, F., Brana, A. F., Sanchez-Puelles, J. M., Mendez, C., Salas, J. A., 2006. Deciphering the biosynthesis pathway of the antitumor thiocoraline from a marine actinomycete and its expression in two *streptomyces* species. Chembiochem. 7**,** 366-76.

Lu, C., Zhang, X., Jiang, M., Bai, L., 2016. Enhanced salinomycin production by adjusting the supply of polyketide extender units in *Streptomyces albus*. Metab Eng. 35**,** 129-137.

Ludwig, W., Euzéby, J., Schumann, P., Busse, H.-J., Trujillo, M. E., Kämpfer, P., Whitman, W. B., 2012. Road map of the phylum *Actinobacteria*. In: Goodfellow, M., Kämpfer, P., Busse, H.-J., Trujillo, M. E., Suzuki, K.-i., Ludwig, W., Whitman, W. B., Eds.), Bergey's Manual® of Systematic Bacteriology: Volume Five The Actinobacteria, Part A and B. Springer New York, New York, NY, pp. 1-28.

Lukezic, T., Pikl, S., Zaburannyi, N., Remskar, M., Petkovic, H., Muller, R., 2020. Heterologous expression of the atypical tetracycline chelocardin reveals the full set of genes required for its biosynthesis. Microb Cell Fact. 19**,** 230.

Luo, Y., Zhang, L., Barton, K. W., Zhao, H., 2015. Systematic Identification of a Panel of Strong Constitutive Promoters from *Streptomyces albus*. ACS Synth Biol. 4**,** 1001-10.

Ma, Z., Hu, Y., Liao, Z., Xu, J., Xu, X., Bechthold, A., Yu, X., 2020. Cloning and Overexpression of the Toy Cluster for Titer Improvement of Toyocamycin in *Streptomyces diastatochromogenes*. Front Microbiol. 11.

Macagnan, D., Romeiro, R. d. S., de Souza, J. T., Pomella, A. W. V., 2006. Isolation of actinomycetes and endospore-forming bacteria from the cacao pod surface and their antagonistic activity against the witches' broom and black pod pathogens. Phytoparasitica. 34**,** 122-132.

Macleod, A. J., Ross, H. B., Ozere, R. L., Digout, G., Van, R., 1964. Lincomycin: A New Antibiotic Active against *Staphylococci* and Other Gram-Positive Cocci: Clinical and Laboratory Studies. Can Med Assoc J. 91**,** 1056-60.

Magnus, J. B., Hollwedel, D., Oldiges, M., Takors, R., 2006. Monitoring and modeling of the reaction dynamics in the valine/leucine synthesis pathway in *Corynebacterium glutamicum*. Biotechnol Prog. 22**,** 1071-83.

Makitrynskyy, R., Rebets, Y., Ostash, B., Zaburannyi, N., Rabyk, M., Walker, S., Fedorenko, V., 2010. Genetic factors that influence moenomycin production in streptomycetes. J Ind Microbiol Biotechnol. 37**,** 559-66.

Mantione, K. J., Kream, R. M., Kuzelova, H., Ptacek, R., Raboch, J., Samuel, J. M., Stefano, G. B., 2014. Comparing bioinformatic gene expression profiling methods: microarray and RNA-Seq. Med Sci Monit Basic Res. 20, 138-42.

Mao, X. M., Luo, S., Li, Y. Q., 2017. Negative regulation of daptomycin production by DepR2, an ArsR-family transcriptional factor. J Ind Microbiol Biotechnol. 44, 1653-1658.

Marahiel, M. A., Essen, L. O., 2009. Chapter 13 Nonribosomal Peptide Synthetases: Mechanistic and Structural Aspects of Essential Domains. Methods in Enzymology. vol. 458. Academic Press, pp. 337-351.

Massey, L. K., Sokatch, J. R., Conrad, R. S., 1976. Branched-chain amino acid catabolism in bacteria. Bacteriol Rev. 40, 42-54.

Matthews, P. C., Barrett, L. K., Warren, S., Stoesser, N., Snelling, M., Scarborough, M., Jones, N., 2016. Oral fosfomycin for treatment of urinary tract infection: a retrospective cohort study. BMC Infectious Diseases. 16, 556.

McCann, P. A., Pogell, B. M., 1979. Pamamycin: a new antibiotic and stimulator of aerial mycelia formation. J Antibiot (Tokyo). 32, 673-8.

McCord, J. P., Kohanov, Z. A., Lowell, A. N., 2022. Thermorubin Biosynthesis Initiated by a Salicylate Synthase Suggests an Unusual Conversion of Phenols to Pyrones. ACS Chem Biol. 17, 3169-3177.

Medema, M. H., Blin, K., Cimermancic, P., de Jager, V., Zakrzewski, P., Fischbach, M. A., Weber, T., Takano, E., Breitling, R., 2011. antiSMASH: rapid identification, annotation and analysis of secondary metabolite biosynthesis gene clusters in bacterial and fungal genome sequences. Nucleic Acids Res. 39, 14.

Méndez, C., Brana, A. F., Manzanal, M. B., Hardisson, C., 1985. Role of substrate mycelium in colony development in *Streptomyces*. Canadian Journal of Microbiology. 31, 446-450.

Menges, R., Muth, G., Wohlleben, W., Stegmann, E., 2007. The ABC transporter Tba of *Amycolatopsis balhimycina* is required for efficient export of the glycopeptide antibiotic balhimycin. Appl Microbiol Biotechnol. 77, 125-34.

Mensa, L., Marco, F., Vila, J., Gascon, J., Ruiz, J., 2008. Quinolone resistance among *Shigella spp*. isolated from travellers returning from India. Clin Microbiol Infect. 14, 279-81.

Meza, E., Becker, J., Bolivar, F., Gosset, G., Wittmann, C., 2012. Consequences of phosphoenolpyruvate:sugar phosphotranferase system and pyruvate kinase

isozymes inactivation in central carbon metabolism flux distribution in *Escherichia coli*. Microb Cell Fact. 11, 127.

Miguelez, E. M., Hardisson, C., Manzanal, M. B., 1999. Hyphal death during colony development in *Streptomyces antibioticus*: morphological evidence for the existence of a process of cell deletion in a multicellular prokaryote. J Cell Biol. 145, 515-25.

Miyairi, N., 1966. Studies on new antibiotics, cineromycins A and B. J Antibiotics Ser. 19, 56-62.

Mo, J., Wang, S., Zhang, W., Li, C., Deng, Z., Zhang, L., Qu, X., 2019. Efficient editing DNA regions with high sequence identity in actinomycetal genomes by a CRISPR-Cas9 system. Synthetic and systems biotechnology. 4, 86-91.

Monk, J. M., Koza, A., Campodonico, M. A., Machado, D., Seoane, J. M., Palsson, B. O., Herrgård, M. J., Feist, A. M., 2016. Multi-omics Quantification of Species Variation of *Escherichia coli* Links Molecular Features with Strain Phenotypes. Cell Syst. 3, 238-251.e12.

Montaser, R., Kelleher, N. L., 2020. Discovery of the Biosynthetic Machinery for Stravidins, Biotin Antimetabolites. ACS Chem Biol. 15, 1134-1140.

Moore, B. S., 2008. Extending the biosynthetic repertoire in ribosomal peptide assembly. Angew Chem Int Ed Engl. 47, 9386-8.

Morimoto, Y., Baba, T., Sasaki, T., Hiramatsu, K., 2015. Apigenin as an anti-quinolone-resistance antibiotic. Int J Antimicrob Agents. 46, 666-73.

Morimoto, Y., Igarashi, M., Baba, T., Hiramatsu, K., 2013. P42 Antimicrobial activity of nybomycin against *Escherichia coli*. Int J Antimicrob Agents. 42, S54.

Murray, C. J. L., Ikuta, K. S., Sharara, F., Swetschinski, L., Robles Aguilar, G., Gray, A., Han, C., Bisignano, C., Rao, P., Wool, E., et al., 2022. Global burden of bacterial antimicrobial resistance in 2019: a systematic analysis. The Lancet. 399, 629-655.

Myronovskyi, M., Luzhetskyy, A., 2013. Genome engineering in actinomycetes using site-specific recombinases. Appl Microbiol Biotechnol. 97, 4701-12.

Myronovskyi, M., Luzhetskyy, A., 2016. Native and engineered promoters in natural product discovery. Nat Prod Rep. 33, 1006-19.

Myronovskyi, M., Rosenkranzer, B., Nadmid, S., Pujic, P., Normand, P., Luzhetskyy, A., 2018. Generation of a cluster-free *Streptomyces albus* chassis strains for

improved heterologous expression of secondary metabolite clusters. Metab Eng. 49, 316-324.

Myronovskyi, M., Rosenkranzer, B., Stierhof, M., Petzke, L., Seiser, T., Luzhetskyy, A., 2020. Identification and Heterologous Expression of the Albucidin Gene Cluster from the Marine Strain *Streptomyces Albus* Subsp. *Chlorinus* NRRL B-24108. Microorganisms. 8.

Myronovskyi, M., Tokovenko, B., Brotz, E., Ruckert, C., Kalinowski, J., Luzhetskyy, A., 2014. Genome rearrangements of *Streptomyces albus* J1074 lead to the carotenoid gene cluster activation. Appl Microbiol Biotechnol. 98, 795-806.

Nelson, M. L., Levy, S. B., 2011. The history of the tetracyclines. Ann N Y Acad Sci.

Nett, M., Ikeda, H., Moore, B. S., 2009. Genomic basis for natural product biosynthetic diversity in the actinomycetes. Nat Prod Rep. 26, 1362-84.

Nonejuie, P., Burkart, M., Pogliano, K., Pogliano, J., 2013. Bacterial cytological profiling rapidly identifies the cellular pathways targeted by antibacterial molecules. Proc Natl Acad Sci U S A. 110, 16169-74.

Novakova, R., Mingyar, E., Feckova, L., Homerova, D., Csolleiova, D., Rezuchova, B., Sevcikova, B., Javorova, R., Kormanec, J., 2022. A New Family of Transcriptional Regulators Activating Biosynthetic Gene Clusters for Secondary Metabolites. Int J Mol Sci. 23.

Oh, Y.-K., Palsson, B. O., Park, S. M., Schilling, C. H., Mahadevan, R., 2007. Genome-scale Reconstruction of Metabolic Network in *Bacillus subtilis* Based on High-throughput Phenotyping and Gene Essentiality Data*. Journal of Biological Chemistry. 282, 28791-28799.

Ohtake, T., Pontrelli, S., Laviña, W. A., Liao, J. C., Putri, S. P., Fukusaki, E., 2017. Metabolomics-driven approach to solving a CoA imbalance for improved 1-butanol production in *Escherichia coli*. Metab Eng. 41, 135-143.

Ostash, B., Doud, E., Walker, S., 2012. ABC transporter genes from *Streptomyces ghanaensis* moenomycin biosynthetic gene cluster: roles in antibiotic production and export. Arch Microbiol. 194, 915-922.

Ottesen, E. A., Campbell, W., 1994. Ivermectin in human medicine. Journal of Antimicrobial Chemotherapy. 34, 195-203.

Paddon, C. J., Westfall, P. J., Pitera, D. J., Benjamin, K., Fisher, K., McPhee, D., Leavell, M. D., Tai, A., Main, A., Eng, D., et al., 2013. High-level semi-synthetic production of the potent antimalarial artemisinin. Nature. 496, 528-532.

Parekh, S., Vinci, V. A., Strobel, R. J., 2000. Improvement of microbial strains and fermentation processes. Appl Microbiol Biotechnol. 54, 287-301.

Park, S. H., Kim, H. U., Kim, T. Y., Park, J. S., Kim, S.-S., Lee, S. Y., 2014. Metabolic engineering of *Corynebacterium glutamicum* for L-arginine production. Nat Commun. 5, 4618.

Park, S. J., Tseng, C. P., Gunsalus, R. P., 1995. Regulation of succinate dehydrogenase (sdhCDAB) operon expression in *Escherichia coli* in response to carbon supply and anaerobiosis: role of ArcA and Fnr. Mol Microbiol. 15, 473-82.

Parkinson, E. I., Bair, J. S., Nakamura, B. A., Lee, H. Y., Kuttab, H. I., Southgate, E. H., Lezmi, S., Lau, G. W., Hergenrother, P. J., 2015. Deoxynybomycins inhibit mutant DNA gyrase and rescue mice infected with fluoroquinolone-resistant bacteria. Nat Commun. 6, 6947.

Parthasarathy, A., Cross, P. J., Dobson, R. C. J., Adams, L. E., Savka, M. A., Hudson, A. O., 2018. A Three-Ring Circus: Metabolism of the Three Proteogenic Aromatic Amino Acids and Their Role in the Health of Plants and Animals. Front Mol Biosci. 5, 29.

Paulus, C., Myronovskyi, M., Zapp, J., Rodríguez Estévez, M., Lopatniuk, M., Rosenkränzer, B., Palusczak, A., Luzhetskyy, A., 2022. Miramides A-D: Identification of Detoxin-like Depsipeptides after Heterologous Expression of a Hybrid NRPS-PKS Gene Cluster from *Streptomyces mirabilis* Lu17588. Microorganisms. 10.

Pavoncello, V., Barras, F., Bouveret, E., 2022. Degradation of Exogenous Fatty Acids in *Escherichia coli*. Biomolecules. 12.

Pereira, D. A., Williams, J. A., 2007. Origin and evolution of high throughput screening. Br J Pharmacol. 152, 53-61.

Pereira, H., Silva, P. C., Johansson, B., 2023. Bacteria and Yeast Colony PCR. In: Domingues, L., (Ed.), PCR: Methods and Protocols. Springer US, New York, NY, pp. 209-221.

Pereira, T., Nikodinovic, J., Nakazono, C., Dennis, G. R., Barrow, K. D., Chuck, J. A., 2008. Community structure and antibiotic production of Streptomyces nodosus bioreactors cultured in liquid environments. Microb Biotechnol. 1, 373-81.

Pérez-Victoria, I., Oves-Costales, D., Lacret, R., Martín, J., Sánchez-Hidalgo, M., Díaz, C., Cautain, B., Vicente, F., Genilloud, O., Reyes, F., 2019. Structure elucidation

and biosynthetic gene cluster analysis of caniferolides A–D, new bioactive 36-membered macrolides from the marine-derived *Streptomyces caniferus* CA-271066. Org Biomol Chem. 17**,** 2954-2971.

Peters-Wendisch, P. G., Eikmanns, B. J., Thierbach, G., Bachmann, B., Sahm, H., 1993. Phosphoenolpyruvate carboxylase in *Corynebacterium glutamicum* is dispensable for growth and lysine production. FEMS Microbiol Lett. 112**,** 269-274.

Petersen, F., Zähner, H., Metzger, J. W., Freund, S., Hummel, R. P., 1993. Germicidin, an autoregulative germination inhibitor of *Streptomyces viridochromogenes* NRRL B-1551. J Antibiot (Tokyo). 46**,** 1126-38.

Petkovic, H., Cullum, J., Hranueli, D., Hunter, I. S., Peric-Concha, N., Pigac, J., Thamchaipenet, A., Vujaklija, D., Long, P. F., 2006. Genetics of *Streptomyces rimosus*, the oxytetracycline producer. Microbiol Mol Biol Rev. 70**,** 704-28.

Pickford, R., 2019. Mass Spectrometry-Based Metabolomic Analysis. In: Ranganathan, S., Gribskov, M., Nakai, K., Schönbach, C., Eds.), Encyclopedia of Bioinformatics and Computational Biology. Academic Press, Oxford, pp. 410-425.

Pinu, F. R., Goldansaz, S. A., Jaine, J., 2019. Translational Metabolomics: Current Challenges and Future Opportunities. Metabolites. 9.

Pizer, E. S., Thupari, J., Han, W. F., Pinn, M. L., Chrest, F. J., Frehywot, G. L., Townsend, C. A., Kuhajda, F. P., 2000. Malonyl-coenzyme-A is a potential mediator of cytotoxicity induced by fatty-acid synthase inhibition in human breast cancer cells and xenografts. Cancer Res. 60**,** 213-8.

Poblete-Castro, I., Hoffmann, S.-L., Becker, J., Wittmann, C., 2020. Cascaded valorization of seaweed using microbial cell factories. Curr Opin Biotechnol. 65**,** 102-113.

Pontrelli, S., Chiu, T.-Y., Lan, E. I., Chen, F. Y. H., Chang, P., Liao, J. C., 2018. Escherichia coli as a host for metabolic engineering. Metab Eng. 50**,** 16-46.

Pope, M. K., Green, B. D., Westpheling, J., 1996. The bld mutants of *Streptomyces coelicolor* are defective in the regulation of carbon utilization, morphogenesis and cell–cell signalling. Mol Microbiol. 19**,** 747-756.

Price, L. B., Vogler, A., Pearson, T., Busch, J. D., Schupp, J. M., Keim, P., 2003. In vitro selection and characterization of *Bacillus anthracis* mutants with high-level resistance to ciprofloxacin. Antimicrob Agents Chemother. 47**,** 2362-5.

Puglisi, M. P., 2004. Natural Products: the Secondary Metabolites By James R. Hanson (University of Sussex). The Royal Society of Chemistry, Cambridge, UK. 2003. vi + 147 pp. 24.5 × 19 cm. $28.00. ISBN 0-85404-490-6. J Nat Prod. 67, 1772-1773.

Qi, F., Thakker, C., Zhu, F., Pena, M., San, K.-Y., Bennett, G. N., 2018. Improvement of butanol production in *Clostridium acetobutylicum* through enhancement of NAD(P)H availability. Journal of Industrial Microbiology and Biotechnology. 45, 993-1002.

Qiao, K., Wasylenko, T. M., Zhou, K., Xu, P., Stephanopoulos, G., 2017. Lipid production in *Yarrowia lipolytica* is maximized by engineering cytosolic redox metabolism. Nature Biotechnology. 35, 173-177.

Qiu, J., Zhuo, Y., Zhu, D., Zhou, X., Zhang, L., Bai, L., Deng, Z., 2011. Overexpression of the ABC transporter AvtAB increases avermectin production in *Streptomyces avermitilis*. Appl Microbiol Biotechnol. 92, 337-45.

Quinn, G. A., Banat, A. M., Abdelhameed, A. M., Banat, I. M., 2020. *Streptomyces* from traditional medicine: sources of new innovations in antibiotic discovery. J Med Microbiol. 69, 1040-1048.

Rebets, Y., Brotz, E., Manderscheid, N., Tokovenko, B., Myronovskyi, M., Metz, P., Petzke, L., Luzhetskyy, A., 2015. Insights into the pamamycin biosynthesis. Angew Chem Int Ed Engl. 54, 2280-4.

Reed, J. L., Vo, T. D., Schilling, C. H., Palsson, B. O., 2003. An expanded genome-scale model of *Escherichia coli* K-12 (iJR904 GSM/GPR). Genome Biology. 4, R54.

Ribeiro da Cunha, B., Fonseca, L. P., Calado, C. R. C., 2019. Antibiotic Discovery: Where Have We Come from, Where Do We Go? Antibiotics (Basel). 8.

Richter, M. F., Drown, B. S., Riley, A. P., Garcia, A., Shirai, T., Svec, R. L., Hergenrother, P. J., 2017. Predictive compound accumulation rules yield a broad-spectrum antibiotic. Nature. 545, 299-304.

Rodicio, M. R., Chater, K. F., 1988. The *Sal*I (*Sal*GI) restriction-modification system of *Streptomyces albus* G. Gene. 74, 39-42.

Rodrigues, A. L., Trachtmann, N., Becker, J., Lohanatha, A. F., Blotenberg, J., Bolten, C. J., Korneli, C., de Souza Lima, A. O., Porto, L. M., Sprenger, G. A., et al., 2013. Systems metabolic engineering of *Escherichia coli* for production of the antitumor drugs violacein and deoxyviolacein. Metab Eng. 20, 29-41.

Rodriguez, A., Martinez, J. A., Flores, N., Escalante, A., Gosset, G., Bolivar, F., 2014. Engineering *Escherichia coli* to overproduce aromatic amino acids and derived compounds. Microb Cell Fact. 13**,** 126.

Rodríguez Estévez, M., Gummerlich, N., Myronovskyi, M., Zapp, J., Luzhetskyy, A., 2020. Benzanthric Acid, a Novel Metabolite From *Streptomyces albus* Del14 Expressing the Nybomycin Gene Cluster. Front Chem. 7.

Rodriguez Estevez, M., Myronovskyi, M., Gummerlich, N., Nadmid, S., Luzhetskyy, A., 2018. Heterologous Expression of the Nybomycin Gene Cluster from the Marine Strain *Streptomyces albus* subsp. *chlorinus* NRRL B-24108. Mar Drugs. 16.

Rodriguez Estevez, M., Myronovskyi, M., Rosenkranzer, B., Paululat, T., Petzke, L., Ristau, J., Luzhetskyy, A., 2020. Novel Fredericamycin Variant Overproduced by a Streptomycin-resistant *Streptomyces albus* subsp. *chlorinus* Strain. Mar Drugs. 18.

Rohles, C., Pauli, S., Gießelmann, G., Kohlstedt, M., Becker, J., Wittmann, C., 2022. Systems metabolic engineering of *Corynebacterium glutamicum* eliminates all by-products for selective and high-yield production of the platform chemical 5-aminovalerate. Metab Eng. 73**,** 168-181.

Rohles, C. M., Giesselmann, G., Kohlstedt, M., Wittmann, C., Becker, J., 2016. Systems metabolic engineering of *Corynebacterium glutamicum* for the production of the carbon-5 platform chemicals 5-aminovalerate and glutarate. Microb Cell Fact. 15**,** 154.

Roux, F. L., Blokesch, M., 2018. Eco-evolutionary Dynamics Linked to Horizontal Gene Transfer in Vibrios. Annual Review of Microbiology. 72**,** 89-110.

Ruiz, B., Chavez, A., Forero, A., Garcia-Huante, Y., Romero, A., Sanchez, M., Rocha, D., Sanchez, B., Rodriguez-Sanoja, R., Sanchez, S., et al., 2010. Production of microbial secondary metabolites: regulation by the carbon source. Crit Rev Microbiol. 36**,** 146-67.

Sagnak, R., Cochot, S., Molina-Jouve, C., Nicaud, J.-M., Guillouet, S. E., 2018. Modulation of the Glycerol Phosphate availability led to concomitant reduction in the citric acid excretion and increase in lipid content and yield in *Yarrowia lipolytica*. J Biotechnol. 265**,** 40-45.

Salverda, M. L. M., Koomen, J., Koopmanschap, B., Zwart, M. P., de Visser, J. A. G. M., 2017. Adaptive benefits from small mutation supplies in an antibiotic

resistance enzyme. Proceedings of the National Academy of Sciences. 114, 12773-12778.

Sambrook, J. F., Russell, D. W., 2001. Molecular Cloning: A Laboratory Manual, 3rd ed. Cold Spring Harbor Laboratory Press. Vols 1,2 and 3.

Sander, T., Farke, N., Diehl, C., Kuntz, M., Glatter, T., Link, H., 2019. Allosteric Feedback Inhibition Enables Robust Amino Acid Biosynthesis in *E. coli* by Enforcing Enzyme Overabundance. Cell Syst. 8, 66-75 e8.

Santajit, S., Indrawattana, N., 2016. Mechanisms of Antimicrobial Resistance in ESKAPE Pathogens. Biomed Res Int. 2475067, 5.

Sarmiento-Vizcaino, A., Espadas, J., Martin, J., Brana, A. F., Reyes, F., Garcia, L. A., Blanco, G., 2018. Atmospheric Precipitations, Hailstone and Rainwater, as a Novel Source of *Streptomyces* Producing Bioactive Natural Products. Front Microbiol. 9, 773.

Schatz, A., Bugie, E., Waksman, S. A., Hanssen, A. D., Patel, R., Osmon, D. R., 2005. The Classic: Streptomycin, a Substance Exhibiting Antibiotic Activity against Gram-Positive and Gram-Negative Bacteria. Clinical Orthopaedics and Related Research®. 437.

Schilling, O., Frick, O., Herzberg, C., Ehrenreich, A., Heinzle, E., Wittmann, C., Stulke, J., 2007. Transcriptional and metabolic responses of *Bacillus subtilis* to the availability of organic acids: transcription regulation is important but not sufficient to account for metabolic adaptation. Appl Environ Microbiol. 73, 499-507.

Schmidt, A., Kochanowski, K., Vedelaar, S., Ahrné, E., Volkmer, B., Callipo, L., Knoops, K., Bauer, M., Aebersold, R., Heinemann, M., 2016. The quantitative and condition-dependent *Escherichia coli* proteome. Nature Biotechnology. 34, 104-110.

Schwechheimer, S. K., Becker, J., Peyriga, L., Portais, J.-C., Sauer, D., Müller, R., Hoff, B., Haefner, S., Schröder, H., Zelder, O., et al., 2018a. Improved riboflavin production with *Ashbya gossypii* from vegetable oil based on ^{13}C metabolic network analysis with combined labeling analysis by GC/MS, LC/MS, 1D, and 2D NMR. Metab Eng. 47, 357-373.

Schwechheimer, S. K., Becker, J., Peyriga, L., Portais, J. C., Wittmann, C., 2018b. Metabolic flux analysis in *Ashbya gossypii* using (13)C-labeled yeast extract:

industrial riboflavin production under complex nutrient conditions. Microb Cell Fact. 17, 162.

Schwecke, T., Aparicio, J. F., Molnár, I., König, A., Khaw, L. E., Haydock, S. F., Oliynyk, M., Caffrey, P., Cortés, J., Lester, J. B., et al., 1995. The biosynthetic gene cluster for the polyketide immunosuppressant rapamycin. Proc Natl Acad Sci U S A. 92, 7839-43.

Schwentner, A., Feith, A., Münch, E., Stiefelmaier, J., Lauer, I., Favilli, L., Massner, C., Öhrlein, J., Grund, B., Hüser, A. T., et al., 2019. Modular systems metabolic engineering enables balancing of relevant pathways for l-histidine production with *Corynebacterium glutamicum*. Biotechnology for Biofuels. 12.

Seghezzi, N., Amar, P., Koebmann, B., Jensen, P. R., Virolle, M. J., 2011. The construction of a library of synthetic promoters revealed some specific features of strong *Streptomyces* promoters. Appl Microbiol Biotechnol. 90, 615-23.

Sehgal, S. N., 2003. Sirolimus: its discovery, biological properties, and mechanism of action. Transplantation Proceedings. 35, S7-S14.

Seto, H., Imai, S., Tsuruoka, T., Ogawa, H., Satoh, A., Sasaki, T., Otake, N., 1983. Studies on the biosynthesis of bialaphos (SF-1293) Part 3. Production of phosphinic acid derivatives, MP-103, MP-104 and MP-105, by a blocked mutant of *Streptomyces hygroscopicus* SF-1293 and their roles in the biosynthesis of bialaphos. Biochem Biophys Res Commun. 111, 1008-14.

Seyedsayamdost, M. R., 2019. Toward a global picture of bacterial secondary metabolism. J Ind Microbiol Biotechnol. 46, 301-311.

Shen, Y., Sun, F., Zhang, L., Cheng, Y., Zhu, H., Wang, S.-P., Jiao, W.-H., Leadlay, P. F., Zhou, Y., Lin, H.-W., 2020. Biosynthesis of depsipeptides with a 3-hydroxybenzoate moiety and selective anticancer activities involves a chorismatase. Journal of Biological Chemistry. 295, 5509-5518.

Shima, J., Hesketh, A., Okamoto, S., Kawamoto, S., Ochi, K., 1996. Induction of actinorhodin production by *rps*L (encoding ribosomal protein S12) mutations that confer streptomycin resistance in *Streptomyces lividans* and *Streptomyces coelicolor* A3(2). J Bacteriol. 178, 7276-84.

Shiriaev, D. I., Sofronova, A. A., Berdnikovich, E. A., Lukianov, D. A., Komarova, E. S., Marina, V. I., Zakalyukina, Y. V., Biryukov, M. V., Maviza, T. P., Ivanenkov, Y. A., et al., 2021. Nybomycin inhibits both types of *E. coli* DNA gyrase -

fluoroquinolone-sensitive and fluoroquinolone-resistant. Antimicrob Agents Chemother.

Shuai, H., Myronovskyi, M., Nadmid, S., Luzhetskyy, A., 2020. Identification of a Biosynthetic Gene Cluster Responsible for the Production of a New Pyrrolopyrimidine Natural Product-Huimycin. Biomolecules. 10.

Shuai, H., Myronovskyi, M., Rosenkranzer, B., Paulus, C., Nadmid, S., Stierhof, M., Kolling, D., Luzhetskyy, A., 2022. Novel Biosynthetic Route to the Isoquinoline Scaffold. ACS Chem Biol. 17**,** 598-608.

Siegl, T., Tokovenko, B., Myronovskyi, M., Luzhetskyy, A., 2013. Design, construction and characterisation of a synthetic promoter library for fine-tuned gene expression in actinomycetes. Metab Eng. 19**,** 98-106.

Sivalingam, P., Hong, K., Pote, J., Prabakar, K., 2019. Extreme Environment *Streptomyces*: Potential Sources for New Antibacterial and Anticancer Drug Leads? Int J Microbiol. 2019**,** 5283948.

Smanski, M. J., Zhou, H., Claesen, J., Shen, B., Fischbach, M. A., Voigt, C. A., 2016. Synthetic biology to access and expand nature's chemical diversity. Nat Rev Microbiol. 14**,** 135-49.

Stansen, C., Uy, D., Delaunay, S., Eggeling, L., Goergen, J. L., Wendisch, V. F., 2005. Characterization of a *Corynebacterium glutamicum* lactate utilization operon induced during temperature-triggered glutamate production. Appl Environ Microbiol. 71**,** 5920-8.

Staunton, J., Weissman, K. J., 2001. Polyketide biosynthesis: a millennium review. Nat Prod Rep. 18**,** 380-416.

Stone, M. J., Williams, D. H., 1992. On the evolution of functional secondary metabolites (natural products). Mol Microbiol. 6**,** 29-34.

Strelitz, F., Flon, H., Asheshov, I. N., 1955. Nybomycin, a New Antibiotic with Antiphage and Antibacterial Properties. Proc Natl Acad Sci U S A. 41**,** 620-4.

Sun, D., Jeannot, K., Xiao, Y., Knapp, C. W., 2019. Editorial: Horizontal Gene Transfer Mediated Bacterial Antibiotic Resistance. Front Microbiol. 10.

Sun, L., Zeng, J., Cui, P., Wang, W., Yu, D., Zhan, J., 2018. Manipulation of two regulatory genes for efficient production of chromomycins in *Streptomyces reseiscleroticus*. J Biol Eng. 12**,** 9.

Sun, Z., Huang, Y., Wang, Y., Zhao, Y., Cui, Z., 2014. Potassium hydroxide-ethylene diamine tetraacetic acid method for the rapid preparation of small-scale PCR template DNA from *actinobacteria*. Mol Gen Mikrobiol Virusol. 38-40.

Tanaka, K., Henry, C. S., Zinner, J. F., Jolivet, E., Cohoon, M. P., Xia, F., Bidnenko, V., Ehrlich, S. D., Stevens, R. L., Noirot, P., 2012. Building the repertoire of dispensable chromosome regions in *Bacillus subtilis* entails major refinement of cognate large-scale metabolic model. Nucleic Acids Res. 41**,** 687-699.

Teoh, S. T., Kitamura, M., Nakayama, Y., Putri, S., Mukai, Y., Fukusaki, E., 2016. Random sample consensus combined with partial least squares regression (RANSAC-PLS) for microbial metabolomics data mining and phenotype improvement. J Biosci Bioeng. 122**,** 168-175.

Teoh, S. T., Putri, S., Mukai, Y., Bamba, T., Fukusaki, E., 2015. A metabolomics-based strategy for identification of gene targets for phenotype improvement and its application to 1-butanol tolerance in *Saccharomyces cerevisiae*. Biotechnology for Biofuels. 8**,** 144.

Thong, W. L., Shin-ya, K., Nishiyama, M., Kuzuyama, T., 2018. Discovery of an Antibacterial Isoindolinone-Containing Tetracyclic Polyketide by Cryptic Gene Activation and Characterization of Its Biosynthetic Gene Cluster. ACS Chem Biol. 13**,** 2615-2622.

Tippmann, S., Ferreira, R., Siewers, V., Nielsen, J., Chen, Y., 2017. Effects of acetoacetyl-CoA synthase expression on production of farnesene in *Saccharomyces cerevisiae*. J Ind Microbiol Biotechnol. 44**,** 911-922.

Tong, Y., Charusanti, P., Zhang, L., Weber, T., Lee, S. Y., 2015. CRISPR-Cas9 Based Engineering of Actinomycetal Genomes. ACS Synth Biol. 4**,** 1020-1029.

Tsypik, O., Makitrynskyy, R., Yan, X., Koch, H. G., Paululat, T., Bechthold, A., 2021. Regulatory Control of Rishirilide(s) Biosynthesis in *Streptomyces bottropensis*. Microorganisms. 9.

Umezawa, H., 1958. KANAMYCIN: ITS DISCOVERY. Ann N Y Acad Sci. 76**,** 20-26.

van Wezel, G. P., McDowall, K. J., 2011. The regulation of the secondary metabolism of *Streptomyces*: new links and experimental advances. Nat Prod Rep. 28**,** 1311-1333.

van Wezel, G. P., van der Meulen, J., Kawamoto, S., Luiten, R. G., Koerten, H. K., Kraal, B., 2000. ssgA is essential for sporulation of *Streptomyces coelicolor*

A3(2) and affects hyphal development by stimulating septum formation. J Bacteriol. 182, 5653-62.

van Winden, W. A., van Dam, J. C., Ras, C., Kleijn, R. J., Vinke, J. L., van Gulik, W. M., Heijnen, J. J., 2005. Metabolic-flux analysis of *Saccharomyces cerevisiae* CEN.PK113-7D based on mass isotopomer measurements of 13C-labeled primary metabolites. FEMS Yeast Research. 5, 559-568.

Ventura, M., Canchaya, C., Tauch, A., Chandra, G., Fitzgerald, G. F., Chater, K. F., van Sinderen, D., 2007. Genomics of *Actinobacteria*: tracing the evolutionary history of an ancient phylum. Microbiol Mol Biol Rev. 71, 495-548.

Vernel-Pauillac, F., Hogan, T. R., Tapsall, J. W., Goarant, C., 2009. Quinolone resistance in *Neisseria gonorrhoeae*: rapid genotyping of quinolone resistance-determining regions in gyrA and parC genes by melting curve analysis predicts susceptibility. Antimicrob Agents Chemother. 53, 1264-7.

Vestergaard, M., Frees, D., Ingmer, H., 2019. Antibiotic Resistance and the MRSA Problem. Microbiol Spectr. 7.

Vila, J., Ruiz, J., Goni, P., Marcos, A., Jimenez de Anta, T., 1995. Mutation in the gyrA gene of quinolone-resistant clinical isolates of *Acinetobacter baumannii*. Antimicrob Agents Chemother. 39, 1201-3.

Vila, J., Ruiz, J., Marco, F., Barcelo, A., Goni, P., Giralt, E., Jimenez de Anta, T., 1994. Association between double mutation in *gyrA* gene of ciprofloxacin-resistant clinical isolates of *Escherichia coli* and MICs. Antimicrob Agents Chemother. 38, 2477-9.

Vitayakritsirikul, V., Jaemsaeng, R., Lohmaneeratana, K., Thanapipatsiri, A., Daduang, R., Chuawong, P., Thamchaipenet, A., 2016. Improvement of chloramphenicol production in *Streptomyces venezuelae* ATCC 10712 by overexpression of the aroB and aroK genes catalysing steps in the shikimate pathway. Antonie Van Leeuwenhoek. 109, 379-88.

Wagner, S., Baars, L., Ytterberg, A. J., Klussmeier, A., Wagner, C. S., Nord, O., Nygren, P. A., van Wijk, K. J., de Gier, J. W., 2007. Consequences of membrane protein overexpression in *Escherichia coli*. Mol Cell Proteomics. 6, 1527-50.

Waksman, S. A., Lechevalier, H. A., 1949. Neomycin, a New Antibiotic Active against Streptomycin-Resistant Bacteria, including Tuberculosis Organisms. Science. 109, 305-307.

Waksman, S. A., Schatz, A., 1945. Streptomycin–Origin, Nature, and Properties*††Journal Series Paper of the Department of Microbiology of the New Jersey Agricultural Experiment Station, Rutgers University. Journal of the American Pharmaceutical Association (Scientific ed.). 34, 273-291.

Waksman, S. A., Schatz, A., Reynolds, D. M., 2010. Production of antibiotic substances by actinomycetes. Ann N Y Acad Sci. 1213, 112-24.

Walker, G. E., Dunbar, B., Hunter, I. S., Nimmo, H. G., Coggins, J. R., 1996. Evidence for a novel class of microbial 3-deoxy-D-arabino-heptulosonate-7-phosphate synthase in *Streptomyces coelicolor* A3(2), *Streptomyces rimosus* and *Neurospora crassa*. Microbiology. 142 (Pt 8), 1973-82.

Wang, J., Wang, C., Song, K., Wen, J., 2017. Metabolic network model guided engineering ethylmalonyl-CoA pathway to improve ascomycin production in *Streptomyces hygroscopicus* var. *ascomyceticus*. Microb Cell Fact. 16, 169.

Wang, K., Chen, X. A., Li, Y. Q., Mao, X. M., 2019a. Identification of a secondary metabolism-responsive promoter by proteomics for over-production of natamycin in *Streptomyces*. Arch Microbiol. 201, 1459-1464.

Wang, X., Elshahawi, S. I., Ponomareva, L. V., Ye, Q., Liu, Y., Copley, G. C., Hower, J. C., Hatcher, B. E., Kharel, M. K., Van Lanen, S. G., et al., 2019b. Structure Determination, Functional Characterization, and Biosynthetic Implications of Nybomycin Metabolites from a Mining Reclamation Site-Associated *Streptomyces*. J Nat Prod. 82, 3469-3476.

Wang, Y., Tao, Z., Zheng, H., Zhang, F., Long, Q., Deng, Z., Tao, M., 2016. Iteratively improving natamycin production in *Streptomyces gilvosporeus* by a large operon-reporter based strategy. Metab Eng. 38, 418-426.

Washington, J. A., 2nd, Wilson, W. R., 1985. Erythromycin: a microbial and clinical perspective after 30 years of clinical use (2). Mayo Clin Proc. 60, 271-8.

Weiland, F., Barton, N., Kohlstedt, M., Becker, J., Wittmann, C., 2023. Systems metabolic engineering upgrades *Corynebacterium glutamicum* to high-efficiency cis, cis-muconic acid production from lignin-based aromatics. Metab Eng. 75, 153-169.

Weissman, K. J., Leadlay, P. F., 2005. Combinatorial biosynthesis of reduced polyketides. Nat Rev Microbiol. 3, 925-36.

Wendt-Pienkowski, E., Huang, Y., Zhang, J., Li, B., Jiang, H., Kwon, H., Hutchinson, C. R., Shen, B., 2005. Cloning, sequencing, analysis, and heterologous

expression of the fredericamycin biosynthetic gene cluster from *Streptomyces griseus*. J Am Chem Soc. 127, 16442-52.

Werner, G., Fleige, C., Ewert, B., Laverde-Gomez, J. A., Klare, I., Witte, W., 2010. High-level ciprofloxacin resistance among hospital-adapted Enterococcus faecium (CC17). Int J Antimicrob Agents. 35, 119-125.

WHO, 2014. Antimicrobial resistance: global report on surveillance. World Health Organization, Geneva.

Wildermuth, H., 1970. Development and organization of the aerial mycelium in *Streptomyces coelicolor*. J Gen Microbiol. 60, 43-50.

Wildermuth, H., Hopwood, D. A., 1970. Septation during sporulation in *Streptomyces coelicolor*. J Gen Microbiol. 60, 51-9.

Willey, J. M., Gaskell, A. A., 2011. Morphogenetic signaling molecules of the streptomycetes. Chem Rev. 111, 174-87.

Williams, S., Vickers, J., 1988. Detection of actinomycetes in the natural environment: problems and perspectives. Biology of actinomycetes. 88, 265-270.

Winter, J. M., Moffitt, M. C., Zazopoulos, E., McAlpine, J. B., Dorrestein, P. C., Moore, B. S., 2007. Molecular basis for chloronium-mediated meroterpene cyclization: cloning, sequencing, and heterologous expression of the napyradiomycin biosynthetic gene cluster. J Biol Chem. 282, 16362-8.

Wittmann, C., 2007. Fluxome analysis using GC-MS. Microb Cell Fact. 6, 6.

Wittmann, C., Heinzle, E., 2002. Genealogy profiling through strain improvement by using metabolic network analysis: metabolic flux genealogy of several generations of lysine-producing corynebacteria. Appl Environ Microbiol. 68, 5843-59.

Wittmann, C., Krömer, J. O., Kiefer, P., Binz, T., Heinzle, E., 2004. Impact of the cold shock phenomenon on quantification of intracellular metabolites in bacteria. Analytical Biochemistry. 327, 135-139.

Wu, D., Schandry, N., Lahaye, T., 2018. A modular toolbox for Golden-Gate-based plasmid assembly streamlines the generation of Ralstonia solanacearum species complex knockout strains and multi-cassette complementation constructs. Mol Plant Pathol. 19, 1511-1522.

Yang, D., Cho, J. S., Choi, K. R., Kim, H. U., Lee, S. Y., 2017. Systems metabolic engineering as an enabling technology in accomplishing sustainable development goals. Microb Biotechnol. 10, 1254-1258.

Yao, Y. F., Wang, C. S., Qiao, J., Zhao, G. R., 2013. Metabolic engineering of *Escherichia coli* for production of salvianic acid A via an artificial biosynthetic pathway. Metab Eng. 19, 79-87.

Yin, S., Wang, X., Shi, M., Yuan, F., Wang, H., Jia, X., Sun, J., Liu, T., Yang, K., Zhang, Y., et al., 2017. Improvement of oxytetracycline production mediated via cooperation of resistance genes in *Streptomyces rimosus*. Sci China Life Sci. 60, 992-999.

Zaburannyi, N., Rabyk, M., Ostash, B., Fedorenko, V., Luzhetskyy, A., 2014. Insights into naturally minimised *Streptomyces albus* J1074 genome. BMC Genomics. 15, 97.

Zakalyukina, Y. V., Birykov, M. V., Lukianov, D. A., Shiriaev, D. I., Komarova, E. S., Skvortsov, D. A., Kostyukevich, Y., Tashlitsky, V. N., Polshakov, V. I., Nikolaev, E., et al., 2019. Nybomycin-producing *Streptomyces* isolated from carpenter ant *Camponotus vagus*. Biochimie. 160, 93-99.

Zhang, H., Stephanopoulos, G., 2013. Engineering *E. coli* for caffeic acid biosynthesis from renewable sugars. Appl Microbiol Biotechnol. 97, 3333-41.

Zhang, K., Mohsin, A., Dai, Y., Chen, Z., Zhuang, Y., Chu, J., Guo, M., 2019. Combinatorial Effect of ARTP Mutagenesis and Ribosome Engineering on an Industrial Strain of *Streptomyces albus* S12 for Enhanced Biosynthesis of Salinomycin. Front Bioeng Biotechnol. 7, 212.

Zhu, M., Zhang, F., Gan, T., Lin, J., Duan, Y., Zhu, X., 2022. Deciphering the pathway-specific regulatory network for production of ten-membered enediyne Tiancimycins in *Streptomyces* sp. CB03234-S. Microb Cell Fact. 21, 188.

Zhu, Z., Li, H., Yu, P., Guo, Y., Luo, S., Chen, Z., Mao, X., Guan, W., Li, Y., 2017. *SlnR* is a positive pathway-specific regulator for salinomycin biosynthesis in *Streptomyces albus*. Appl Microbiol Biotechnol. 101, 1547-1557.